

Sedimentary Facies, Lithostratigraphy, and Sequence Stratigraphy of the Lower Cretaceous Dina and
Cummings, Alberta, Canada

By

Scott Botterill

A thesis submitted in partial fulfillment of the requirements for the degree of
Doctor of Philosophy

Department of Earth and Atmospheric Sciences
University of Alberta

© Scott Botterill, 2024

Abstract

The Lower Cretaceous Aptian to Albian Dina and Cummings lithostratigraphic units comprise a complex assemblage of siliciclastic strata deposited in the Western Canada Sedimentary Basin (WCSB) during transgression of the Lower Cretaceous Boreal Sea. The internal stratigraphic complexity of this interval results from several factors, including significant topographic variation along the underlying sub-Cretaceous unconformity (more than 50 metres), internal complexity of the constituent continental to shallow marine environments, and the occurrence of several high-frequency base-level fluctuations nested within the lower frequency transgressive system. This complexity has resulted in historical inconsistencies in top placement, geological definitions, and formal rank (Formation versus Member). Despite the production of hydrocarbons ranging from the 1940's to present no regional, high-resolution sedimentary facies and sequence stratigraphic analysis of the Dina and Cummings has been published. Such studies are essential to inform several aspects including exploration and development of hydrocarbon resources, pore space distribution, and the presence of sub-surface intervals suitable for CO₂ sequestration.

The overarching goal of this study is to develop a regional, geologically consistent, stratigraphic framework for the Dina and Cummings lithostratigraphic units in the east-central plains region of Alberta. To achieve this goal, the application of high-resolution sedimentary facies analysis and sequence stratigraphic principles were applied to a subsurface dataset consisting of seventy-two stratigraphic core, and ca. 7800 petrophysical wireline logs in an area between Townships 45-55, Ranges 1-8W4 Meridian (8800 km²). Focus was placed on the analysis of physical sedimentology (lithology, sedimentary structures, lithological accessories) and ichnology (ichnogeneric identification, bioturbation intensity, trace fossil distribution) to identify the range of depositional environments preserved within the Dina and Cummings interval. These sedimentological observations were then used to revise the formal lithostratigraphic stratigraphy and develop a high-resolution sequence stratigraphic framework.

The high-resolution facies and sequence stratigraphic analysis resulted in the identification of seven geologically distinct facies association complexes (FAC-A to FAC-G) bound by seven discontinuity surfaces (S1 to S7). These seven facies association complexes and discontinuity surfaces form the building blocks of depositional sequences at two scales. These sequences are referred to as medium-frequency Sequence 1, within which are nested two higher-frequency depositional sequences – high-frequency Sequence 1 and high-frequency Sequence 2. The goal of establishing a regionally consistent lithostratigraphic framework for the Dina and Cummings was also achieved, with the revision of stratigraphic tops, elevation in rank from Member to Formation, and the recognition of four new members resulting from these high-resolution facies analysis. In ascending stratigraphic order these are the

McLaughlin and Rivercourse members of the Dina Formation, and the Lindbergh and Paradise Valley members of the Cummings Formation.

Preface

All work herein is the author's own, with the final product being representative of inputs and edits of his doctoral committee (Dr. Murray Gingras, Dr. John-Paul Zonneveld, Dr. Mike Ranger, Dr. James MacEachern, and Dr. Daniel Hembree). A version of Chapters 3 and 4 will be submitted for publication in academic journals after submission of this thesis and may differ in terms of format, content, and coauthor contribution. Dr. Mattias Grobe and Dr. Eric Timmer provided edits and discussion for Chapter 3. Dr. Sarah Schultz provided edits and discussion for Chapter 4. Dr. Eric Timmer contributed to the petrophysical analysis component in Chapter 3.

Dedication

I dedicate this thesis to my wife, Erin. My gratitude for your support and the sacrifices you made during the completion of this thesis are beyond words. Without you, I could never have completed this endeavour. Thank you.

Acknowledgements

Completing this thesis would not have been possible without the help of several people. First, I thank my wife Erin, and daughter, Ella for being so patient and supportive throughout this endeavour. You are the two most important people in my life and without you I would be lost. To my parents, Mark, and Dorothy, and my second parents, Ann, and Dennis, I deeply appreciate the support you all have given me throughout this endeavour. Time is a precious thing, and you have all given me that in spades. Finally, Ellen and George Andrews are thanked for their contribution that made the pursuit of my PhD possible.

I am sincerely grateful to the Alberta Geological Survey, in particular Kelsey McCormack and Chris Filewich for so strongly supporting this project. This thesis has benefitted from several excellent AGS scientists. David Herbers, Eric Timmer, Sarah Schultz, Tiffany Playter, Tyler Hauck, Jesse Peterson, Greg Hartman, Dan Utting, Calla Knudsen, Alex MacNeil, and Matt Grobe are all thanked for their invaluable discussion on all things sedimentology, ichnology, and stratigraphy. Matt Grobe is thanked for his other-worldly editing skills. Ryan King is thanked for all the support and knowledge he has passed down to me since the start of my first stint as a graduate student in the IRG lab more than a decade ago. I am grateful to the members of my committee, Dr. James MacEachern, Dr. Mike Ranger, and Dr. J-P Zonneveld. Each of you have made significant contributions to my development as a geologist throughout the time I have known you all, and it is not lost on me how fortunate I am to have such incredible mentors. Dr. Brian Zaitlin, and Jason Lavigne are thanked for their willingness to engage in discussions on all things Mannville geology. There is never a conversation I have with either of you that I do not learn something meaningful.

It is with regret that I cannot personally thank Dr. George Pemberton for the influence he has had on me and countless other IRG students throughout his years at the U of A. I had the privilege of being one of the last students to have George as part of their candidacy exam and the memory of hearing him tell stories to the rest of my examiners while I sat out in the hallway waiting to learn my fate is something I will not forget. It was not a short wait, as Georges stories grew in grandeur with each telling.

Finally, to my supervisor Dr. Murray Gingras, it is difficult to express how much gratitude I feel for your mentorship throughout the nearly 20 years I have known you. I have benefitted so much from your knowledge, and just as importantly your friendship. You are an incredible geologist, and an even better person. Thank you, Mur.

Table of Contents

| | | |
|------------|---|-----------|
| 1 | INTRODUCTION | 1 |
| 1.1 | Introduction | 1 |
| 1.2 | Organization of the Dissertation | 2 |
| 1.3 | References | 4 |
| 2 | HIGH RESOLUTION FACIES ANALYSIS OF THE LOWER MANNVILLE DINA AND CUMMINGS INTERVAL, EAST-CENTRAL PLAINS REGION, ALBERTA | 8 |
| 2.1 | Introduction | 8 |
| 2.2 | Regional Geology | 9 |
| 2.3 | Study Area, Dataset, and Methods | 10 |
| 2.4 | Results and Interpretations | 14 |
| 2.4.1 | Facies Association Complexes | 14 |
| 2.4.1.1 | Facies Association Complex A | 14 |
| 2.4.1.2 | Facies Association Complex B – Upper to Middle Estuary | 24 |
| 2.4.1.3 | Facies Association Complex C – River- and Wave-Influenced Embayment | 28 |
| 2.4.1.4 | Facies Association Complex D – Tidal Channel & Tidal Delta | 29 |
| 2.4.1.5 | Facies Association Complex E – Storm-Dominated Delta | 32 |
| 2.4.1.6 | Facies Association Complex F – Coastal Marine to Offshore | 33 |
| 2.4.1.7 | Facies Association Complex G – Shoreface to Offshore | 35 |
| 2.4.2 | Bounding Surfaces | 35 |
| 2.4.2.1 | Surface 1 | 37 |
| 2.4.2.2 | Surface 2 | 37 |
| 2.4.2.3 | Surface 3 | 37 |
| 2.4.2.4 | Surface 4 | 38 |
| 2.4.2.5 | Surface 5 | 38 |
| 2.4.2.6 | Surface 6 | 38 |
| 2.4.2.7 | Surface 7 | 38 |

| | | |
|------------|--|-----------|
| 2.5 | Discussion | 39 |
| 2.5.1 | Spatio-Temporal Trends in Deposition | 39 |
| 2.6 | Conclusions | 44 |
| 2.7 | References | 46 |
| 3 | STRATIGRAPHIC REVISION OF THE LOWER CRETACEOUS DINA AND CUMMINGS MEMBERS, ALBERTA, CANADA | 54 |
| 3.1 | Introduction | 54 |
| 3.2 | Dataset, Methods, and Historical Background | 56 |
| 3.2.1 | Dataset and Methods | 56 |
| 3.2.2 | Historical Background | 57 |
| 3.2.2.1 | Dina Member | 57 |
| 3.2.2.2 | Cummings Member | 58 |
| 3.3 | Stratigraphic Revision | 59 |
| 3.3.1 | Revision of the Dina Member | 59 |
| 3.3.1.1 | Utility and Rank | 59 |
| 3.3.1.2 | Stratotype and Locality | 59 |
| 3.3.1.3 | Geological Description | 64 |
| 3.3.1.4 | Extent, Thickness and Boundaries | 68 |
| 3.3.1.5 | Age and Correlation | 68 |
| 3.3.2 | Revision of the Cummings Member | 71 |
| 3.3.2.1 | Utility and Rank | 71 |
| 3.3.2.2 | Stratotype and Locality | 71 |
| 3.3.2.3 | Geological Description | 71 |
| 3.3.2.4 | Extent, Thickness, and Boundaries | 73 |
| 3.3.2.5 | Age and Correlation | 74 |
| 3.4 | Discussion | 78 |
| 3.4.1 | Revised Definition | 78 |
| 3.4.1.1 | Dina Formation | 78 |
| 3.4.1.2 | Cummings Formation | 78 |
| 3.4.2 | Limitations | 79 |

| | | |
|------------|--|------------|
| 3.5 | Conclusions | 80 |
| 3.6 | References | 83 |
| 4 | APPLICATION OF FACIES ANALYSIS IN HIGH-RESOLUTION SEQUENCE STRATIGRAPHY: A CASE STUDY FROM THE LOWER MANNVILLE GROUP, EAST-CENTRAL PLAINS REGION, ALBERTA, CANADA | 86 |
| 4.1 | Introduction | 86 |
| 4.2 | Scale of Stratigraphic Units and Discontinuities | 88 |
| 4.3 | Overview of Dina and Cummings Geology | 91 |
| 4.4 | Dataset and Methodology | 93 |
| 4.5 | Scale of Units and Bounding Surface | 97 |
| 4.5.1 | Bounding Surfaces | 98 |
| 4.5.1.1 | Subaerial Unconformity and Correlative Conformity – SU & CC | 98 |
| 4.5.1.2 | Transgressive Surface - TS | 100 |
| 4.5.1.3 | Ravinement Surface - RS | 100 |
| 4.5.1.4 | Maximum Flooding Surface - MFS | 100 |
| 4.5.2 | Sedimentological Surfaces | 101 |
| 4.6 | Depositional Sequences | 102 |
| 4.6.1 | High- Frequency Depositional Sequence 1 | 102 |
| 4.6.1.1 | Lowstand Systems Tract | 102 |
| 4.6.1.2 | Transgressive Systems Tract | 103 |
| 4.6.1.3 | Highstand Systems Tract | 104 |
| 4.6.2 | Sequence 1 – 2 Bounding Surface | 106 |
| 4.6.3 | High-Frequency Depositional Sequence 2 | 106 |
| 4.6.3.1 | Lowstand Systems Tract | 106 |
| 4.6.3.2 | Transgressive Systems Tract | 106 |
| 4.6.3.3 | Highstand Systems Tract | 110 |
| 4.7 | Depositional Evolution | 112 |
| 4.8 | Conclusions | 113 |

| | | |
|-----|--|-----|
| 4.9 | References----- | 116 |
| 5 | SUMMARY AND CONCLUSIONS ----- | 125 |
| 5.1 | Sedimentary Facies and Depositional Environments ----- | 125 |
| 5.2 | Revised Lithostratigraphic Framework----- | 125 |
| 5.3 | Sequence Stratigraphic Framework----- | 126 |
| | REFERENCES ----- | 128 |
| | APPENDIX----- | 144 |

LIST OF FIGURES

| | |
|--|-----|
| 2-1) CROSS-SECTION AND STRATIGRAPHIC CHART OF THE DINA AND CUMMINGS | 11 |
| 2-2) LOCATION MAP | 12 |
| 2-3) SYMBOL LEGEND | 13 |
| 2-4) CONTINENTAL TO ESTUARINE DISTRIBUTION OF A-FA1, A-FA3, AND B-FA4 | 21 |
| 2-5) CORE AND PETROPHYSICAL LOGS OF FACIES ASSOCIATION COMPLEXES A-G | 22 |
| 2-6) FACIES ASSOCIATION COMPLEX A | 23 |
| 2-7) CORE AND PETROPHYSICAL LOGS OF FACIES ASSOCIATION COMPLEX A-G | 25 |
| 2-8) FACIES ASSOCIATION COMPLEXES B AND C | 26 |
| 2-9) FACIES ASSOCIATION COMPLEXES D AND E | 30 |
| 2-10) FACIES ASSOCIATION COMPLEXES F AND G | 36 |
| 2-11) REGIONAL NW-SE AND W-E CROSS-SECTIONS | 40 |
| 2-12) STRATIGRAPHIC SURFACE CHARACTERISTICS | 41 |
| 2-13) STRATIGRAPHIC FENCE DIAGRAM | 41 |
| 3-1) SUMMARY OF TOP PLACEMENT AND LOCATION MAP | 55 |
| 3-2) LEGEND OF SYMBOLS | 57 |
| 3-3) STRATIGRAPHIC COLUMN | 60 |
| 3-4) REFERENCE LOGS | 61 |
| 3-5) MCLAUGHLIN AND RIVERCOURSE MEMBER FACIES | 66 |
| 3-6) CONTINENTAL TRACE FOSSIL ASSEMBLAGES | 67 |
| 3-7) ISOPACH MAP OF THE DINA FORMATION | 69 |
| 3-8) NW-SE STRATIGRAPHIC CROSS-SECTIONS | 70 |
| 3-9) CORE AND PETROPHYSICAL SIGNATURE OF THE DINA-CUMMINGS CONTACT | 72 |
| 3-10) HISTOGRAM AND VIOLIN PLOTS | 75 |
| 3-11) FACIES OF THE LINDBERGH AND PARADISE VALLEY MEMBERS | 76 |
| 3-12) ISOPACH MAP OF THE CUMMINGS FORMATION | 77 |
| 3-13) LITHOSTRATIGRAPHIC COMPARISON OF THE LLOYDMINSTER AND ATHABASCA AREAS | 82 |
| 4-1) ICHNOLOGICALLY DEMARCATED DISCONTINUITIES | 88 |
| 4-2) STRATIGRAPHY OF THE MANNVILLE GROUP IN ALBERTA AND WESTERN SASKATCHEWAN | 90 |
| 4-3) SCHEMATIC DIAGRAM OF SEQUENCE STRATIGRAPHIC AND SEDIMENTOLOGICAL DISCONTINUITIES | 91 |
| 4-4) LOCATION MAP AND WELL DATASET | 93 |
| 4-5) SEQUENCE AND SEDIMENTOLOGICAL SURFACES | 99 |
| 4-6) CORE LOGS AND PHOTOS OF HF SEQUENCE 1 | 102 |
| 4-7) FACIES OF HF SEQUENCE 1 | 105 |
| 4-8) NW-SE AND W-E CROSS-SECTIONS | 107 |

4-9) CORE AND PETROPHYSICAL CHARACTERISTICS OF HF SEQUENCE 1-2 CONTACT-----108
4-10) CORE LOGS AND PHOTOS OF HF SEQUENCE 2-----109
4-11) FACIES OF HF SEQUENCE 2 -----111

LIST OF TABLES

| | |
|------------------------|----|
| TABLE 2-1 | 17 |
| TABLE 3-1 | 62 |
| TABLE 4-1 | 95 |

1 Introduction

1.1 Introduction

The lower Cretaceous Dina and Cummings members of the Mannville Group in the east-central plains region of Alberta consist of a spatially complex assemblage of clastic sediments deposited during southward transgression of the Boreal Sea. The Dina and Cummings comprise the transgressive systems tract of the Mannville Group third-order depositional sequence of Cant (1996) and Cant and Abrahamson (1996). The internal complexity of strata results from several factors, including significant topographic relief along the sub-Cretaceous unconformity (more than 50 metres), the high lithologic variability inherent in the constituent continental and shallow marine environments, and the nested architecture of higher frequency sequences within the third order transgressive systems tract. As a result, previous publications have led to discrepancies between assignment of formal rank (formation versus member), identification of their stratigraphic tops, and the interpretation of depositional environments (e.g., Nauss 1945; Wickenden, 1948; Ambler, 1951; Kent, 1959; Orr et al., 1977; Vigrass, 1977; Wilson, 1984; Zaitlin and Schultz, 1984; Christopher, 1997; Bauer et al., 2009).

Several factors contribute to these discrepancies. First, the formal definition of the Dina and Cummings by Nauss (1945) was made when the density and quality of core and wireline data was limited. The map provided in Figure 1 of Nauss (1945) shows the location of the seventeen reference wells comprising his dataset between townships 43-56, ranges 1-14W4. The original top placement and definitions, based on that seventeen well dataset, could not be expected to capture the lithological complexity of this interval. Second, most of the previous work focusing specifically on the study area was done using lithostratigraphic correlation before the development of sequence stratigraphic methodologies. Lithostratigraphic placement of tops by early workers relied primarily on electric log signatures. For example, Nauss (1945) and Kent (1959) place the Dina/Cummings contact as “the base of the first shale or siltstone horizon appearing on an electric log” (Kent, 1959, p. 17). In essence, this placed a member-level contact within a continuous fluvial channel, at the base of the inclined heterolithic portion of the syndepositional point-bar. The placement of a contact at this surface has no regional meaning given the lateral complexity of fluvial systems. Finally, while Zaitlin and Schultz, (1984), Christopher (1997), and Bauer et al., (2009) have provided published studies focusing on facies analysis including sedimentology and ichnology for the Dina and Cummings in Saskatchewan, such an integrated study has yet to be published on equivalent strata in Alberta. Facies analysis is an essential component in establishing geologically sound

interpretations of depositional environments. Only after the affinity of depositional environments has been established can a geologically consistent stratigraphic framework be erected.

1.2 Organization of the Dissertation

This thesis is comprised of four chapters, which focus on different geological aspects of the Dina and Cummings lithostratigraphic units located in the east-central plains region of Alberta. The overarching goal of this work is to develop a regional, geologically consistent stratigraphic framework for the Dina and Cummings that can be used to inform several sub-surface uncertainties. Chapter 2 focuses on the detailed facies analysis of seventy-two stratigraphic drill core that intersect intervals within the Dina and Cummings members in an area encompassing townships 45-55, ranges 1-8W4 meridian (8800 km²). This work incorporates sedimentary facies observations including physical sedimentology, ichnology, and lithology to identify the range of depositional environments preserved within the Dina and Cummings members. The combination of sedimentological and ichnological criteria is an essential component in such analysis as it allows for the identification of several physical and chemical stresses affecting sedimentation and biotic distribution during deposition of given facies. Such stresses include the rapid or slow sedimentation rates, storm-induced turbidite deposition, water turbidity, food resource distribution, current strength, oxygenation, substrate consistency, temperature, and shifting substrate. A number of studies have documented the ichnological response to these physico-chemical stresses through research on modern and ancient environments (e.g., Howard et al., 1975; Seilacher, 1978; Pemberton et al., 1982; Ekdale and Bromley, 1984; Moslow and Pemberton, 1988; Savrda and Bottjer, 1991; Pemberton and MacEachern, 1992; Gingras et al., 1998; Gingras et al., 1999; Bann and Fielding, 2004; Hubbard et al., 2004; Coats and MacEachern, 2005; MacEachern et al., 2005; Hauck et al., 2009; Gingras et al., 2012, among many others). Chapter 2 also establishes the presence of stratigraphic discontinuity surfaces that bound distinct units, briefly describes the nature of bounding facies above and below and assesses the stratigraphic extent of these surfaces using petrophysical log correlations. This work represents the first integrated sedimentological and ichnological study of the entire Dina and Cummings interval within the east-central plains of Alberta. The identification of depositional environments in Chapter 2 serves as the basis for the lithostratigraphic and sequence stratigraphic frameworks developed in chapters 3 and 4, respectively.

Chapter 3 addresses issues pertaining to lithostratigraphic nomenclature, geological definitions, and top placements that have persisted from the original formal establishment of the Dina and Cummings members by Nauss (1945) to present day. In this chapter, an attempt is made to resolve these historical inconsistencies in three ways. First, the original stratigraphic tops of Nauss (1945) are revised to conform to discontinuity surfaces in place of arbitrary lithostratigraphic contacts. This results in stratigraphic

correlations that better conform to natural breaks in sedimentation and is more effective at ensuring depositionally related facies are included within the same lithostratigraphic interval. Second, expanded geological definitions are provided for the Dina and Cummings intervals. These criteria enable more regionally consistent identification of these stratigraphic intervals to be made in the subsurface. Finally, through detailed mapping using an extensive wireline dataset tied to core observations, a regional lithostratigraphic framework is erected for the Dina and Cummings in the east-central plains region.

Chapter 4 leverages the detailed facies analysis of Chapter 2 to develop a high-resolution sequence stratigraphic framework for the Dina and Cummings. As with Chapter 2, a published sequence stratigraphic analysis of the Dina and Cummings situated within the boundaries of this study is currently lacking. Due to the absence of outcrop and public availability of seismic datasets, this chapter focuses on leveraging sedimentological and ichnological datasets to identify the stratigraphic significance of discontinuity surfaces that bound the distinct facies associations complexes defined in Chapter 2. Such datasets have been applied to a number of sequence stratigraphic studies of Mannville Group strata throughout the Western Canada Sedimentary Basin (e.g., Vossler and Pemberton, 1988; Pemberton and MacEachern, 1995; Cant, 1996; MacEachern et al., 1999; Wellner et al., 2018; Chateau et al., 2019; Morshedian et al., 2019; Ahmad and Gingras, 2022; Newitt and Pedersen, 2022; Schultz et al., 2022) and basins of various age in a number of countries (e.g., Fielding et al., 2007; Rodriguez-Tovar et al., 2007; Pearson et al., 2012; Bayet-Goll et al., 2017; Rodriguez et al., 2018).

The closing chapter, Chapter 5 summarizes the findings of chapters 2, 3, and 4 and describes the contribution of the thesis to the disciplines of sedimentology, ichnology, and stratigraphy.

1.3 References

- Ahmad, W. and Gingras, M.K., 2022, Ichnology and Sedimentology of the Lower Cretaceous Wabiskaw Member (Clearwater Formation) Alberta, Canada: *Marine and Petroleum Geology*, v. 143, Article 105775.
- Ambler, J.S., 1951, The stratigraphy and structure of the Lloydminster oil and gas area: University of Saskatchewan, M.Sc. thesis.
- Bann, K.L., and Fielding, C.R., 2004, An integrated ichnological and sedimentological comparison of non-deltaic shoreface and subaqueous delta deposits in Permian reservoir units of Australia: *Geological Society, London, Special Publication* v. 228, p. 273-310.
- Bauer, D.B., Hubbard, S.M., Leckie, D.A., and Dolby, G., 2009, Delineation of a sandstone-filled incised valley in the Lower Cretaceous Dina–Cummings interval: implications for development of the Winter Pool, west-central Saskatchewan: *Bulletin of Canadian Petroleum Geology*, v. 57, no. 4, p. 409-429.
- Bayet-Goll, R., Samani, P.N., de Carvalho, C.N., Monaco, P., Khodaie, N., Pour, M.M., Kazemini, H., and Zareiyan, M.H., 2017, Sequence stratigraphy and ichnology of Early Cretaceous reservoirs, Gadvan Formation in southwestern Iran: *Marine and Petroleum Geology*, v. 81, p. 294-319.
- Cant, D.J., 1996, Sedimentological and sequence stratigraphic organization of a foreland clastic wedge, Mannville Group, Western Canada Basin: *Journal of Sedimentary Research*, v. 66, no. 6, p. 1137-1147.
- Chateau, C.C.F., Dashtgard, S.E., MacEachern, J.A., and Hauck, T.E., 2019, Parasequence architecture in a low-accommodation setting, impact of syndepositional carbonate epikarstification, McMurray Formation, Alberta, Canada: *Marine and Petroleum Geology*, v. 104, p. 168-179.
- Christopher, J., 1997, Evolution of the Lower Cretaceous Mannville Sedimentary Basin in Saskatchewan, *in*: Pemberton, S.G., and James, D.P., editors, *Petroleum Geology of the Cretaceous Mannville Group, Western Canada*: Canadian Society of Petroleum Geologists, *Memoir* 18, p. 191-210.
- Coates, L. and MacEachern, J.A. 2005, The ichnological signatures of river- and wave-dominated delta complexes: Differentiating deltaic and non-deltaic shallow marine successions, Lower Cretaceous Viking Formation and Upper Cretaceous Dunvegan Formation, west-central Alberta, *in*: *Applied Ichnology*, MacEachern, J.A., Bann, K.L, Gingras, M.K., and Pemberton, S.G., editors, *Society of Economic Paleontologists and Mineralogists Short Course Notes*, v. 52, p. 221-248.
- Fielding, C.R., Bann, K.L., and Trueman, J.D., 2007, Resolving the architecture of a complex, low-accommodation unit using high-resolution sequence stratigraphy and ichnology: the Late Permian

- Freitag Formation in the Denison Trough, Queensland, Australia: *in*: MacEachern, J.A., Bann, K.L., Gingras, M.K., and Pemberton, S.G., editors, Applied Ichnology: SEPM Short Course Notes, v. 52
- Fuglem 1970, M.O., 1970, Use of core in evaluation of productive sands, Lloydminster area, *in*: Brindele, J.E., and Holmerg, R.A., editors, Saskatchewan Mesozoic Core Seminar, Saskatchewan Geological Society, 12 p.
- Gingras, M.K., MacEachern, J.A., and Pemberton, S.G., 1998, A comparative analysis of the ichnology of wave- and river-dominated allomembers of the Upper Cretaceous Dunvegan Formation; BGGP, v. 46, v. 1, p. 51-73.
- Gingras, M.K., Pemberton, S.G., Saunders, T. and Clifton, H.E. 1999. The ichnology of modern and Pleistocene brackish-water deposits at Willapa Bay, Washington; variability in estuarine settings. *Palaios*, v. 14, no. 4, p. 352–374.
- Gingras, M.K., MacEachern, J.A. and Dashtgard, S.E., 2012, The potential of trace fossils as tidal indicators in bays and estuaries. *Sedimentary Geology*, v. 279, p. 97–106.
- Gross, A.A., 1980, Mannville Channels in east-central Alberta: Lloydminster and Beyond: Geology of Mannville Hydrocarbon, *in*: Beck, L.S., Christopher, J.E., and Kent, D.M., editors, Lloydminster and Beyond: Geology of Mannville Hydrocarbon Reservoirs: Saskatchewan Geological Society, Special Publication 5. p. 33–63.
- Hubbard, S.M, Gingras, M.K., and Pemberton, S.G., 2004, Paleoenvironmental implications of trace fossils in estuary deposits of the Cretaceous Bluesky Formation, Cadotte region, Alberta, Canada: *Fossils and Strata*, v. 51, p. 68–87.
- Howard, J.D., Elders, C.A., and Heinbokel, J.F., 1975, Animal-sediment relationships in estuarine point bar deposits, Ogeechee River-Ossabaw Sound: *Estuaries of the Georgia Coast, U.S.A.: Sedimentology and Biology V, Senckenbergiana Maritima*, v. 7, p. 181-203.
- Kent, D.M., 1959, The Lloydminster oil and gas field, Alberta: University of Saskatchewan, M.Sc. thesis, 92 p.
- MacEachern, J.A., Zaitlin, B.A., and Pemberton, S.G., 1999, A sharp-based sandstone of the Viking Formation, Joffre field, Alberta, Canada: criteria for recognition of transgressively incised shoreface complexes: *Journal of Sedimentary Research*, v. 69, no. 4, p. 876-892.
- MacEachern, J.A., Bann, K.L., Bhattacharya, J.P., and Howell, C.D., 2005, Ichnology of deltas: organism responses to the dynamic interplay of rivers, waves, storms and tides, *in*: Bhattacharya, J.P., and Giosan, L., editors, *River Deltas: Concepts, Models and Examples*, Society of Economic Paleontologists and Mineralogists, Special Publication 83, pp. 49–85.

- Morshedjian, A., MacEachern, J.A., Dashtgard, S.E., Bann, K.L., and Pemberton, S.G., 2019, Systems tracts and their bounding surfaces in the low- accommodation Upper Mannville group, Saskatchewan, Canada: *Marine and Petroleum Geology*, v. 110, p. 35-54.
- Nauss, A.W., 1945, Cretaceous stratigraphy of Vermillion area, Alberta, Canada: *Bulletin of the American Association of Petroleum Geologists*, v. 29, no. 11, p. 1605-1629.
- Newitt, K.J., and Pederson, P.K., 2022, Observational data-based sequence stratigraphy of a clastic wedge within an active foreland basin, Spirit River Formation, west-central Alberta, Canada: *Marine and Petroleum Geology*, v. 140, 105681.
- Orr, R.D., Johnston, J.R., and Manko, E.M., 1977, Lower Cretaceous geology and heavy-oil potential of the Lloydminster area: *Bulletin of Canadian Petroleum Geology*, v. 25, no. 6, p. 1187-1221.
- Pearson, N.J., Mangano, M.G., Buatois, L.A., Casadio, and Raising, M.R., 2012, Ichnology, sedimentology, and sequence stratigraphy of outer-estuarine and coastal-plain deposits: Implications for the distinction between allogenic and autogenic expressions of the *Glossifungites* Ichnofacies: *Palaeogeography, Palaeoclimatology, Palaeoecology*, v. 333, 192-217.
- Pemberton, S.G., and MacEachern, J.A., 1995, The sequence stratigraphic significance of trace fossils: examples from the Cretaceous foreland basin of Alberta, Canada. *in*: Van Wagoner, J.C., and Bertram, G., editors, *Sequence Stratigraphy of Foreland Basin Deposits: Outcrop and Subsurface Examples from the Cretaceous of North America*, American Association of Petroleum Geologists, Memoir 64, p. 429–475.
- Rodriguez, W., Buatois, L.A., Mangano, M.G., and Solórzano, E., 2018, Sedimentology, ichnology, and sequence stratigraphy of the Miocene Oficina Formation, Junín and Boyacá areas, Orinoco Oil Belt, Eastern Venezuela Basin: *Marine and Petroleum Geology*, v. 92, p. 213-233.
- Rodriguez-Tovar, F.J., Perez-Valera, F., and Perez-Lopez, A., 2007, Ichnological analysis in high-resolution sequence stratigraphy: The *Glossifungites* ichnofacies in Triassic successions from the Betic Cordillera (southern Spain): *Sedimentary Geology*, v. 198, p. 293-307.
- Schultz, S.K., MacEachern, J.A., Catuneanu, O., Dashtgard, S.E., and Diaz, N., 2022, High-resolution sequence stratigraphic framework for the late Albian Viking Formation in central Alberta: *Marine and Petroleum Geology*, v. 139, 105627.
- Seilacher, A., 1978, Use of trace fossil assemblages for recognizing depositional environments: *Trace Fossil Concepts*, Society of Economic Paleontologists and Mineralogists, Special Publication 5, p. 185-201.

- Vigrass, L.W., 1977, Trapping of Oil at Intra-Mannville (Lower Cretaceous) Disconformity in Lloydminster Area, Alberta, and Saskatchewan: The American Association of Petroleum Geologists Bulletin, v. 61, no. 7, p. 1010-1028.
- Vossler, S.M., and Pemberton, S.G., 1988, Ichnology of the Cardium Formation (Pembina oilfield): implications for depositional and sequence stratigraphic interpretations, *in*: James, D.P., and Leckie, D.A., editors, Sequences, Stratigraphy, Sedimentology: Surface and Subsurface. Canadian Society of Petroleum Geology, Memoir 15, p. 237–253.
- Wellner, R.W., Varban, B.L., Roca, X, Flaum, J.A., Stewart, E.K., and Blum, M.D., 2018, Simple is better when it comes to sequence stratigraphy: The Clearwater Formation of the Mannville Group reinterpreted using a genetic body approach: American Association of Petroleum Geologists Bulletin, v. 102, no. 3, p. 447-482.
- Wickenden, R.T.D., 1948, The Lower Cretaceous of the Lloydminster oil and gas area, Alberta, and Saskatchewan: Geological Survey of Canada, Paper 48-21, 15 p.
- Wilson, M., 1984, Depositional environments of the Mannville Group (Lower Cretaceous) in the Tangleflags area, Saskatchewan, *in*: Lorsche, J.A., and Wilson, M., editors, Oil and Gas in Saskatchewan: Saskatchewan Geological Society, Special Publication Number 7, p. 119-134.
- Zaitlin, B.A., and Schultz, B.C., 1984, An estuarine-embayment fill model from the Lower Cretaceous Mannville Group, west-central Saskatchewan, *in*: Stott, D.F., and Glass, D.J., editors, The Mesozoic of Middle North America: Canadian Society of Petroleum Geologists, Memoir 9, p. 455-469.

2 High Resolution Facies Analysis of the Lower Mannville Dina and Cummings Interval, East-Central Plains Region, Alberta

2.1 Introduction

Facies analysis of core datasets is an essential component in establishing the genetic affinity of ancient sub-surface depositional systems. Establishing geologically sound interpretations of depositional systems is, in turn, a crucial component in sequence stratigraphic analysis as it is the affinity of these environments that define systems tracts, and stratigraphic sequences. The need for high-resolution facies analyses in complex lithological intervals lacking associated outcrop and/or seismic datasets can not be overstated. Although petrophysical logs are an essential component in characterizing reservoir parameters, and mapping the extent of stratigraphic breaks, they do not provide direct information about the physico-chemical stresses influencing sedimentation and biotic distribution within a given depositional system. For example, prograding/shoaling-upward cycles observed on logs are likely to be characterized by decreasing-upward gamma ray, increasing-upward neutron porosity, and decreasing-upward density log profiles representing the transition from mudstone to interbedded mudstone and sandstone, to sandstone. This profile could represent a prograding strandplain shoreface, wave-dominated delta front, or a sandy tidal dune. In core, each of these examples will be characterized by unique combinations of sedimentological and ichnological characteristics. These unique characteristics record the interplay of physico-chemical parameters present within each environment during deposition, with subtle differences (e.g., preponderance of wave- versus tide-generated structures) likely to go undetected on traditional wireline logs. As reservoir lithofacies distribution will be unique to each environment, interpretations made from facies characteristics in core will result in more informed and predictive models of both porous and non-porous media.

A critical aspect of facies analysis in reconstructing depositional environments in core datasets is the application of process sedimentological and process ichnological methodologies. Both methodologies are concerned with identifying the process-response relationship between preserved sedimentary and biogenic structures and the physical and chemical parameters acting upon the environment during deposition. Examples of common stresses in paralic and marine environments include but are not limited to, rates of deposition, shifting substrate, water turbidity, food resource distribution, salinity, oxygenation, substrate consistency, and temperature. Leveraging an integrated sedimentologic and ichnologic approach to identify physico-chemical parameters in paralic and marine environments has been shown to be a valuable aspect in more refined interpretations of depositional environments (e.g., Seilacher, 1978;

Pemberton et al., 1982; Savarda and Bottjer, 1989; Frey, 1990; MacEachern et al., 1992; Bann and Fielding, 2004; Hubbard et al., 2004; Martin, 2004; McIlroy, 2004; MacEachern et al., 2005; Bhattacharya and MacEachern, 2009; Carmona et al., 2009; Buatois et al., 2008; 2019; Gingras et al., 2012; Botterill et al., 2016; Campbell et al., 2016; Solórzano et al., 2017; MacEachern and Bann, 2020; Shchepetkina et al., 2020; Ahmad and Gingras, 2022). The ichnological response to stresses in continental environments is not as well established (e.g., water table fluctuation, soil moisture, sediment characteristics). However, several studies and summary papers are significantly advancing the ability of workers to utilize trace fossil characteristics to identify and refine sub-environments in the continental realm (e.g., Buatois and Mangano, 1995; Hasiotis, 2002; Hasiotis, 2007; Melchor et al., 2012; Hembree, 2018; Metz, 2020). Despite a history of hydrocarbon production spanning from the 1940s to present, a detailed sedimentological and ichnological analysis is currently lacking. This manuscript focuses on the geology and architecture of strata comprising the Dina and Cummings members in the subsurface of east-central Alberta. Detailed facies analysis and petrophysical log correlations were utilized to identify, interpret, and map distinct stratigraphic units which were, in turn, leveraged to interpret the depositional evolution of this interval. The results of this work advance the geological understanding of the study interval in three main ways. First, facies analysis established the presence of multiple depositional environments encompassing the previously described continental Dina and marine Cummings (e.g., Nauss, 1945; Wickenden, 1948; Kent, 1959). Second, it establishes a revised lithostratigraphic framework that can be consistently applied at the regional scale (discussed in Chapter 3). Finally, this study establishes a high-resolution sequence stratigraphic framework that can be used to assess the distribution of reservoir and non-reservoir facies strata comprising the Dina and Cummings members (discussed in Chapter 4).

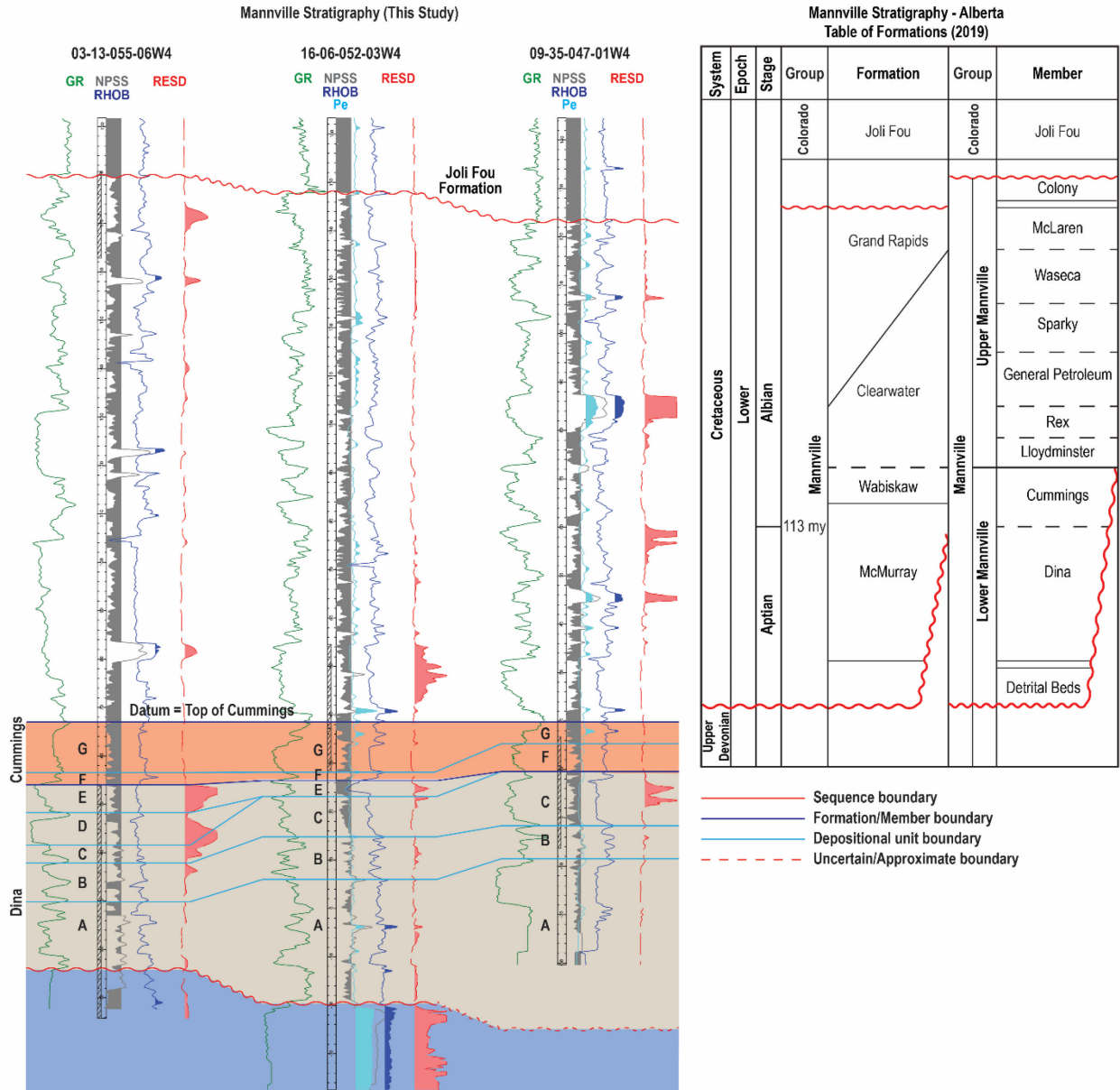
2.2 Regional Geology

The Mannville Group in east-central Alberta consists of continental, marginal marine and marine strata that comprise a third-order, unconformity-bound sequence (Cant, 1996; Cant and Abrahamson, 1996) (Fig. 2.1). Here, the Mannville Group unconformably overlies Paleozoic and minor Jurassic strata (referred to as the Sub-Cretaceous Unconformity), a surface with significant topographic relief resulting from deep incision due to isostatic rebound (Cant and Abrahamson, 1996) and fault reactivation (Wadsworth et al., 2002). The Dina and Cummings members record the progressive southward migration of the Boreal Sea. In general, this transgression is expressed as continental to marginal marine strata at the base becoming progressively overlain by paralic and marine strata. This interval comprises the transgressive systems tract of the third-order Mannville sequence of Cant (1996) and Cant and

Abrahamson (1996), with the maximum flooding surface (MFS) occurring at the top of the Cummings Member (Fig. 2.1).

2.3 Study Area, Dataset, and Methods

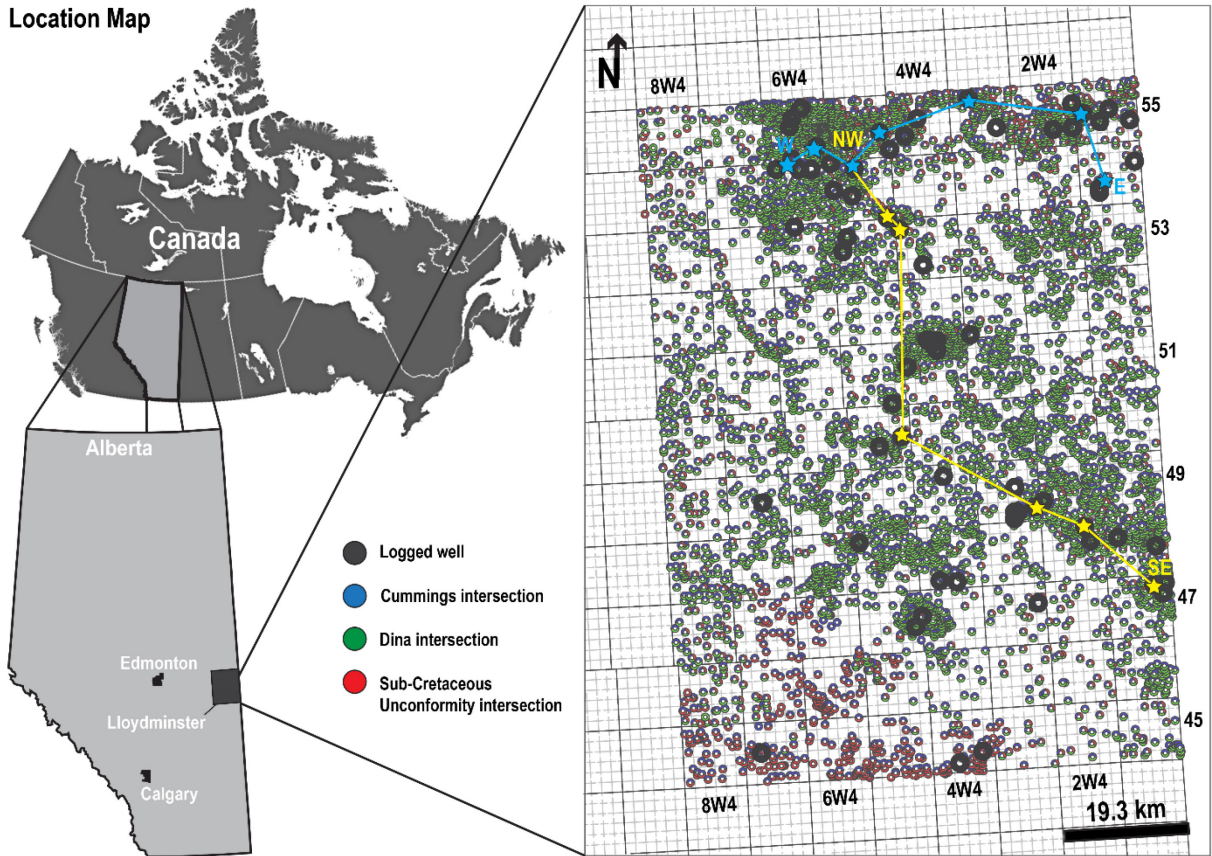
The study interval is in the east-central plains region of Alberta, between Townships 45-55, Ranges 1-8W4 Meridian (total area of 8,800 km²) (Fig. 2.2). The dataset consists of seventy-two cored, and approximately 7800 petrophysical logs wherein digital log curves were available. Core were logged at the facies scale with emphasis on documenting lithology, sedimentary structures, bioturbation index, ichnogenic, trace-fossil distribution, relative trace-fossil size, lithological accessories, and the nature of contacts. Figure 2.3 provides a legend for sedimentary structures, trace fossils, lithological accessories, and contacts for logs presented in various figures. Also provided in Figure 2.3 are abbreviations codes for facies and paleosol modifiers. The naming scheme for facies expands on the fluvial facies scheme of Miall (2006) to encompass structures not commonly observed in fluvial environments. Paleosol modifiers are based on the paleosol identification scheme of Mack et al., (1993). Bioturbation index was assigned a value of 0-6 (Reineck, 1967; Taylor and Goldring, 1993) with a BI 0 value representing an absence of bioturbation and a value of BI 6 representing complete homogenization of sediment. Assigning an ichnological diversity and general size for trace fossils for a specific unit can be done in relation to other units within the same study. The highest diversity assemblages and most robust trace fossil sizes occur in facies association complex G, which serves as the comparative standard for all other units. This is because FAC-G is the closest expression to the archetypal Seilacherian *Skolithos* and *Cruziana* ichnofacies occurring within the Dina and Cummings interval. These archetypal expressions represent ethological groupings of trace fossils developed predominantly under ambient conditions in fully marine environments. The ternary framework of Ainsworth et al., (2011) was used to identify the primary, secondary, and tertiary influence of wave, tide, and fluvial processes. Discontinuity surfaces observed in core were transferred to the corresponding wireline log in Petra[®]. These reference logs underpin the stratigraphic framework of the project area. The confidence in correlation is highest near cored wells and decreases with increasing distance from these reference wells.



2-1) Cross-Section and stratigraphic chart of the Dina and Cummings

Well log cross-section and stratigraphic chart illustrating the stratigraphic position of the Dina and Cummings within the Lower Cretaceous Mannville Group. Also shown is the stratigraphic position of facies association complexes A-G. Stratigraphic chart modified from the Alberta Geological Survey Table of Formation, 2019.

Location Map



2-2) Location Map

Location map illustrating the distribution of wireline logs, core dataset (black circles), and existence within each well of the sub-Cretaceous unconformity (red circles), top of Dina Member/Depositional Unit C (green circles), and top of Cummings Member/Facies Association Complex G (blue circles). Also shown are the locations of cross-sections illustrated in Figure 2.11.

Legend

Core Logs

Sedimentary Structures

| | | | |
|---|-------------------------------------|--|---------------------------|
| M | Massive | | Sedimentary scour |
| | Low-angle cross-lamination | | Convolute bedding |
| | High-angle cross-lamination | | Dish structures |
| | Hummocky cross-lamination | | Synsedimentary fault |
| | Herringbone cross-lamination | | Mottled |
| | Planar cross-stratification | | Flame structure |
| | Trough cross-stratification | | Injection feature |
| | Bioturbated | | Gutter cast |
| | Crypto-bioturbation | | Fracture |
| | Vague low-angle cross-lamination | | Soft sediment deformation |
| | Oscillation ripple cross-lamination | | Slickensides |
| | Isolated wave ripples | | Loaded ripples |
| | Combined flow ripple cross-lam | | Undiff cross-bedding |
| | Current ripple cross-lamination | | Lenticular bedding |
| | Climbing ripple cross-lamination | | Flaser bedding |
| | Starved wave ripples | | Dewatering structure |
| | Wavy bedded | | Lenses |
| | Normally graded beds | | Contorted |
| | Reverse graded beds | | Boudinage |
| | Load structures | | Bioturbated mud laminae |
| | Synaeresis cracks | | Bioturbated mud beds |
| | Double mud drape | | Wavy mud beds |
| | Mud crack | | Pinstrip bedding |
| | Reactivation surface | | |

Ichnofossils

| | | | |
|--|---------------------|--|----------------|
| | Skolithos | | Cylindrichnus |
| | Diplocraterion | | Berguaria |
| | Asterosoma | | Rhizocorallium |
| | Chondrites | | Arenicolites |
| | Zoophycos | | Gyrolithes |
| | Palaeophycus | | Taenidium isp. |
| | fugichnia | | Scolicia |
| | Thalassinoides | | Macaronichnus |
| | Planolites | | Nereites |
| | Ophiomorpha | | Cosmoraphe |
| | Rosselia | | Conichnus |
| | Schaubcylindrichnus | | Navichnia |
| | Helminthopsis | | Undiff Burrow |
| | Phycosiphon | | Lockeia |
| | Teichichnus | | Shell Debris |

Surfaces

| | |
|--|----------------------------|
| | Formation Contact |
| | Member Unit Contact |
| | Depositional Unit Contact |
| | Facies Association Contact |
| | Unconformity |

Accessories

| | | | |
|--|---------------------|--|-------------------|
| | Coal laminae | | Granule/pebble |
| | Coal fragment | | Siderite layer |
| | Mudstone interclast | | Shale laminae |
| | Pyrite | | Sand laminae |
| | Glauconite | | Silt laminae |
| | Wood fragments | | Plant debris |
| | Carbonaceous debris | | Kaolinite |
| | Carbonaceous drapes | | Mud-filled crack |
| | Siderite nodules | | Sand-filled crack |
| | Rootlets | | |

Bioturbation Index



Lithology

| | |
|--|--------------|
| | Missing core |
| | Coal |

Facies Abbreviation Codes

Lithology

| | |
|---|----------------|
| G | = Gravel |
| S | = Sand |
| H | = Heterolithic |
| F | = Fines |
| P | = Paleosol |
| C | = Coal |

Lithology Modifiers

| | |
|-----|---|
| t | = trough cross-bedding |
| l | = low-angle cross-lamination |
| h | = horizontal bedding |
| c | = curvilinear cross-lamination |
| p | = planar cross-beds |
| o | = oscillation ripple cross-lamination |
| cr | = current ripple cross-lamination |
| cfr | = combined flow ripple cross-lamination |
| m | = massive |
| s | = scours |
| mb | = mud clast breccia |
| f | = flaser bedding |
| ln | = lenticular bedding |
| sm | = sand - silt/mud |
| ms | = silt/mud - sand |
| r | = massive, roots, biot. |
| mm | = matrix supported, weak grading |
| mg | = matrix supported, graded |
| ci | = clast supported, inverse grading |
| cm | = clast supported, massive |

Paleosol Modifiers

| | |
|---|--------------|
| h | = Histosol |
| p | = Protosol |
| v | = Vertisol |
| g | = Gleysol |
| c | = Calcisol |
| g | = Gypsisol |
| a | = Argillisol |
| s | = Spodosol |
| o | = Oxisol |

2-3) Symbol Legend

Legend of symbols, abbreviation codes, and surfaces present in core logs and Table 2.1.

2.4 Results and Interpretations

2.4.1 Facies Association Complexes

Seven distinct facies association complexes were identified in core. In ascending stratigraphic order these are termed FAC-A to FAC-G (Fig. 2.1, Table 2.1). Facies association complexes are comprised of facies associations of which twenty-one were identified (Table 2.1). Facies associations consist of an extensive number of individual sedimentary facies characterized by different combinations of physical sedimentary structures, lithological composition, trace fossil characteristics, and mineralogy.

2.4.1.1 Facies Association Complex A

FAC-A is composed of five facies associations (Fig. 2.4, position 1 and 2, Fig. 2.5, Fig. 2.6; Table 2.1). These five facies associations can be placed geographically within three zones defined by the tidal and brackish-water limits (Fig. 2.4). These zones are continental fluvial (Zone 1), fluvio-tidal transition (Zone 2), and lower delta plain (Zone 3). Facies associations comprising FAC-A are generally of limited aerial extent on wireline logs and are lithologically complex. These zonation's are hypothetical geographical locations, as the dataset and scope of the study are beyond the resolution of establishing the chronostratigraphic relationship between various depositional environments along this continuum.

Zone 1: Continental Strata

Description:

A-FA1: consists of sharp-based, metre-scale fining-upward cycles of fine- to medium-grained sandstone, interbedded fine-grained sandstone, and mudstone, and silty to organic mudstone (Fig. 2.5, Fig. 2.6 a-f; Table 2.1). Sedimentary structures transition upward from high-energy trough and planar-tabular cross-bedding to lower energy low-angle, and ripple cross-lamination. Mudstone beds are massive to laminated with predominantly sharp bases and tops and may contain ripple cross-laminated siltstone laminae (Fig. 2.6b). Organic detritus such as disseminated grains and organic laminae, coal fragments, and wood clasts are common to abundant in A-FA1 strata (Fig. 2.6b). Bioturbation is absent to sporadic in sandstone facies, with BI of 0-1. Bioturbation in mudstone beds is absent to high (BI 0-5). Ichnogenera observed in A-FA1 include *Taenidium boweni*, *Planolites*, and *Taenidium isp.*

A-FA2: consists of fine-grained aggradational to weakly coarsening-upward sequences of silty mudstone, siltstone, muddy sandstone, and organic-rich mudstone (Fig. 2.6 d-f). Pedogenic overprinting is common and includes horizonation, color mottling, pedogenic slickensides, rhizoturbation, ped development, and nodules and concretions (Fig. 2.6 d, e). Common lithological accessories include pyrite, coal, siderite nodules, plant debris, iron staining, and silty sandstone interbeds and laminae. A-FA2 is characterized by sporadic to homogeneous distribution of bioturbation, with BI of (0-5). Ichnogenera

observed in A-FA2 include *Taenidium bowni*, *Palaeophycus*, *Planolites*, and *Taenidium isp.* Other biogenic sedimentary structures include rootlets and rhizoliths (Fig. 2.6 d-f).

Interpretation:

A-FA1 and A-FA2 are interpreted to record deposition in fluvial channel, point-bar, and bar-top (A-FA1), and floodplain (A-FA2) settings, respectively. The fining-upward architecture of A-FA1, in concert with the transition upward from high-energy to progressively lower-energy physical sedimentary structures is consistent with fluvial channel facies models (e.g., Allen, 1964; Allen, 1970; Walker and Cant, 1982). Intervals of inter-bedded sandstone and mudstone are interpreted as IHS (*sensu* Thomas et al., 1987) which record the lateral and down-stream migration of point-bars. The interpretation of A-FA2 as floodplain strata is based upon the overall fine grain size, abundant rooting and bioturbation, and the presence of horizonation, color mottling, pedogenic slickensides, rhizoturbation, ped development, and nodules and concretions, each of which evidence paleosol development (e.g., Retallack, 1988; Wright 1992; Kraus, 1999; Tabor et al., 2017). Ichnological evidence for continental conditions includes a lack of trace fossils indicative of brackish-water sedimentation, which include *Cylindrichnus*, *Gyrolithes*, *Psilonichnus*, and *Teichichnus* (e.g., Pemberton et al., 1982; Beynon et al., 1988; Gingras et al., 1999; Gingras et al., 2012; Gingras et al., 2016). In concert with a lack of observable tidal structures (double mudstone drapes, rhythmites) these ichnological characteristics suggest deposition of channel and floodplain elements occurred landward of both tidal modulation and brackish-water incursion (Position 1, Fig. 2.4).

Zone 2: Fluvio-Tidal Transition Strata

Description

A-FA3 consists of fining-upward cycles of fine- to medium-grained sandstone, interbedded fine-grained sandstone and mudstone, and mudstone similar in scale, sedimentological characteristics, and ichnology to fluvial channel facies of A-FA1 (Fig. 2.6 g-i). Distinguishing characteristics include an overall higher proportion of mudstone (based on limited observations), the presence of double mudstone drapes, and apparent tidal rhythmites. Sandstone facies are sparsely burrowed, with BI of (0-2). Mudstone beds are more variable, with BI's of (0-6). Ichnological diversity is relatively low, with ichnogenera including *Arenicolites*, *Taenidium bowni*, *Palaeophycus*, *Planolites*, and *Taenidium isp* (Fig. 2.6 h, i). Other biogenic structures include rootlets and rhizoliths.

Interpretation

A-FA3 is interpreted to represent deposition of channel, point-bar, and bar-top facies within the fluvio-tidal transition zone. The presence of double mudstone drapes and apparent rhythmicity is taken as evidence of modulation by tidal currents (e.g., Neo and Yang, 1991; Dalrymple, 2010; Longhitano, 2012).

It is important to note here, and in all other facies associations where rhythmicity is observed that this observation is of apparent rhythmicity. Fine-scale lamination is not solely the product of tidal currents (Longhitano et al., 2012). The use of analytical methods such as those applied by Kvale (1999; 2012) and Timmer et al., (2016) would be necessary to determine if the rhythmicity observed preserves a true tidal periodicity.

Table 2-1

Facies, facies associations, and facies association complexes comprising the Dina and Cummings lithostratigraphic intervals.

| FAC | FA | Facies | Sedimentary Structures | Ichnogenera | | | Accessories | Ter. Frm | Interpretation |
|-------|-------|---|--|---------------------|-----------------|--|---|----------|--|
| | | | | BI (rng) | BI (ave) | Ichnogenera | | | |
| FAC-A | A-FA1 | St, Sp, Sl, Sh, Sm, So, Scr, Fln, Fr | trough & planar tabular cross-bedding, low-angle & planar cross-lamination, current ripples, grain striping, massive fabric, soft-sediment deformation | S=0-1; F=0-6 | S=0; F=2 | <i>Planolites, Palaeophycus, Skolithos, Taenidium, rootlets, rhizoliths</i> | carbonaceous detritus, wood debris, pyrite, mud clasts | F | continental fluvial channel, point-bar |
| | A-FA2 | Sr, Sm, So, Hsm, Hms, Fm, Fh, Pp, Pg | current ripples, low-angle planar lamination, mottled, massive, convolute lamination, soft-sediment deformation, lenticular bedding, normally-graded beds, pedogenic slickensides | F=1-3; S=1-3 | F=1; S=2 | <i>Taenidium bowni, Taenidium, Skolithos, Planolites, rootlets, rhizoliths</i> | pyrite, coal fragments, siderite nodules, plant debris, iron staining, sand laminae, silt laminae | F | floodplain - proximal to distal |
| | A-FA3 | St, Sp, Sl, Scr, Sm, Scfr, Hcr, Mb, Pp | trough & planar tabular cross-bedding, low-angle planar, current & combined flow ripple cross lamination, massive, wavy-bedded, mottled, lenticular bedding, convolute lamination, double mudstone drapes, rhythmic lamination | S=0-1; F=2-5 | S=0; F=3 | <i>Arenicolites, Planolites, Palaeophycus, Skolithos, Taenidium, rootlets</i> | pyrite (nodular and disseminated), carbonaceous detritus, coal fragments, mud clasts | Ft | fluvially dominated, tide-influenced channel, point-bar, and bar-top |
| | A-FA4 | Sl, Sr, Sm, Sb, So, Pp | low-angle planar & current ripple cross-lamination, faint cross-lamination, massive, mottled, double mudstone drapes | S=0-3 | S=1 | <i>?Conichnus, fugichnia, Lockeia, Planolites, rootlets, Skolithos, Taenidium isp, Rhizoliths</i> | organic detritus, rare mud drapes, pyrite | Ft | distributary channel |
| | A-FA5 | Scr, Sl, Sb, Sm, So, Hsm, Hms, Hb, Fb, Pp | wavy bedded, bioturbated, lenticular, current ripple & low-angle cross-laminated, convolute lamination, mottled. | S=1-5; F=0-4 | S=3; F=2 | <i>Cylindrichnus, Gyrolithes, rootlets, Planolites, Skolithos, Taenidium, Teichichnus</i> | organic detritus, pyrite, granules, iron stain, coal laminae, clasts with altered rims | Ft | Interdistributary bay fill/crevasse splay |
| FAC-B | B-FA1 | Sl, Scr, Scfr, Sh, Hms, Hsm, Hb, Fln, Fm | wavy bedding, lenticular bedding, flaser bedding, convolute lamination, low-angle planar, current & combined flow ripple cross-lamination, normally graded beds, synaeresis cracks, load casts | Fsm=0-3; Fms=0-2 | Fsm=3; Fms=1 | <i>Arenicolites, Cylindrichnus, fugichnia, Lockeia, Palaeophycus, Planolites, rootlets, Skolithos, Taenidium, Teichichnus, Thalassinoides</i> | mud clasts, organic detritus, pyrite | Tfw | tide-influenced, wave-affected tidal delta |
| | B-FA2 | Sl, Scr, Sor, Sb, Sm, Hsm, Hms, Hb, Fln, Fm, Fb, Fr, Fo | low-angle planar, current, and oscillation ripple cross-lamination, hummocky cross-stratification, wavy bedding, mottled, lenticular bedding, massive, faint low-angle cross-lamination | F=2-5; S=0-3 | F=3; S=1 | <i>Arenicolites, Cylindrichnus, Diplocraterion, fugichnia, Gyrolithes, Paleophycus, Planolites, Siphonichnus, Taenidium, Teichichnus, Thalassinoides</i> | pyrite, organic detritus, coal fragments, silt laminae, siderite cement | Wtf | wave- and tide-influenced bay-margin |
| | B-FA3 | Sor, Sb, Hsm, Hms, Hb, Fln, Fm, Fb, Fr, Fo | oscillation ripple cross-lamination, wavy bedding, mottled, lenticular bedding, massive, faint low-angle cross-lamination | F=2-5; S=2-5 | F=3; S=3 | <i>Arenicolites, Cylindrichnus, Diplocraterion, fugichnia, Gyrolithes, Paleophycus, Planolites, Siphonichnus, Taenidium, Teichichnus, Thalassinoides</i> | pyrite, organic detritus, coal fragments, silt laminae, siderite cement | Wtf | wave-influenced bay-margin |
| | B-FA4 | St, Sp, Sl, Sm, Scr, Scfr, Sb, Hsm, Fm, Fb, Fln | trough & planar tabular cross-bedding, massive, low-angle, planar, current ripple, & combined flow ripple cross-lamination, grain-striping, double mudstone drapes, rhythmic lamination | S=0-2; F=0-5 | S=0; F=2 | <i>Arenicolites, Cylindrichnus, Gyrolithes, Planolites, Psilonichnus, rootlets, Skolithos, Taenidium</i> | mud clasts, organic detritus | Tf | tide- and fluvially influenced channel, point-bar, and tidal flat |

| | | | | | | | | | |
|-------|-------|--|--|-----------------|-------------|--|---|-----|---|
| FAC-C | C-FA1 | St, Sl, Sc, Scfr, Sf, So, Sor, Hng, Hb-ld, Fl, C, Pp | trough cross bedding, low-angle planar & hummocky cross-stratification, convolute lamination, combined flow-ripple cross-lamination, synaeresis cracks, normally graded beds, micro-faults, fluid escape structures. | S=0-2; F=0-3 | S=0; F=1 | <i>Cylindrichnus, fugichnia, Palaeophycus, Planolites, rootlets, Skolithos, Taenidium, Teichichnus</i> | coal fragments, pyrite, organic detritus, carbonaceous drapes | Fwt | river-dominated, wave-influenced delta |
| | C-FA2 | St, Sl, Sc, Scfr, Sf, So, Sor, Hng, Hb-ld, Fl, C, Pp | hummocky cross-stratification, trough cross bedding, low-angle planar & convolute lamination, combined flow-ripple cross-lamination, synaeresis cracks, normally graded beds, micro-faults, fluid escape structures. | S=0-2; F=0-3 | S=0; F=1 | <i>Cylindrichnus, fugichnia, Palaeophycus, Planolites, rootlets, Skolithos, Taenidium, Teichichnus</i> | coal fragments, pyrite, organic detritus, carbonaceous drapes | Wft | wave-dominated delta |
| | C-FA3 | Sl, Shc, Sor, Sf, Sb, Hb, Hng, Fb, C, Pp | low-angle planar & vague cross-lamination, combined flow ripples, flaser bedding, oscillation & combined flow ripple cross-lamination, convolute lamination, synaeresis cracks, normally graded beds | S=1-5; F=1-4 | S=3; F=2 | <i>Arenicolites, Asterosoma, Berguaeria, Cylindrichnus, fugichnia, Gyrolithes, Helminthopsis, Ophiomorpha, Palaeophycus, Planolites, rhizoliths, rootlets, Skolithos, Taenidium, Teichichnus, Thalassinoides</i> | organic detritus, coal fragments, wood debris, pyrite, carbonaceous drapes | Wtf | bay-margin shoreface to offshore |
| FAC-D | D-FA1 | St, Sl, Sm, Scfr, Hng, Hcr, Hor, Fln, Fm, Fg | trough cross-bedding, low-angle planar cross-lamination, massive fabric, combined flow ripples, dish and pillar, flame structure, fluid escape structures, double mud drapes, convolute lamination, synaeresis cracks, load casts, pinstripe lamination, micro-folds | S=0-2; F=0-2 | S=1; F=1 | <i>Berguaeria, fugichnia, navichnia, Rhizocorallium, Planolites, Skolithos, Teichichnus, Thalassinoides</i> | coal fragments, carbonaceous debris, plant debris, pyrite, siderite cement, siltstone laminae | Twf | tide-, wave-, and river-influenced distributary channel |
| | D-FA2 | St, Sl, Sm, Scfr, Hng, Hcr, Hor, Fln, Fm, Fg | trough cross-bedding, low-angle planar cross-lamination, hummocky cross-stratification, massive fabric, combined flow ripples, double mud drapes, convolute lamination, synaeresis cracks, load casts, pinstripe lamination | S=0-2; F=0-5 | S=1; F=3 | <i>Berguaeria, fugichnia, navichnia, Rhizocorallium, Planolites, Skolithos, Teichichnus, Thalassinoides</i> | coal fragments carbonaceous debris, plant debris, pyrite, siderite cement, siltstone laminae | Twf | tide-, wave-, and river-influenced delta front |
| | D-FA3 | St, Sl, Sm, Scfr, Sm, Fl, Fm, Fo | trough cross-bedding, low-angle planar cross-lamination, massive fabric, combined flow ripple cross-lamination, lenticular bedding | S=0-1; F=0-1 | S=0; F=0 | <i>Planolites</i> | abundant coal fragments, pyrite, wood debris | T | mouth bar |
| FAC-E | E-FA1 | St, Sl, Shc, Scfr, Sf, Ss, Sb, Hb, Fln, Fm, Fb, C | trough cross-bedding, low-angle planar, & hummocky cross-stratification, climbing ripples, flame structures, convolute lamination, flaser bedding, flaser bedding, load casts, double mud drapes, scour surfaces | S=0-3; F=1-3 | S=1; F=1 | <i>Berguaeria, Chondrites, Cylindrichnus, Diplocraterion, fugichnia, Lockeia, Macaronichnus, navichnia, Ophiomorpha, Palaeophycus, Phycosiphon, Planolites, Rhizocorallium, Rosselia, Skolithos, Teichichnus, Thalassinoides</i> | organic detritus, coal fragments, wood fragments, pyrite, siderite cement | Wft | storm-influenced marine delta |
| | E-FA2 | Sr, Sm, So, Hsm, Hms, Fm, Fh, Pp, Pg | current ripples, mottled, massive, convolute lamination, soft-sediment deformation, lenticular bedding, pedogenic slickensides | F=1-3; S=1-3 | F=1; S=2 | <i>Taenidium bowni, Taenidium, Skolithos, Planolites, rootlets, rhizoliths</i> | pyrite, coal fragments, plant debris, sand laminae, silt laminae | F | delta plain |
| FAC-F | F-FA1 | St, Sl, Sh, Scfr, Scr, Sor, Hsm, Hms, Hb | low-angle, planar, & hummocky cross-stratification, oscillation, & combined flow ripples, soft sediment deformation, fluid escape structures, synaeresis cracks, normally graded beds, convolute lamination, load casts, fluid muds, double mud drapes | S=0-2; F=1-3 | S=1; F=2 | <i>Arenicolites, Asterosoma, Berguaeria, Cylindrichnus, Diplocraterion, fugichnia, Gyrolithes, Helminthopsis, Ophiomorpha, Palaeophycus, Phycosiphon, Planolites, Rhizocorallium, Rosselia, Skolithos, Teichichnus, Thalassinoides</i> | pyrite, organic detritus | Tw | river- and wave-influence delta |

| | | | | | | | | | |
|-------|-------|---|--|-----------------|-------------|---|---|-----|---------------------------------|
| | F-FA2 | Sl, Src, Sor, Scfr, Hsm, Hms, Hb, Fm, Fln | low-angle planar & hummocky cross-stratification, current, combined flow, & oscillation ripple cross-lamination, fluid mud, convolute lamination, load casts, micro-faults, flame structure, double mud drapes, fluid escape structures, | S=0-4; F=0-3 | S=1; F=2 | <i>Arenicolites, Asterosoma, Berguaeria, Chondrites, Cylindrichnus, Cosmorhappe, Diplocraterion, Helminthopsis, Palaeophycus, Phycosiphon, Planolites, Rhizocorallium, Skolithos, Teichichnus, Thalassinoides, Zoophycos</i> | glauconite, organic detritus, pyrite, coal fragments, calcite cement | Wtf | tide- and wave-influenced delta |
| | F-FA3 | Sl, Shc, Scfr, Sm, Sor, Sb, Hb, Hsm, Hms | low-angle planar & hummocky cross-stratification, combined flow & oscillation ripple cross-lamination, normally graded beds, double mud drapes | S=0-3; F=0-3 | S=1; F=2 | <i>Arenicolites, Asterosoma, Chondrites, Cylindrichnus, Helminthopsis, navichnia, Palaeophycus, Phycosiphon, Planolites, Rhizocorallium, Scolicia, Skolithos, Teichichnus, Thalassinoides, Zoophycos</i> | glauconite, carbonaceous debris, pyrite, siderite, shell debris, granules | Wtf | transgressive lag |
| FAC-G | G-FA1 | Sl, Sc, Sh, Sor, Scfr, Sb, Hsm, Hms, Hb, Fb | low-angle planar & hummocky cross-stratification, combined flow & oscillation ripple cross-lamination | S=0-5; F=1-5 | S=2; F=3 | <i>Arenicolites, Asterosoma, Berguaeria, Chondrites, Cosmorhappe, Cylindrichnus, Diplocraterion, Helminthopsis, Nereites, Ophiomorpha, Palaeophycus, Phoebichnus, Phycosiphon, Planolites, Rhizocorallium, Rosselia, Schaubcylindrichnus freyi, Scolicia, Skolithos, Teichichnus, Thalassinoides, Zoophycos</i> | glauconite, carbonaceous debris, pyrite | W | marine lower shoreface to shelf |

The ichnological assemblage preserved in A-FA3 is consistent with characteristics of the *Scoyenia* Ichnofacies (e.g., Ekdale, et al., 1984; Frey et al., 1984; Buatois and Mangano, 1995; Melchor et al., 2012). Such criteria include a predominance of meniscate burrows, arthropod trackways and bilobed burrows/trails, and low diversity (Melchor et al., 2012). The combined sedimentological and ichnological observations are consistent with deposition in the fluvio-tidal transition zone (FTZ) as defined by Shchepetkina et al., (2019). This places A-FA3 at Position 2 of Figure 2.4, basinward of the tidal limit, but landward of brackish-water incursion.

Zone 3: Fresh to Brackish-Water Transition Strata

Description

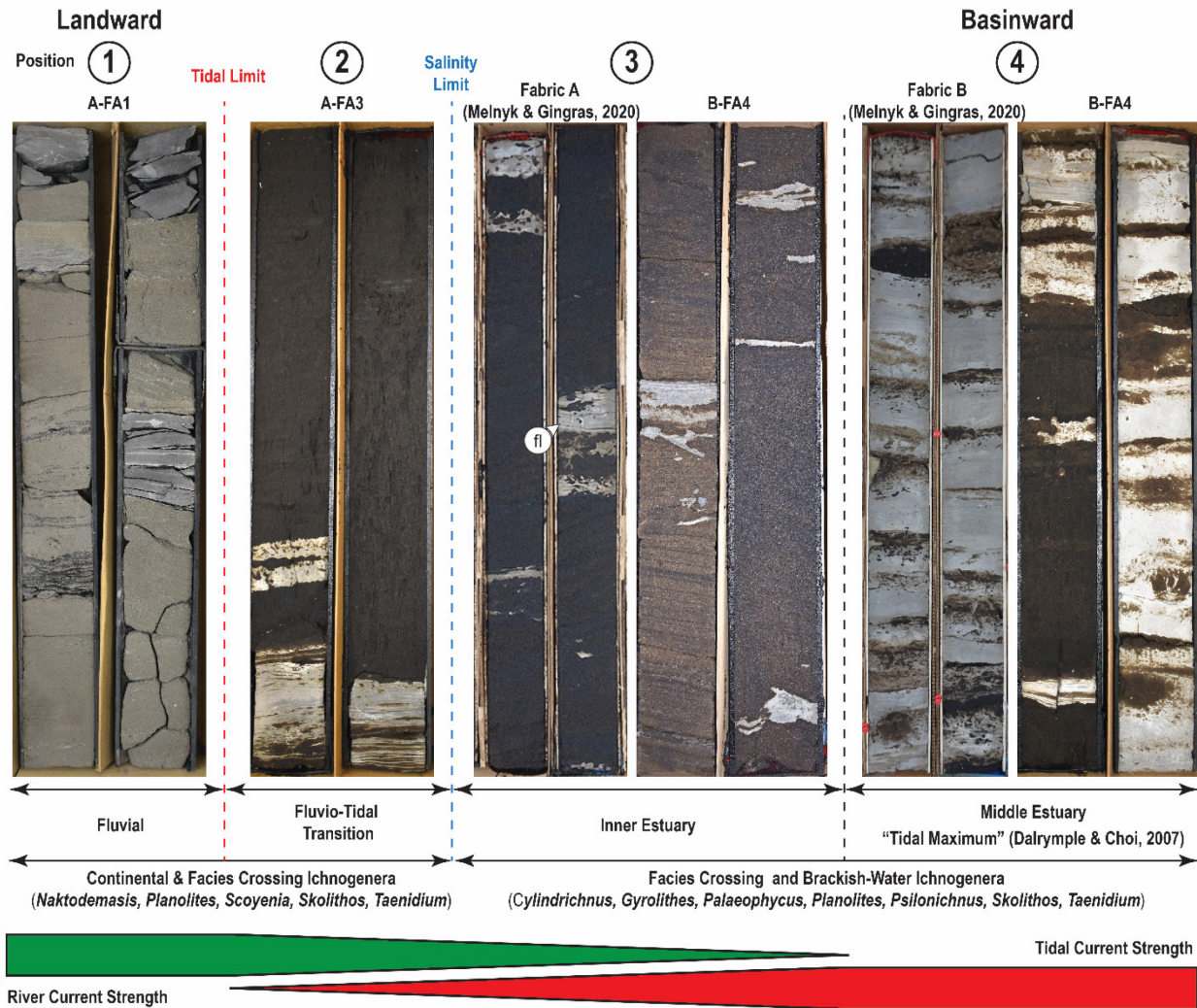
A-FA4 consists of a thin (<2 m) weakly fining-upward cycles of fine-grained to very fine-grained sandstone (Fig. 2.6 j-l). The basal 50 cm are characterized by low-angle planar cross-lamination, ripple cross-lamination, massive fabric, and rare double mudstone drapes. There is a progressive upward decrease in the preservation of primary sedimentary structures that is accompanied by an increase in organic detritus and color alteration. This upper portion fits the criteria of a protosol (*sensu* Mack et al., 1993). Bioturbation in distributary channels is absent to locally homogeneous, with BI of (0-5), and a low-diversity trace fossil assemblage consisting of *Conichnus, fugichnia, Lockeia, Planolites,*

Skolithos, and *Taenidium isp* (Fig. 2.6j). Other biogenic structures include rootlets and rhizoliths (Fig. 2.6 k, l).

A-FA5 consist of stacked, thin, coarsening-upward sequences of sandy mudstone, muddy sandstone, and sandstone (Fig. 2.6 m-o; Fig. 2.7, well 03-13). Bioturbate and pedogenic fabric have largely disrupted the original depositional fabric. Wavy and lenticular bedding are locally preserved, as are low-angle cross-lamination and ripple cross-lamination (Fig. 2.6 m, n, o). Organic detritus, pyrite, granules, coal laminae and clasts, and clasts with altered rims were also observed. A-FA5 facies are characterize by absent to high bioturbation indices (0-5). The trace-fossil suite is highly impoverished, with a low-diversity suite consisting of *Cylindrichnus*, *Gyrolithes*, and *Teichichnus* (Fig. 2.6 m). Overprinting of brackish-water trace fossil suites by continental forms (i.e., *Taenidium boweni*) is common (Fig. 2.6 m, n).

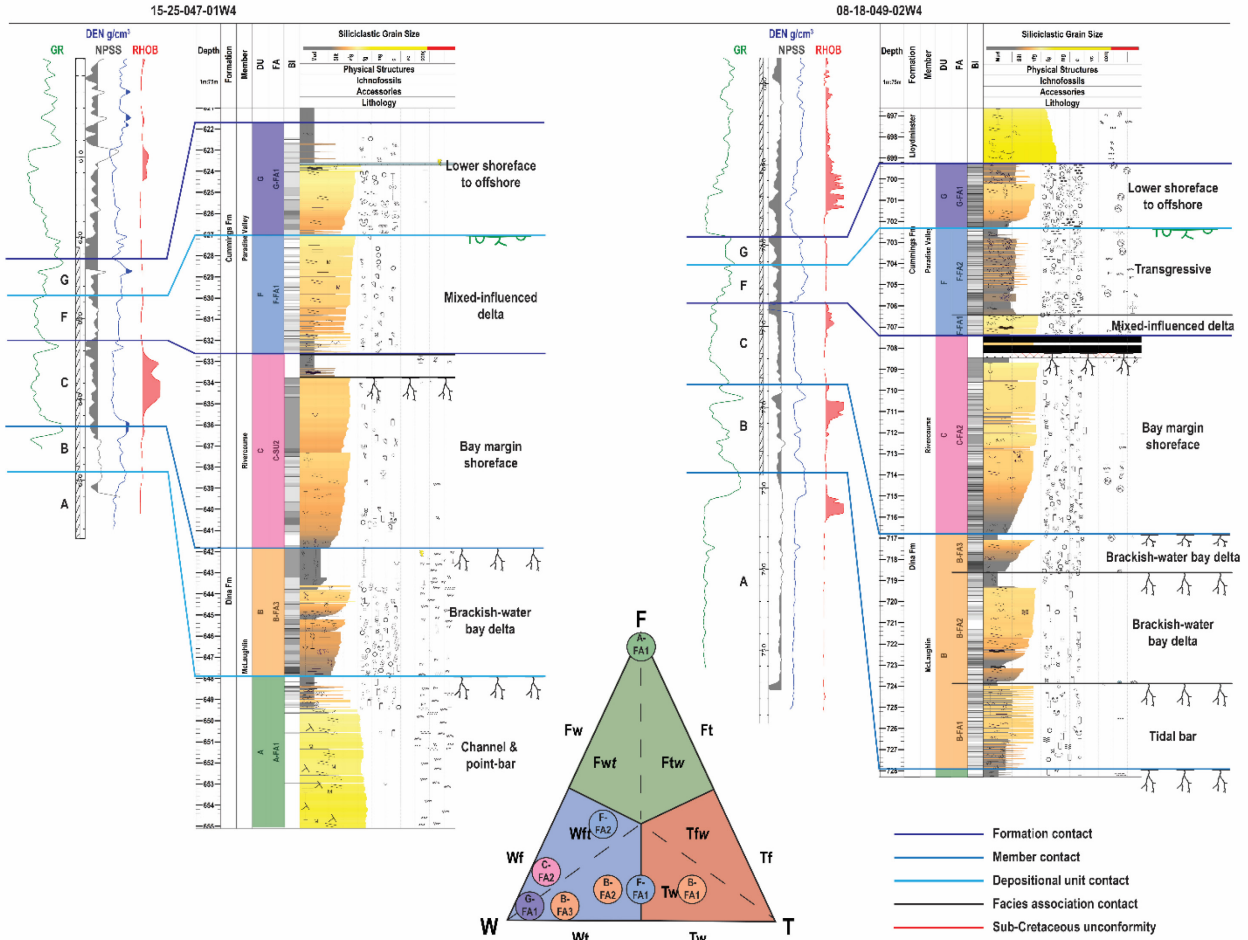
Interpretation

A-FA4 and A-FA5 are interpreted as preserving deposition in small distributary channel (A-FA4) and crevasse splay or minor deltas (A-FA5) in a lower delta plain environment. This interpretation is based on the following observations. Individual cycles are thin (<2-3 m) indicating deposition into shallow waterbodies of relatively low-energy which allows for high rates of bioturbation. The presence of brackish-water trace fossils (i.e., *Cylindrichnus*, *Gyrolithes*, *Teichichnus*) indicate at least periodic incursion of the salt-water wedge. The overprinting of brackish-water by continental assemblages and pedogenic alteration requires alternating sub-aerial conditions of sufficient time for incipient pedogenesis to commence. Paleosol development is influenced by several factors including climate, parent material, topographic location, and sedimentation rates (e.g., Bown and Kraus, 1987; Wright, 1992; Kraus, 1999; Hasiotis 2007), making the time of formation difficult to confidently assess. However, the stacked nature, preservation of non-pedogenically altered sediment occurring between paleosol horizons, and their weakly-developed nature are consistent with deposition in an aggradational system with little erosion and steady sediment accumulation (Kraus, 1999; Catuneanu, 2006). A depositional system that accounts for these observations is the lower delta plain environment described by Reading and Collinson (1996) and Bhattacharya (2010) of which distributary channels, crevasse splays, and minor interdistributary bay deltas are a common component. A-FA4 and A-FA5 are similar in description to minor mouth bars formed by crevasse splays of distributary channels in the lower delta plain of the Lower Westphalian A in north-west England by Fielding (1987).



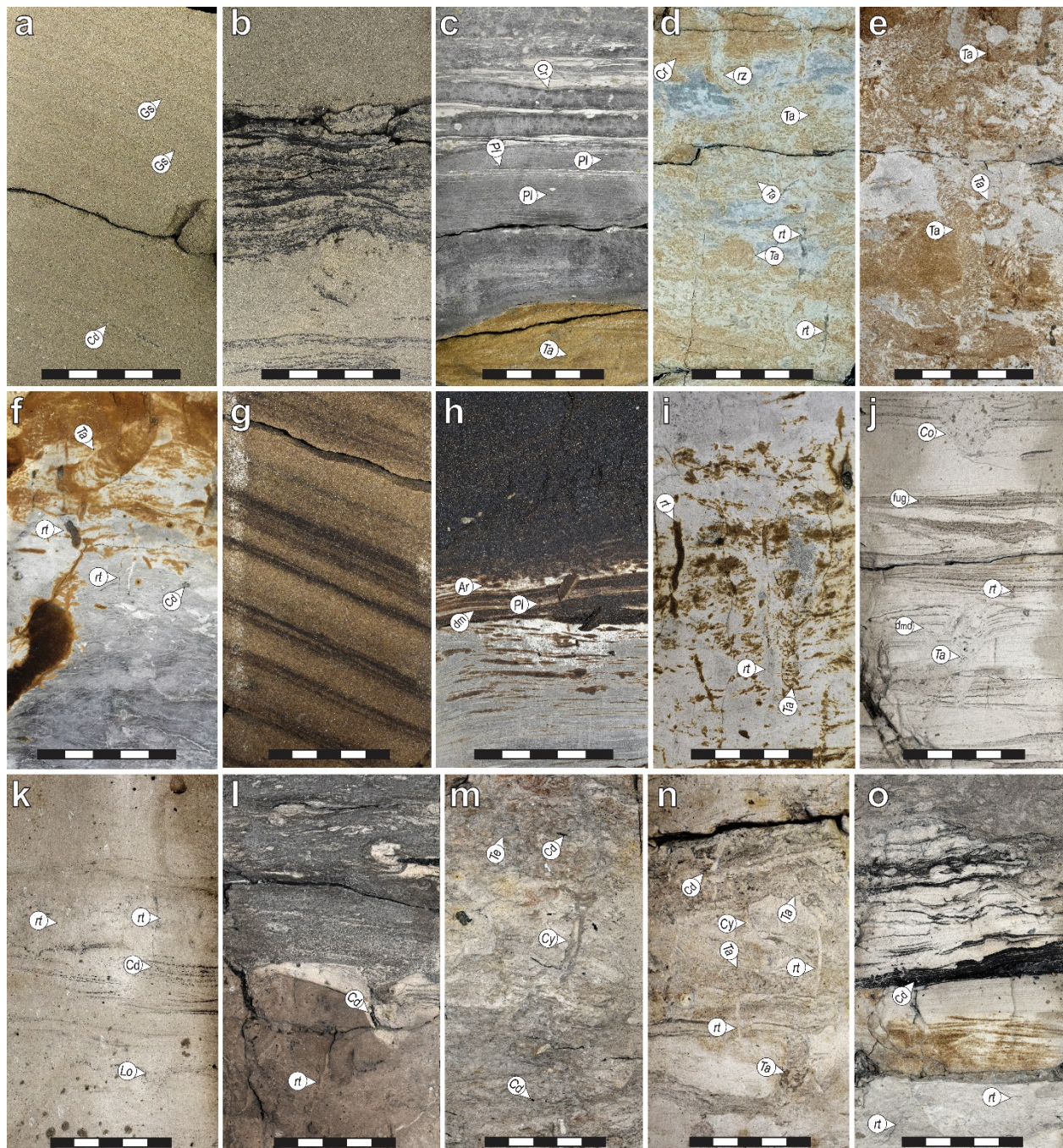
2-4) Continental to Estuarine Distribution of A-FA1, A-FA3, and B-FA4

Theoretical geographical distribution of different channel facies of Facies Association Complex A and B. Zones 1-3 are defined by the location of the tidal limit and salinity limit. The tidal limit is defined by the first preserved evidence of tidal sedimentation including double mudstone drapes and apparent rhythmicity of sedimentation. The brackish-water limit is defined by the persistent occurrence of brackish-water ichnogenera including *Cylindrichnus*, *Gyrolithes*, *Psilonichnus*, and *Teichichnus*. FAC-B channel facies are shown in comparison to Fabric A and Fabric B of the stratigraphic equivalent McMurray Formation (Melnik and Gingras, 2020).



2-5) Core and Petrophysical Logs of Facies Association Complexes A-G

Core and petrophysical logs illustrating the geological attributes, depositional environments and stratigraphic architecture of facies association complexes A, B, C, F, and G. Abbreviations are GR = gamma ray, 0-150 API, NPSS = neutron porosity, 0.45--0.15, RHOB = density, 1.5-3 g/cm³. Shaded cut off for NPSS = 0.33, RHOB = 2.5 g/cm³.



2-6) Facies Association Complex A

Facies association complex A. a-c) Channel and point-bar facies of continental fluvial A-FA1 strata with abundant carbonaceous detritus and a low-diversity sparse ichnological assemblage with *Planolites* and *Taenidium*. Photos a, b from 15-25-047-01W4, depth 651.7m, photo c is from Well 16-03-049-03W4, depth 732.1m. d-f) Highly bioturbated, rooted sandy mudstone from overbank deposits of A-FA2. Roots (rt), rhizoliths (rz), and *Taenidium isp* (Ta) are accompanied by colour mottling suggesting mild pedogenic alteration. Photo d, e from 09-35-047-01W4, depth 653.2m. Photo F from 02-30-051-04W4, depth 592.2 m. g-l) Channel and point-bar facies of A-FA3 characterized by a low-diversity assemblage of *Arenicolites* (Ar) and *Planolites* (Pl), apparent rhythmicity (g), and double mudstone drapes (h) indicating tidal influenced on sedimentation. Photo g, well 16-03-049-03W4,

depth 729.8m, photo h, i, well 02-30-051-04W4, depth 602.1m, 593.2 m. j-p) Upper delta plain facies of A-FA4 and A-FA5 with a low-diversity trace fossil suite including *Conichnus* (*Co*), *Lockeia* (*Lo*), and *Taenidium bowni* (*Ta b.*). Carbonaceous detritus is common on bedding planes. Photos j-l, well 03-13-055-06W4, depths 622.6m, 622.4m, and 621m. m-o) Cleaning-upward interdistributary bay facies of A-SU6 displaying elevated levels of bioturbation with preservation of thin ripple cross-laminated sand beds. The original brackish-water trace fossil suite consisting of *Cylindrichnus* (*Cy*) and *Teichichnus* (*Te*) appears to be overprinted by a continental assemblage consisting of *Taenidium bowni* (*Ta b.*), and rootlets. Photos m-o, well 03-13-055-06W4, depths 620.75m (m), 620.2m (n), 619.4m (o).

2.4.1.2 Facies Association Complex B – Upper to Middle Estuary

Description

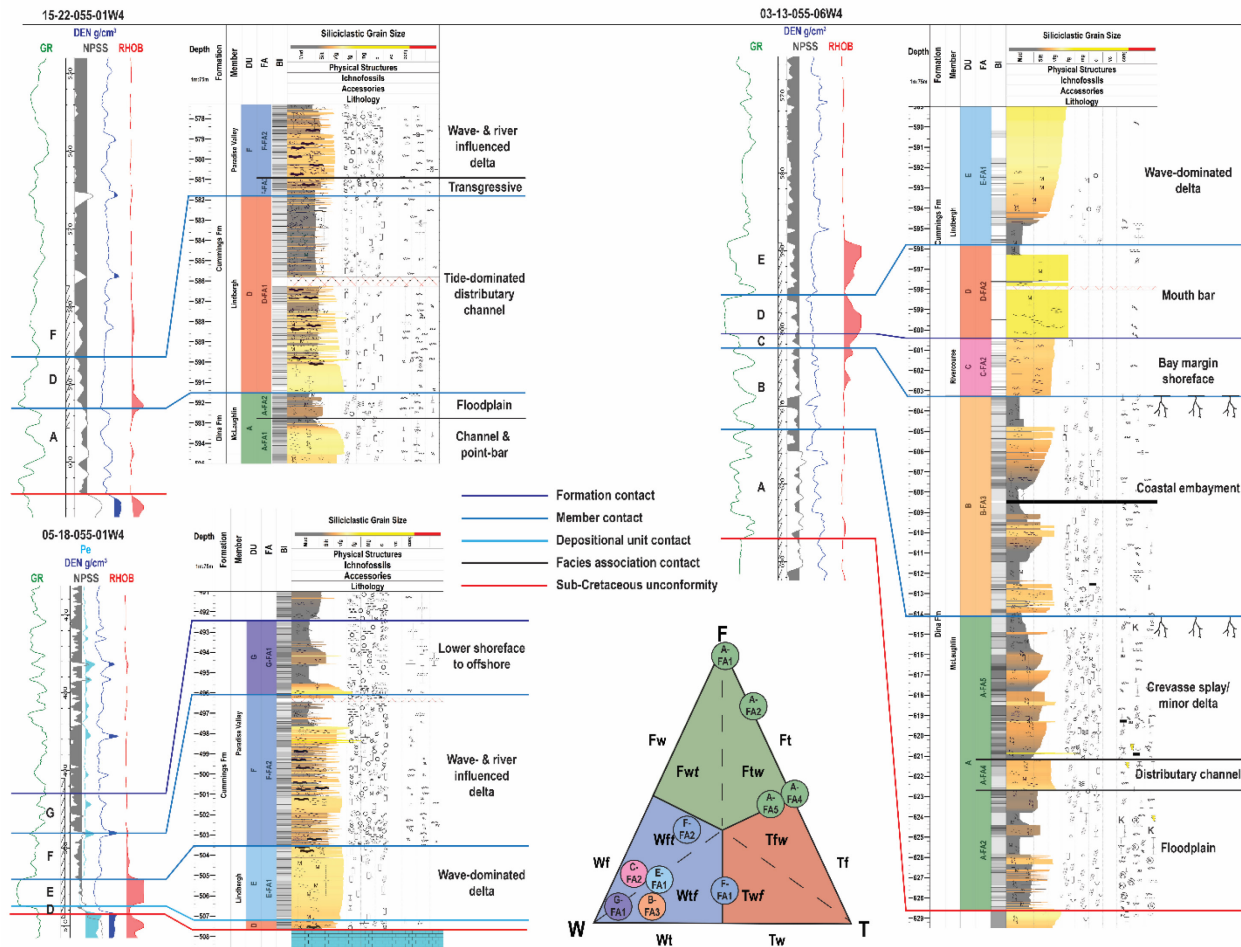
B-FA1: consists of coarsening-upward cycles of lenticular mudstone, wavy-bedded mudstone and sandstone and sandstone capped by organic-rich, variably pedogenically altered silty mudstone beds of variable thickness. Sedimentary structures include lenticular, wavy, and flaser bedding, with combined-flow ripple cross-lamination, mud drapes, rare normally graded beds, and rare synaeresis cracks. Lithological accessories include mud clasts, organic detritus, and pyrite. Bioturbation indices are low to moderate, with BI of 0-3, and have a sporadic distribution (Fig. 2.5, Fig. 2.7, well 03-13, Fig. 2.8 a, b). Ichnogenera include *Arenicolites*, *Cylindrichnus*, *fugichnia*, *Lockeia*, *Palaeophycus*, *Planolites*, *Skolithos*, *Taenidium*, *Teichichnus*, and *Thalassinoides*. Other biogenic structures include rootlets.

B-FA2: consists of coarsening-upward cycles of lenticular mudstone, wavy-bedded mudstone and sandstone, and sandstone capped by organic-rich, variably pedogenically altered silty mudstone beds of variable thickness. Sedimentary structures include low-angle, oscillation, and hummocky cross-stratification in sandstone facies (Fig. 2.8 d-e). Lithological accessories include pyrite, organic detritus, coal fragments, silt laminae, and siderite cement. Bioturbation is high in basal mudstone facies, BI 2-5, with sandstone intervals characterized by absent to moderate values of BI (0-3). Ichnogenera include *Arenicolites*, *Cylindrichnus*, *Diplocraterion*, *fugichnia*, *Gyrolithes*, *Paleophycus*, *Planolites*, *Siphonichnus*, *Taenidium*, *Teichichnus*, and *Thalassinoides* (Fig. 2.8 c-e)

B-FA3: consists of coarsening-upward cycles of from bioturbated lenticular mudstone, wavy-bedded mudstone and sandstone, and sandstone and are capped by organic-rich, variably pedogenically altered silty mudstone beds of variable thickness. Sedimentary structures include locally preserved oscillation ripple cross-lamination, low-angle lamination, and lenticular to wavy bedding. Lithological accessories consist of pyrite, organic detritus, coal fragments, silt laminae, siderite cement. B-FA3 is bioturbated throughout, with moderate to high bioturbation values of BI (2-5). Ichnogenera include

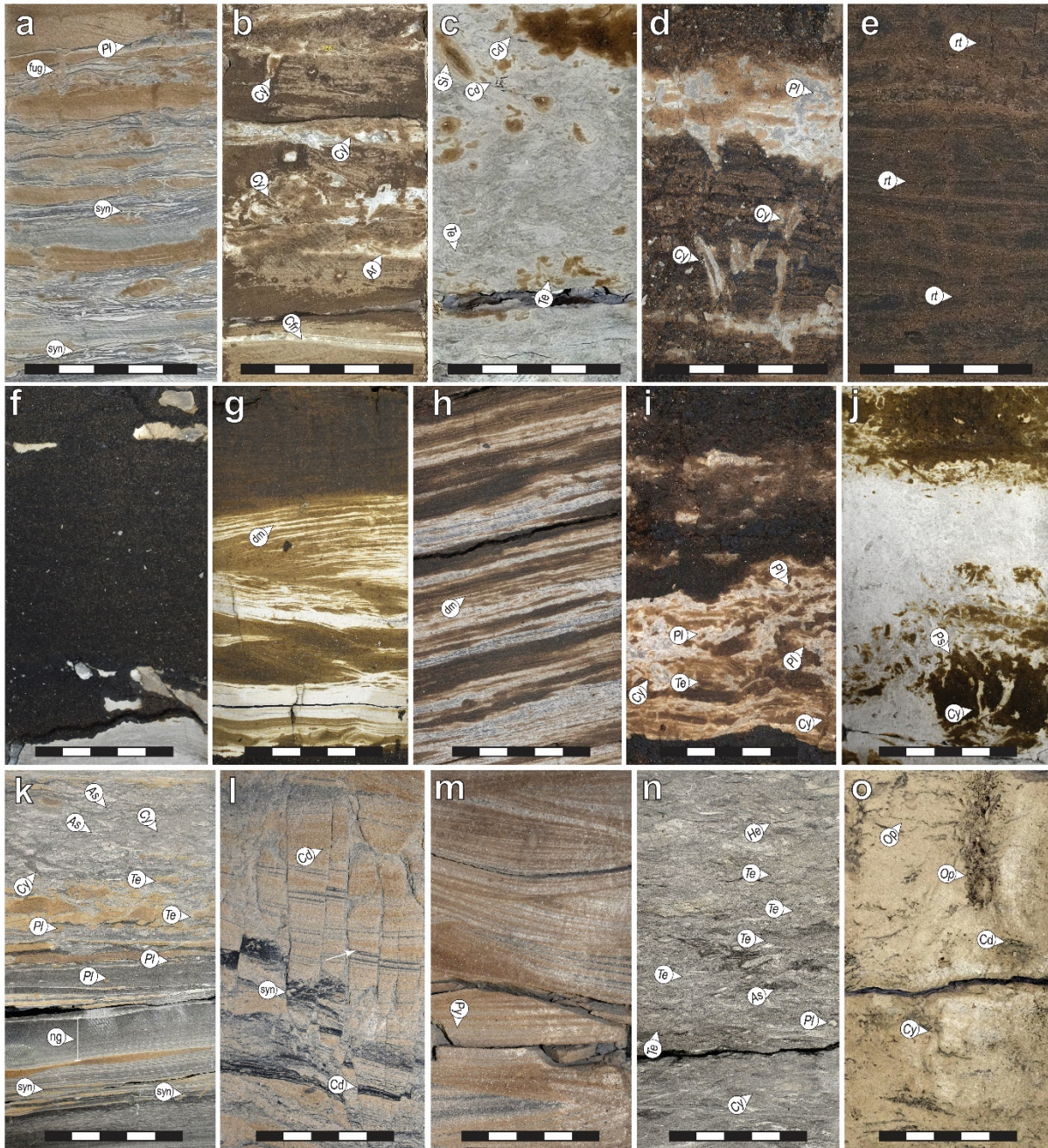
Arenicolites, Asterosoma, Cylindrichnus, Diplocraterion, fugichnia, Gyrolithes, Lockeia, Palaeophycus, Planolites, Ppsilonichnus, Siphonichnus, Skolithos, Taenidium, Teichichnus, and Thalassinoides.

B-FA4: consists of metre-scale, fining-upward sequences of sandstone, interbedded sandstone and mudstone, and silty mudstone. Sedimentary structures grade upward from trough and planar tabular cross-bedding and low-angle planar lamination to ripple cross-lamination and planar lamination. Grain-size striping, double mudstone drapes, and apparent rhythmicity are also present in B-FA4. Bioturbation is absent to locally homogeneous, with BI of (0-5), and a low-diversity, diminutive trace-fossil assemblage.



2-7) Core and Petrophysical Logs of Facies Association Complex A-G

Core and petrophysical logs illustrating the geological attributes, depositional environments and stratigraphic architecture of facies association complexes A, B, C, F, and G. Abbreviations are GR = gamma ray, 0-150 API, NPSS = neutron porosity, 0.45--0.15, RHOB = density, 1.5-3 g/cm³. Shaded cut off for NPSS = 0.33, RHOB = 2.5 g/cm³.



2-8) Facies Association Complexes B and C

a, b) Heterolithic tidal bar/dune facies of B-FA1 with synaeresis cracks (syn), combined flow ripples (cfr) and a low-diversity assemblage including *Cylindrichnus* (Cy), *fugichnia* (fug), and *Planolites* (Pl). Well 08-18-049-02W4, depths 726.4m (a), and 726.1m (b). c-e) brackish embayment facies of A-FA2. c) highly bioturbated basal mudstone with carbonaceous detritus (Cd), *Siphonichnus* (Si) and *Teichichnus* (Te). d) Bioturbated heterolithic facies of B-FA2 with *Cylindrichnus* (Cy), and *Planolites* (Pl). e) rooted, low-angle planar laminated sandstone from the upper zone of the coarsening-upward cycle. Photos c, e, well 08-18-049-02W4, depth 718.3m (c) and 722m (e), 03-13-055-06W4, depth 606.4m (d). f-j) Tidal channel and point-bar facies of B-FA4. Mudstone clasts embedded in fine-grained channel sandstone (f). Point-bar facies characterized by double mudstone drapes, rhythmic sedimentation, and

low-diversity bioturbated mudstone laminae with *Cylindrichnus* (*Cy*), *Planolites* (*Pl*), and *Teichichnus* (*Te*) indicating tidal influence and brackish-water conditions. j) Large *Psilonichnus* (*Ps*) burrow with intersecting *Cylindrichnus* (*Cy*) in bar top/tidal flat facies of B-FA4. Photos f, g, j from well 09-25-054-01W4, depths 554.7m (f), 547 m (g), and 545.5m (j). Photos h, i from well 13-27-055-06W4, depths 606.4m (h). 602.8m (i). k-o) Core photos of Facies Association Complex C. k, l) Prodelta (d) and distal delta front (l), and delta front (m) facies of C-FA1 characterized by abundant syneresis cracks (syn) with well developed normal graded beds (ng) and carbonaceous detritus (Cd). Photo k from well 09-35-047-01, depth 649.95m, photo l and m from well 08-31-048-05, depth 673.45m and 672.2m (m). n, o) Bioturbated silty mudstone and sandstone facies of C-FA3 with a moderated diversity assemblage including *Asterosoma* (*As*), *Cylindrichnus* (*Cy*), *Helminthopsis* (*He*), *Ophiomorpha* (*Op*), *Planolites* (*Pl*), and *Teichichnus* (*Te*). Photo n from well 02-32-053-03W4, depth 601.4m, photo o from well 06-24-048-01W4, depth 637.5m.

Identified ichnogenera include *Arenicolites*, *Cylindrichnus*, *Gyrolithes*, *Palaeophycus*, *Planolites*, *Psilonichnus*, *Skolithos*, *Taenidium*, and *Teichichnus* (Fig. 2.6 k-o)

Interpretation

Facies associations of FAC-B are interpreted to comprise various sub-environments within a tide- and wave-influenced, brackish-water estuary. B-FA1 to B-FA3 are interpreted as small tide- and wave-influenced deltaic lobes prograding into shallow brackish-water interdistributary bays. This interpretation is based upon the coarsening-upward geometry of individual cycles, the presence of tidal sedimentary structures including double mudstone drapes, and wave-generated structures including oscillation ripple cross-lamination and small-scale hummocky cross-stratification. The diminutive, low-diversity trace fossil suite indicates persistent brackish-water conditions (e.g., Pemberton et al., 1982; Beynon et al., 1988; Gingras and MacEachern, 2012; Gingras et al., 2016). The varying degrees of bioturbation intensity between B-FA1, B-FA2, and B-FA3 reflects spatial variability in physical conditions with higher intensities corresponding to more protected locales. These coarsening-upward cycles resemble Facies Associations 3 and 4 (tide-dominated, and wave-dominated, tide-influenced, fluvial-affected deltas) documented by Chateau et al., (2021) from the stratigraphically equivalent McMurray Formation of the Athabasca oil sands. FAC-B strata are also sedimentologically analogous to estuarine point-bar, tidal flat and marginal marine deposits of stratigraphic units MM2 and MM3 described by Barton (2016), and the B Sequence of the AEUB Regional Geological Study (EUB, 2003).

B-FA4 is interpreted to record deposition in tidal channel, point-bar, and tidal flat environments. The sedimentological and ichnological characteristics of tidal channel strata are analogous to inner (Fabric A) and middle estuary (Fabric B) facies documented in the stratigraphically equivalent McMurray Formation by Melnyk and Gingras et al., (2020). This places B-FA4 at Positions 3 and 4 on Figure 2.4, basinward of both tidal and salinity limits.

2.4.1.3 Facies Association Complex C – River- and Wave-Influenced Embayment

Description

C-FA1: metre-scale coarsening-upward cycles of silty mudstone, interbedded silty mudstone and sandstone, and sandstone, with cycles often capped by a thin coal seam or organic mudstone facies (Fig. 2.5, Fig. 2.7 well 03-13). Sedimentary structures include trough cross bedding, low-angle planar and hummocky cross-stratification, convolute lamination, combined flow-ripple cross-lamination, syneresis cracks, normally graded beds, micro-faults, and fluid escape structures (Fig. 2.8 k, l, m). Lithological accessories include coal fragments, pyrite, organic detritus, and carbonaceous drapes. Bioturbation is absent to moderate (BI 0-3), and sporadically distributed. Ichnogenera include *Cylindrichnus*, *fugichnia*, *Palaeophycus*, *Planolites*, *Skolithos*, *Taenidium*, and *Teichichnus*.

C-FA2: metre-scale coarsening-upward cycle of silty mudstone, interbedded silty mudstone and sandstone, and sandstone, with cycles often capped by a thin coal seam or organic mudstone facies. Sedimentary structures include hummocky cross-stratification, trough cross bedding, low-angle planar and convolute lamination, combined flow-ripple cross-lamination, syneresis cracks, normally graded beds, micro-faults, and fluid escape structures. Lithological accessories include coal fragments, pyrite, organic detritus, carbonaceous drapes. Bioturbation indices are absent to moderate (BI 0-3), and distribution is sporadic. Ichnogenera identified include *Cylindrichnus*, *fugichnia*, *Palaeophycus*, *Planolites*, *Skolithos*, *Taenidium*, and *Teichichnus*.

C-FA3: metre-scale coarsening-upward cycle of bioturbated silty mudstone, interbedded silty mudstone and sandstone, and sandstone, with cycles often capped by a thin coal seam or organic mudstone facies. Sedimentary structures include low-angle planar and vague cross-lamination, combined flow ripples, flaser bedding, oscillation and combined flow ripple cross-lamination, convolute lamination, syneresis cracks, and rare normally graded beds. Lithological accessories consist of organic detritus, coal fragments, wood debris, pyrite, carbonaceous drapes. Bioturbation indices are low to high, with distribution being more homogeneous than in C-FA1 or C-FA2. Ichnogenera identified include *Arenicolites*, *Asterosoma*, *Berguaeria*, *Cosmorhapha*, *Cylindrichnus*, *fugichnia*, *Gyrolithes*, *Helminthopsis*, *Ophiomorpha*, *Palaeophycus*, *Phycosiphon*, *Planolites*, *Skolithos*, *Taenidium*, *Teichichnus*, and *Thalassinoides*.

Interpretation

FAC-C is interpreted to record deposition in a wave- and river-influenced delta prograding into an open brackish-water to near-marine salinity embayment. This interpretation is based upon the following observations. Physical sedimentary structures such as hummocky, trough and low-angle cross-stratification, and massive fabric recorded in C-FA1 and C-FA3 indicate deposition under high-energy

conditions subject to spatial and temporal changes in the magnitude of fluvial and wave processes. Normal to reverse-graded beds in prodelta mudstone facies are consistent with hyperpycnites resulting from high suspended sediment concentrations associated with elevated river discharge (Mulder et al., 2001; 2003; Bhattacharya and MacEachern, 2009). River input is also indicated by an abundance of coal fragments and organic detritus interpreted as phytodetrital pulses, which are commonly associated with hyperpycnal discharge (Zavala et al., 2012). The presence of syneresis cracks, which are attributed to the settling and dewatering of flocculated fresh-water clays introduced into saline water (Plummer and Gostin, 1981) can also be taken as evidence for the presence of freshwater discharge. The highly sporadic distribution of trace fossils in high-energy facies is consistent with rates of high deposition and shifting substrata (e.g., MacEachern et al., 2005). Higher bioturbation indices indicate C-FA2 was deposited in more sheltered areas within the embayment under ambient salinity. As with FAC-B, facies associations of FAC-C bear a high degree of similarity to coarsening-upward cycles of the McMurray Formation. These include the A Sequence (EUB, 2003), stratigraphic unit MM4 (Barton, 2016), and facies associations 1 and 2 of Weleschuk and Dashtgard (2019).

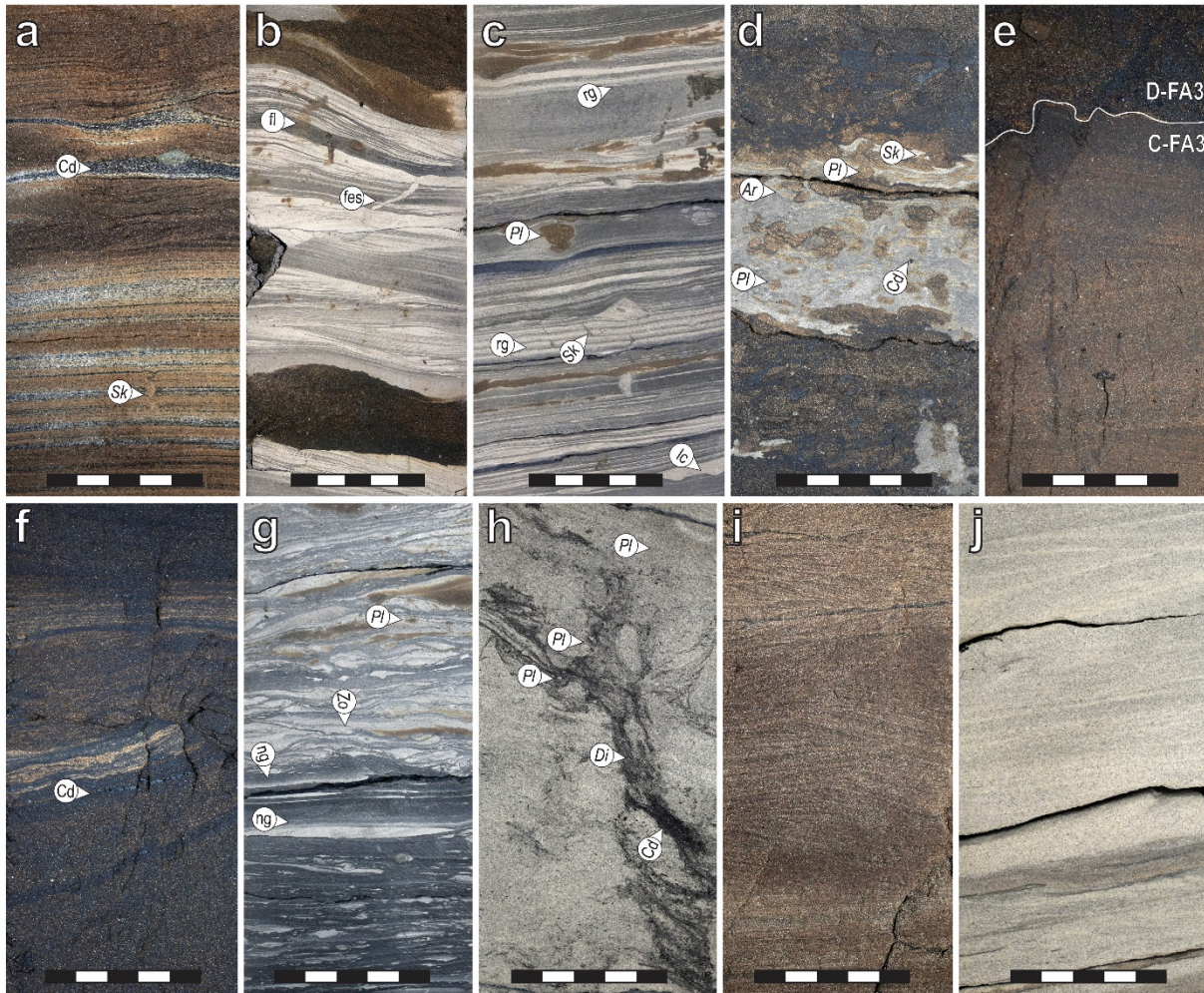
2.4.1.4 Facies Association Complex D – Tidal Channel & Tidal Delta

Description

D-FA1: consists of a fining-upward cycle of trough and planar tabular cross-bedded sandstone, interbedded sandstone and blue-grey mudstone, and blue-grey mudstone (Fig. 2.7, well 15-22, Fig. 2.9 a-c). Mudstone beds are sharp to erosively based, massive to laminated, contain abundant siltstone laminae, with common convolute lamination, load casts, and display local normal- to reverse-grading (Fig. 2.9 b, c). Mudstone beds with abundant silt to very fine-grained sandstone laminae commonly preserve ripple cross-lamination and internal grading. Sandstone facies are very fine- to fine-grained and are characterized by trough cross-bedding, low-angle planar cross-lamination, micro-hummocky cross-stratification, ripple cross-lamination, combined flow-ripple cross-lamination, and possible reactivation surfaces. Individual mudstone beds range from a few cm to several dm's and are characterized by highly sporadic bioturbation, with BI of (0-1), and a low-diversity assemblage. Ichnogenera observed include *Arenicolites*, *Berguaria*, *fugichnia*, *navichnia*, *Planolites*, *Rhizocorallium*, *Skolithos*, and *Thalassinoides*.

D-FA2: consists of a fining-upward cycle of trough and planar tabular cross-bedded sandstone, interbedded sandstone and blue-grey mudstone, and blue-grey mudstone. Mudstone beds are thinner than those of D-FA1, but still contain abundant siltstone and very fine-grained sandstone laminae with low-angle lamination and ripple cross-lamination being common (Fig. 2.9 d). Bioturbation indices are

significantly higher than D-FA1, with BI (1-4). Ichnogenera include *Arenicolites*, *Berguaria*, *fugichnia*, *navichnia*, *Planolites*, *Rhizocorallium*, *Skolithos*, and *Thalassinoides*.



2-9) Facies Association Complexes D and E

a-e) Tidal channel and delta front facies of FAC-D. a) Low-angle cross-laminated to rippled sandstone facies of D-FA1 with abundant carbonaceous laminae indicating emplacement of phytodetrital pulses. Photo from well 04-14-055-02W4, depth 504.9m. b, c) interbedded sandstone and silty mudstone with ripple cross-lamination, fluid mud beds (fl), and fluid escape structure (fes) (b) and dark grey mudstone with load casts (lc) and reverse-graded beds (rg). Note the highly impoverished trace fossil assemblage of *Planolites* (Pl) and *Skolithos* (Sk) with low BI values. Photos from well 15-22-055-01W4, depths 588.9m (b), and 585.8m (c). d) Bioturbated mudstone and sandstone facies of D-FA2 with carbonaceous detritus (cd) a low-diversity assemblage of *Arenicolites* (Ar), *Planolites* (Pl), and *Skolithos* (Sk). Photo from well 12-20-055-01W4, depth 518.6m. e-f) Fine- to medium-grained sandstone of D-FA3. e) erosive contact between D-FA3 and underlying C-FA3 facies. f) carbonaceous laminae interpreted as phytodetrital pulses. Photos from well 03-13-055-06W4, depths 600.4m, and 599.7 m. g-j) Storm-influenced prodelta to delta front facies of FAC-E. g) Prodelta mudstone and interbedded siltstone with normally graded beds (ng) and an impoverished trace fossil assemblage of *Planolites* (Pl) and *Zoophycos* (Zo). Photo from well 03-05-055-06W4, depth 600.6m. h) Robust *Diplocraterion* (Di) and *Carbonicola* (Cc).

with *Planolites (Pl)* and abundant carbonaceous detritus in distal delta front sandstone of E-FA1. Photo from well 14-34-054-06W4, depth 604.6m. i) Climbing ripple cross-lamination of the delta front indicating rapid sediment deposition. Photo from well 03-05-055-06W4, depth 599.2m. j) High-angle planar and hummocky cross-lamination of proximal delta front facies. Photo from well 14-34-054-06W4, depth 601.8m.

D-FA3: consists of fine- to medium-grained sand and local dark-grey, centimetre to decimetre scale carbonaceous mudstone beds with sharp bases and tops (Fig. 2.9 e, f). Low-angle planar, planar, and trough cross-stratification are common, with lesser combined flow ripple cross-lamination, and massive fabric. Organic detritus, both as disseminated grains and along bedding planes are common (Fig. 2.9 f). Bioturbation in sandstone facies appears absent but may be obscured by oil staining. Mudstone beds have extremely low BI of 0-1 and are restricted to *Planolites*.

Interpretation

FAC-D is interpreted to record deposition in a tide-dominated, wave- and river-influenced channel (D-FA1) delta front (D-FA2) and mouth bar (D-FA3). This interpretation is based upon the following sedimentological observations and comparisons to tidal channel and tidal delta deposits with similar characteristics. The thick (often >10 cm thick) blue-grey mudstone beds of D-FA1 and D-FA2 resemble those interpreted as tidal mudstones of the Bluesky Formation, as described by MacKay and Dalrymple (2011) and sub-tidal channel wall facies along the Holocene tidal flats of the North Sea (Reineck, 1975). The sedimentological characteristics of FAC-D resemble the tidal-fluvial channel, mouth-bar and terminal distributary channel, and delta front deposits of the Tilje Formation of offshore Norway as described by Ichaso and Dalrymple, (2009). Those authors noted that anomalously thick, internally structureless to laminated mudstone beds were a common component of tidal-fluvial channel and terminal distributary channel elements and interpreted them as fluid muds resembling those in the tidal-fluvial transition of moder estuaries and deltas (Ichaso and Dalrymple, 2009 and references therein). They also noted the presence of interbeds of hummocky cross-stratification within their delta front deposits which they interpret to preserve event beds associated with storm waves. Preservation of similar hummocky cross-stratified beds occur within D-FA1 and D-FA2. The sedimentological and ichnological characteristics of FAC-D (particularly the characteristic thick, grey-blue color mudstone beds) are also like tide- and wave-influenced deltaic strata of the Bluesky Formation (Botterill et al., 2016; Campbell et al., 2016), and Wabiskaw Member of the Clearwater Formation (Ahmad and Gingras, 2022).

2.4.1.5 Facies Association Complex E – Storm-Dominated Delta

Description

E-FA1: consists of one to two coarsening-upward cycles of lenticular mudstone, interbedded siltstone and mudstone, and sandstone. In some cases, the mudstone and heterolithic interval is missing or are very thin (<20 cm), with sandstone facies sitting sharply above facies association complex C or D strata. E-FA1 is characterized by trough, low-angle, and hummocky cross-stratification, climbing ripple and oscillation ripple cross-lamination, and scour surfaces (Fig. 2.9 g-j). Synaeresis cracks, load casts, graded beds, and convolute lamination are common in prodelta to distal delta front facies. Bioturbation is sporadic (fine-grained facies) to highly sporadic (sandstone facies), with BI of (0-3) for fine-grained and (0-1) for sandstone intervals. The trace-fossil assemblage is diverse, and forms are robust. Ichnogenera include *Arenicolites*, *Berguaria*, *Chondrites*, *Cylindrichnus*, *Diplocraterion*, *fugichnia*, *Lockeia*, *Macaronichnus*, *navichnia*, *Ophiomorpha*, *Palaeophycus*, *Phycosiphon*, *Planolites*, *Rhizocorralium*, rootlets, *Rosselia*, *Skolithos*, *Teichichnus*, *Thalassinoides*, and *Zoophycos*.

E-FA2: consists of variably thick poorly stratified silty to sandy mudstone, muddy to silty sandstone wavy bedded mudstone, siltstone, and sandstone, organic mudstone and sandstone, and coal. Sedimentary structures are largely obscured by pedogenic alteration, but local preservation of low-angle to planar cross-lamination, ripple cross-lamination, convolute lamination, wavy bedding, load casts, and fluid escape structures are observed. Organic detritus, pyrite, coal fragments and thin laminae. Bioturbation is absent to locally intense with BI of (0-5). Ichnogenera identified include *Palaeophycus*, *Planolites*, and *Skolithos*. Other biogenic structures include rootlets and rhizoliths.

Interpretation

FAC-E is interpreted to record deposition in a storm-influenced marine delta front to prodelta (E-FA1) and delta plain (E-FA2) complex. This interpretation is based on a number of criteria. Sedimentary structures such as hummocky cross-stratification, combined flow-ripple cross-lamination, and climbing ripple cross-lamination record erosion and deposition by oscillatory and unidirectional currents (Harms et al., 1975; Dott and Bourgeois, 1982; Duke, 1985; Dumas et al., 2005; Dumas and Arnott, 2006). The interbedding of bioturbated and non-bioturbated beds record alternations between fair-weather sedimentation and tempestite deposition (lam-scam, MacEachern and Pemberton, 1992). The lack of dominance of one bed type within E-FA1 is consistent with the characteristics of moderately storm-dominated shoreface environment (Pemberton et al., 2012). A marine depositional setting is inferred from the diversity and robust nature of the trace-fossil assemblage, in particular those normally associated with marine salinities (e.g., *Phycosiphon*, *Zoophycos*). The interpretation of E-FA2 as delta plain strata is based

on similar sedimentological evidence to continental floodplain facies of FAC-A. E-FA2 facies are commonly rooted, poorly sorted, locally organic rich, and lack trace fossils associated with brackish-water settings. This interpretation is limited by the overall lack of cored examples of E-FA2 and the fact that when present these facies are typically less than 2 metres thick.

2.4.1.6 Facies Association Complex F – Coastal Marine to Offshore

Description

F-FA1: consist of one to two, coarsening-upward cycles of lenticular mudstone, wavy-bedded silty mudstone and very fine-grained sandstone, and sandstone (Fig. 2.5, well 15-25, Fig. 2.10 a-c). Primary sedimentary structures include low-angle, planar, and hummocky cross-stratification, flaser, wavy, and lenticular bedding, oscillation and combined flow ripples, fluid escape structures, fluid muds, double mudstone drapes, convolute lamination, normally graded beds, and rare sphaerulite cracks. Lithological accessories consist of carbonaceous detritus, glauconite, shell fragments, and pyrite. Trace fossil distribution in F-FA1 is sporadic to locally homogeneous, with low to moderate BI of (0-4). Diversity is high in F-FA1 with traces being of moderate to large size. Ichnogenera include *Arenicolites*, *Asterosoma*, *Berguaeria*, *Chondrites*, *Cylindrichnus*, *Cosmorhapha*, *Diplocraterion*, *fugichnia*, *Gyrolithes*, *Helminthopsis*, *Nereites*, *Ophiomorpha*, *Palaeophycus*, *Phycosiphon*, *Planolites*, *Rhizocorallium*, *Rosselia*, *Skolithos*, *Teichichnus*, *Thalassinoides* and *Zoophycos*.

F-FA2: consists of one to two, coarsening-upward cycles of wavy-bedded mudstone and very fine-grained sandstone, flaser bedded very fine-grained sandstone, and sandstone. Sedimentological characteristics are essentially identical to F-FA1, apart from the following. F-FA2 has a higher sand-to-mud ratio, with a lesser fluid mudstone component, and a lower occurrence of deformational structures such as convolute lamination, and load casting. F-FA2 also lacks shell fragments and visible glauconite, but still contains carbonaceous detritus and pyrite. Trace fossil distribution is sporadic with BI (0-3). Ichnological diversity is slightly less than observed in F-FA1 with ichnogenera including *Arenicolites*, *Asterosoma*, *Berguaeria*, *Cylindrichnus*, *Diplocraterion*, *fugichnia*, *Gyrolithes*, *Ophiomorpha*, *Palaeophycus*, *Phycosiphon*, *Planolites*, *Rhizocorallium*, *Rosselia*, *Skolithos*, *Teichichnus*, *Thalassinoides*.

F-FA3: consists of a fining-upward interval (less than 10 cm to ca. 1 metre) of poorly sorted glauconitic, muddy sandstone and sandy mudstone. Local occurrence of low-angle planar lamination, oscillation ripple cross-lamination, combined flow ripple cross-lamination, and mud drapes are preserved. Visible glauconite grains, shell fragments, pyrite, and organic detritus are quite common with lesser presence of granules. Bioturbation indices are low to high (BI 0-5), with homogeneous to sporadic distribution. Ichnogenera include *Arenicolites*, *Asterosoma*, *Chondrites*, *Cylindrichnus*, *Helminthopsis*,

navichnia, *Palaeophycus*, *Phycosiphon*, *Planolites*, *Rhizocorallium*, *Scolicia*, *Skolithos*, *Teichichnus*, *Thalassinoides*, and *Zoophycos*.

Interpretation

FAC-F is interpreted to represent preservation of multiple mixed-influence marine delta lobes (F-FA1 and F-FA2) and interstratified transgressive lags (F-FA3). This interpretation is based on several observations. The abundant occurrence of massive to graded dark-grey mudstone beds, interpreted as river-induced hyperpycnal flows indicates significant influence of river induced sedimentation (Mulder et al., 2001; 2003; Bhattacharya and MacEachern, 2009). Accumulations of interbedded centimetre scale fluid mudstone and oscillation ripple cross-laminated sandstone show similar characteristics to those of E-FA1 wherein alternations of low and high bioturbation values are preserved. In low bioturbation intervals trace fossil diversity is highly suppressed with near monospecific assemblages of *Chondrites* with variable presence of *Phycosiphon*. Interbedded bioturbated zones are significantly higher in diversity with common *Asterosoma*, *Cosmorhaphé*, *Helminthopsis*, *Phycosiphon*, *Scolicia*, and *Zoophycos*. The occurrence of monospecific *Chondrites* has been associated with dysoxic conditions in bottom and pore waters (e.g., Bromley and Ekdale, 1984; Savrda and Bottjer, 1991), conditions that are common in prodelta mudstone deposits (MacEachern et al., 2005). Given the dark color of fluid mudstone beds of F-FA1 and the visible detrital organic component it is possible that the alternating low-BI – high-BI zones record variation in oxygen in the prodelta environment. Alternatively, intervals of low BI may reflect rates of deposition that are too high for colonization, or periods where salinity stress associated with freshets precludes substrate colonization by marine organisms. The presence of double mudstone drapes which are common in FAC-F, indicates that tidal modulation influences sedimentation, particularly in upper prodelta and delta front facies. Despite the evidence of fluvial-, tidal-, wave-generated physical and associated chemical stresses (salinity fluctuation, possible dysoxia), the overall trace fossil diversity is indicative of ambient conditions of marine chemistry. In particular, the presence of robust *Asterosoma*, *Cosmorhaphé*, *Phycosiphon*, and *Zoophycos* are strong indicators of fully marine environments (e.g., MacEachern et al., 2010; Gingras et al., 2011, Buatois et al., 2019).

F-FA3 is consistent with the diagnostic criteria of transgressive lag deposits. As described by Kidwell (1989), transgressive lag deposits are thin (0.5-2m) intervals of consisting of conglomerate, glauconite, or bioclastic material which occur at the base of shallow marine units. Transgressive lags occur at the base of FAC-F, and locally at contacts between stacked F-FA1 or F-FA2 cycles. The juxtaposition of offshore marine facies of FAC-F over delta front/delta plain strata of FAC-E provides additional evidence to the interpretation of F-FA3 having a transgressive depositional origin.

2.4.1.7 Facies Association Complex G – Shoreface to Offshore

Description

G-FA1: consist of one to several, metre-scale coarsening-upward cycles of glauconitic sandy mudstone, interbedded mudstone and sandstone, and sandstone (Fig. 2.8, well 15-25, Fig. 2.10 k-o). The base of G-FA1 cycles is often sharp, erosional, and may be mantled by a lag of coarser-grained sandstone, glauconite grains, pyrite, and carbonaceous debris. Sedimentary structures, where preserved consist primarily of low-angle and hummocky cross-stratification, horizontal, combined flow, and oscillation ripple cross-lamination with local scour surfaces. Glauconite is abundant, with lesser pyrite and carbonaceous debris. Bioturbation is sporadic to homogeneous with BI of (0-5), diversity is exceedingly high (23 ichnogenera), and traces are very robust. Ichnogenera include *Arenicolites*, *Asterosoma*, *Berguaeria*, *Chondrites*, *Cosmorhapha*, *Cylindrichnus*, *Diplocraterion*, *Helminthopsis*, *navichnia*, *Nereites*, *Ophiomorpha*, *Palaeophycus*, *Phoebichnus*, *Phycosiphon*, *Planolites*, *Rhizocorallium*, *Rosselia*, *Schaubcylindrichnus freyi*, *Scolicia*, *Skolithos*, *Teichichnus*, *Thalassinoides*, and *Zoophycos* (Fig. 2.10 k-o).

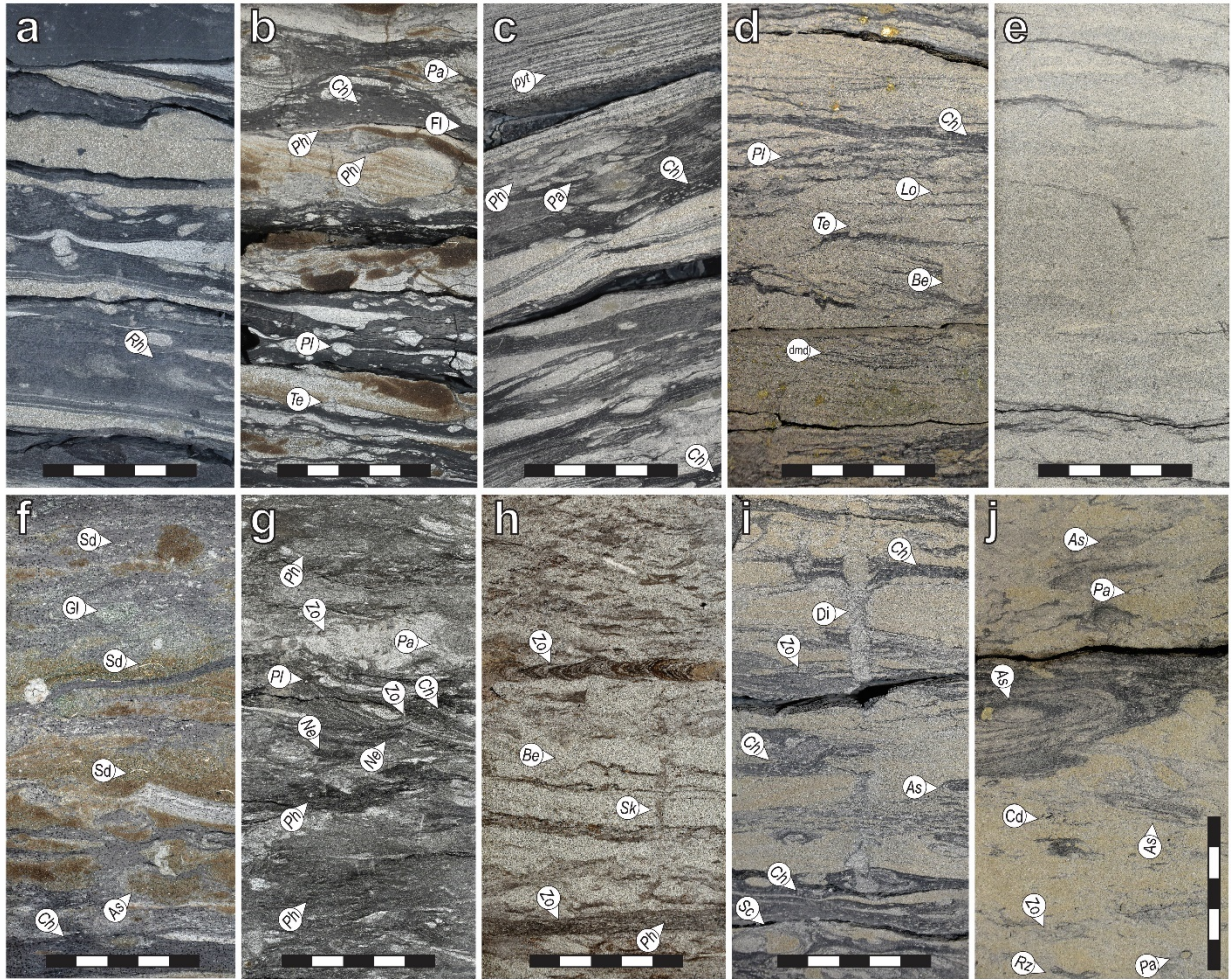
Interpretation

FAC-G is interpreted to preserve multiple cycles of sediment deposited from lower offshore/shelf to proximal lower shoreface settings following the criteria of MacEachern and Bann, (2008) and Pemberton et al. (2012). In a typical cycle G-FA1 consists of dark, burrowed, silty mudstone with rare very fine-grained sandstone or siltstone laminae and a trace fossil assemblage consistent with the *Zoophycos* Ichnofacies (i.e., *Zoophycos*, *Cosmorhapha*, *Phycosiphon*, *Helminthopsis*, and *Nereites*) (MacEachern and Bann, 2008). The lack of appreciable sandstone laminae and *Zoophycos* Ichnofacies suggests deposition in low-energy settings near or below storm-weather wave-base (Pemberton et al., 2012). As the cycle coarsens upward the sandstone fraction and bed thickness increases, wave-ripple cross-lamination becomes progressively preserved and the diversity and ethology of trace fossils increases (Fig. 2.11). The most proximal expression of G-FA1 preserved in the core dataset is interpreted to represent the proximal lower shoreface. In addition to the ichnological evidence for fully marine conditions, the presence of glauconite grains is indicative of open marine environments with low rates of terrigenous input and low-rates of sedimentation (e.g., Velde, 2014).

2.4.2 Bounding Surfaces

The seven facies association complexes described above are separated by seven discontinuity surfaces (S1-S7). Each surface demarcates a juxtaposition of facies that violate Walther's law. These surfaces are independent of the lithology of bounding units, making them useful in correlating genetically related strata at a local to regional scale. All seven surfaces are preserved in the north-west corner of the

study area (Fig. 2.11, E-W cross-section wells 16-04 and 03-13), with each surface except for S6 and S7 overlapping Paleozoic highs or merging to become composite surfaces (Fig. 2.11). The nature of facies relationships and the lateral extents of S1-S7 are summarized in Figure 2.12. The sequence stratigraphic significance of surfaces S1-S7 are discussed in Chapter 4.



2-10) Facies Association Complexes F and G

a-c) Prodelta facies of F-FA1 with abundant dark-grey massive fluid mudstone beds (fl), phytodetrital pulses (pyt), and a low-diversity, sporadically distributed trace fossil assemblage of *Chondrites* (Ch), *Palaeophycus* (Pa), *Phycosiphon* (Ph), *Planolites* (Pl), *Rhizocorallium* (Rh) and *Teichichnus* (Te) indicating a stressed environment with rapid deposition of river-derived sediment. Photos from well 08-31-048-05W4, depths 666.3m (a) and 667.3m (c), and well 04-14-055-02W4, depth 501.9m (b). d, e) Distal (d) and proximal (e) delta front facies of F-FA2 displaying double mudstone drapes (dmd) and an ichnological assemblage consisting of *Planolites* (Pl), *Berguaria* (Be), *Lockeia* (Lo), and *Chondrites* (Ch). Photos from well 09-35-047-01W4, depths 638.5 (d) and 637.6m (e). f) Transgressive lag deposit of F-FA3 with visible glauconite (gl), shell debris (sd), and a trace-fossil assemblage consisting of *Chondrites* (Ch), and *Asterosoma* (As). Photo from well 04-14-055-02W4, depth 503.6m. g-j) Offshore to lower shoreface facies of FAC-G. g) Offshore mudstone with high bioturbation indices and a diverse marine trace fossil assemblage consisting of

Palaeophycus (Pa), *Phycosiphon (Ph)*, *Planolites (Pl)*, *Nereites (Ne)*, and *Zoophycos (Zo)*. Photo from well 09-33-054-05W4, depth 571.1m. h-j) Interbedded bioturbated and laminated beds (lam-scram) recording alternating fair-weather conditions punctuated by tempestite emplacement. Ichnological diversity is high, and forms are very robust indicating marine conditions. Ichnogenera include *Asterosoma (As)*, *Berguaria (Be)*, *Chondrites (Ch)*, *Diplocraterion (Di)*, *Rhizocorallium (Rh)*, *Scolicia (Sc)* and *Zoophycos (Zo)*. Photos from wells 09-33-054-05W4, depth 572.5m (h), and well 15-25-047-01W4, depths 625.5m (i), and 623.7m (j). Scale bars are all 5 centimetres in width.

2.4.2.1 Surface 1

S1 separates continental and lower delta plain (FAC-A) from inner to middle tide- and wave-influenced estuary strata (FAC-B) (Fig. 2.11, Fig. 2.12, Fig. 2.13). Regardless of which facies association is present below this surface, the uppermost facies (in cored examples) are characterized by weak to pedogenic alteration (Fig. 2.12). Above S1, inner to middle estuary facies are comprised of bioturbated silty mudstone with trace fossils indicating stressed brackish-water deposition (i.e., *Cylindrichnus*, *Gyrolithes*, *Teichichnus*). S1 is difficult to correlate regionally due to the lithological heterogeneity of both underlying delta plain and overlying estuary strata. As the contact is in part defined by the presence of continental or continental overprinted brackish-water ichnofossil assemblages below and persistent brackish-water assemblages above, stratigraphic correlations require calibration to known cored intersections.

2.4.2.2 Surface 2

S2 separates inner to middle estuary (FAC-B) from wave- and river-dominated open embayment facies (FAC-C) and is mappable over much of the study area, except where it onlaps Paleozoic highs (Fig. 2.11, Fig. 2.13). Below S2, strata of facies association complex B are characterized by weakly to moderately pedogenically altered facies with common rooting, ped development, and mottling (Fig. 2.12). Above S2 is the first regional bioturbated brackish- to stressed-marine embayment or prodelta mudstone of facies association complex C. S2 is not observed to be incised (in cored examples) and can be mapped on a regional scale.

2.4.2.3 Surface 3

S3 separates wave- and river-dominated open embayment (FAC-C) from tide-, river- and wave-influenced channel, mouth-bar, and delta front facies (FAC-D) (Fig. 2.11, Fig. 2.12). This surface is sharp and visibly erosional with a significant increase in grain-size across the contact (Fig. 2.9 e; Fig. 2.12). There are two expressions of this surface. The first expression occurs at the base of tidal channel strata of D-FA1 where incision as deep as FAC-A is observed in core. Where D-FA3 is present, S3 occurs at the base of mouth-bar facies erosionally overlying upper embayment shoreface/deltaic cycles of facies association complex C (Fig. 2.11, Fig. 2.12). Surface S3 is difficult to map away from cored occurrences due to the

limited core dataset and the restricted occurrence of FAC-D north of Township 53 (Fig. 2.11). S3 merges with S4 at the zero edge of facies association complex D (Fig. 2.11).

2.4.2.4 Surface 4

S4 separates facies association complex C or D (where present) below from storm-influenced deltaic strata of facies association complex E above. This contact is placed at the top of the regional coal seam and correlative organic mudstone capping FAC-C or FAC-D facies (Fig. 2.11, Fig. 2.12). In a northwest to southeast direction, S4 merges with S5 due to the progressive thinning and facies transition of delta front (E-FA1) to delta plain (E-FA2).

2.4.2.5 Surface 5

S5 separates delta front or delta plain strata of facies association complex C or E from prodelta to delta front facies of FAC-F or offshore to lower shoreface strata of FAC-G (Fig. 2.11, Fig. 2.12, Fig. 2.13). This surface has variable expressions depending on location. In wells where offshore deposits of facies association complex G overlie FAC-E, S5 is commonly sharp and an erosional lag consisting of shell material, granules, and organic detritus may be preserved (Fig. 2.12). Locally, a thin coal seam is preserved at the top of FAC-E. Where S5 is overlain by prodelta deposits of facies association complex F, the coal defining the top of FAC-E is preserved, and the contact is sharp, with no clear evidence of erosion. S5 demarcates the contact between the Dina and Cummings formations as revised in Chapter 3.

2.4.2.6 Surface 6

S6 separates lower shoreface to offshore facies of FAC-G above from prodelta to delta front or delta plain facies of FAC-F below (Fig. 2.12, Fig. 2.13). In core, S6 is commonly expressed as a *Glossifungites* surface that is exceptionally well-developed where underlying FAC-F facies consist of fine-grained prodelta sediment (Fig. 2.12). Where FAC-F facies are comprised of sandstone this *Glossifungites* surface is more subtle, but still present. Across S6, an appreciable increase in the size of trace fossils and the homogeneity of trace fossils occurs, accompanied by a small increase in ichnodiversity.

2.4.2.7 Surface 7

S7 represents the contact between the Cummings Formation and Lloydminster Member interval and has 2 expressions depending on the depositional affinity of Lloydminster strata. Where regional, coarsening-upward cycles of the Lloydminster are present, S7 occurs within a variably thick succession of mudstone (Fig. 2.11). Here, the exact location of S7 is cryptic with offshore mudstone of the Cummings overlain by offshore/prodelta mudstone of the Lloydminster Member. In core, S7 is placed at the point where silt or very fine-grained sandstone beds of Lloydminster prodelta deposits begin increasing. This is

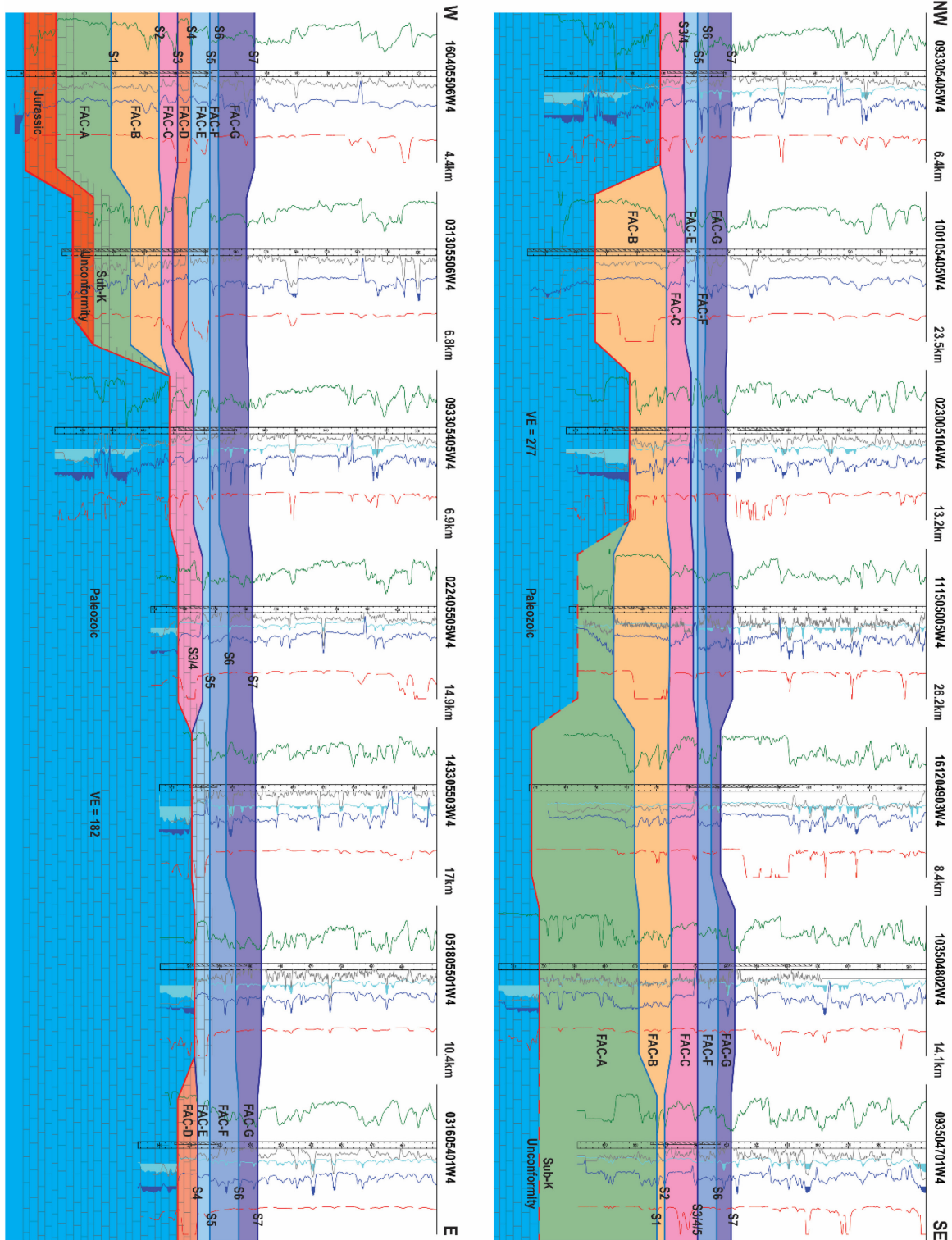
interpreted to represent the transition from transgressive Cummings Formation facies to regressive strata of the Lloydminster. On logs, S7 is placed at the point of maximum gamma ray and neutron porosity values (Fig. 2.11, Fig. 2.12). The second expression is readily identifiable as it occurs at the base of thick (up to 40 m thick) Lloydminster-aged, incised valley fill deposits which may incise down to the coal seam capping FAC-E (Fig. 2.11, Fig. 2.12). The conformable expression of S7 is mappable across the entire study area whereas the incisional expression forms elongate trends corresponding to the orientation of the incised valleys in which estuarine channel strata is deposited.

2.5 Discussion

Currently, published interpretation of Dina and Cummings member strata relevant to this study are sparse and provide only brief descriptions and interpretations for these lithostratigraphic units (Nauss, 1945; Wickenden, 1948; Ambler, 1951; Kent, 1959; Vigrass, 1977). In these papers, the Dina and Cummings are identified as comprising continental and marine strata, respectively, with attempts at regional correlations based solely on mineralogy, paleontology, and lithostratigraphic correlation of wireline logs. The current study has established that a significant proportion of the Dina and Cummings members preserves deposition in numerous environments between the continental and marine realms. Additionally, through detailed sedimentological and ichnological analysis this study has established the presence of disconformity surfaces that can be correlated on a sub-regional (township) to regional (multiple township) scale. The identification of constituent depositional environments and the presence and nature of stratigraphic discontinuities allow for a more refined understanding of the depositional evolution of the Dina and Cummings to be established.








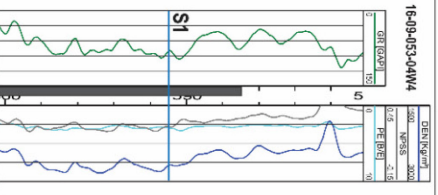
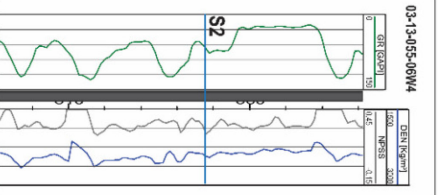
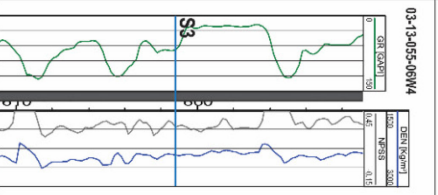
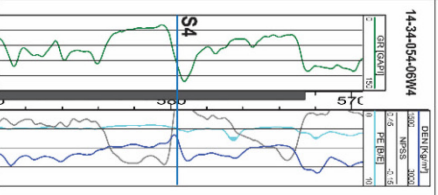
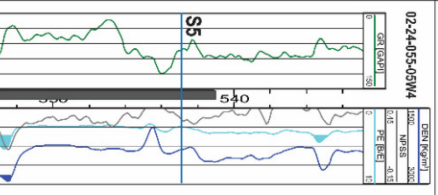
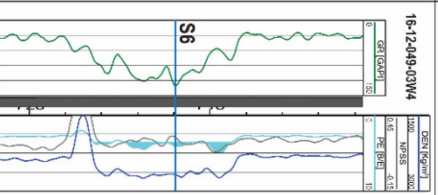
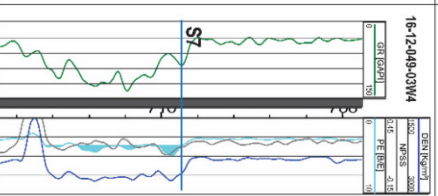
2.5.1 Spatio-Temporal Trends in Deposition

The ichnologic and sedimentologic characteristics of depositional units indicate that the Dina and Cummings members preserve deposition across a continuum of environments from continental, fluvio-tidal, estuarine/deltaic, and shoreface to offshore settings. The oldest preserved strata consist of facies associations comprising FAC-A and FAC-B. Within this continental through estuarine interval are numerous stratigraphic horizons characterized by paleosols which are of limited correlatability. Facies associations of these complexes are characterized by either purely continental trace fossil assemblages (i.e., *Scoyenia*, *Taenidium bowni*), or have low-diversity brackish-water assemblages overprinted by continental forms. Deposition of estuarine facies of facies association complex B record the onset of permanently brackish-water conditions and modulation by tidal currents.



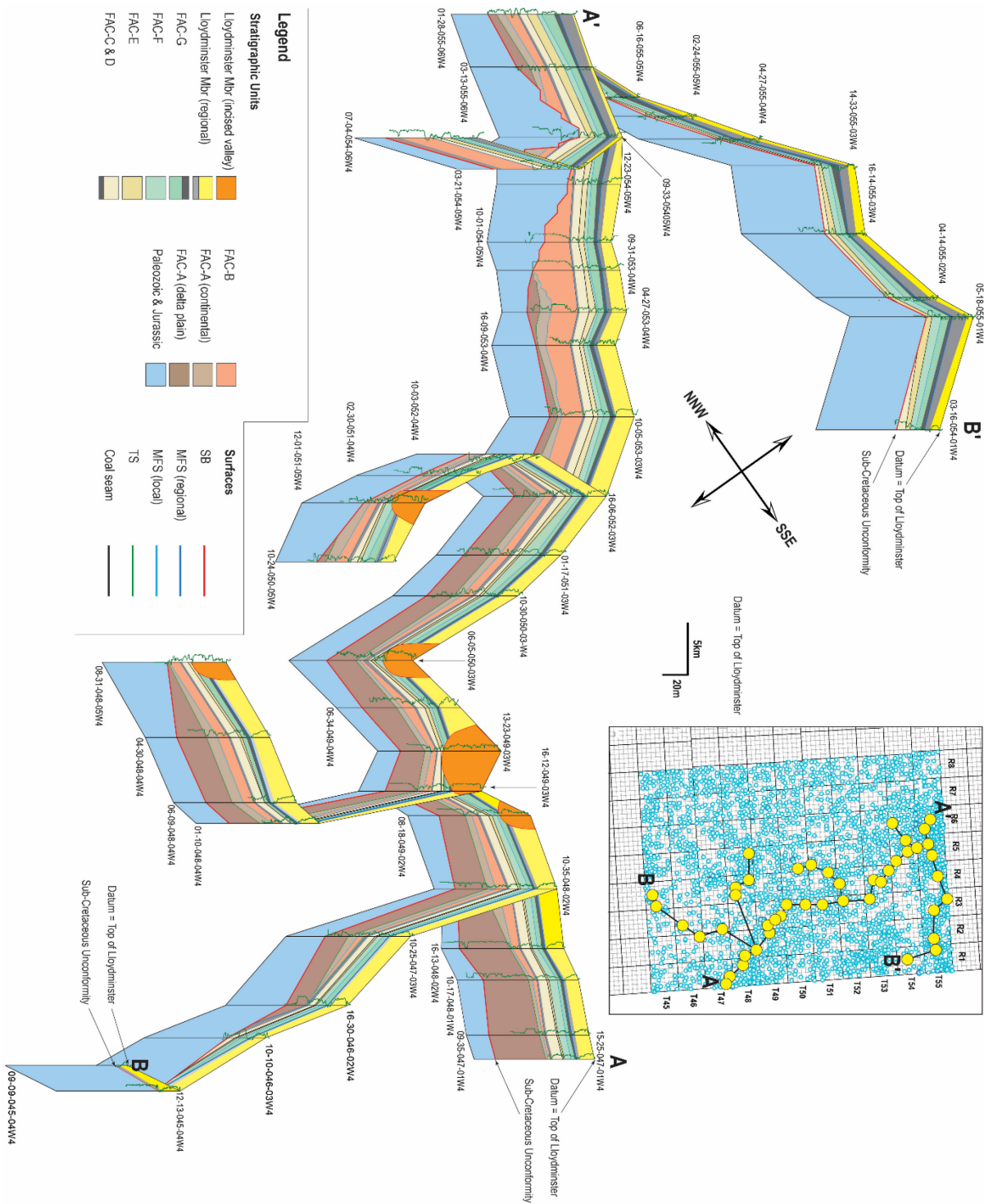
2-11) Regional NW-SE and W-E Cross-Sections

Cross-sections oriented down-dip (NW-SE) and across strike (W-E) showing the stratigraphic relationship and interpreted distribution of facies association complexes A-G. Note the different scales of vertical exaggeration. Cross-Section location shown in Figure 2.2.

| Surface Type | Bounding Facies | | Core Example | | | | |
|-----------------------------|---|---|--|--|---|---|---|
| | Above | Below | | | | | |
| Sharp ± Erosional | Lower delta plain | Floodplain |  | | | | |
| Sharp ± Erosional | Delta front/central basin | Coastal plain |  | | | | |
| Erosional | Tidal Channel/Mouth-bar | Delta front/central basin |  | | | | |
| Sharp ± Erosional | Storm-dominated delta | Delta front/central basin/ mouth-bar |  | | | | |
| Erosional | Offshore/transgressive/marine delta | Storm-dominated delta |  | | | | |
| Sharp ± Erosional | Lower shoreface | Offshore/transgressive |  | | | | |
| Erosional or Gradational | Offshore or tidal channel | Lower shoreface to offshore |  | | | | |
| Ichnio-Facies | Above | <i>Cruziana</i> (brackish) | Correlatability | | | | |
| | Below | <i>Scopelina</i> | | | | | |
| Petrophysical Log Signature | 16-09-053-04W4 | 03-13-055-06W4 | 03-13-055-06W4 | 14-34-054-06W4 | 02-24-055-09W4 | 16-12-049-03W4 | 16-12-048-03W4 |
| |  |  |  |  |  |  |  |
| | Limited - <10 km | Regional - up to 10 s km | Limited - up to <10 km | Limited - <10 km | Regional - up to 10 s km | Regional - up to 10 s km | Regional - up to 10 s km or Limited - <10 km |
| | | <i>Cruziana</i> (brackish) | <i>Skolithos</i> (brackish) | <i>Cruziana</i> (stressed marine) | <i>Cruziana</i> (stressed marine) | <i>Cruziana</i> (stressed marine) | <i>Cruziana</i> (marine) or <i>Skolithos</i> (brackish) |
| | | <i>Scopelina</i> | <i>Scopelina</i> | <i>Cruziana</i> or <i>Skolithos</i> (brackish) | <i>Skolithos</i> (stressed marine) | <i>Cruziana</i> (stressed marine) | <i>Cruziana</i> (marine) |

2-12) Stratigraphic Surface Characteristics

Core expression, descriptions of bounding facies, and petrophysical example of surfaces S1-S7.



2-13) Stratigraphic Fence Diagram

Fence diagram illustrating the interpreted architecture of Dina, Cummings, and Lloyminster Member strata within the study area. Continental and delta plain facies of FAC-A are strongly controlled by paleotopography associational with underlying Paleozoic and Jurassic strata and thin in an SSE-NNW direction with an associated thickening of estuary strata of FAC-B. All overlying FAC's are

characterized by more sheet-type geometry, with basal brackish-water mudstones of both FAC-C and marine offshore mudstones of FAC-G appearing correlative over several 10's of kilometres. FAC-A to FAC-G show a retrogradational stacking pattern with maximum transgression occurring near the contact between FAC-G and the regional Lloydminster Member (thick blue line). Abbreviations: SB = sequence boundary, MFS = maximum flooding surface, TS = transgressive surface.

Deposition of FAC-C represents the first regional incursion of brackish- to near-marine salinity waters and a change in processes from dominantly tide-modulated estuary facies to wave- and fluviually influenced coarsening upward deltaic cycles (Fig. 2.12). The thickness and aerial extent of internal coarsening-upward cycles of FAC-C are significantly greater than those of FAC-B. This suggests that deposition of facies association complex C occurred in a setting of greater accommodation and a less restricted shoreline geomorphology. The geological characteristics and stratigraphic relationships between facies association complexes A, B, and C resemble the stratigraphic architecture of the McMurray C, B, and A units defined in the AEUB Regional Geological Study (EUB, 2003).

Deposition of facies association complex D is more difficult to assess with respect to shoreline trajectory. S3, which is the contact between FAC-D and C (where mouth bar facies are present) or A (where tidal distributary channel facies are present) is clearly erosive. At least two scenarios for the genesis of facies association complex D can be proposed. In the first scenario, the scoured contacts are a result of tidal ravinement during transgression, with the sediment caliber increase resulting from the juxtaposition of high-energy channel and mouth-bar sandstone over finer-grained open embayment strata (Fig. 2.11, Table 2.1). In this scenario, S3 represents a tidal ravinement surface. A second scenario involves a basinward shift of facies resulting in incision and subsequent deposition of mixed influence incised valley fill strata. The most parsimonious interpretation is that of scenario one, due to the following observations. First, the stacking of depositional units D-F is retrogradational, displaying punctuated shoreline movement (*cf.* Helland-Hanson and Gjelberg, 1994). FAC-D is the only unit with significant evidence of tidal modulation; each successive unit is marine and wave- or storm-dominated. In scenario one, surfaces S4, S5, and S6 represent ravinement surfaces cut during transgression of the shoreline. In transgressive coasts, whether wave- or tide-dominated the tidal ravinement surface occurs stratigraphically below the wave ravinement surface (Cattaneo and Steel, 2003).

As discussed in the deposition of FAC-D, Facies association complexes E-G represent retrogradationally stacked marine deltaic and shoreface strata comprised of higher-frequency progradational cycles of sedimentation. The contacts between these depositional units fit criteria associated with ravinement surfaces including coarse lags of organic debris, granules, pyrite, shell fragments, glauconite, and substrate-controlled *Glossifungites* ichnofacies assemblages (Zecchin, 2017)

(Fig. 2.12). The top of FAC-G represents the point of maximum transgression within the Dina and Cummings interval, as sedimentological and ichnological observations of the overlying Lloydminster Member strongly suggest the onset of progradation. In contrast to underlying marine shoreface and offshore Cummings strata cored observations of the Lloydminster Member indicate significantly high-energy depositional conditions (Fig. 2.12).

It is worth discussing that the interpretation of depositional units and bounding discontinuities in this study are based on a relatively sparse core dataset, particularly when compared to other heavy oil and bitumen deposits within the WCSB (Peace River, Cold Lake, Athabasca). The limitations resulting from this paucity of data include:

- Identifying lateral sedimentological and ichnological changes within and between facies associations is significantly limited, as areas of up to 1200 km² may lack a single stratigraphic core.
- Identification of all constituent depositional environments preserved within the Dina-Cummings interval, particularly in facies association complexes A and B where stratigraphic core is biased toward channel intersections. There are almost certainly facies associations that are not represented in the core dataset.
- Assessing chronostratigraphic relationships, particularly in facies association complexes A and B is not possible at a regional scale.
- The degree of confidence with which stratigraphic surfaces can be correlated decreases with increasing distance from core control. Despite the attempt to correlate surfaces S1 to S7 using a high density petrophysical dataset (average of ca. 90 wells per township) the lithological complexity of facies has without question resulted in errors of stratigraphic correlations. As such, the placement of each surface is subject to revision in the presence of new data.

While integrated sedimentological and ichnological datasets are highly effective, the integration of other data types (e.g., seismic, coal petrology, biostratigraphy, geochronology) would better constrain the chronological and architectural relationships of various facies associations.

2.6 Conclusions

The Lower Cretaceous Dina and Cummings member in the east-central plains region of Alberta preserves strata spanning the continuum from fully continental to fully marine offshore environments. At a regional scale, these strata can be separated into seven facies association complexes. These are termed in ascending stratigraphic order FAC-A to FAC-G. These facies association complexes are comprised of 21 facies associations. Facies association complexes are bound, above and below by discontinuity surfaces of variable extent and genesis which are termed in ascending order S1-S7. These surfaces were identified

through a combination of sedimentological, lithological, and ichnological observations indicating the juxtaposition of environments that violate Walther's Law. Across each discontinuity surface (except for S3) there is a progressive increase in ichnological diversity and trace fossil size. The first indication of brackish-water sedimentation occurs in the upper facies associations of FAC-A as interpreted by the presence of ichnogenera including *Cylindrichnus*, *Gyrolithes*, and *Teichichnus*. The first presence of fully marine conditions occurs at the onset of deposition of FAC-E. Facies association complexes A-G are characterized by a retrogradational architecture, with internal facies associations being dominantly progradational with deposition resulting from punctuated shoreline movement.

Given the absence of previous detailed facies analysis within the project area, this study has added significant resolution and understanding of the depositional environments and evolution of the Dina and Cummings member interval. We have also demonstrated the utility of facies analysis in the identification of stratigraphic discontinuity surfaces in lithologically complex strata that are mappable beyond the pool scale and are independent of lithology. This work also provides a framework for subsurface activity in that it forwards the understanding of the regional distribution of both reservoir and non-reservoir baffle/barrier horizons.

2.7 References

- Ainsworth, R.B., Vakarelov, B.K., and Nanson, R.A., 2011, Dynamic spatial and temporal prediction of changes in depositional processes on clastic shorelines: Toward improved subsurface uncertainty reduction and management: *American Association of Petroleum Geologists Bulletin*, v. 95, no. 2, p. 267-297.
- Ahmad, W., and Gingras, M.K., 2022, Ichnology and sedimentology of the lower Cretaceous Wabiskaw Member (Clearwater Formation), Alberta, Canada: *Marine and Petroleum Geology*, v. 143, 105775.
- Alberta Energy and Utilities Board, 2003, Athabasca Wabiskaw-McMurray regional geological study: Alberta Energy and Utilities Board, Report 2003-A, 195 p.
- Allen, J.R.L., 1964, Studies in fluvial sedimentation: six cyclothems from the Lower Old Red Sandstone, Anglo-Welsh Basin: *Sedimentology*, v. 3, p. 163-198.
- Allen, J.R.L., 1970, Studies in fluvial sedimentation: A comparison of fining-upward cyclothems, with special reference to coarse-member composition and interpretation: *Journal of Sedimentary Petrology*, v. 40, p. 298-323.
- Ambler, J.S., 1951, The stratigraphy and structure of the Lloydminster oil and gas area: University of Saskatchewan, M.Sc. thesis
- Bann, K.L., and Fielding, C.R., 2004, An integrated ichnological and sedimentological comparison of non-deltaic shoreface and subaqueous delta deposits in Permian reservoir units of Australia: *Geological Society, London, Special Publication* v. 228, p. 273-310.
- Barton, M.D., 2016, The architecture and variability of valley-fill deposits within the Cretaceous McMurray Formation, Shell Albian sands lease, northeast Alberta: *Bulletin of Canadian Petroleum Geology*, v. 64, no. 2, p. 166-198.
- Beynon, B.M., Pemberton, S.G., Bell, D.F., and Logan, C.A., 1988, Environmental implications of ichnofossil from the Lower Cretaceous Grand Rapids Formation, Cold Lake oil sands deposit, *in*: James, D.P., and Leckie, D.A., editors, *Sequences, Stratigraphy, and Sedimentology: Surface and Subsurface*, Canadian Society of Petroleum Geologists, Memoir 15, p. 275-290.
- Bhattacharya, J.P., 2010, Deltas. *in*: James, N.P., and Dalrymple, R.W., editors, *Facies Models 4*, Geologic Association of Canada, p. 233-264.
- Bhattacharya, J.P., and MacEachern, J.A., 2009, Hyperpycnal rivers and prodeltaic shelves in the Cretaceous seaway of North America: *Journal of Sedimentary Research*, v. 79, p. 184–209.

- Botterill, S.E., Campbell, S.G., Timmer, E.R., Gingras, M.K., and Pemberton, S.G., 2016, Recognition of wave-influenced deltaic and bay-margin sedimentation, Bluesky Formation, Alberta: *Bulletin of Canadian Petroleum Geology*, v. 64, p. 389–414.
- Bown, T.M. and Kraus, M.J., 1987, Integration of channel and floodplain suites in aggrading fluvial systems I. Developmental sequence and lateral relations of lower Eocene alluvial palaeosols, Willwood Formation, Bighorn Basin, Wyoming: *Journal of Sedimentary Petrology*, v. 57, p. 587-601.
- Bromley, R.G., and Ekdale, A.A., 1984, *Chondrites*: a trace fossil indicator of anoxia in sediments: *Science*, v. 224, p. 872-874.
- Buatois, L.A., and Mangano, M.G., 1995, The paleoenvironmental and paleoecological significance of the lacustrine *Mermia* Ichnofacies: an archetypical subaqueous nonmarine trace fossil assemblage: *Ichnos*, v. 4, no. 2, p. 151–161.
- Buatois, L.A., Santiago, N., Parra, K., and Steel, R., 2008, Animal-Substrate interactions in an early Miocene wave-dominated tropical delta: delineating environmental stresses and depositional dynamics (Tacata Field, eastern Venezuela): *Journal of Sedimentary Research*, v. 86, p. 458-479.
- Buatois, L.A., Mangano, M.G., and Pattison, S.A., 2019, Ichnology of prodeltaic hyperpycnite-turbidite channel complexes and lobes from the upper Cretaceous Prairie Canyon member of the Mancos Shale, Book Cliffs, Utah, USA: *Sedimentology*, v. 66, p. 1825-1860.
- Campbell, S.G., Botterill, S.E., Gingras, M.K., and MacEachern, J.A., 2016, Event sedimentation, deposition rate, and paleoenvironment using crowded *Rosselia* assemblages of the Bluesky Formation: *Journal of Sedimentary Research*, v. 86, p. 380-393.
- Cant, D.J., 1996, Sedimentological and sequence stratigraphic organization of a foreland clastic wedge, Mannville Group, Western Canada Basin: *Journal of Sedimentary Research*, v. 66, no. 6, p. 1137-1147.
- Cant, D.J., and Abrahamson, B., 1996, Regional distribution and internal stratigraphy of the Lower Mannville: *Bulletin of Canadian Petroleum Geology*, v. 44, no. 3, 508-529.
- Carmona, N.B., Buatois, L.A., Ponce, J.J., and Mangano, M.G., 2009, Ichnology and sedimentology of a tide-influenced delta, Lower Miocene Chenque Formation, Patagonia, Argentina: trace-fossil distribution and response to environmental stresses: *Palaeogeography, Palaeoclimatology, Palaeoecology*: v. 273, p. 75–86.
- Cattaneo, A., and Steel, R.J., 2003, Transgressive deposits: a review of their variability: *Earth Science Reviews*, v. 62, no. 3, p. 187-228.
- Catuneanu, O., 2006, *Principles of Sequence Stratigraphy*: Amsterdam, Elsevier, 375 p.

- Chateau, C.C.F., Dashtgard, S.E., MacEachern, J.A., and Hauck, T.E., 2019, Parasequence architecture in a low-accommodation setting, impact of syndepositional carbonate epikarstification, McMurray Formation, Alberta, Canada: *Marine and Petroleum Geology*, v. 104, p. 168-179.
- Dalrymple, R.W. 2010, Tidal Depositional Systems. *in*: James, N.P., Dalrymple, R.W. editors, *Facies Models 4*, Geologic Association of Canada, p. 199-208.
- Dalrymple, R.W., and Choi, K., 2007, Morphological and facies trends through the fluvial-marine transition in tide-dominated depositional systems: a schematic framework for environmental and sequence stratigraphic interpretation, *Earth-Science Reviews*, v. 81, no. 3-4, p. 135-174.
- Dott, R.H., Jr and Bourgeois, J., 1982, Hummocky cross-stratification: significance of its variable bedding sequences: *Geological Society of America Bulletin*, v. 93, p. 663-680.
- Duke, W.L., 1985, Hummocky cross-stratification, tropical hurricanes, and intense storms: *Sedimentology*, v. 32, p. 167-194.
- Dumas, S., and Arnott, R.W.C., 2006, Origin of hummocky and swaley cross-stratification – The Controlling influence of unidirectional current strength and aggradation rate: *Geology*, v. 34, p. 1073-1076.
- Dumas, S., Arnott, R.W.C., and Southard, J.B., 2005, Experiments on oscillatory-flow and combined-flow bed forms: implications for interpreting parts of the shallow-marine sedimentary record: *Journal of Sedimentary Research*, v. 75, p. 501-513.
- Ekdale, A.A., Bromley, R.G., Pemberton, S.G., 1984. *Ichnology: The Use of Trace Fossils in Sedimentology and Stratigraphy*. SEPM Short Course Notes 15, 1–316.
- Fielding, C.R., 1987, Lower delta plain interdistributary deposits – an example from the Westphalian of the Lancashire Coalfield, northwest England: *Geological Journal*, v. 22, no. 2, p. 151-162.
- Frey, R.W., Pemberton, S.G., Fagerstrom, J.A., 1984. Morphological, ethological, and environmental significance of the ichnogenera *Scoyenia* and *Ancorichnus*. *J. Paleontol.* 58, 511–528.
- Frey, R.W., Pemberton, S.G., and Saunders, T.D.A., 1990, Ichnofacies and bathymetry: a passive relationship: *Journal of Paleontology*, v. 64, no. 1, p. 155-158.
- Gingras, M.K., Pemberton, S.G., Saunders, T. and Clifton, H.E. 1999. The ichnology of modern and Pleistocene brackish-water deposits at Willapa Bay, Washington; variability in estuarine settings. *Palaios*, v. 14, no. 4, p. 352–374.
- Gingras, M.K., MacEachern, J.A. and Dashtgard, S.E., 2011. Process ichnology and the elucidation of physico-chemical stress. *Sedimentary Geology*, v. 237, no. 3, p.115–134.
- Gingras, M.K., MacEachern, J.A. and Dashtgard, S.E., 2012. The potential of trace fossils as tidal indicators in bays and estuaries. *Sedimentary Geology*, v. 279, p. 97–106.

- Gingras, M.K., MacEachern, J.A., Dashtgard, S.E., Ranger, M.J., and Pemberton, S.G., 2016, The significance of trace fossils in the McMurray Formation, Alberta, Canada: *Bulletin of Canadian Petroleum Geology*, v. 64, no. 2, p. 233-250.
- Harms, J.C., Southard, J.B., Spearing, D.R., and Walker, R.G., 1975, Depositional environments as interpreted from primary sedimentary structures and stratification sequences: *Society of Economic Paleontologists and Mineralogists Short Course 2*, 161 p.
- Hasiotis, S.T. 2002, Continental Trace Fossils: *Society of Economic Mineralogist and Palaeontologists. Short Course No. 51*, 132 p.
- Hasiotis, S.T., 2007, Continental ichnology: fundamental processes and controls on trace fossil distribution, *in: Miller, W., Trace Fossil Concepts, Problems, and Prospects*, Elsevier, Amsterdam, p. 268-284.
- Helland-Hansen, W., and Martinsen, O.J., 1994, Shoreline trajectories and sequences: description of variable depositional-dip scenarios: *Journal of Sedimentary Research*, v. 66, no. 4, 670-688.
- Hembree, D., 2018, The role of continental trace fossils in Cenozoic paleoenvironmental and paleoecological reconstructions, *in: Croft, D.A., Su, D.F., and Simpson, S.W., editors, Methods in Paleocology: Reconstructing Cenozoic Terrestrial Environments and Ecological Communities, Vertebrate Paleobiology and Paleoanthropology Series*, p. 185-214.
- Hubbard, S.M, Gingras, M.K., and Pemberton, S.G., 2004, Paleoenvironmental implications of trace fossils in estuary deposits of the Cretaceous Bluesky Formation, Cadotte region, Alberta, Canada: *Fossils and Strata*, v. 51, p. 68–87.
- Ichaso, A.A., and Dalrymple, R.W., 2009, Tide- and wave-generated fluid mud deposits in the Tilje Formation (Jurassic), offshore Norway, *Geology*, v. 37, p. 539-542.
- Kent, D.M., 1959, The Lloydminster oil and gas field, Alberta: University of Saskatchewan, M.Sc. thesis, 92 p.
- Kidwell, S.M., 1989, Stratigraphic condensation of marine transgressive records; origin of major shell deposits in the Miocene of Maryland: *Journal of Geology*, v. 97, p. 1-24.
- Kraus, M.J., 1999, Paleosols in clastic sedimentary rocks: their geologic applications: *Earth-Science Reviews*, v. 47, p. 41-70.
- Kvale, E.P. 2012. Tidal constituents of modern and ancient tidal rhythmites: criteria for recognition and analyses, *in: Davis, R.A., Davis Jr, R.A., and Dalrymple, R.W., editors, Principles of Tidal Sedimentology*, Springer Netherlands, p. 1–17.
- Kvale, E.P., Johnson, H.W., Sonett, C.P., Archer, A.W. and Zawistoski, A. 1999. Calculating lunar retreat rates using tidal rhythmites. *Journal of Sedimentary Research*, v. 69, no. 6, 1154-1168.

- Longhitano, S.G., Mellere, D., Steel, R.J., and Ainsworth, R.B., 2012, Tidal depositional systems in the rock record: A review and new insights: *Sedimentary Geology*, v. 279, p. 2-22.
- MacEachern, J.A., and Pemberton, S.G., 1992, Ichnological aspects of Cretaceous shoreface successions and shoreface variability in the Western Interior Seaway of North America, *in*: Pemberton, S.G., editor, *Applications of Ichnology to Petroleum Exploration, A Core Workshop, Core Workshop 17*, SEPM Society for Sedimentary Geology, Tulsa, OK. p. 57–84.
- MacEachern, J.A., and Bann, K.L., 2008, The role of ichnology in refining shallow marine facies models, *in*: Hampson, G., Steel, R., Burgess, P., and Dalrymple, R.W., editors, *Recent Advances in Models of Siliciclastic Shallow-Marine Stratigraphy*. Society of Economic Paleontologist and Mineralogists Special Publication, v. 90, p. 73-116.
- MacEachern, J.A., and Bann, K.L., 2020, The *Phycosiphon* ichnofacies and *Rosselia* ichnofacies: two new ichnofacies for marine deltaic environments: *Journal of Sedimentary Research*, v. 90, p. 855-886.
- MacEachern, J.A., Bann, K.L., Bhattacharya, J.P., and Howell, C.D., 2005, Ichnology of deltas: organism responses to the dynamic interplay of rivers, waves, storms and tides, *in*: Bhattacharya, J.P., and Giosan, L., editors, *River Deltas: Concepts, Models and Examples*, Society of Economic Paleontologists and Mineralogists, Special Publication 83, pp. 49–85.
- MacEachern, J.A., Pemberton, S.G., Gingras, M.K., and Bann, K.L., 2010, Ichnology and facies models. *in*: James, N.P., and Dalrymple, R.W. editors, *Facies Models*, edition 4: Geological Association of Canada, St. Johns, Newfoundland, p. 19–58.
- Mack, G.H., James, W.C., and Monger, H.C., 1993, Classification of paleosols: *Geological Society of America Bulletin*, v. 105, p. 129-136.
- Mackay, D.A. and Dalrymple, R.W., 2011, Dynamic mud deposition in a tidal environment: the record of fluid-mud deposition in the Cretaceous Bluesky Formation, Alberta Canada: *Journal of Sedimentary Research*, v. 81, p. 901-920.
- Martin, K.D., 2004. A re-evaluation of the relationship between trace fossils and dysoxia, *in*: McIlroy, D. editor, *The Application of Ichnology to Paleoenvironmental and Stratigraphic Analysis*: Geological Society of London, Special Publication, v. 228, p. 141–156.
- McIlroy, D., 2004, Some Ichnological Concepts, Methodologies, Applications, and Frontiers: Geological Society of London, Special Publication, v. 288, p. 3-27.
- Melchor, R.N., Genise, J.F., Buatois, L.A., and Umazano, A.M., 2012, Fluvial environments, *in*: Knaust, D., Bromley, R.G. editors, *Trace fossils as indicators of sedimentary environments*. *Developments in Sedimentology*, v. 64, p. 329-378.

- Melnyk, S., and Gingras, M.K., 2020, Using ichnological relationships to interpret heterolithic fabrics in fluvio-tidal settings: *Sedimentology*, v. 67, p. 1069-1083.
- Metz, R., 2020, Trace fossils in fluvial deposits of the uppermost Stockton Formation (Late Triassic), Newark Basin, New Jersey: *Ichnos*, v. 27, no. 2, p. 142-151.
- Miall, A.D. 2006. The geology of fluvial deposits: Sedimentary facies, basin analysis, and petroleum geology. Springer-Verlag, Berlin.
- Mulder, T., and Alexander, J., 2001, The physical character of subaqueous sedimentary density currents and their deposits: *Sedimentology*, v. 48, p. 269-299.
- Mulder, T., Syvitski, J.P.M., Migeon, S., Faugères, J.C., and Savoye, B., 2003, Marine hyperpycnal flows: initiation, behaviour, and related deposits. A review: *Marine and Petroleum Geology*, v. 20p. 861-882.
- Nauss, A.W., 1945, Cretaceous stratigraphy of Vermillion area, Alberta, Canada: *American Association of Petroleum Geologists Bulletin*, v. 29, no. 11, p. 1605-1629.
- Nio, S.D., and Yang, C.S., 1991, Diagnostic attributes of clastic tidal deposits: a review, *in*: Smith, D.G., Reinson, C.G., Zaitlin, B.A., and Rahmani, R.A., editors, *Clastic Tidal Sedimentology*, Canadian Society of Petroleum Geology, Memoir 16, p. 3-28.
- Pemberton, S.G., Flach, P.D., and Mossop, G.D., 1982, Trace fossils from the Athabasca Oil Sands, Alberta, Canada: *Science*, v. 217, p. 825–827.
- Pemberton, S.G., MacEachern, J.A., Dashtgard, S.E., Bann, K.L., Gingras, M.K., and Zonneveld, J.P., 2012, Shorefaces. *in*: Knaust, D., and Bromley, R.G., editors, *Trace fossils as indicators of sedimentary environments*. *Developments in Sedimentology*, v. 64, p. 563-603.
- Plummer, P.S., and Gostin, V.A., 1981, Shrinkage cracks: desiccation or syneresis? *Journal of Sedimentary Petrology*, v. 51, no. 4, p. 1147-1156.
- Reading, H.G., and Collinson, J.D., 1996, *Clastic Coasts*, *in*: Reading, H.G., editor, *Sedimentary Environments: Processes, Facies and Stratigraphy*, Third Addition, Blackwell, p. 154-231.
- Reineck, H.E., 1967. Parameter von Schichtung und bioturbation. *Geologische Rundschau*, v. 56, p. 420–438.
- Reineck, H.E., 1975, German North Sea tidal flats: *in*: Ginsburg, R.N., editor, *Tidal Deposits: A casebook of recent examples and fossil counterparts*, Springer-Verlag, New York.
- Retallack, G.J., 1988, Field recognition of paleosols: *in*: Reinhardt, J., and Sigleo, W.R., editors, *Paleosols and weathering through geologic time*, Geological Society of America Special Paper, v. 2016, p. 1-20

- Savrda, C.E., and Bottjer, D.J., 1989, Trace-fossil model for reconstructing oxygenation histories of ancient marine bottom waters: application to Upper Cretaceous Niobrara Formation, Colorado: *Palaeogeography, Palaeoclimatology, Palaeoecology*, v. 74, p. 49–74.
- Shchepetkina, A., Ponce, J.J., Carmona, N.B., Mangano, M.G., Buatois, L.A., Ribas, S., and Benvenuto, M.C.V., 2020, Sedimentological and ichnological analyses of the continental to marginal-marine Centenario formation (Cretaceous), Neuquén basin, Argentina: reservoir implications: *Marine and Petroleum Geology*, v. 119, 104471.
- Seilacher, A., 1978, Use of trace fossil assemblages for recognizing depositional environments: *Trace Fossil Concepts*, Society of Economic Paleontologists and Mineralogists, Special Publication 5, p. 185-201.
- Solórzano, E.J., Buatois, L.A., Rodríguez, W.J., and Mangano, M.G., 2017, From freshwater to fully marine: exploring animal-substrate interactions along a salinity gradient (Miocene Oficina Formation of Venezuela): *Palaeogeography, Palaeoclimatology, Palaeoecology*, v. 482, p. 30-47.
- Tabor, N.J., Myers, T.S., and Michel, L.A., 2017, Sedimentologists guide for recognition, description, and classification of paleosol: *in: Zeigler, K.E., and Parker, W.G., editors, Terrestrial Depositional Systems: Deciphering complexities through multiple stratigraphic methods*, Elsevier, p. 165-208.
- Taylor, A.M. and Goldring, R. 1993. Description and analysis of bioturbation and ichnofabric; *Organisms and sediments; relationships and applications*. *Journal of the Geological Society of London*, v. 150, p. 141–148. Thomas et al., 1987
- Thomas, R.G., Smith, D.G., Wood, J.M., Visser, J., Calverley-Range, E.A. and Koster, E.H. 1987. Inclined heterolithic stratification—terminology, description, interpretation, and significance. *Sedimentary Geology*, v. 53, no. 1, p. 123–179.
- Timmer, E.R., Gingras, M.K., Morin, M.L., Ranger, M.J., and Zonneveld, J.P., 2016, Laminae-scale rhythmicity of inclined heterolithic stratification, Lower Cretaceous McMurray Formation, NE Alberta, Canada: *Canadian Society of Petroleum Geology*, v. 64, no. 2, 199-217.
- Velde, B., 2014, Green Clay Minerals: *in: Mackenzie, F.T., editor, Sediments, Diagenesis, and Sedimentary Rocks*, *in: Holland, H.D., and Turekian, K.K., editors, Treatise on Geochemistry*, v. 7, Elsevier-Pergamon, Oxford
- Vigrass, L.W., 1977, Trapping of Oil at Intra-Mannville (Lower Cretaceous) Disconformity in Lloydminster Area, Alberta, and Saskatchewan: *American Association of Petroleum Geologists Bulletin*, v. 61, no. 7, p. 1010-1028.
- Wadsworth, J., Boyd, R., Diessel, C., and Leckie, D., 2002, Stratigraphic style of coal and non-marine strata in a tectonically influenced intermediate accommodation setting: the Mannville Group of the

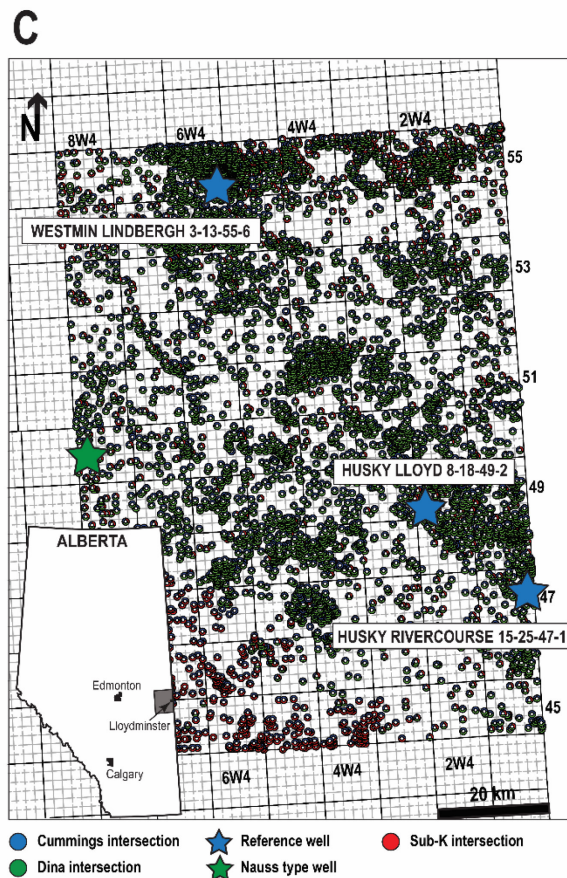
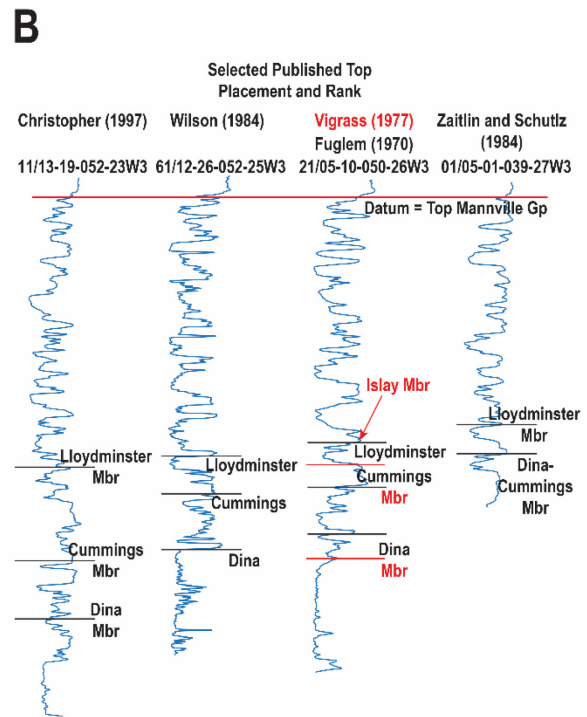
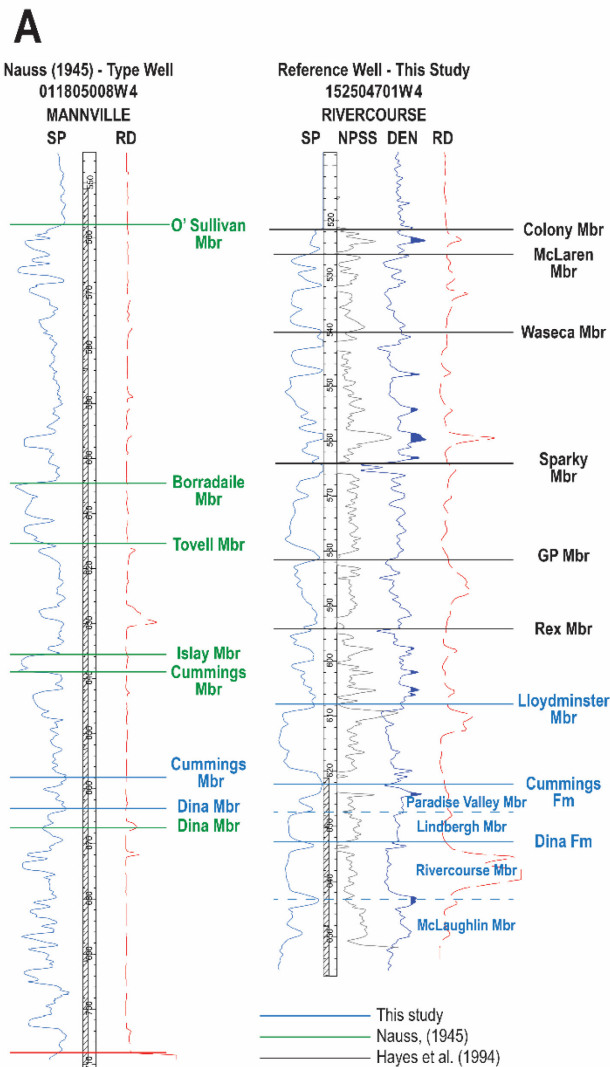
- Western Canadian Sedimentary Basin, south-central Alberta: *Bulletin of Canadian Petroleum Geology*, v. 50, no. 4, p. 507-541.
- Walker, R.G., and Cant, D.J. 1984, Sandy fluvial systems. *in*: Walker, R.G., editor, *Facies models*, Second Edition: Geological Association of Canada, 1984.
- Weleschuk, Z.P., and Dashtgard, S.E., 2019, Evolution of an ancient (Lower Cretaceous) marginal-marine system from a tide-dominated to wave-dominated deposition, McMurray Formation: *Sedimentology*, v. 66, p. 2354-2391.
- Wickenden, R.T.D., 1948, The Lower Cretaceous of the Lloydminster oil and gas area, Alberta, and Saskatchewan: Geological Survey of Canada, Paper 48-21, 15 p.
- Wright, V.P., 1992, Paleosol recognition: a guide to early diagenesis, *in*: Wolf, K.H., and Chilingarian, G.V., editors, *Diagenesis III, Developments in Sedimentology*, v. 47, p. 591-619.
- Zavala, C., Arcuri, M., and Blanco-Valiente, L., 2012, The importance of plant remains as diagnostic criteria for the recognition of ancient hyperpycnites: *Revue De Paleobiologie, Special Volume 11*, p. 457-469.
- Zecchin, M., Catuneanu, O., and Caffau, M., 2017, High-resolution sequence stratigraphy of clastic shelves V: criteria to discriminate between stratigraphic sequences and sedimentological cycles: *Marine and Petroleum Geology*, v. 85, p. 259-271.

3 Stratigraphic Revision of the Lower Cretaceous Dina and Cummings Members, Alberta, Canada

3.1 Introduction

The Lower Cretaceous Aptian to early Albian Dina and Cummings members in the east-central plains region of Alberta comprise continental, paralic, and marine siliciclastic strata deposited during southward transgression of the Boreal Sea. Together, the Dina and Cummings preserve the transgressive systems tract of the third-order Mannville depositional sequence (Cant, 1996). Comprising this third-order transgressive systems tract are several higher-order transgressive-regressive cycles which in conjunction with the inherent lithological variability characteristic of shallow marine and backshore settings has resulted in a complex spatial architecture. This complexity has led to inconsistencies in published stratigraphic top placement, hierarchical rank, and the defining geological characteristics of the Dina and Cummings interval (e.g., Nauss, 1945; Wickenden, 1948; Ambler, 1951; Kent, 1959; Fuglem 1970; Orr et al., 1977; Vigrass, 1977; Gross, 1980; Zaitlin and Schultz, 1984; Wilson, 1984; Hayes et al., 1994; Christopher, 1997; McPhee and Pemberton, 1997; Bauer et al., 2009) (Fig. 3.1A, B).

These inconsistencies can be attributed to several factors. First, many of the previous studies use a lithostratigraphic approach to correlation wherein the choice of lithological contact does not scale to regional correlations. An example with specific relevance to the study interval is the placement of the Dina top by Nauss (1945) and Kent (1959) which they define “as the base of the first shale or siltstone horizon appearing on an electric log” (Kent, 1959, p. 17). In effect, this separates channel sandstone strata from overlying syndepositional point-bar and bar-top facies into separate members. Given the potential lateral complexity of channel and floodplain environments, the placement of the Dina top at this lithological boundary has little regional meaning. Second, much of the published work on the Dina and Cummings interval within the study area was done between 1945 and 1977 when the density and quality of wireline logs and drill core was significantly less than today. Finally, the original geological interpretations of the constituent depositional environments formally defined by Nauss (1945) are not consistent with the sedimentological and ichnological characteristics of these intervals. Certainly, this is not a criticism of early workers as they lacked the high-quality datasets (core and petrophysical logs) available today. Just as importantly, they could not benefit from the decades of research in sedimentology, ichnology, and stratigraphy that enable current researchers to make more refined interpretations of depositional environments and to differentiate stratigraphic surfaces that are of local and regional significance.



3-1) Summary of Top Placement and Location Map

Variations in top placement for the Dina and Cummings interval and study location. A) Original type well of Nauss (1945) and reference well 15-25 of this study showing the original (green) and revised (blue) Dina and Cummings top placement on type well Northwest Mannville No. 1 (01-18-050-08W4M). Unit tops in black on 15-25 are interpreted from correlations with Hayes et al. (1994). B) Variation in top placement from selected publications. C) Location map showing the distribution of well intersections with the Cummings, Dina, and sub-Cretaceous unconformity on petrophysical logs.

To resolve the stratigraphic issues mentioned above a regional core and petrophysical study was undertaken. The goals of this study are two-fold: 1) to identify and assess the regional correlatability of geologically distinct stratigraphic units and their bounding surfaces over an area of 8800 km² in the east-central plains region of Alberta; and 2) if warranted, revise the definitions, boundaries, and rank of the Dina and Cummings members following the guidelines of the 2005 North American Stratigraphic Code (NASCN, 2005).

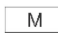

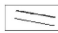






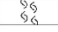

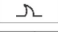


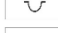











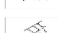
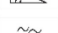





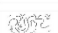



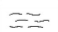









3.2 Dataset, Methods, and Historical Background

3.2.1 Dataset and Methods






The study area is in the east-central plains region of Alberta between Townships 45 and 55, and Ranges 1 and 8W4M, an area covering 8800 km² (Fig. 3.1C). The dataset consists of seventy-two drill core and petrophysical wireline logs from ca. 7800 wells. Core logging was completed at the facies scale using WellCAD[®] software with a focus on the documentation of lithology, sedimentary structures, bioturbation index, ichnogeneric identification, lithological accessories, and the presence and nature of contacts (core log symbol legend provide in Figure 3.2). Contacts observed in core were transferred to the corresponding well in Petra[®] and used as a framework for regional correlations and isopach map generation. In the absence of comprehensive geochemical datasets, a petrophysical analysis was run on a subset of 225 wells using .LAS (Log ASCII Standard) files for all available curves to evaluate the petrophysical similarity of distinct facies association complexes. For this process we started by aliasing all .LAS files to the following curve names: "GR", "DEN", "NPSS", "NPLS", "NPDL", "DPSS", "DPLS", "DPDL", "DTC", "RESD", "CILD", and "PE". Once aliased, several cut-off-based corrections were applied to the curves. Density porosity curves were converted to sandstone matrix, if necessary, by subtracting 0.04 from limestone matrix and 0.12 from dolostone matrix. Neutron porosity curves were converted to sandstone matrix, if necessary, by adding 0.03 or 0.08 to limestone or dolostone scaled curves, respectively. Neutron and density porosity curves were clipped to a range of [-.015 ,1]. Bulk density curves where culled wherever data was less than 1000 kg/m³. Deep conductivity curves were converted to deep resistivity (1000/conductivity = resistivity); resistivity values of less than 0 ohm/m were culled. Gamma-ray curves were clipped to the range of [0, 1000]. For any given curve, groups of missing values, comprising twenty or less consecutive missing values were imputed using linear interpolation.

Legend

Sedimentary Structures

| | |
|---|--|
|  Massive |  Sedimentary scour |
|  Low-angle cross-lamination |  Convolute bedding |
|  High-angle cross-lamination |  Dish structures |
|  Hummocky cross-lamination |  Synsedimentary fault |
|  Herringbone cross-lamination |  Mottled |
|  Planar cross-stratification |  Flame structure |
|  Trough cross-stratification |  Injection feature |
|  Bioturbated |  Gutter cast |
|  Crypto-bioturbation |  Fracture |
|  Vague low-angle cross-lamination |  Soft-sediment deformation |
|  Oscillation ripple cross-lamination |  Slickensides |
|  Isolated wave ripples |  Loaded ripples |
|  Combined flow ripple cross-lamination |  Undifferentiated cross-bedding |
|  Current ripple cross-lamination |  Lenticular bedding |
|  Climbing ripple cross-lamination |  Flaser bedding |
|  Starved wave ripples |  Dewatering structure |
|  Wavy bedded |  Lenses |
|  Normally graded beds |  Contorted |
|  Reverse graded beds |  Boudinage |
|  Load structures |  Bioturbated mud laminae |
|  Synaeresis cracks |  Bioturbated mud beds |
|  Double mud drape |  Wavy mud beds |
|  Mud crack |  Pinstripe bedding |
|  Reactivation surface | |














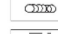




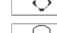

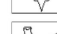
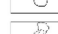



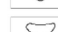
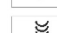
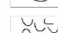

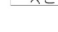
Surfaces

| | |
|---|----------------------------|
|  | Formation contact |
|  | Member unit contact |
|  | Depositional unit contact |
|  | Facies association contact |
|  | Unconformity |



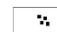
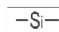



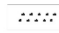
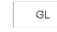


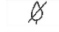


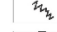

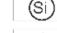


Lithology

| | |
|---|--------------|
|  | Missing core |
|  | Coal |

Ichnofossils

| | | | |
|---|----------------------------|---|-----------------------|
|  | <i>Skolithos</i> |  | <i>Cylindrichnus</i> |
|  | <i>Diplocraterion</i> |  | <i>Bergaueria</i> |
|  | <i>Asterosoma</i> |  | <i>Rhizocorallium</i> |
|  | <i>Chondrites</i> |  | <i>Arenicolites</i> |
|  | <i>Zoophycos</i> |  | <i>Gyrolithes</i> |
|  | <i>Palaeophycus</i> |  | <i>Taenidium isp.</i> |
|  | <i>fugichnia</i> |  | <i>Scolicia</i> |
|  | <i>Thalassinoides</i> |  | <i>Macaronichnus</i> |
|  | <i>Planolites</i> |  | <i>Nereites</i> |
|  | <i>Ophiomorpha</i> |  | <i>Cosmoraphe</i> |
|  | <i>Rosselia</i> |  | <i>Conichnus</i> |
|  | <i>Schaubcylindrichnus</i> |  | <i>Navichnia</i> |
|  | <i>Helminthopsis</i> |  | <i>Undiff Burrow</i> |
|  | <i>Phycosiphon</i> |  | <i>Lockeia</i> |
|  | <i>Teichichnus</i> |  | <i>Shell Debris</i> |

Accessories

| | | | |
|---|---------------------|---|-------------------|
|  | Coal laminae |  | Granule/pebble |
|  | Coal fragment |  | Siderite layer |
|  | Mudstone interclast |  | Shale laminae |
|  | Pyrite |  | Sand laminae |
|  | Glauconite |  | Silt laminae |
|  | Wood fragments |  | Plant debris |
|  | Carbonaceous debris |  | Kaolinite |
|  | Carbonaceous drapes |  | Mud-filled crack |
|  | Siderite nodules |  | Sand-filled crack |
|  | Rootlets | | |

Bioturbation Index



3-2) Legend of Symbols

Legend of symbols appearing on core logs.

3.2.2 Historical Background

3.2.2.1 Dina Member

Nauss (1945) was the first to formally define the Dina as a member within his Mannville Formation from type well Northwest Mannville No. 1 (01-18-050-08W4M) (Fig. 3.1). They defined the Dina as consisting of well-rounded and frosted quartz grains with interbedded silt and shale ranging from 0–150 feet in thickness. They noted that thicker intervals correspond to lows along the “Paleozoic unconformity.” Their depositional interpretation of the Dina Member was that it represented a beach-type sandstone deposit. Nauss (1945) chose member rank for the Dina based on his observation that the interval was of

limited areal extent. Noting similar lithological characteristics, Ambler (1951) and Kent (1959) agreed with Nauss (1945) that the Dina was attributable to deposition in a beach setting. Based on data not available to Nauss, Kent (1959) proposed elevating the Dina to formation rank and placed the top of the Dina at the base of the first shale horizon observed on electric logs. Wickenden (1948) interpreted the Dina as being a member in their basal division of the Mannville and considered the Dina to be continental in origin. Orr et al. (1977) identified the Dina as a formation within the Mannville, defining it as the course-grained sandstone filling topographic lows along the “Paleozoic unconformity”. Vigrass (1977) defined the Dina as a member within his lower Mannville and described it as a quartz sandstone with partings of coaly material and dark-grey shale. Vigrass (1977) seemingly first pointed out that the position of the Dina top at the start of the initial shale interval did not distinguish between continental and marine strata. He further suggested that such placement was simply a matter of convenience for the industry. Gross (1980) attempted to map the distribution of “shoe-string” and blanket sand bodies of the Dina and Lloydminster (among others) over a large area of Alberta based upon log motifs. They interpreted depositional environment from these log motifs by assigning “electro-facies.” They interpreted the shoe-string sand bodies (i.e., Dina) as being comprised of channel deposits. Zaitlin and Schultz (1984) refer to the Dina and Cummings interval in the Senlac Heavy Oil Pool (Townships 38–39, Ranges 26–27 W3M) as the Dina-Cummings Member. They describe the interval as “a 10-30 m fining-upward sequence of sandstone, siltstone and shales containing pyritized rootlets and a restricted trace fossil assemblage (*Palaeophycus heberti*, *Conichnus*, *Lockeia*, and *Thalassinoides*) (Zaitlin and Schultz, 1984, p. 1). Christopher (1997) classifies the Dina and Cummings as members of the Cantaur Formation, which they demonstrated to straddle the boundary region between the provinces of Alberta and Saskatchewan (Christopher, 1997, Fig. 2, p. 3). Christopher (1997) interpreted the Dina as comprising fining-upward meandering fluvial to estuarine channels, and coarsening upward estuarine bars, bay mouth bars, or lower estuary shoreface bars. Kohlruss (2012) conducted a study on the Dina Member in northwest Saskatchewan over a four-township area and recognized the Dina as comprising fluvial to fluvio-tidal channel and overbank facies filling incised valleys.

3.2.2.2 *Cummings Member*

Nauss (1945) was the first to formally define the Cummings as a member within what they defined as the Mannville Formation from type well Northwest Mannville No. 1 (01-18-050-08W4M). They described the Cummings as a dark grey to black shale with abundant pyrite, foraminifera, and salt-and-pepper sands with a basal coal seam. Kent (1959) considered the Cummings Formation to be the light-grey glauconitic sand, siltstone, and shale interval containing foraminifera. They placed the upper contact at the last occurrence of glauconite/first occurrence of quartz sand and the basal contact at the first

occurrence of shale visible on electric logs. Vigrass (1977) described the Cummings Member as a fine-grained glauconitic sandstone with interbeds of shale containing marine forams and other marine fossils. Christopher (1997) interpreted the Cummings as back-barrier or bay-chenier facies, lagoons, and tidal inlets.

3.3 Stratigraphic Revision

A review of previous publications highlights the differences in interpretation of stratigraphic top placement, rank, and constituent geological facies. The work of Nauss (1945) represents the establishment of the Dina and Cummings members and his definitions for these lithostratigraphic intervals have not been formally revised. Based on the facies (Chapter 2) and petrophysical analysis, a revised definition of the Dina and Cummings is proposed. Below, we provide the elements required by the North American Stratigraphic Code (NASCN, 2005) to formally revise the Dina and Cummings of Alberta (Fig. 3.3). The revised definitions provide a more robust and inclusive set of criteria for identifying both units within the subsurface, with a primary focus on both sedimentological characteristics observable in core and petrophysical attributes that are useful for regional correlations.

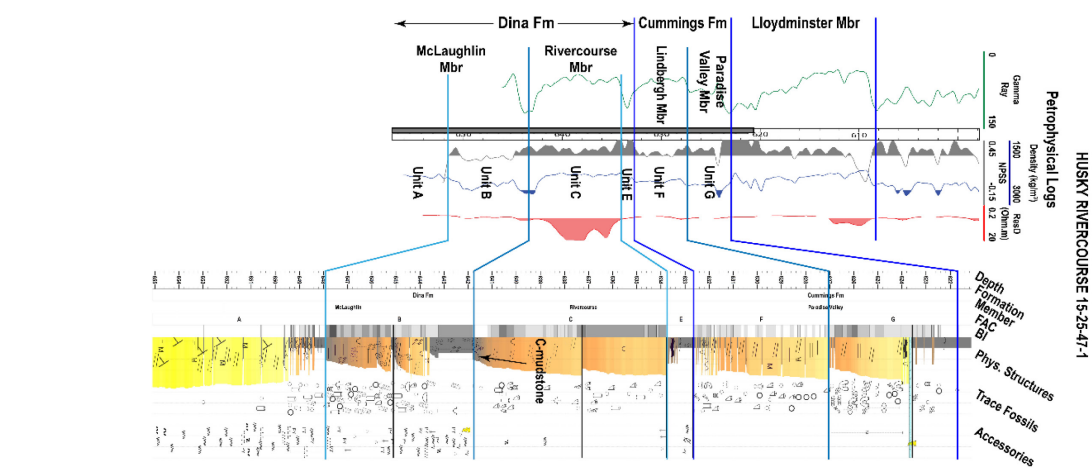
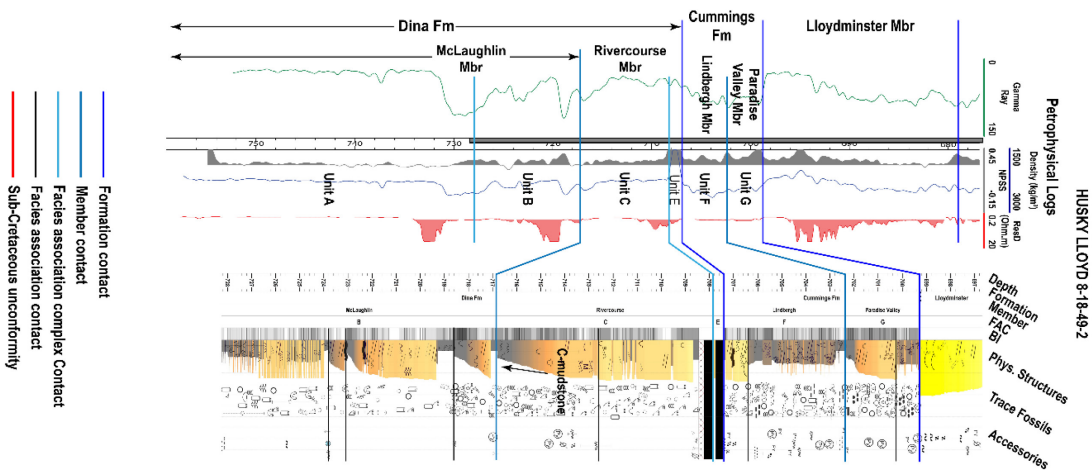
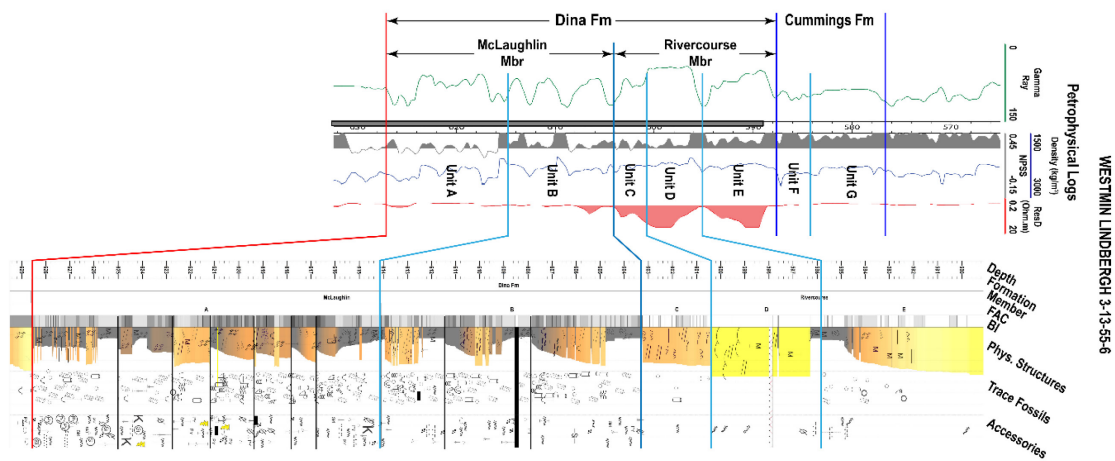
3.3.1 Revision of the Dina Member

3.3.1.1 *Utility and Rank*

Revising the geological definition and boundaries of the Dina Member of Nauss (1945) by using stratigraphic disconformity surfaces in place of arbitrary lithological contacts enables more geologically consistent regional correlations. The advantage of establishing a uniform framework is that it addresses regulatory matter. This includes resolving issues like pore space competition, identifying regional reservoirs, and determining potential connections between hydrocarbon pools and aquifers. Having a framework based on stratigraphic breaks, rather than on lithological tops, will aid in reducing such issues of disagreement or equity among operators and other stakeholders. We propose elevation of the Dina Member (Nauss, 1945) to formation rank, with the formal recognition of two internal members, the McLaughlin, and Rivercourse (Fig. 3.1, Fig. 3.3, Fig. 3.4, Fig. 3.5; Table 3.1). These members derive their names from the nearby communities of McLaughlin and Rivercourse which are situated close to type wells designated as HUSKY RIVERCOURSE 15-25-47-1 and HUSKY LLOYD 08-18-49-2, respectively.

3.3.1.2 *Stratotype and Locality*

The composite stratotype for the revised Dina Formation consists of the interval from 664.5 m to 707.4 m TVD in the original type section in Northwest Mannville No. 1 (01-18-050-08W4M) (Fig. 3.1) as well as reference section intervals in three wells: HUSKY RIVERCOURSE 15-25-47-1 (hereafter referred to



- Formation contact
- Member contact
- Facies association complex Contact
- Facies association contact
- Sub-Cretaceous unconformity

3-4) Reference Logs

Revised stratigraphic top placement of the Dina and Cummings formations, and McLaughlin, Rivercourse, Lindbergh, and Paradise Valley members, and facies association complexes A–G in reference wells WESTMIN LINDBERGH 3-13-55-06, HUSKY LLOYD 8-18-49-2 and HUSKY RIVERCOURSE 15-25-47-1. A legend of symbols on core logs is provided in Figure 3.3. Shaded cut-offs are 40% for NPSS log, 2500 kg/m³ for the density log, and 3 ohm/m for the deep resistivity log.

Table 3-1

Sedimentological and ichnological characteristics of facies associations and facies association complexes of the Dina and Cummings lithostratigraphic units.

| FAC | FA | Sedimentary Structures | Ichnogenera | | | Accessories | Interpretation |
|-------|-------|--|---------------------|-----------------|--|---|---|
| | | | BI (rng) | BI (ave) | Ichnogenera | | |
| FAC-A | A-FA1 | trough & planar tabular cross-bedding, low-angle & planar cross-lamination, current ripples, grain striping, massive fabric, soft-sediment deformation | S=0-1; F=0-6 | S=0; F=2 | <i>Planolites, Palaeophycus, Skolithos, Taenidium, rootlets, rhizoliths</i> | carbonaceous detritus, wood debris, pyrite, mud clasts | continental fluvial channel, point-bar |
| | A-FA2 | current ripples, low-angle planar lamination, mottled, massive, convolute lamination, soft-sediment deformation, lenticular bedding, normally-graded beds, pedogenic slickensides | F=1-3; S=1-3 | F=1; S=2 | <i>Taenidium bowni, Taenidium, Skolithos, Planolites, rootlets, rhizoliths</i> | pyrite, coal fragments, siderite nodules, plant debris, iron staining, sand laminae, silt laminae | floodplain - proximal to distal |
| | A-FA3 | trough & planar tabular cross-bedding, low-angle planar, current & combined flow ripple cross lamination, massive, wavy-bedded, mottled, lenticular bedding, convolute lamination, double mudstone drapes, rhythmic lamination | S=0-1; F=2-5 | S=0; F=3 | <i>Arenicolites, Planolites, Palaeophycus, Skolithos, Taenidium, rootlets</i> | pyrite (nodular and disseminated), carbonaceous detritus, coal fragments, mud clasts | fluviially dominated, tide-influenced channel, point-bar, and bar-top |
| | A-FA4 | low-angle planar & current ripple cross-lamination, faint cross-lamination, massive, mottled, double mudstone drapes | S=0-3 | S=1 | <i>?Conichnus, fugichnia, Lockeia, Planolites, rootlets, Skolithos, Taenidium isp, Rhizoliths</i> | organic detritus, rare mud drapes, pyrite | distributary channel |
| | A-FA5 | wavy bedded, bioturbated, lenticular, current ripple & low-angle cross-laminated, convolute lamination, mottled. | S=1-5; F=0-4 | S=3; F=2 | <i>Cylindrichnus, Gyrolithes, rootlets, Planolites, Skolithos, Taenidium, Teichichnus</i> | organic detritus, pyrite, granules, iron stain, coal laminae, clasts with altered rims | Interdistributary bay fill/crevasse splay |
| FAC-B | B-FA1 | wavy bedding, lenticular bedding, flaser bedding, convolute lamination, low-angle planar, current & combined flow ripple cross-lamination, normally graded beds, synaeresis cracks, load casts | Fsm=0-3; Fms=0-2 | Fsm=3; Fms=1 | <i>Arenicolites, Cylindrichnus, fugichnia, Lockeia, Palaeophycus, Planolites, rootlets, Skolithos, Taenidium, Teichichnus, Thalassinoides</i> | mud clasts, organic detritus, pyrite | tide-influenced, wave-affected tidal delta |
| | B-FA2 | low-angle planar, current, and oscillation ripple cross-lamination, hummocky cross-stratification, wavy bedding, mottled, lenticular bedding, massive, faint low-angle cross-lamination | F=2-5; S=0-3 | F=3; S=1 | <i>Arenicolites, Cylindrichnus, Diplocraterion, fugichnia, Gyrolithes, Paleophycus, Planolites, Siphonichnus, Taenidium, Teichichnus, Thalassinoides</i> | pyrite, organic detritus, coal fragments, silt laminae, siderite cement | wave- and tide-influenced bay-margin |
| | B-FA3 | oscillation ripple cross-lamination, wavy bedding, mottled, lenticular bedding, massive, faint low-angle cross-lamination | F=2-5; S=2-5 | F=3; S=3 | <i>Arenicolites, Cylindrichnus, Diplocraterion, fugichnia, Gyrolithes, Paleophycus, Planolites, Siphonichnus, Taenidium, Teichichnus, Thalassinoides</i> | pyrite, organic detritus, coal fragments, silt laminae, siderite cement | wave-influenced bay-margin |

| | | | | | | | |
|-------|-------|--|-----------------|-------------|--|---|--|
| | B-FA4 | trough & planar tabular cross-bedding, massive, low-angle, planar, current ripple, & combined flow ripple cross-lamination, grain-stripping, double mudstone drapes, rhythmic lamination | S=0-2; F=0-5 | S=0; F=2 | <i>Arenicolites, Cylindrichnus, Gyrolithes, Planolites, Psilonichnus, rootlets, Skolithos, Taenidium</i> | mud clasts, organic detritus | tide- and fluviially influenced channel, point-bar, and tidal flat |
| FAC-C | C-FA1 | trough cross bedding, low-angle planar & hummocky cross-stratification, convolute lamination, combined flow-ripple cross-lamination, synaeresis cracks, normally graded beds, micro-faults, fluid escape structures. | S=0-2; F=0-3 | S=0; F=1 | <i>Cylindrichnus, fugichnia, Palaeophycus, Planolites, rootlets, Skolithos, Taenidium, Teichichnus</i> | coal fragments, pyrite, organic detritus, carbonaceous drapes | river-dominated, wave-influenced delta |
| | C-FA2 | hummocky cross-stratification, trough cross bedding, low-angle planar & convolute lamination, combined flow-ripple cross-lamination, convolute lamination, synaeresis cracks, normally graded beds, micro-faults, fluid escape structures. | S=0-2; F=0-3 | S=0; F=1 | <i>Cylindrichnus, fugichnia, Palaeophycus, Planolites, rootlets, Skolithos, Taenidium, Teichichnus</i> | coal fragments, pyrite, organic detritus, carbonaceous drapes | wave-dominated delta |
| | C-FA3 | low-angle planar & vague cross-lamination, combined flow ripples, flaser bedding, oscillation & combined flow ripple cross-lamination, convolute lamination, synaeresis cracks, normally graded beds | S=1-5; F=1-4 | S=3; F=2 | <i>Arenicolites, Asterosoma, Berguaeria, Cylindrichnus, fugichnia, Gyrolithes, Helminthopsis, Ophiomorpha, Palaeophycus, Planolites, rhizoliths, rootlets, Skolithos, Taenidium, Teichichnus, Thalassinoides</i> | organic detritus, coal fragments, wood debris, pyrite, carbonaceous drapes | bay-margin shoreface to offshore |
| FAC-D | D-FA1 | trough cross-bedding, low-angle planar cross-lamination, massive fabric, combined flow ripples, dish and pillar, flame structure, fluid escape structures, double mud drapes, convolute lamination, synaeresis cracks, load casts, pinstripe lamination, micro-folds | S=0-2; F=0-2 | S=1; F=1 | <i>Berguaeria, fugichnia, navichnia, Rhizocorallium, Planolites, Skolithos, Teichichnus, Thalassinoides</i> | coal fragments, carbonaceous debris, plant debris, pyrite, siderite cement, siltstone laminae | tide-,wave-, and river-influenced distributary channel |
| | D-FA2 | trough cross-bedding, low-angle planar cross-lamination, hummocky cross-stratification, massive fabric, combined flow ripples, double mud drapes, convolute lamination, synaeresis cracks, load casts, pinstripe lamination | S=0-2; F=0-5 | S=1; F=3 | <i>Berguaeria, fugichnia, navichnia, Rhizocorallium, Planolites, Skolithos, Teichichnus, Thalassinoides</i> | coal fragments carbonaceous debris, plant debris, pyrite, siderite cement, siltstone laminae | tide-,wave-, and river-influenced delta front |
| | D-FA3 | trough cross-bedding, low-angle planar cross-lamination, massive fabric, combined flow ripple cross-lamination, lenticular bedding | S=0-1; F=0-1 | S=0; F=0 | <i>Planolites</i> | abundant coal fragments, pyrite, wood debris | mouth bar |
| FAC-E | E-FA1 | trough cross-bedding, low-angle planar, & hummocky cross-stratification, climbing ripples, flame structures, convolute lamination, flaser bedding, flaser bedding, load casts, double mud drapes, scour surfaces | S=0-3; F=1-3 | S=1; F=1 | <i>Berguaeria, Chondrites, Cylindrichnus, Diplocraterion, fugichnia, Lockeia, Macaronichnus, navichnia, Ophiomorpha, Palaeophycus, Phycosiphon, Planolites, Rhizocorallium, Rosselia, Skolithos, Teichichnus, Thalassinoides</i> | organic detritus, coal fragments, wood fragments, pyrite, siderite cement | storm-influenced marine delta |
| | E-FA2 | current ripples, mottled, massive, convolute lamination, soft-sediment deformation, lenticular bedding, pedogenic slickensides | F=1-3; S=1-3 | F=1; S=2 | <i>Taenidium bowni, Taenidium, Skolithos, Planolites, rootlets, rhizoliths</i> | pyrite, coal fragments, plant debris, sand laminae, silt laminae | delta plain |

| | | | | | | | |
|-------|-------|---|-----------------|-------------|--|---|---------------------------------|
| FAC-F | F-FA1 | low-angle, planar, & hummocky cross-stratification, oscillation, & combined flow ripples, soft sediment deformation, fluid escape structures, syneresis cracks, normally graded beds, convolute lamination, load casts, fluid muds, double mud drapes | S=0-2; F=1-3 | S=1; F=2 | <i>Arenicolites, Asterosoma, Berguaeria, Cylindrichnus, Diplocraterion, fugichnia, Gyrolithes, Helminthopsis, Ophiomorpha, Palaeophycus, Phycosiphon, Planolites, Rhizocorallium, Rosselia, Skolithos, Teichichnus, Thalassinoides</i> | pyrite, organic detritus | river- and wave-influence delta |
| | F-FA2 | low-angle planar & hummocky cross-stratification, current, combined flow, & oscillation ripple cross-lamination, fluid mud, convolute lamination, load casts, micro-faults, flame structure, double mud drapes, fluid escape structures, | S=0-4; F=0-3 | S=1; F=2 | <i>Arenicolites, Asterosoma, Berguaeria, Chondrites, Cylindrichnus, Cosmorhaphie, Diplocraterion, Helminthopsis, Palaeophycus, Phycosiphon, Planolites, Rhizocorallium, Skolithos, Teichichnus, Thalassinoides, Zoophycos</i> | glauconite, organic detritus, pyrite, coal fragments, calcite cement | tide- and wave-influenced delta |
| | F-FA3 | low-angle planar & hummocky cross-stratification, combined flow & oscillation ripple cross-lamination, normally graded beds, double mud drapes | S=0-3; F=0-3 | S=1; F=2 | <i>Arenicolites, Asterosoma, Chondrites, Cylindrichnus, Helminthopsis, navichnia, Palaeophycus, Phycosiphon, Planolites, Rhizocorallium, Scolicia, Skolithos, Teichichnus, Thalassinoides, Zoophycos</i> | glauconite, carbonaceous debris, pyrite, siderite, shell debris, granules | transgressive lag |
| FAC-G | G-FA1 | low-angle planar & hummocky cross-stratification, combined flow & oscillation ripple cross-lamination | S=0-5; F=1-5 | S=2; F=3 | <i>Arenicolites, Asterosoma, Berguaeria, Chondrites, Cosmorhaphie, Cylindrichnus, Diplocraterion, Helminthopsis, Nereites, Ophiomorpha, Palaeophycus, Phoebichnus, Phycosiphon, Planolites, Rhizocorallium, Rosselia, Schaubcylindrichnus freyi, Scolicia, Skolithos, Teichichnus, Thalassinoides, Zoophycos</i> | glauconite, carbonaceous debris, pyrite | marine lower shoreface to shelf |

3.3.1.3 Geological Description

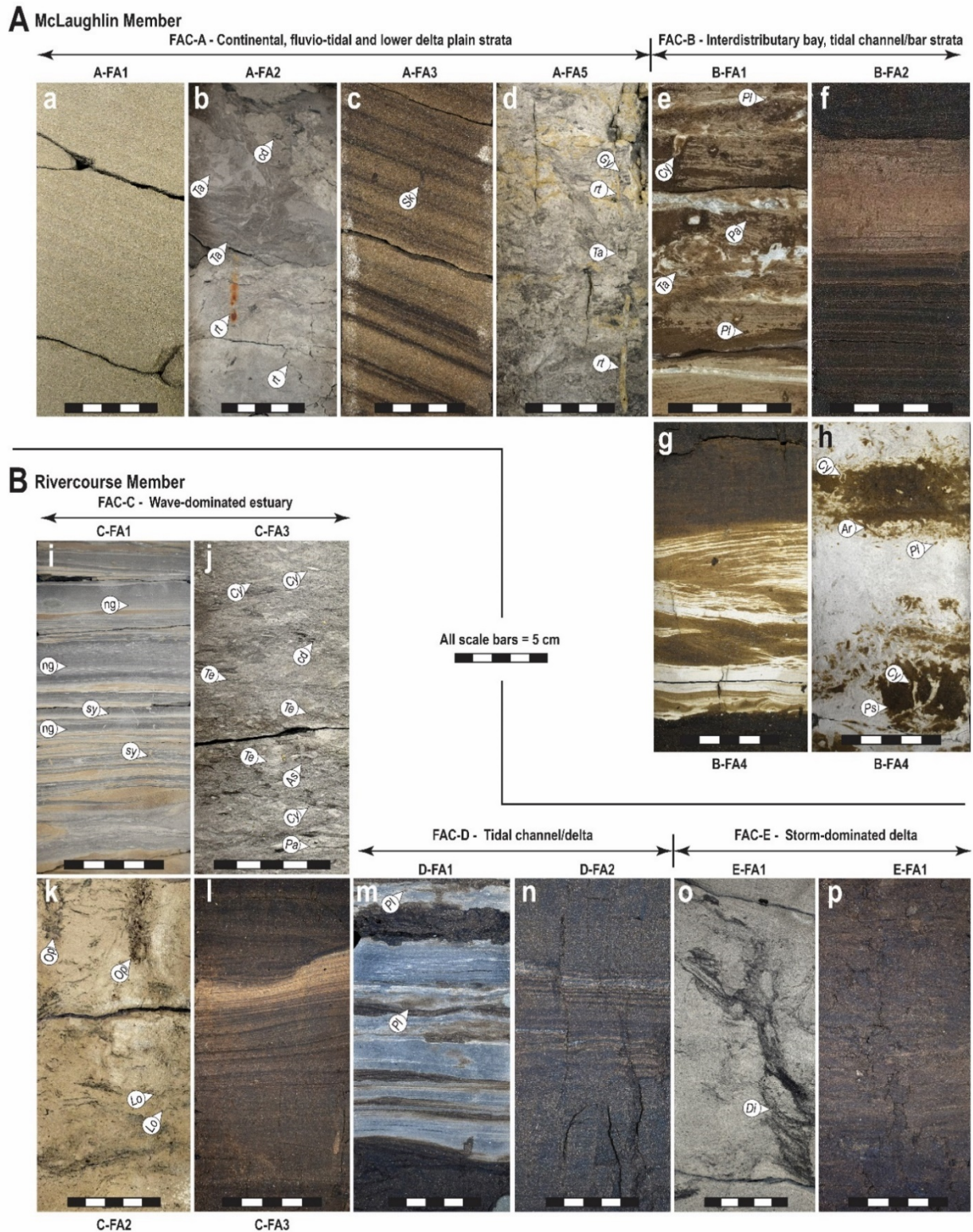
McLaughlin Member

The McLaughlin Member consists of retrogradationally stacked fluvial, fluvio-tidal, and upper to middle estuary strata of FAC-A and FAC-B (Table 3.1) and is the lowermost Cretaceous unit preserved within the study area (Fig. 4.4, Table 4.1). Within the study area, it unconformably overlies Devonian or Jurassic strata. The defining geological characteristics of the McLaughlin are as follows. Strata include deposition in a continuum of environments from continental channel and floodplain through to various paralic environments including lower delta plain distributary channels and interdistributary bays, and tidal channel and tidal flat settings (Chapter 2). In all core observations of the McLaughlin Member, the vertical succession consists of continental or fluvio-tidal strata progressively overlain by paralic facies. Where multiple channels are preserved in the same vertical succession, an upward increase in tidal sedimentary structures is observed. Second, within the McLaughlin are several horizons characterized by variable degrees of pedogenic alteration, with paleosol types including protosols, vertisols, histosols, and gleysols (terminology after Mack et al., 1993). These paleosol horizons are typically of limited correlatability and represent hiatal surfaces of non-deposition or sediment bypass. Third, as with the aforementioned

paleosol horizons, facies associations within the McLaughlin are of limited areal extent. This leads to difficulty in establishing chronostratigraphic relationships between different facies associations. Fourth, facies associations are characterized primarily by sedimentary structures generated by tidal and fluvial currents, with wave-generated structures largely confined to the uppermost facies of facies association complex B (Fig. 3.5A). Finally, the McLaughlin is characterized by a distinct type and range of trace fossil assemblages not observed within overlying members. These include: 1) a continental assemblage characterized by abundant meniscate backfilled burrows including *Taenidium bowni*, and *Scoyenia* with abundant roots and rhizoliths; 2) assemblages characteristic of brackish-water sedimentation including *Cylindrichnus*, *Gyrolithes*, *Psilonichnus*, and *Teichichnus* that are overprinted by the previously described continental fabric; and 3) brackish-water assemblages lacking overprint by continental forms, with this assemblage type restricted to facies association complex B (Fig. 3.6). No trace fossils strongly associated with marine salinity conditions were observed (e.g., *Cosmorhapha*, *Nereites*, *Phycosiphon*, *Scolicia*, *Zoophycos*) were observed.

Rivercourse Member

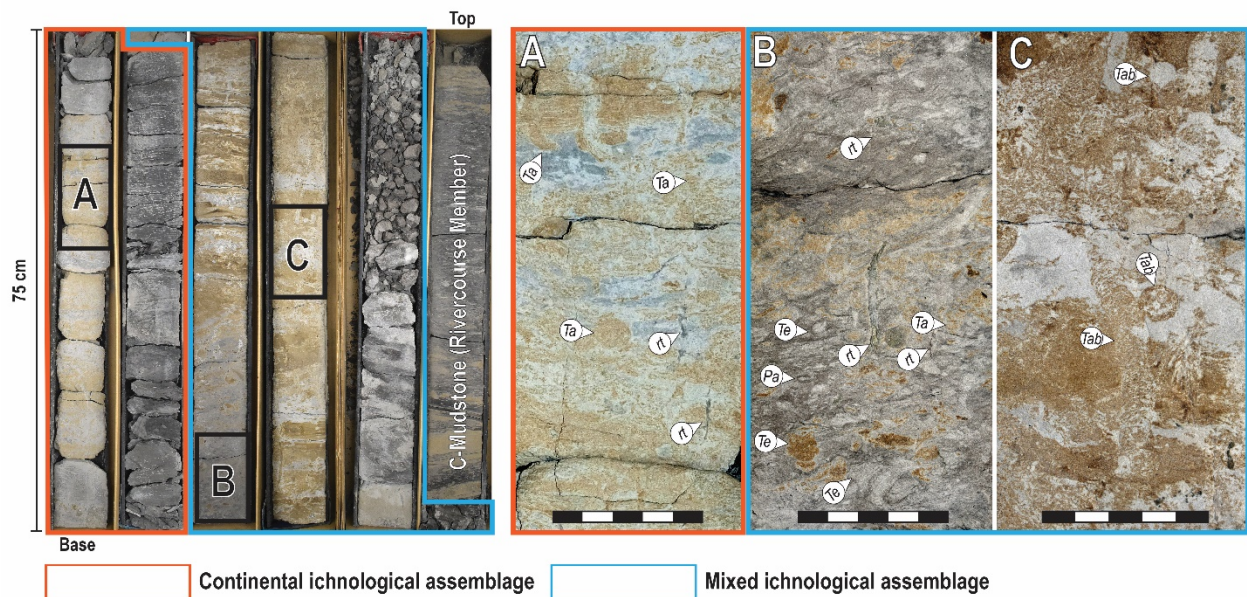
The Rivercourse Member consists of one to multiple coarsening-upward progradational cycles bound by local stratigraphic discontinuities that are interpreted to represent within-trend flooding surfaces (Fig. 3.4, Fig. 3.5; Table 3.1). The Rivercourse is composed of facies deposited in wave-dominated estuary (FAC-C), tidal channel and mouth-bar (FAC-D), and storm-dominated deltaic environments (FAC-E). Facies association complex C is further divisible into three syndepositional environments: bayhead delta (C-FA1), bay margin and central basin (C-FA2), and barrier bar (C-FA3). Superficially, facies of FAC-C resemble those of McLaughlin strata of FAC-B. However, the average thickness and lateral extent of coarsening-upward cycles and bioturbated mudstone horizons are greater and more laterally continuous in the Rivercourse Member. Facies association complex's C and E of the Rivercourse Member are characterized by a moderate to diverse trace-fossil assemblage, with highly variable bioturbation index values. The ichnological assemblage includes *Arenicolites*, *Asterosoma*, *Berguaeria*, *Chondrites*, *Cylindrichnus*, *Diplocraterion*, *fugichnia*, *Gyrolithes*, *Helminthopsis*, *Lockeia*, *navichnia*, *Ophiomorpha*, *Palaeophycus*, *Planolites*, *rhizoliths*, *rootlets*, *Skolithos*, *Taenidium*, *Teichichnus*, and *Thalassinoides*. In contrast, FAC-D is characterized by absent to low bioturbation index values and a comparatively low-diversity assemblage consisting of *Berguaeria*, *fugichnia*, *navichnia*, *Rhizocorallium*, *Planolites*, *Skolithos*, *Teichichnus*, and *Thalassinoides*.



3-5) McLaughlin and Rivercourse Member Facies

Selected facies of the McLaughlin (A) and Rivercourse (B) members, including examples from the broader 72 core dataset. A) a–c, channel sandstone from fluvial (a) and tidal-fluvial (c) channels with possible rhythmicity in C and floodplain facies (b) with

visible pedogenic alteration including colour mottling and rooting, and (c) low-angle cross-stratification. d) highly bioturbated silty to muddy sandstone interdistributary bay facies with sand-filled rootlets (rt), *Gyrolithes* (Gy), and *Taenidium isp* (Ta). e–h, brackish embayment facies including tidal bar (e), bay margin shoreface (f), and point-bar and tidal flat (G, H). Tidal modulation is inferred from the presence of double mudstone drapes (g), with brackish water indicated by *Cylindrichnus* (Cy), and *Psilonichnus* (Ps). B) i, j, prodelta and central embayment mudstone facies of C-FA1 and C-FA2 (Table 1, Botterill et al., 2023, in prep) displaying graded beds, and syneresis cracks (sy), and abundant *Teichichnus* (Te), and lesser *Cylindrichnus* (Cy) and *Palaeophycus* (Pa) (B). k, l, sandstone facies of C-FA2 and C-FA3 displaying *Ophiomorpha* (Op), *Cylindrichnus* (Cy), and *Planolites* (Pl) (k) and low-angle curvilinear cross-lamination (l). M, N, heterolithic tidal channel/delta facies with characteristic blue-grey mudstone beds. o, p, storm-dominated deltaic facies with robust *Diplocraterion* (Di) with low-angle cross-laminations. Photos a, i from well 15-25-047-01W4, core depths 651.5 m and 641.5 m, respectively. Photos b, d, p from well 03-13-055-06W4, core depths 623.25 m, 618.5 m, and 591.7 m, respectively. Photo c, well 16-03, core depth 729.8 m. Photos e, f from well 08-18-049-02W4, core depths 726.1 m, 721.2 m, respectively. Photos g, h, from well 09-25-054-01W4, core depths 547.0 m and 545.4 m, respectively. Photo j from well 02-32-053-05W4, core depth 601.3m. Photo k from well 06-24-048-01W4, core depth 637.6 m. Photo o, well 14-34-054-06W4, core depth 602.6 m.



3-6) Continental Trace Fossil Assemblages

Examples of continental (orange outline) and mixed brackish-water/continental (blue outline) trace fossil assemblages of the McLaughlin Member. Photo A shows of *Taenidium isp* (Ta), and rootlet (rt) structures in A-FA2. The continental interval is mottled with development of ped structures and weak horizonation in the upper mudstone interval (second sleeve from left) which is interpreted as a gleyed protosol or gleysol. B, C, overprinted assemblage with brackish-water *Teichichnus* (Te) and continental *Taenidium isp* (Ta), and *Taenidium bowni* (Tab). The sharp walls of *Taenidium bowni* in photo C suggest a firm substrate. This interval is interpreted as a protosol. Scale bar in B is 5 cm.

3.3.1.4 *Extent, Thickness and Boundaries*

The Dina Formation extends across the entire 88 townships of the study area reaching a maximum thickness of 79.5 metres and thinning to a zero edge where strata onlap Paleozoic highs (Fig. 3.7, Fig. 3.8). The base of the Dina Formation corresponds to the contact with underlying Paleozoic and Jurassic strata, or the contact with the underlying Lower Cretaceous Detrital Beds, if present. The upper contact is defined as the top of the Rivercourse Member. This contact occurs at the top of a regional coal seam, informally termed here as the E-coal, or correlative organic-rich mudstone that caps FAC-E (Fig. 3.9). On petrophysical logs, the contact is readily identified by a persistent shift to higher values for the photoelectric factor log, and significant drop in density porosity log values across the very low-density, high porosity values associated with the E-coal (Fig. 3.9). These petrophysical shifts are also readily apparent on the histogram plots illustrated in Figure 3.10A. The boundary between the McLaughlin and Rivercourse members is placed at the base of the first regional brackish-water bioturbated mudstone of facies association complex C, informally termed here as the (C-Mudstone, Fig. 3.4, Fig. 3.5 I, J Fig. 3.9). This contact juxtaposes shallow marine above pedogenically altered silty to sandy, rooted mudstone strata of underlying facies association complex B facies.

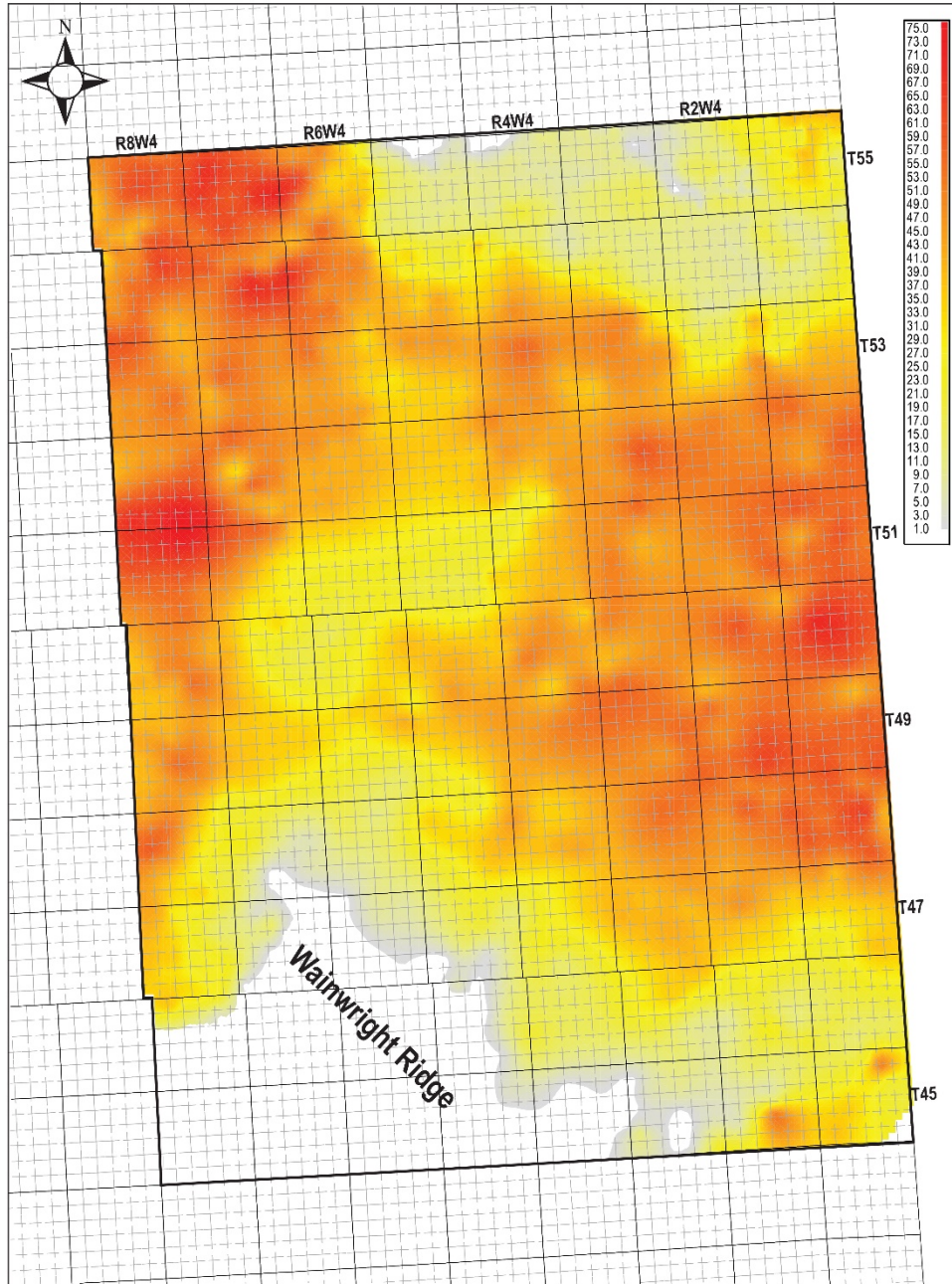
3.3.1.5 *Age and Correlation*

As the Dina top has not been consistently placed it is difficult to establish correlations with other formally defined strata. To the north, the Dina Formation as defined here correlates closely with the McMurray Formation and the Wabiskaw Member of the Clearwater Formation. In particular, facies association complexes A, B, and C are sedimentologically analogous with the McMurray C, B, and A sequences defined in the EUB Regional Geological Study (EUB, 2003). Facies association complexes D and E are sedimentologically similar to the D and B units of the Wabiskaw Member (unpublished observation). Further correlation will be required to confidently establish this relationship. Southward, the Dina is traced as far as Township 35 (100 km south of the base of the study area), where it remains a distinctly mappable unit and is broadly age equivalent to the Cutbank and Sunburst sandstone members of southern Alberta. Westward, the Dina is stratigraphically equivalent with the Ellerslie Member of central Alberta.

At present, no geochronological or biostratigraphical studies have been published on the Dina Formation. The Alberta Table of Formations (AGS, 2019) places the Dina within the Aptian, which is in alignment with ages obtained for the McMurray Formation based on biostratigraphic and geochronologic studies (e.g., Demchuk et al., 2007; Dolby et al., 2013; Rinke-Hardekopf et al., 2022). Confirmation of this age would require high-resolution correlations between Dina and McMurray strata where age dates are

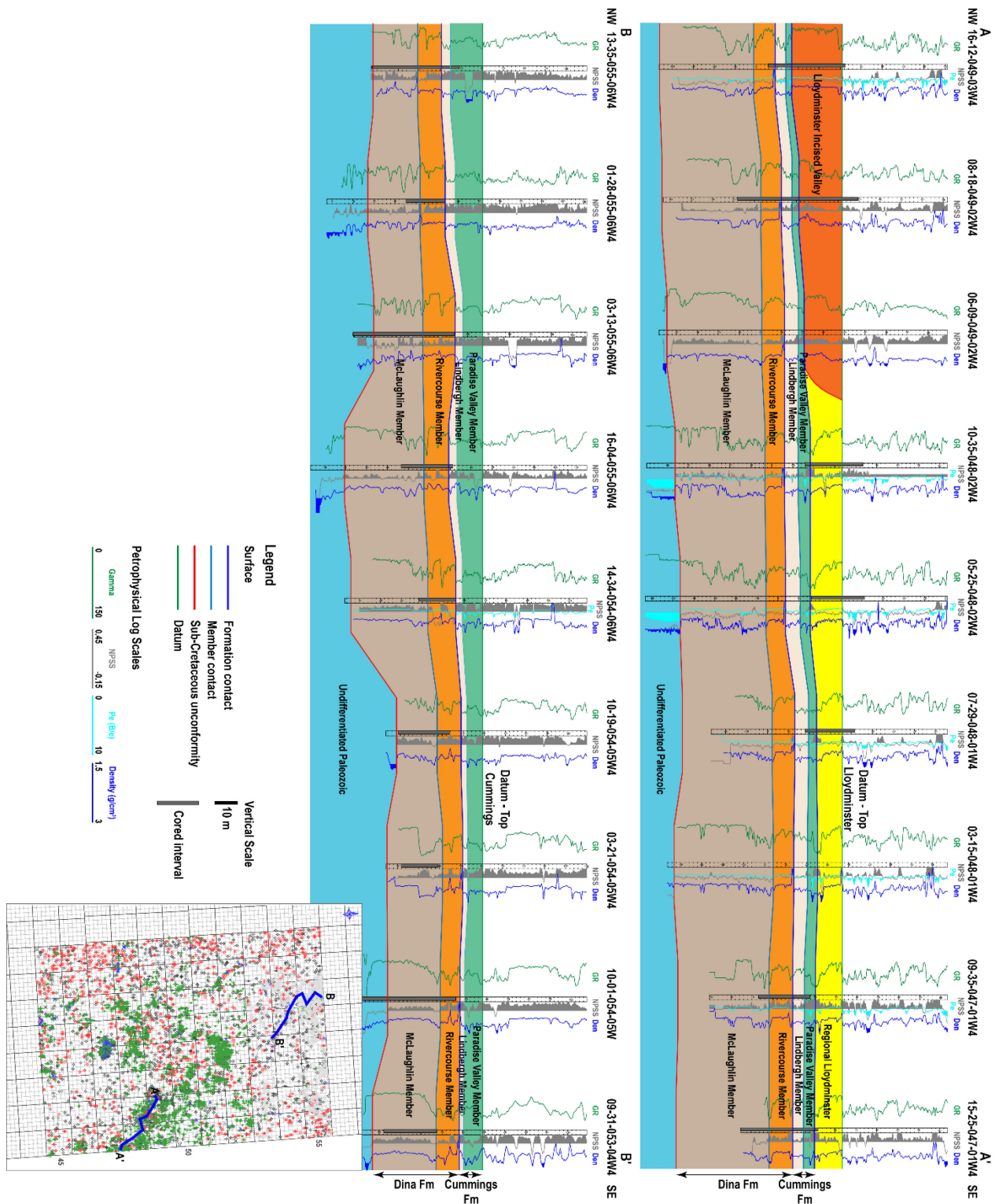
established, or more preferably, geochronological analysis of the Dina Formation within the east-central plains region of Alberta.

Isopach Map of the Dina Formation



3-7) Isopach Map of the Dina Formation

Isopach maps of the Dina Formation. White area in southwest corner illustrates where Dina Formation strata overlap a Paleozoic high (Wainwright Ridge). Each Township is 10 kilometres by 10 kilometres.



3-8) NW-SE Stratigraphic Cross-Sections

NW-SE cross-sections illustrating the stratigraphic relationship between the Dina and Cummings formations, and Lloydminster Member and the interpreted lateral extent of the McLaughlin, Rivercourse, Lindbergh, and Paradise Valley members.

3.3.2 Revision of the Cummings Member

3.3.2.1 *Utility and Rank*

Revising the geological definition and boundaries of the Cummings Member is warranted as the type section of Nauss (1945) is overly broad and encompasses the interval that is widely recognized as the Lloydminster Member in both subsequent publications and industry usage (Fig. 3.1). The revised boundaries proposed here result in a Cummings Formation that is more restricted in definition. Geological facies and petrophysical log characteristics are distinctly different from strata above and below. Due to the unique geological and petrophysical characteristics and regional nature (across and beyond the study area limits) we propose elevation of the Cummings from member to formation rank is warranted. Within the Cummings Formation, I formally propose two new internal members. These are the Lindbergh and Paradise Valley members (Fig. 3.4, Fig. 3.8, Fig. 3.9). These members are named after the communities of Lindbergh and Paradise Valley which are located within the boundaries of the study area.

3.3.2.2 *Stratotype and Locality*

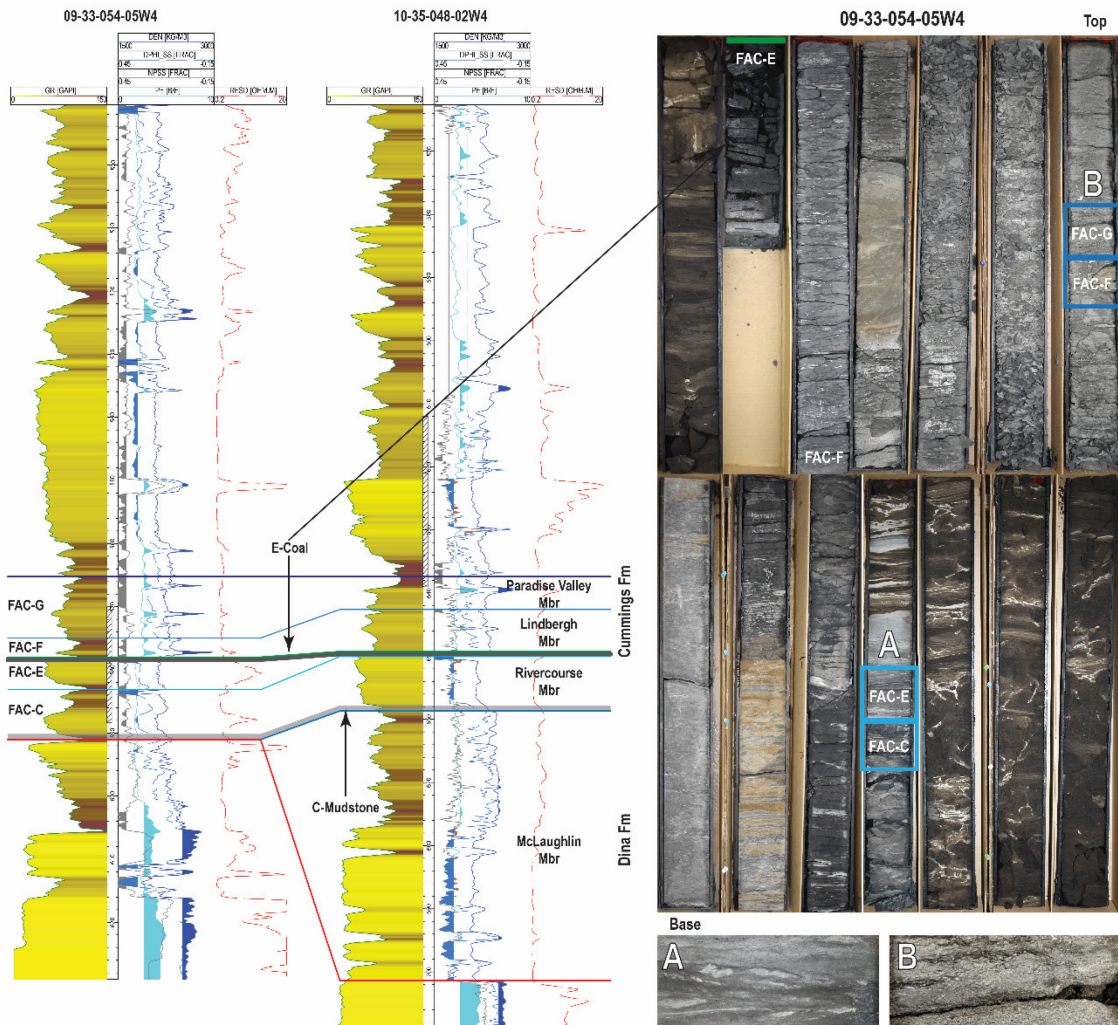
The composite stratotype for the revised Cummings Formation comprises the interval from 658 m to 664.5 m TVD in the original type section in Northwest Mannville No. 1 (01-18-050-08W4M) (Fig. 3.1) as well as reference section intervals in two wells: HUSKY RIVERCOURSE 15-25-47-1 from 621.85–632.75 m TVD, and HUSKY LLOYD 8-18-49-2 from 699.2–707.5 m TVD (Fig. 3.4, Fig. 3.11; Table 3.1). The Cummings Formation has two geologically distinct members, termed in ascending stratigraphic order the Lindbergh and Paradise Valley members. The Lindbergh Member stratigraphic top occurs in reference well 15-25 at 627 m TVD, and in well 08-18 at 702.3 m TVD. These members correspond to facies association complexes F and G of Chapter 2. Table 3.1 provides a summary of these stratigraphic units.

3.3.2.3 *Geological Description*

Lindbergh Member

The Lindbergh Member consists of facies association complex F (Fig. 3.4, reference wells 08-18 and 15-25, Fig. 3.11) and has three facies associations—F-FA1, F-FA2, and F-FA3 (Table 3.1)—which are interpreted as marine deltaic and transgressive strata characterized by thin coarsening-upward (deltaic) and fining-upward (transgressive) cycles (Fig. 3.4). Cycles are separated by sharp, erosive, or gradational contacts and are difficult to map at the regional scale. In core, the Lindbergh is commonly glauconitic, and contains internal lags of organic debris (including pyritized wood), pyrite, shell debris and granules (Fig. 3.11 f). These lags are present at the contacts between internal facies associations and at the surface bounding facies association complexes F and G (Fig. 3.9 B). In core, there is a sharp contrast in ichnological

characteristics between the Lindbergh and underlying McLaughlin Member units. Ichnological diversity and trace fossil size increase across this contact and ichnogenera that are indicative of marine salinities. These include *Cosmorhaphe*, *Nereites*, *Phycosiphon*, *Scolicia*, and *Zoophycos*. No definitive examples of these ichnogenera were identified below the Lindbergh Member



3-9) Core and Petrophysical Signature of the Dina-Cummings Contact

Petrophysical log suite and core example across facies association complex boundaries FAC-C/FAC-E (A), FAC-E/FAC-F, and FAC-F/FAC-G (B). Core photos are from well 09-33-054-05W4 (hachured interval in depth column). Also shown are the stratigraphic horizons corresponding to the C-mudstone and E-coal marker beds that define the McLaughlin-Rivercourse and Dina-Cummings boundary, respectively.

Paradise Valley Member

The Paradise Valley Member consists of facies association complex G (Fig. 3.4, reference wells 08-18 and 15-25, Fig. 3.11 B). In core, the Paradise Valley Member is composed of several sharp-based cleaning-upward cycles of bioturbated glauconitic sandstone, siltstone, and mudstone (Fig. 3.11 B). These comprise marine offshore to lower shoreface depositional environments characterized by the most diverse, robust trace fossil assemblage of any stratigraphic interval within the Dina and Cummings formations, and from any observed cored interval of the overlying Lloydminster Member. Twenty-three ichnogenera are present within the Paradise Valley Member including abundant marine-associated forms including *Cosmorhappe*, *Nereites*, *Phycosiphon*, *Scolicia*, and *Zoophycos*. Internal contacts between sequences of FAC-G and the contact between the Paradise Valley and underlying Lindbergh Member are commonly demarcated by well-developed *Glossifungites* Ichnofacies-bearing surfaces characterized by *Diplocraterion*, *Skolithos*, and *Thalassinoides* (e.g., Fig. 3.9 B Fig. 3.11 K).

3.3.2.4 Extent, Thickness, and Boundaries

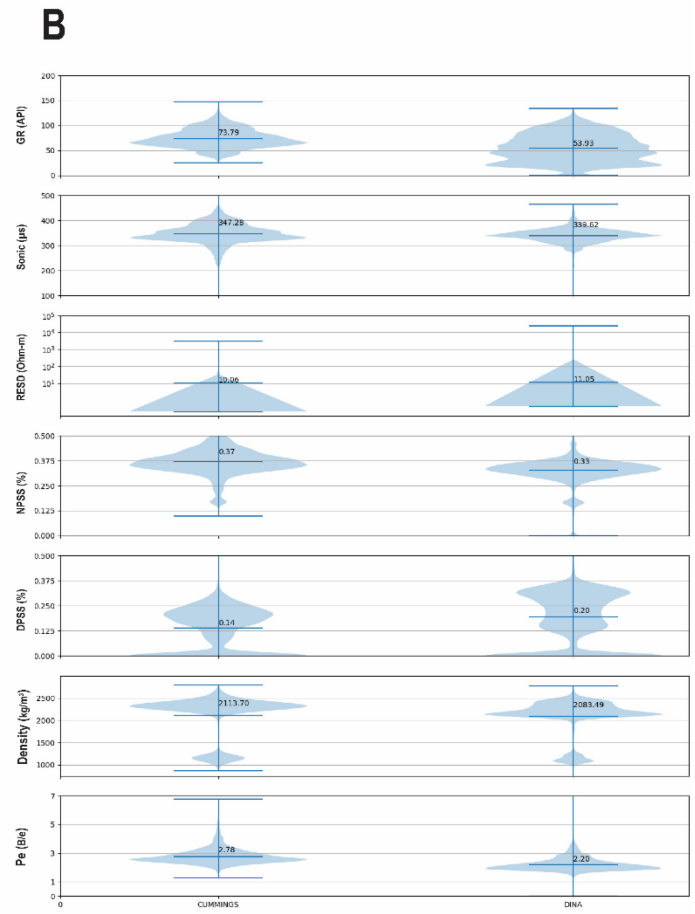
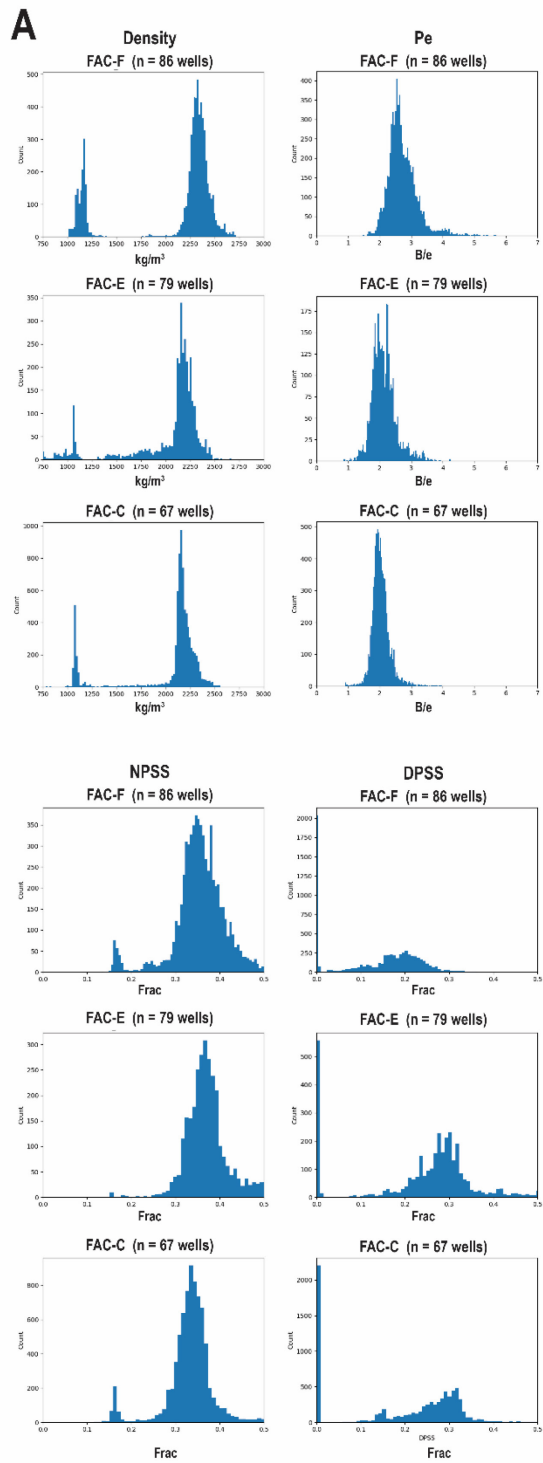
The Cummings Formation extends across and beyond the study area in all directions, except where it onlaps Paleozoic highs of the Wainwright Ridge in the southwest corner of the study area. The Cummings reaches a maximum thickness of 25.5 m (Fig. 3.12). The basal boundary occurs at the Lindbergh-Rivercourse contact (FAC-F–FAC-E or –FAC-C) and is well developed in both core and petrophysical log datasets (Fig. 3.9). In core, the basal boundary is an erosional surface juxtaposing offshore marine mudstone facies of the Lindbergh Member over coastal deltaic or delta plain facies of the Rivercourse Member (Fig. 3.9 B). An erosional lag of glauconite, shell debris, pyrite, granules, and carbonate clasts are often present within the basal portion of the Lindbergh Member (Fig. 3.11 E). Visual observations, confirmed by petrophysical analysis show a study-wide, persistent shift toward higher photoelectric factor, density porosity, and density values (Fig. 3.9 a, 3.10 A). The petrophysical analyses shows clearly differences in grouped average values of Dina and Cummings facies association complexes. This is demonstrated by plotting the shape of the distribution of various petrophysical properties in violin plots for the Dina and Cummings (Fig. 3.10 B). The gamma ray log distribution has a narrower value range, is unimodal and has a higher mean value in the Cummings (73.8 API) when compared to the Dina, which is bimodal and has a mean value of 53.9 API. Mean density porosity (which is more representative of total porosity than neutron porosity) is higher in the Dina (20 %) compared to the Cummings (14 %). Both the Dina and the Cummings have relatively important coal proportions by volume (i.e., zones with bulk density values of less than 1250 kg/m³). Mean photoelectric effect (PE) values are closer to typical shale PE values (approximately 3 B/e) in the Cummings compared to the Dina where mean PE values are closer to a typical

Quartz response (approximately 1.8 B/e). Mean neutron porosity is higher in the Cummings compared to the Dina, which might be a response to higher glauconitic content relative to the Dina. The higher overall gamma ray readings in the Cummings might be attributable to this as well. Overall, the petrophysical analyses demonstrates that both the Cummings and the Dina contain coal zones and that the Cummings contains more radioactive minerals (likely glauconite), lower porosity and is more lithologically homogeneous than the Dina.

The upper boundary of the Cummings has two expressions depending on the nature of the overlying Lloydminster Member. Based on core observations and wireline correlations the Lloydminster Member in the east-central plains region of Alberta has two general environments of deposition (Fig. 3.8). The first, informally referred to here as the regional Lloydminster consists of one to several coarsening-upward cycles of mudstone, interbedded mudstone and sandstone, sandstone, and coal that record the progradation of wave- and river-influenced deltaic deposits. The second general environment consists of thick (up to 40 m) estuarine channel, point-bar, and bar top strata that incise the regional Lloydminster coarsening-upward cycles and facies association complexes F and G. Chapter 4 discusses the sequence stratigraphic relationships between the Lloydminster expression and the underlying Dina and Cummings interval and provides a more detailed summary of the sedimentology and ichnology of the regional expression. Where the regional Lloydminster Member is present, the contact with the Cummings Formation is gradational, occurring within a variably thick mudstone interval (Fig. 3.4, well 15-25). In this instance, the boundary is placed on logs at the maximum gamma-ray, neutron porosity, and density porosity value within the mudstone interval. This surface is interpreted as the maximum flooding surface (MFS) defining the boundary between the lower and upper Mannville Group. Where incision by Lloydminster-aged (or younger) channels has eroded parts of the Cummings Formation, the base of the channel represents the upper boundary of the Cummings Formation (Fig. 3.4, well 08-18).

3.3.2.5 Age and Correlation

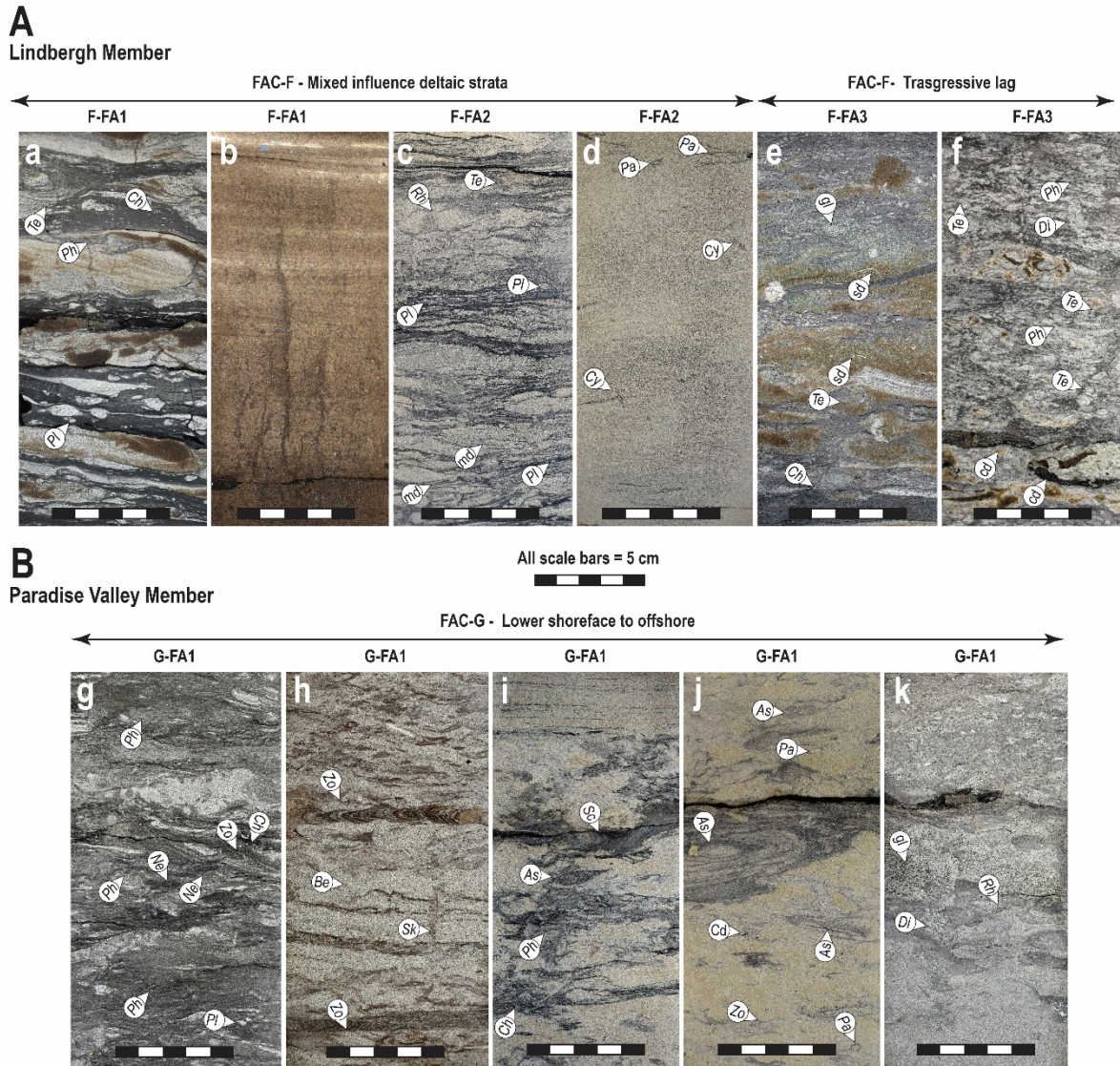
As with the Dina, no direct age dates are available for the Cummings Member within the type section area. Facies of the Lindbergh and Paradise Valley members are sedimentologically, ichnologically, and lithologically similar to those described from the A unit of the Wabiskaw Member and lower Clearwater Formation strata in the Athabasca Oil Sands region and to select facies of the Bluesky Formation and overlying Wilrich Member in the Peace River Oil Sands region (Hubbard et al., 1999; EUB, 2003; Botterill et al., 2016). To the south and west of the study area, the Cummings is shown as being stratigraphically equivalent with the Ostracod Beds (AGS, 2019).



3-10) Histogram and Violin Plots

Histogram (A) and violin plots (B) comparing the range and average petrophysical properties of the Dina and Cummings formations. A) Comparison of the distribution of values from the density, photoelectric factor, neutron porosity, and density

porosity logs between FAC-C, FAC-E, and FAC-F. The most significant differences occur on the photoelectric factor and density porosity logs. B) Violin plot comparing the average and range of petrophysical values for the Dina and Cummings formations.

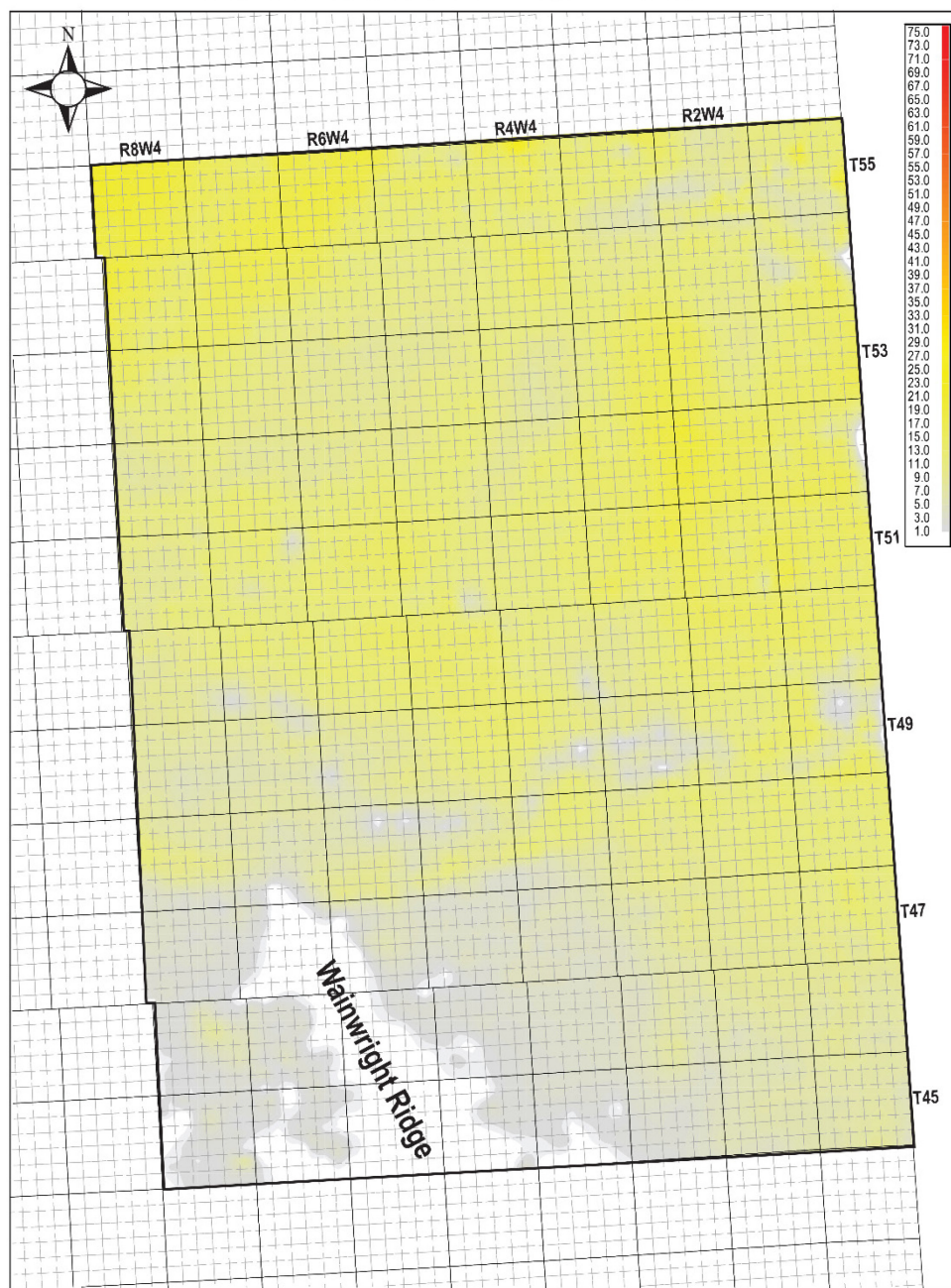


3-11) Facies of the Lindbergh and Paradise Valley Members

Selected facies of the Lindbergh (A) and Paradise Valley (B) members, including examples from the broader dataset. A) a, b, wave- and river-influenced prodelta and delta front facies of F-FA1. c, d, tide- and wave-influenced deltaic facies of F-FA2 with double mudstone drapes and faint low-angle cross-laminations. Fluid mudstone beds and laminae are common in prodelta facies with trace fossils including *Chondrites* (Ch), *Phycosiphon* (Ph), and *Teichichnus* (Te) (a) and *Planolites* (Pl), *Rhizocorallium* (Rh), *Palaeophycus* (Pa), and *Cylindrichnus* (Cy) (c and d). e, f, transgressive facies consisting of poorly sorted muddy to silty sandstone with visible glauconite grains (gl), shell debris (sd), and carbonaceous detritus (cd). Both examples are heavily bioturbated with *Chondrites* (Ch), *Phycosiphon* (Ph), *Diplocraterion* (Di), *Teichichnus* (Te), and *Palaeophycus* (Pa). B) g, j, bioturbated offshore to lower shoreface facies of the Paradise Valley Member. Trace fossil diversity and average size are the highest and largest of any facies within the Dina-Cummings interval. k, internal *Glossifungites* surface with accompanying glauconite concentration above.

Trace fossils include *Asterosoma* (As), *Berguaria* (Be), *Chondrites* (Ch), *Diplocraterion* (Di), *Helminthopsis* (He), *Nereites* (Ne), *Palaeophycus* (Pa), *Phycosiphon* (Ph), *Scolicia* (Sc), *Zoophycos* (Zo). Photos A, B, and J from well 15-25-047-01W4, core depths 631 m, and 630.4 m, 623.8 m, respectively. Photos C, E from well 04-14-055-02W4, core depths 501.85 m, 503 m, respectively. Photo D, well 13-09-054-01W4, core depth 514 m. Photo E, well 16-12-049-03W4, core depth 714.6 m. Photos G, H, K from well 09-33-054-05W4, core depths 571.2 m, 572.4 m, 571.4 m. Photo, well 07-29-048-01W4, core depth 620.6 m.

Isopach Map of the Cummings Formation



3-12) Isopach Map of the Cummings Formation

Isopach map of the Cummings Formation generated using the same depth range as Figure 3.7 to illustrate the thickness and distribution differences with the Dina Formation. The elongate WSW-ENE trending thin to absent thickness corresponds to the presence of Lloydminster-aged, incised valley fills. Each Township is 10 kilometres by 10 kilometres.

3.4 Discussion

3.4.1 Revised Definition

With the above documentation of the sedimentological, ichnological, and stratigraphic characteristics of the Dina and Cummings interval, revised definitions of the bounding surfaces, rank, and general geological attributes are proposed below.

3.4.1.1 *Dina Formation*

The Dina Formation consists of all strata bound between the sub-Cretaceous unconformity—or where present the Detrital Beds—below and the bioturbated glauconitic sandstone, siltstone, and mudstone of the Cummings Formation above. Both bounding contacts are disconformable, sharp, and locally erosional in nature. The Dina Formation comprises of two formal members, the basal McLaughlin and overlying Rivercourse. Depositional environments include continental, fluvio-tidal, estuary, open embayment, and deltaic strata preserved in a retrogradational stacking pattern. The McLaughlin Member is characterized by high lithological variability, numerous internal disconformities (paleosols), and an absence of regionally correlative marker horizons within internal depositional environments comprised of channel and floodplain, fluvio-tidal channel and floodplain, and lower delta plain distributary channel and embayment strata. The Rivercourse Member is characterized by multiple metre-scale, coarsening-upward cycles that are both thicker and more laterally continuous than those present in the McLaughlin Member. In core (within the study area), the trace fossil assemblage is restricted to continental, brackish-water, and stressed marine coastal facies (specifically E-FA1). The Dina Formation is petrophysically distinct from underlying Paleozoic carbonate strata and overlying glauconitic strata of the Cummings Formation.

3.4.1.2 *Cummings Formation*

The Cummings Formation consists of all strata bound between the Dina Formation below and Lloydminster Member above. The basal contact is sharp, disconformable, and locally erosional, while the upper contact is either gradational or erosional depending on the affinity of overlying Lloydminster Member facies. The Cummings Formation comprises two formal members, the Lindbergh and Paradise Valley. The Lindbergh consists of deltaic and transgressive strata containing glauconitic sandstone, siltstone, and mudstone. Contacts between internal facies associations of the Lindbergh are commonly erosional with the development of lags consisting of organic debris, pyrite, glauconite, and shell debris.

The Paradise Valley consists of marine offshore to lower shoreface glauconitic, bioturbated sandstone, siltstone, and mudstone. Internal contacts are commonly erosive with the development of *Glossifungites* surfaces. The contact between the Lindbergh and Paradise Valley is sharp, laterally continuous over tens of kilometres, and characterized by a very well-developed *Glossifungites*-demarcated surface of erosion. The Cummings Formation is petrophysically distinct from adjacent lithostratigraphic units, particularly with respect to average DPSS (lower), Pe (higher), and bulk density (higher) values. The top of the Cummings corresponds to the maximum extent of Boreal Sea transgression, and as such corresponds to the maximum flooding surface of the third-order Mannville depositional sequence of Cant (1996), and Cant and Abrahamson (1996).

3.4.2 Limitations

Limitations of this revised lithostratigraphic framework are largely attributable to the paucity and distribution of cored intersections of the Dina and Cummings. Overall, the 88-township area contains less than 100 stratigraphic cores, many of which are concentrated in certain areas of higher economic potential, such as in the area encompassed within Twp. 54–55, Rge. 5–6, where 17 of the total 72 stratigraphic cores are located. In contrast, the area encompassed between Twp. 50 and 53, Rges.1–3W4 has one core intersecting the Cummings Formation (Chapter 2). In total, 56 out of the 88 townships in the study area contain no cored intersections of the Dina or Cummings interval. Specific limitations of the framework resulting from the nature of the core dataset include the following. First, given the extensive areas lacking core control and the lithological heterogeneity of strata, the geological descriptions are almost certainly incomplete. Second, while the contact between the McLaughlin and Rivercourse members is readily identifiable in locations where depositional unit C cycles and the basal C-Mudstone are well developed (e.g., type wells 15-25, 08-18) it becomes more difficult to trace into areas where core is lacking, and the cycles of FAC-C become thinner and less well developed. Third, establishing the chronostratigraphic relationship of coarsening-upward sequences defining FAC-B, FAC-C, and FAC-E is beyond the scale of this framework. This difficulty in differentiating and correlating distinct facies association complexes occurs in the northwest and west-central areas of the study where the number of individual coarsening-upward cycles within a single vertical section increases (Fig. 8). In type wells 15-25 and 08-18 there are only three to four stacked cycles and only two coal seams present at the tops of FAC-C and FAC-E (Fig. 4, Fig. 8). In type well 03-13, a number of coaly shale/shaley coal horizons are present and it becomes much more difficult to correlate distinct horizons over regional distances when no core is available. This makes the placement of the McLaughlin-Rivercourse contact more problematic in areas of increased accommodation.

An alternative lithostratigraphic model that was considered was to include facies association complexes D and E within the Cummings Formation, as FAC-D is similar in appearance to the Wabiskaw Member D of the lower Clearwater Formation in the Athabasca Oil Sands region (Fig. 13). In that model, FAC-A to FAC-C would be lithostratigraphically equivalent to the McMurray C, B, and A units as defined by the EUB Regional Geological Study (EUB, 2003), and FAC-D to FAC-G lithostratigraphically equivalent to the Wabiskaw Member and lower Clearwater Formation (Fig. 13). In either model, the Wabiskaw B, A, and lower Clearwater Formation would be lithostratigraphically equivalent to the Cummings Formation facies association complexes F and G. This general model of the McMurray-Wabiskaw interval in the Athabasca Oil Sands region, while not completely accounting for all the geological complexity is applicable at regional scales because of the significant density of drill core available to confidently correlate these units. This model, applied to the Lloydminster area would have made the placement of the Dina-Cummings boundary more difficult to establish in any area where FAC-D or FAC-E are present. This is due to the difficulty in correlating individual coarsening-upward cycles in absence of core, and because the petrophysical characteristics of facies association complexes C, D, and E are similar when compared to facies association complexes F and G.

In defining the Dina-Cummings boundary as proposed above, the contact is readily visible on petrophysical logs and while the facies contrast across this surface is significant, core is not necessary to confidently identify this lithological boundary at a regional scale. The proposed placement of the Dina-Cummings boundary also reduces the possibility of conflating hydrocarbon pool nomenclature in regulatory or exploration activities as the newly defined Cummings is in effect a regional stratigraphic seal for the primary producing intervals within the lower Mannville of the Lloydminster heavy oil region.

3.5 Conclusions

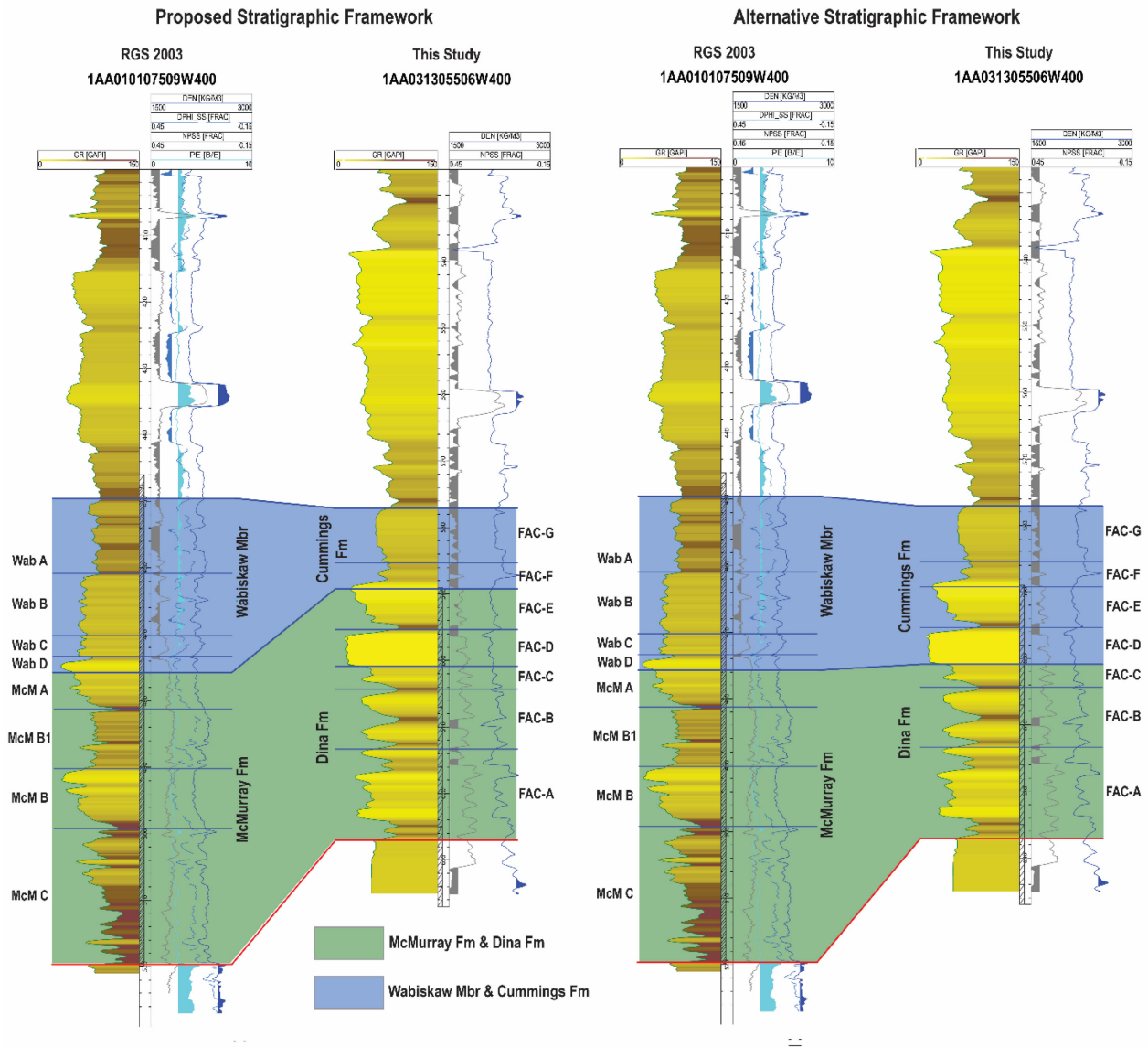
The initial definitions of the Dina and Cummings intervals in the east-central Alberta by Nauss (1945) were established using a core and petrophysical dataset of low density and quality. However, subsequent researchers and the petroleum industry have not consistently embraced this original definition. As a consequence, there have been discrepancies in the placement of the interval's top, formal rank assignment, and the description and interpretation of its constituent strata. In this study we conducted a detailed analysis of seventy-two stratigraphic drill core, and correlation of ca. 7800 petrophysical logs to identify the range of depositional environments and presence of stratigraphic breaks that may be useful in constructing a predictable and consistent lithostratigraphic framework. In addition, we conducted analysis on a sub-set of 225 wells to assess differences in petrophysical parameters. This analysis showed highlighted differences in average gamma ray values and distribution, density porosity, and photoelectric

effect. These data indicated that the Dina Formation is likely higher in quartz content, whereas the Cummings Formation is enriched in radioactive minerals (likely glauconite) and is likely more lithologically homogeneous. Based on this research, I propose revising the top placements for the Dina and Cummings intervals and elevating their rank to Formation. To that end, comprehensive geological descriptions of the Dina and Cummings formations are provided. Finally, I propose four new members, namely the McLaughlin and Rivercourse members within the Dina Formation, and the Lindbergh and Paradise Valley members within the Cummings Formation.

The revised definition of the Dina is as follows. “All strata bound between the sub-Cretaceous unconformity, or where present, the Detrital Beds below and the glauconitic, marine Cummings Formation above. Bounding surfaces are unconformable, and bounding strata are sedimentologically, ichnologically, petrophysically, and geometrically distinct. Dina Formation strata consist of two members, the McLaughlin and Rivercourse which comprise continental, fluvio-tidal, paralic, and shoreline environments. The McLaughlin Member is characterized by high spatial lithological heterogeneity and a lack of regionally correlative internal marker horizons. The Rivercourse is characterized by more uniform, sheet-like coarsening-upward facies occurring in isolation or as stacked cycles.”

The revised definition of the Cummings is as follows. “All strata bound between the Dina Formation below and Lloydminster Member above. The basal boundary is unconformable and locally visibly erosive. The upper boundary is either gradational or unconformable depending on the geological characteristics of the Lloydminster Member (regional coarsening-upward or incised valley fill, respectively). The Cummings Formation is sedimentologically, ichnologically, and petrophysically distinct from bounding units and is comprised of two internal members, the Lindbergh and Paradise Valley which comprise marine environments including deltaic, transgressive, and lower shoreface to offshore environments. Both members have sheet-like geometries, are visibly glauconitic and contain multiple internal disconformity surfaces which are often expressed by the *Glossifungites* ichnofacies.

Despite limited core data leading to uncertainties in correlating members and their constituent facies association complexes, the distinct geological and petrophysical differences between the redefined Dina and Cummings formations are easily discernible. As such, this updated stratigraphy offers a more consistent framework, thereby reducing uncertainty in correlations and potentially mitigating uncertainties in various subsurface activities, such as pool definition, pore space competition, and subsurface disposal activities.



3-13) Lithostratigraphic Comparison of the Lloydminster and Athabasca Areas

Lithostratigraphic comparison of the Dina-Cummings and McMurray-Wabiskaw intervals in the Lloydminster heavy oil and Athabasca regions, respectively. The right-hand logs show theoretical correlations between these areas based on the revised lithostratigraphic framework proposed in this study. The left-hand logs illustrate an alternative interpretation based on an interpretation that FAC-D is equivalent to the Wabiskaw D unit. This would shift the Dina-Cummings boundary downward several metres.

3.6 References

- Alberta Energy and Utilities Board, 2003, Athabasca Wabiskaw-McMurray regional geological study: Alberta Energy and Utilities Board, Report 2003-A, 195 p.
- Ambler, J.S., 1951, The stratigraphy and structure of the Lloydminster oil and gas area: University of Saskatchewan, M.Sc. thesis,
- Bauer, D.B., Hubbard, S.M., Leckie, D.A., and Dolby, G., 2009, Delineation of a sandstone-filled incised valley in the Lower Cretaceous Dina–Cummings interval: implications for development of the Winter Pool, west-central Saskatchewan: *Bulletin of Canadian Petroleum Geology*, v. 57, no. 4, p. 409-429.
- Botterill, S.E., Campbell, S.G., Timmer, E.R., Gingras, M.K., and Pemberton, S.G., 2016, Recognition of wave-influenced deltaic and bay-margin sedimentation, Bluesky Formation, Alberta: *Bulletin of Canadian Petroleum Geology*, v. 64, p. 389–414.
- Cant, D.J., 1996, Sedimentological and sequence stratigraphic organization of a foreland clastic wedge, Mannville Group, Western Canada Basin: *Journal of Sedimentary Research*, v. 66, no. 6, p. 1137-1147.
- Cant, D.J., and Abrahamson, B., 1996, Regional distribution and internal stratigraphy of the Lower Mannville: *Bulletin of Canadian Petroleum Geology*, v. 44, no. 3, 508-529.
- Christopher, J., 1997, Evolution of the Lower Cretaceous Mannville Sedimentary Basin in Saskatchewan, *in*: Pemberton, S.G., and James, D.P., editors, *Petroleum Geology of the Cretaceous Mannville Group, Western Canada*: Canadian Society of Petroleum Geologists, Memoir 18, p. 191-210.
- Demchuk, T. D., Dolby, G., McIntyre, D.J., and Suter, J.R., 2007, The utility of palynofloral assemblages for the interpretation of depositional paleoenvironments and sequence-stratigraphic systems tracts in the McMurray Formation at Surmont, Alberta, *in*: Suter, J.R., Leckie, D.A., and Larter, S., editors, *Heavy oil and bitumen in foreland basins: From processes to products*, AAPG Hedberg Research Conference, Banff, Alberta, Canada, 5 p.
- Dolby, G., Demchuk, T.D., and Suter, J.R., 2013, The significance of palynofloral assemblages from the Lower Cretaceous McMurray Formation and associated strata, Surmont and surrounding areas in north-central Alberta, *in*: Hein, F.J., Leckie, D.A., Larter, S., and Suter, J.R., editors, *Heavy-oil and oil-sand petroleum systems in Alberta and beyond*, American Association of Petroleum Geologists Studies in Geology 64, p. 251-272.
- Fuglem 1970, M.O., 1970, Use of core in evaluation of productive sands, Lloydminster area, *in*: Brindele, J.E., and Holmerg, R.A., editors, *Saskatchewan Mesozoic Core Seminar*, Saskatchewan Geological Society, 12 p.

- Gross, A.A., 1980, Mannville Channels in east-central Alberta: Lloydminster and Beyond: Geology of Mannville Hydrocarbon, *in*: Beck, L.S., Christopher, J.E., and Kent, D.M., editors, Lloydminster and Beyond: Geology of Mannville Hydrocarbon Reservoirs: Saskatchewan Geological Society, Special Publication 5. p. 33–63.
- Hayes, B.J.R., Christopher, J.E., Rosenthal, L.L., McKercher, B., Minken, D., Tremblay, Y.M., and Fennel, J., 1994, Cretaceous Mannville Group of the Western Canada Sedimentary Basin, *in*: Mossop, G.D., and Shetson, I., editors, Geological Atlas of the Western Canada Sedimentary Basin, Canadian Society of Petroleum Geologists and Alberta Research Council.
- Hubbard, S.M., Pemberton, S.G. and Howard, E.A. 1999, Regional geology and sedimentology of the basal Cretaceous Peace River Oil Sands deposit, north–central Alberta: Bulletin of Canadian Petroleum Geology, v. 47, p. 270–297.
- Kent, D.M., 1959, The Lloydminster oil and gas field, Alberta: University of Saskatchewan, M.Sc. thesis, 92 p.
- Kohlruss, D. J., 2012, Stratigraphic architecture and facies analysis of the Lower Cretaceous Dina Member of the Mannville Group in northwest Saskatchewan: University of Regina, M.Sc. thesis, 200 p.
- Mack, G.H., James, W.C., and Monger, H.C., 1993, Classification of paleosols: Geological Society of America Bulletin, v. 105, p. 129-136.
- Nauss, A.W., 1945, Cretaceous stratigraphy of Vermillion area, Alberta, Canada: Bulletin of the American Association of Petroleum Geologists, v. 29, no. 11, p. 1605-1629.
- North American Commission on Stratigraphic Nomenclature, 2005, North American Stratigraphic Code: American Association of Petroleum Geologists Bulletin, v. 89, no. 11, p. 1547-1491.
- Orr, R.D., Johnston, J.R., and Manko, E.M., 1977, Lower Cretaceous geology and heavy-oil potential of the Lloydminster area: Bulletin of Canadian Petroleum Geology, v. 25, no. 6, p. 1187-1221.
- Rinke-Hardekopf, L., Dashtgard, S.E., MacEachern, J.A., and Gingras, M.K., 2022, Resolving stratigraphic architecture and constraining ages of paralic strata in a low-accommodation setting, Firebag Tributary, McMurray Formation, Canada, Depositional Record, v. 8, p. 754-785.
- Vigrass, L.W., 1977, Trapping of Oil at Intra-Mannville (Lower Cretaceous) Disconformity in Lloydminster Area, Alberta, and Saskatchewan: The American Association of Petroleum Geologists Bulletin, v. 61, no. 7, p. 1010-1028.
- Wickenden, R.T.D., 1948, The Lower Cretaceous of the Lloydminster oil and gas area, Alberta, and Saskatchewan: Geological Survey of Canada, Paper 48-21, 15 p.

Wilson, M., 1984, Depositional environments of the Mannville Group (Lower Cretaceous) in the Tangleflags area, Saskatchewan, *in*: Lorscheider, J.A., and Wilson, M., editors, Oil and Gas in Saskatchewan: Saskatchewan Geological Society, Special Publication Number 7, p. 119-134.

Zaitlin, B.A., and Schultz, B.C., 1984, An estuarine-embayment fill model from the Lower Cretaceous Mannville Group, west-central Saskatchewan, *in*: Stott, D.F., and Glass, D.J., editors, The Mesozoic of Middle North America: Canadian Society of Petroleum Geologists, Memoir 9, p. 455-469.

4 Application of Facies Analysis in High-Resolution Sequence Stratigraphy: A Case Study from the Lower Mannville Group, East-Central Plains Region, Alberta, Canada

4.1 Introduction

Sedimentary facies analysis including process sedimentological and ichnological observations is an essential component in the interpretation of depositional environments and placement of those environments within a sequence stratigraphic framework. In high-resolution sequence stratigraphic studies below seismic scale, interpreting the genetic nature and significance of stratigraphic discontinuities is dependent on careful analysis of bounding strata (e.g., Zecchin and Catuneanu, 2013; Catuneanu, 2019b). Although petrophysical logs are an essential component in establishing the extent of these discontinuities, the genesis of such surfaces can only be inferred in the absence of core- or outcrop-based sedimentological observations. High-frequency sequence stratigraphic analysis has a direct application to hydrocarbon exploration and production as the distribution and quality of reservoir and non-reservoir facies is controlled by the systems tract(s) in which they are contained (e.g., Catuneanu, 2006; Zecchin and Catuneanu, 2015).

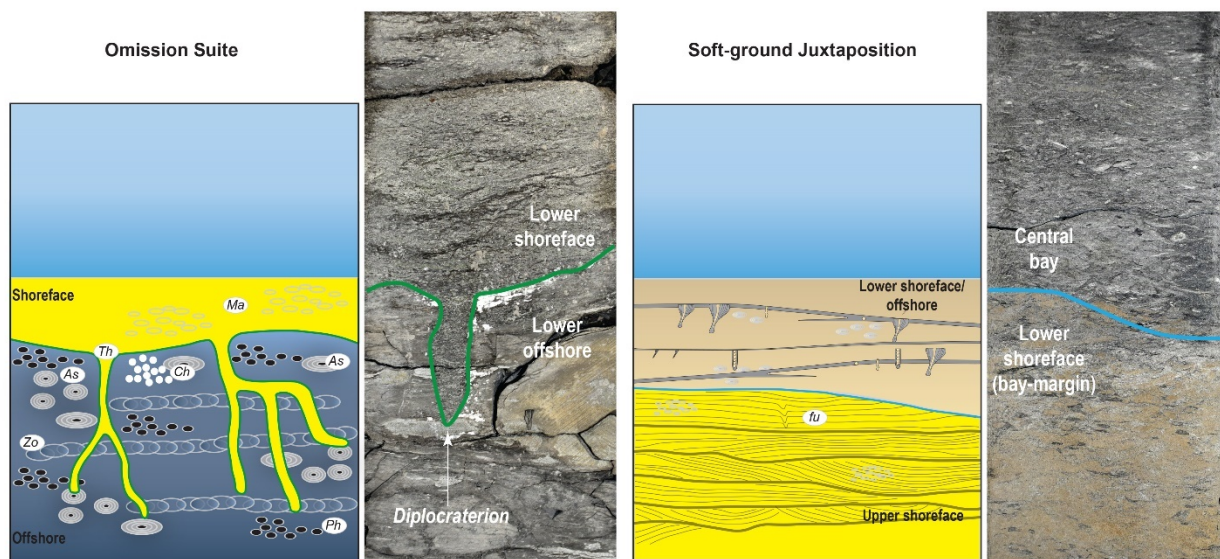
The primary roles that facies-level ichnological and sedimentological observations play in sequence stratigraphic analysis is in the identification of key bounding surfaces (MacEachern et al., 2012 and references therein) and the recognition of spatio-temporal changes in environmental conditions (e.g., wave vs. tide vs. fluvial magnitude, ambient and fluctuating salinity, rates of deposition, etc.). The two types of bounding surfaces in which ichnological and sedimentological criteria are most useful to identify are 1) omission suites, and 2) juxtaposition of soft-ground facies (Fig. 4.1) (e.g., MacEachern et al., 1992; MacEachern et al., 2012). Omission suites are characterized by: 1) trace fossils that cross-cut primary sedimentary fabric or older trace fossil suites; 2) trace fossils that are passively filled with sediment from above the discontinuity; 3) commonly consist of unlined, sharp-walled burrows; 4) trace fossils that may occur in lithologies that do not normally host the preserved ethological groupings; and 5) trace fossils that may show little or no compaction (Bromley, 1975; MacEachern et al., 1992; Pemberton et al., 2004; MacEachern et al., 2007b; MacEachern et al., 2012). The second direct application of facies analysis to sequence stratigraphy is to recognize surfaces wherein bounding strata violate Walther's Law. Before the presence, magnitude, and direction (i.e., basinward, landward, no shift) of facies dislocations can be established, informed interpretations of the bounding units based upon an integrated sedimentological and ichnological dataset must be established. As an example, consider two expressions of discontinuity

surfaces bound by mudstone facies. The first expression is characterized by a high-diversity trace fossil suite including *Cosmorhapha*, *Nereites*, *Phycosiphon*, *Scolicia*, and *Zoophycos* above, and a highly impoverished, diminutive trace fossils suite consisting of *Cylindrichnus*, *Gyrolithes*, and *Teichichnus* in rooted, pedogenically altered mudstone below, both of which are characterized by high bioturbation indices. The second expression has the same high diversity assemblage, but this time underlying the contact, with a sporadically bioturbated mudstone facies above characterized by abundant graded beds, phytodetrital pulses, and synaeresis cracks, with common *Phycosiphon* and rare, but present *Cosmorhapha*, *Scolicia*, and *Zoophycos*. The first example indicates a bounding surface characterized by a significant landward shift of facies placing brackish-water coastal plain mudstone overlying marine offshore deposits. In the second example, the sedimentological criteria suggest a shift in depositional processes from low rates of sedimentation in the offshore to rapid emplacement of river-derived sediment of a prodeltaic facies above. The second example represent a rapid basinward shift of facies from offshore to prodelta. However, the similarity in trace fossil suites suggests that ambient salinity in both facies was likely marine and that the magnitude of dislocation is significantly less than in the first example. The application of soft-ground facies juxtapositions have been successfully applied in numerous subsurface and outcrop sequence stratigraphic studies (e.g., Ekdale and Bromley, 1984; Vossler and Pemberton, 1988; MacEachern and Pemberton, 1994; Pemberton and MacEachern, 1995; Bann and Fielding, 2004; Pemberton et al., 2004; Fielding et al., 2007; MacEachern et al., 2007; Rodriguez-Tovar et al., 2007; Pearson et al., 2012; Bayet-Goll et al., 2017; Rodriguez et al., 2018; Chateau et al., 2019; Morshedien et al., 2019; Ahmad and Gingras, 2022; Schultz et al., 2022).

The Lower Cretaceous, Aptian to early Albian Dina, Cummings, and Lloydminster lithostratigraphic members in the east-central plains of Alberta represent an excellent case study for the application of high-resolution, facies-based sequence stratigraphic analysis. Numerous workers have conducted sequence stratigraphic studies of variable resolution on Mannville Group strata throughout Alberta and Saskatchewan, utilizing a number of datasets. These include sedimentary facies and wireline analysis (e.g., Cant, 1996; Leckie et al., 1997; Pemberton et al., 2000; Pouderoux et al., 2016; Wellner et al., 2018; Morshedien et al., 2019; Newitt and Pederson, 2022), coal stratigraphy (e.g., Banerjee et al., 1996; Holz et al., 2002; Wadsworth et al., 2002; Chalmers et al., 2013; Deschamps et al., 2017), seismic (e.g., Sarzalejo and Hart, 2006, Silva and Hart, 2013; Smaili and Hart, 2018), mineralogical (e.g., Zaitlin et al., 2002), and chemostratigraphic methodologies (e.g., Ratcliffe et al., 2004; Hildred et al., 2010). Among these studies, only Chalmers et al. (2013) has specifically addressed the Dina and Cummings formations within the Lloydminster heavy oil area. Notably, the current study covers an area approximately fifty kilometers south

of the northern boundary of Chalmers et al. (2013) research. The Dina and Cummings interval encompasses a diverse range of strata, spanning from continental to marine environments, and is characterized by several internal discontinuity surfaces with varying origins and stratigraphic importance. In this study, we establish the sequence stratigraphic significance of the facies associations complexes and discontinuity surfaces documented in the high-resolution facies analysis study of Chapter 2. We then use this analysis to construct systems tracts and sequences at hierarchical levels below the third-order depositional sequence of Cant (1996) (i.e., high-frequency sequences).

Ichnological Expressions of Stratigraphic Discontinuities



4-1) Ichnologically Demarcated Discontinuities

Illustrative diagrams and core examples of omission surfaces and soft-ground juxtaposition. In the omission suite example, the disconformable surface is cut by wave erosion (WRS) into cohesive offshore mudstone during forced regression and is colonized by organisms resulting in a *Glossifungites* surface. Burrows are infilled with sediment deposited subsequent to colonization. In the softground example, deeper water facies overlie more proximal strata indicating a landward shift in sedimentation. The contact is gradational and represents a high-frequency transgressive surface (TS). Illustrative diagrams are modified from MacEachern et al., 2007b.

4.2 Scale of Stratigraphic Units and Discontinuities

The resolution to which a sequence stratigraphic analysis can be achieved is dependent upon the scale of the available dataset and purpose of study (Catuneanu, 2019a). Therein it is argued that because sequences, systems tracts, and their bounding surfaces exist at different hierarchies, a scale-independent approach to the use of stratigraphic terminology is desirable. In a scale-independent model, determining

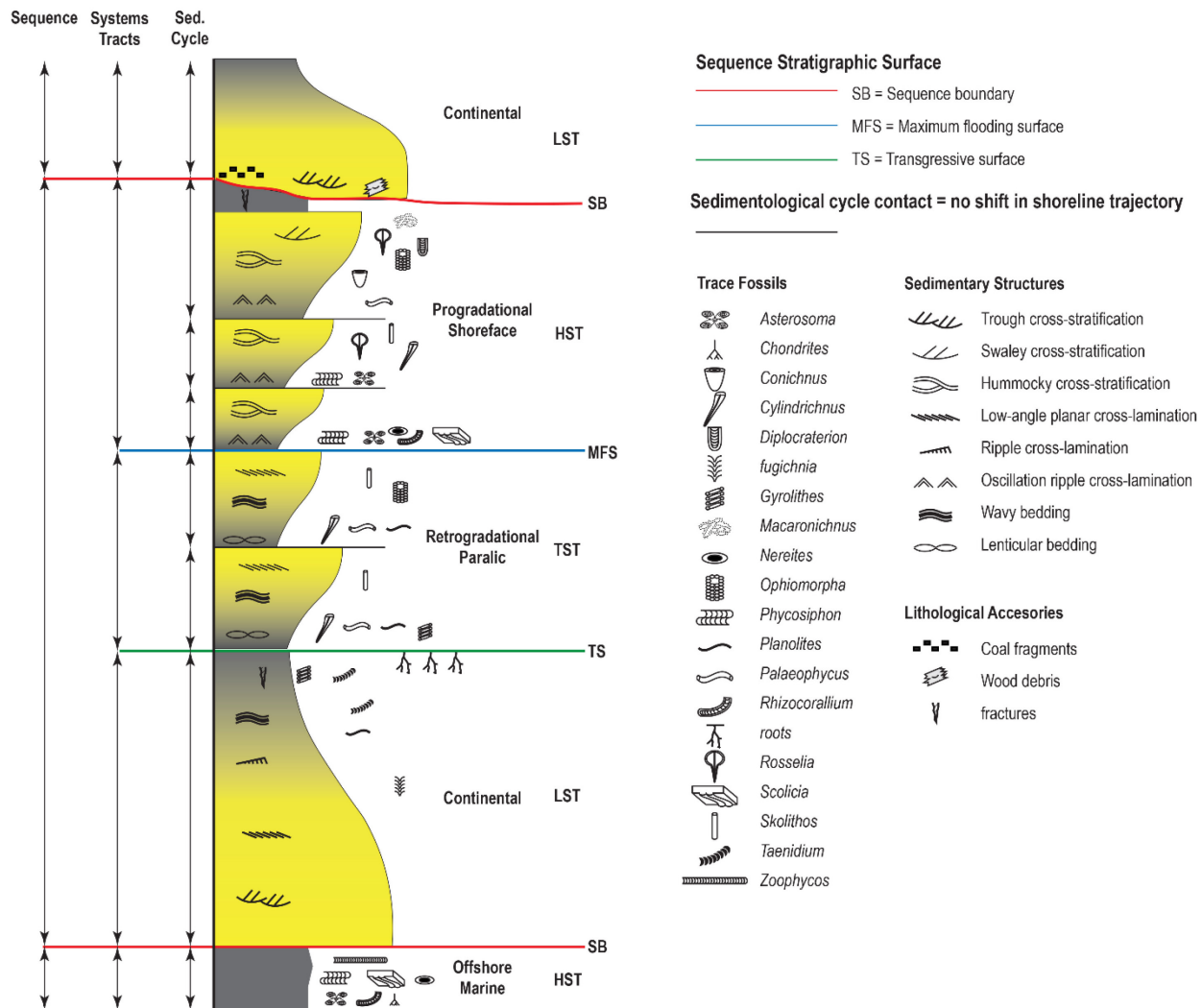
the hierarchy of sequences, systems tracts, and bounding surfaces requires a baseline for which the rank of these elements can be compared. Cant (1996) and Cant and Abrahamson (1996) have interpreted the Mannville Group as comprising a third-order depositional sequence, with the lower Mannville Dina and Cummings interval comprising the third-order transgressive systems tract. This implies that the contact between the Cummings and overlying Lloydminster Member represents a third-order maximum flooding surface (Fig. 4.2 A, thick blue line). This surface is recognized within the presented dataset and will be used as the baseline to which all higher or lower frequency sequences, systems tracts, and bounding surfaces will be compared (Fig. 4.2 B). In place of assigning a number value to sequences within the dataset, the qualitative terms low-, medium-, and high-frequency will be used with the third-order sequence of Cant (1996) representing the low-frequency category.

In high-frequency sequence stratigraphic analysis, a crucial distinction lies in differentiating between sedimentological cycles and stratigraphic sequences. According to Van Wagoner et al. (1990), sedimentological cycles are described as "a relatively conformable succession of genetically related beds bounded by surfaces of erosion, non-deposition, or their correlative conformities."

On the other hand, stratigraphic sequences can be defined using various approaches, but fundamentally, they consist of systems tracts and form in response to changes in base level. Bedsets or sedimentological cycles are nested within these systems tracts and primarily develop due to autocyclic processes, independent of shoreline shifts. Examples include prograding strandplain clinofolds or retrograding bayhead delta lobes, as shown in Fig. 4.3 (Catuneanu and Zecchin, 2013).

Zecchin et al. (2017) provides seven criteria that aid in discerning between high-frequency stratigraphic sequences and sedimentological cycles. These are: 1) occurrence of environmental change across bounding surfaces; 2) water depth changes across bounding surfaces; 3) the physical appearance of bounding surfaces (including the presence of substrate-controlled ichnofacies); 4) lateral extent of bounding surfaces; 5) presence of condensed deposits; 6) cycle thicknesses; and 7) recognition of a set of clinofolds in a regressive shoreface-shelf succession. With respect to core datasets, sedimentological and ichnological observations are well suited to the identification of environmental change, water depth change, the physical appearance of the bounding surfaces, as well as the presence of condensed deposits.

illustrating the stratigraphic relationships between the Dina, Cummings, and Lloydminster lithostratigraphic units including the third-order maximum flooding surface of Cant (1996) and the medium-frequency sequence boundaries of this study.



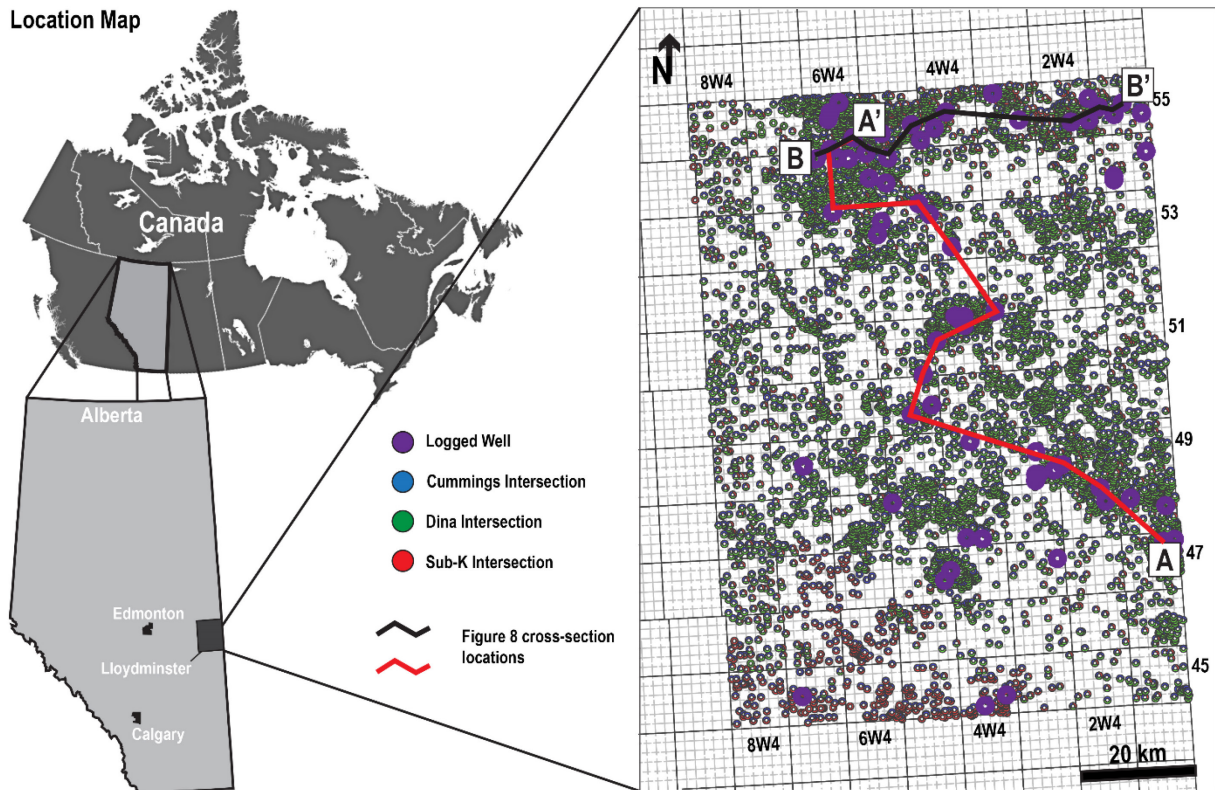
4-3) Schematic Diagram of Sequence Stratigraphic and Sedimentological Discontinuities

Illustration of scale and genetic differences between discontinuity surfaces of sequence stratigraphic and sedimentological significance. Sequence stratigraphic surfaces mark changes in stratal stacking patterns and define systems tracts. Bedset boundaries and sedimentological cycles occur within systems tracts, and do not correlate beyond the boundaries of the depositional system in which are depositionally related. LST = lowstand systems tract, TST = transgressive systems tract, HST = highstand systems tract.

4.3 Overview of Dina and Cummings Geology

The Lower Cretaceous Aptian to early Albian Dina and Cummings members consists of a spatially complex assemblage of continental, paralic, and marine strata (e.g., Nauss, 1945; Wickenden, 1948; Kent,

1959; Fulgem 1970; Orr et al., 1977; Vigrass, 1977; Zaitlin and Schultz, 1984; Wilson, 1984; Hayes et al., 1994; Christopher, 1997; McPhee and Pemberton, 1997; Bauer et al., 2009). In Chapter 2, a high-resolution facies analysis study was conducted on the Dina and Cummings members within the east-central plains region of Alberta covering an area of 8800 km² between Townships 45-55, Ranges 1-8W4 (Fig. 4.4). They combined sedimentological, ichnological, and petrophysical analyses to identify and interpret the range of depositional environments and the presence of discontinuity surfaces within this interval. This type of integrated dataset had not previously been completed for the Dina and Cummings in the sub-surface of Alberta. Table 1 provides a summary of the facies associations, and facies association complexes documented in Chapter 2. A brief summary follows below. Following the lithostratigraphic revision of Chapter 3, the Dina and Cummings formations preserve strata deposited along a continuum from continental to paralic to offshore marine. Continental facies consist of fluvial channel, overbank, and floodplain strata characterized by varying degrees of pedogenic alteration, and a trace assemblage restricted to continental ichnogenera (e.g., *Taenidium bowni*, *Scoyenia*), or those documented to occur across the spectrum from fresh to marine salinities (e.g., *Planolites*, *Skolithos*, *Taenidium isp.*). Paralic strata include lower delta plain, tide-influenced estuary, river- and wave-influenced deltaic, and open embayment facies, which are characterized by brackish-water to stressed marine ichnological assemblages. This interval comprises the Dina Formation (Chapter 3). Marine facies consist of deltaic and shoreface to shelf strata characterized by glauconitic sandstone, siltstone, and mudstone with high diversity, robust ichnological assemblages with forms normally confined to marine saline conditions (e.g., *Cosmorhapha*, *Nereites*, *Phycosiphon*, *Scolicia*, and *Zoophycos*) (Gingras et al., 2011). Marine strata comprise the Cummings Formation (Chapter 3). The bounding surfaces defining the top and base of the Dina are disconformable, sharp, and locally erosional. Bounding surfaces of the Cummings are sharp, and locally erosional (base) and gradational or erosional (top) depending on the nature of the overlying Lloydminster Member. Where the Lloydminster comprises regionally extensive progradational strata the contact is conformable (Fig. 4.2 B, wells 10-35 and 15-25). Where the Lloydminster Member comprises incised valley fill deposits, the contact is demonstrably incisional as regional strata and their bounding surfaces of the Cummings Member are truncated against channel walls (Fig. 4.2 B, wells 12-01 and 08-18). Within the Dina and Cummings members are numerous stratigraphic discontinuity surfaces of variable origin and extent. It is the nature of these internal surfaces that is crucial to adding resolution to the third-order depositional sequence of Cant (1996) and Cant and Abrahamson (1996) in which the Dina, Cummings, and Lloydminster lithostratigraphic intervals reside.



4-4) Location Map and Well Dataset

Location map showing the density and distribution of wells utilized in regional correlations. Note the significant areas lacking core data (purple circles) particularly in the west and east-central areas.

4.4 Dataset and Methodology

The dataset comprising this study includes stratigraphic drill core and petrophysical wireline data. The cores available within the study are limited (approximately one hundred stratigraphic cored intervals across 8800km²), with only one core intersecting the entire Dina and Cummings interval. Core are unevenly distributed and are absent across as much as 1200km² in some parts of the study area. The petrophysical dataset consists of approximately 7,800 wells for which digital log curves consisting of at least one of gamma ray, spontaneous potential, neutron porosity, density porosity, density, photoelectric factor, or deep resistivity are available. No publicly available seismic data are available, and no outcrop sections of the Dina and Cumming formations occur within the study limits. The lack of seismic and outcrop data places greater importance on the interpretation of sedimentary facies, particularly those in contact with stratigraphic discontinuities. A high-resolution facies analysis on a 72-core dataset focused on identifying the range of depositional environments preserved within the Dina and Cummings interval constitute

Chapter 2. Discontinuity surfaces were documented and briefly described in terms of bounding strata and their extent but were not discussed in terms of their sequence stratigraphic significance. Seven facies association complexes (FAC-A to G) were identified, which encompass 21 facies associations. These are summarized in Table 4.1.

Table 4-1

Geological characteristics of facies associations and facies association complexes comprising the Dina, Cummings, and Lloydminster lithostratigraphic units. Also shown are the systems tracts and sequences which they comprise. Seq. = Sequence, S.T. = Systems tract.

| Seq. | S.T | FAC | FA | Sedimentary Structures | Ichnogenera | Accessories | Interpretation |
|---------------------------|-----|-------|-------|--|--|---|--|
| High-Frequency Sequence 1 | LST | FAC-A | A-FA1 | trough & planar tabular cross-bedding, low-angle & planar cross-lamination, current ripples, grain striping, massive fabric, soft-sediment deformation | <i>Planolites, Palaeophycus, Skolithos, Taenidium, rootlets, rhizoliths</i> | carbonaceous detritus, wood debris, pyrite, mud clasts | continental fluvial channel, point-bar |
| | | | A-FA2 | current ripples, low-angle planar lamination, mottled, massive, convolute lamination, soft-sediment deformation, lenticular bedding, normally-graded beds, pedogenic slickensides | <i>Taenidium bowni, Taenidium, Skolithos, Planolites, rootlets, rhizoliths</i> | pyrite, coal fragments, siderite nodules, plant debris, iron staining, sand laminae, silt laminae | floodplain - proximal to distal |
| | | | A-FA3 | trough & planar tabular cross-bedding, low-angle planar, current & combined flow ripple cross lamination, massive, wavy-bedded, mottled, lenticular bedding, convolute lamination, double mudstone drapes, rhythmic lamination | <i>Arenicolites, Planolites, Palaeophycus, Skolithos, Taenidium, rootlets</i> | pyrite (nodular and disseminated), carbonaceous detritus, coal fragments, mud clasts | fluvially dominated, tide-influenced channel, point-bar, and bar-top |
| | | | A-FA4 | low-angle planar & current ripple cross-lamination, faint cross-lamination, massive, mottled, double mudstone drapes | <i>?Conichnus, fugichnia, Lockeia, Planolites, rootlets, Skolithos, Taenidium isp, Rhizoliths</i> | organic detritus, rare mud drapes, pyrite | distributary channel |
| | | | A-FA5 | wavy bedded, bioturbated, lenticular, current ripple & low-angle cross-laminated, convolute lamination, mottled. | <i>Cylindrichnus, Gyrolithes, rootlets, Planolites, Skolithos, Taenidium, Teichichnus</i> | organic detritus, pyrite, granules, iron stain, coal laminae, clasts with altered rims | interdistributary bay fill/crevasse splay |
| | TST | FAC-B | B-FA1 | wavy bedding, lenticular bedding, flaser bedding, convolute lamination, low-angle planar, current & combined flow ripple cross-lamination, normally graded beds, synaeresis cracks, load casts | <i>Arenicolites, Cylindrichnus, fugichnia, Lockeia, Palaeophycus, Planolites, rootlets, Skolithos, Taenidium, Teichichnus, Thalassinoides</i> | mud clasts, organic detritus, pyrite | tide-influenced, wave-affected tidal delta |
| | | | B-FA2 | low-angle planar, current, and oscillation ripple cross-lamination, hummocky cross-stratification, wavy bedding, mottled, lenticular bedding, massive, faint low-angle cross-lamination | <i>Arenicolites, Cylindrichnus, Diplocraterion, fugichnia, Gyrolithes, Paleophycus, Planolites, Siphonichnus, Taenidium, Teichichnus, Thalassinoides</i> | pyrite, organic detritus, coal fragments, silt laminae, siderite cement | wave- and tide-influenced bay-margin |
| | | | B-FA3 | oscillation ripple cross-lamination, wavy bedding, mottled, lenticular bedding, massive, faint low-angle cross-lamination | <i>Arenicolites, Cylindrichnus, Diplocraterion, fugichnia, Gyrolithes, Paleophycus, Planolites, Siphonichnus, Taenidium, Teichichnus, Thalassinoides</i> | pyrite, organic detritus, coal fragments, silt laminae, siderite cement | wave-influenced bay-margin |

| | | | | | | |
|-----|-------|-------|--|--|---|--|
| HST | FAC-C | B-FA4 | trough & planar tabular cross-bedding, massive, low-angle, planar, current ripple, & combined flow ripple cross-lamination, grain-stripping, double mudstone drapes, rhythmic lamination | <i>Arenicolites, Cylindrichnus, Gyrolithes, Planolites, Psilonichnus, rootlets, Skolithos, Taenidium</i> | mud clasts, organic detritus | tide- and fluviially influenced channel, point-bar, and tidal flat |
| | | C-FA1 | trough cross bedding, low-angle planar & hummocky cross-stratification, convolute lamination, combined flow-ripple cross-lamination, synaeresis cracks, normally graded beds, micro-faults, fluid escape structures. | <i>Cylindrichnus, fugichnia, Palaeophycus, Planolites, rootlets, Skolithos, Taenidium, Teichichnus</i> | coal fragments, pyrite, organic detritus, carbonaceous drapes | river-dominated, wave-influenced delta |
| | | C-FA2 | hummocky cross-stratification, trough cross bedding, low-angle planar & convolute lamination, combined flow-ripple cross-lamination, synaeresis cracks, normally graded beds, micro-faults, fluid escape structures. | <i>Cylindrichnus, fugichnia, Palaeophycus, Planolites, rootlets, Skolithos, Taenidium, Teichichnus</i> | coal fragments, pyrite, organic detritus, carbonaceous drapes | wave-dominated delta |
| | | C-FA3 | low-angle planar & vague cross-lamination, combined flow ripples, flaser bedding, oscillation & combined flow ripple cross-lamination, convolute lamination, synaeresis cracks, normally graded beds | <i>Arenicolites, Asterosoma, Berguaeria, Cylindrichnus, fugichnia, Gyrolithes, Helminthopsis, Ophiomorpha, Palaeophycus, Planolites, rhizoliths, rootlets, Skolithos, Taenidium, Teichichnus, Thalassinoides</i> | organic detritus, coal fragments, wood debris, pyrite, carbonaceous drapes | bay-margin shoreface to offshore |
| | FAC-D | D-FA1 | trough cross-bedding, low-angle planar cross-lamination, massive fabric, combined flow ripples, dish and pillar, flame structure, fluid escape structures, double mud drapes, convolute lamination, synaeresis cracks, load casts, pinstripe lamination, micro-folds | <i>Berguaeria, fugichnia, navichnia, Rhizocorallium, Planolites, Skolithos, Teichichnus, Thalassinoides</i> | coal fragments, carbonaceous debris, plant debris, pyrite, siderite cement, siltstone laminae | tide-, wave-, and river-influenced distributary channel |
| | | D-FA2 | trough cross-bedding, low-angle planar cross-lamination, hummocky cross-stratification, massive fabric, combined flow ripples, double mud drapes, convolute lamination, synaeresis cracks, load casts, pinstripe lamination | <i>Berguaeria, fugichnia, navichnia, Rhizocorallium, Planolites, Skolithos, Teichichnus, Thalassinoides</i> | coal fragments carbonaceous debris, plant debris, pyrite, siderite cement, siltstone laminae | tide-, wave-, and river-influenced delta front |
| | | D-FA3 | trough cross-bedding, low-angle planar cross-lamination, massive fabric, combined flow ripple cross-lamination, lenticular bedding | <i>Planolites</i> | abundant coal fragments, pyrite, wood debris | mouth bar |
| | FAC-E | E-FA1 | trough cross-bedding, low-angle planar, & hummocky cross-stratification, climbing ripples, flame structures, convolute lamination, flaser bedding, flaser bedding, load casts, double mud drapes, scour surfaces | <i>Berguaeria, Chondrites, Cylindrichnus, Diplocraterion, fugichnia, Lockeia, Macaronichnus, navichnia, Ophiomorpha, Palaeophycus, Phycosiphon, Planolites, Rhizocorallium, Rosselia, Skolithos, Teichichnus, Thalassinoides</i> | organic detritus, coal fragments, wood fragments, pyrite, siderite cement | storm-influenced marine delta |
| | | E-FA2 | current ripples, mottled, massive, convolute lamination, soft-sediment deformation, lenticular bedding, pedogenic slickensides | <i>Taenidium boweni, Taenidium, Skolithos, Planolites, rootlets, rhizoliths</i> | pyrite, coal fragments, plant debris, sand laminae, silt laminae | delta plain |

| | | | | | | | |
|---------------------------|-----|-------|-------|---|---|---|----------------------------------|
| High-Frequency Sequence 2 | LST | FAC-F | F-FA1 | low-angle, planar, & hummocky cross-stratification, oscillation, & combined flow ripples, soft sediment deformation, fluid escape structures, synaeresis cracks, normally graded beds, convolute lamination, load casts, fluid muds, double mud drapes | <i>Arenicolites, Asterosoma, Berguaeria, Cylindrichnus, Diplocraterion, fugichnia, Gyrolithes, Helminthopsis, Ophiomorpha, Palaeophycus, Phycosiphon, Planolites, Rhizocorallium, Rosselia, Skolithos, Teichichnus, Thalassinoides</i> | pyrite, organic detritus | river- and wave-influence delta |
| | | | F-FA2 | low-angle planar & hummocky cross-stratification, current, combined flow, & oscillation ripple cross-lamination, fluid mud, convolute lamination, load casts, micro-faults, flame structure, double mud drapes, fluid escape structures, | <i>Arenicolites, Asterosoma, Berguaeria, Chondrites, Cylindrichnus, Cosmorhapha, Diplocraterion, Helminthopsis, Palaeophycus, Phycosiphon, Planolites, Rhizocorallium, Skolithos, Teichichnus, Thalassinoides, Zoophycos</i> | glauconite, organic detritus, pyrite, coal fragments, calcite cement | tide- and wave-influenced delta |
| | | | F-FA3 | low-angle planar & hummocky cross-stratification, combined flow & oscillation ripple cross-lamination, normally graded beds, double mud drapes | <i>Arenicolites, Asterosoma, Chondrites, Cylindrichnus, Helminthopsis, navichnia, Palaeophycus, Phycosiphon, Planolites, Rhizocorallium, Scolicia, Skolithos, Teichichnus, Thalassinoides, Zoophycos</i> | glauconite, carbonaceous debris, pyrite, siderite, shell debris, granules | transgressive lag |
| | TST | FAC-G | G-FA1 | low-angle planar & hummocky cross-stratification, combined flow & oscillation ripple cross-lamination | <i>Arenicolites, Asterosoma, Berguaeria, Chondrites, Cosmorhapha, Cylindrichnus, Diplocraterion, Helminthopsis, Nereites, Ophiomorpha, Palaeophycus, Phoebichnus, Phycosiphon, Planolites, Rhizocorallium, Rosselia, Schaubcylindrichnus freyi, Scolicia, Skolithos, Teichichnus, Thalassinoides, Zoophycos</i> | glauconite, carbonaceous debris, pyrite | marine lower shoreface to shelf |
| | | | HST | trough, planar tabular, low-angle, & hummocky cross-stratification, oscillation & combined flow ripple cross-lamination, flaser bedding, normal & reverse-graded beds, synaeresis cracks, load casts, flame structure, mudstone drapes, soft-sediment deformation, convolute lamination | <i>Arenicolites, Asterosoma, Berguaeria Chondrites, Conichnus, Cylindrichnus, fugichnia, Palaeophycus, Phycosiphon, Planolites, Rhizocorallium, Rosselia, Skolithos, Teichichnus, Thalassinoides,</i> | organic detritus, pyrite, wood fragments | Storm- and river-dominated delta |

4.5 Scale of Units and Bounding Surface

The seven facies association complexes documented in Chapter 2 and summarized in Table 4.1 represent the building blocks of systems tracts that comprise three scales of units. Together the seven units comprise the low-stand and transgressive systems tracts of the third-order depositional sequence of Cant (1996) and Cant and Abrahamson (1996). The Dina, Cummings, and regional Lloydminster lithostratigraphic units form a complete depositional sequence one hierarchical scale below this third-order sequence. This is hereafter referred to as MF Sequence 1 (MF – medium frequency). MF Sequence 1 consists of two higher-frequency depositional sequences, hereafter termed HF Sequence 1 and 2. We apply Depositional Sequence IV (Hunt and Tucker, 1992; Helland-Hansen and Gjelberg, 1994) which recognizes four systems tracts: FSST, LST, TST, and HST.. Surface nomenclature follows that of Cattaneo

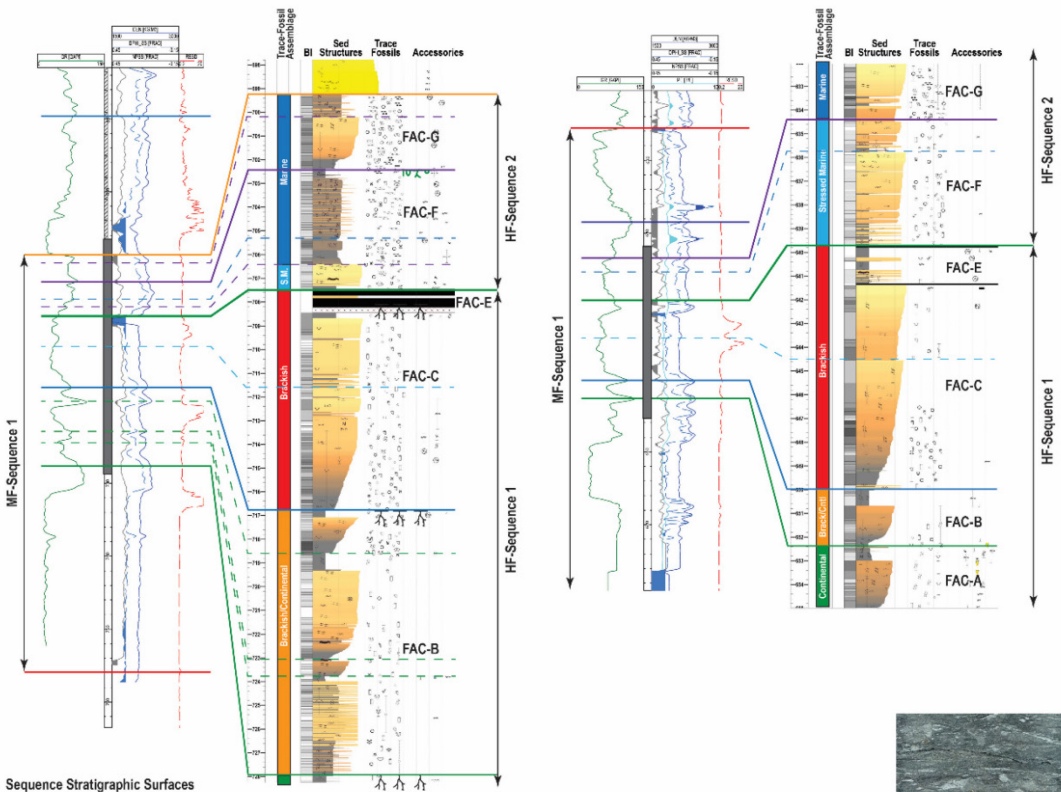
and Steel, (2003), Catuneanu (2006), and Zecchin and Catuneanu (2013). The following section describes the major sequence stratigraphic surfaces that occur within the interval of study. These are summarized in Table 4.2. These will then be combined with the facies associations and facies association complexes to interpret the systems tracts and overall sequence stratigraphic architecture of the Dina, Cummings, and Lloydminster lithostratigraphic units.

4.5.1 Bounding Surfaces

Based on facies analysis and the correlatability of surfaces on wireline logs, five sequence stratigraphic surfaces are recognized. Examples are shown in Figure 4.5. Both surface types are given the same name, with sedimentological cycles differentiated with an HF. Surfaces at both scales may be coplanar. In such cases the younger surface type is listed first, followed by the precursor. The primary genetic differences between sequence stratigraphic and sedimentological discontinuity surfaces are the degree of correlatability and stratal stacking pattern of the bounding units (e.g., Catuneanu et al., 2011; MacEachern et al., 2012; Catuneanu, 2019a,b). Sequence stratigraphic surfaces exhibit continuity beyond the boundaries of a single depositional environment and are linked to variations in base level, leading to distinct stratal stacking patterns both above and below these surfaces. By contrast, sedimentological surfaces are confined within specific depositional environments and do not arise from alterations in shoreline trajectory related to base-level changes (Fig. 4.3).

4.5.1.1 *Subaerial Unconformity and Correlative Conformity – SU & CC*

The SU (Sloss et al., 1949) forms under subaerial conditions that may be accompanied by erosion, non-deposition and/or paleosol development. Within the Dina-Cummings-Lloydminster interval two sequence stratigraphically significant SUs occur. These are the bounding surfaces of MF Sequence 1. The basal SU occurs at the base of fluvial, fluvio-tidal, or tidal channel strata of FAC-A and B (Fig. 4.5). In the latter two instances it is reworked by the tidal ravinement surface (TRS) and overlain by deposits of the TST. It must be noted that these surfaces may correspond to sedimentological contacts where fluvio-tidal and tidal channels have incised into floodplain facies as a result of autogenic processes (e.g., channel avulsion) The second occurrence is at the base of Lloydminster-aged, incised valley fills, where the SU is likewise reworked by the TRS.

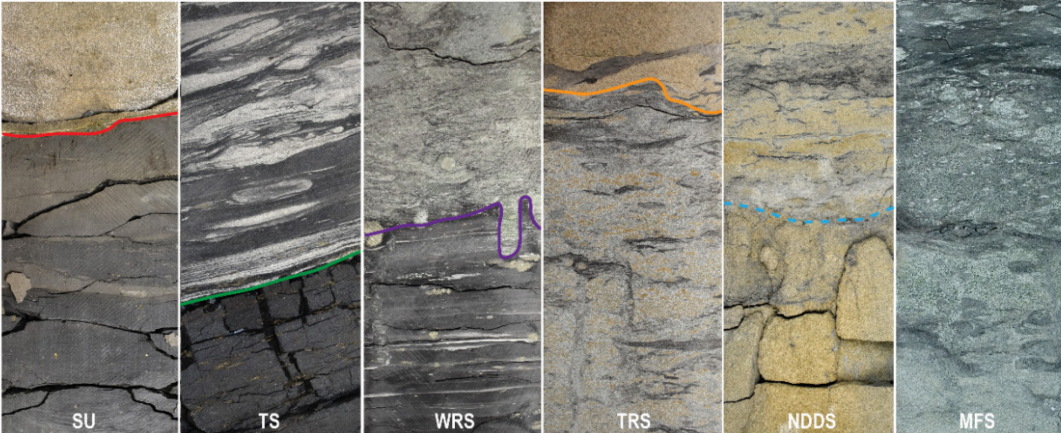


Sequence Stratigraphic Surfaces

- Subaerial unconformity
- Transgressive surface
- Maximum flooding surface
- Wave Ravinement surface
- Tidal Ravinement surface

High-Frequency Sedimentological Surfaces

- - - Wave Ravinement surface
- - - Non-depositional discontinuity surface
- - - Transgressive surface



4-5) Sequence and Sedimentological Surfaces

Core logs and photos illustrating the nested relationship of facies association complexes A-G, high-frequency sequences 1 and 2, and medium frequency sequence 1 and the placement and core expression of their bounding discontinuities. In these examples, only the NDDS is a sedimentological contact (dashed blue line) with all other surfaces being of stratigraphic significance.

4.5.1.2 *Transgressive Surface - TS*

The transgressive surface (TS, Cattaneo and Steel, 2003) (=MRS, Helland-Hansen and Martinsen, 1996) demarcates the turnaround from regression to transgression. The TS also coincides with the MFS if transgressive deposits are not preserved/deposited (Cattaneo and Steel, 2003). In the context of this study the transgressive surface terminology is applied to surfaces where no evidence of erosion is preserved. Two sequence stratigraphic TSs occur within the Dina-Cummings-Lloydminster interval: 1) at the contact between continental strata of facies associations A-FA1 and A-FA2 and delta plain to estuary strata of facies associations A-FA3 – FA5, and FAC-B; and 2) at the contact between delta front and delta plain facies of FAC-E, and marine deltaic to offshore facies of FAC-F and G (Fig. 4.5). In both instances the change in ichnological characteristics across the TS persist in the overlying facies associations. This differs from the repetition of similar trace fossil characteristics across TSs of sedimentological significance. In the lower stratigraphic occurrence, the TS marks the first appearance of brackish-water ichnofauna (e.g., *Cylindrichnus*, *Gyrolithes*, *Teichichnus*) and/or tidally generated sedimentation (appearance of double mudstone drapes, apparent rhythmicity). The upper TS marks the persistent presence of diverse ichnological assemblages associated with marine salinity conditions (e.g., *Cosmorhappe*, *Nereites*, *Phycosiphon*, *Scolicia*, *Zoophycos*). The upper occurrence of the TS at the contact between FAC-E and FAC-F or G becomes reworked in a basinward direction by the RS (Fig. 4.6, well 14-34).

4.5.1.3 *Ravinement Surface - RS*

The ravinement surface (RS) is an erosional transgressive surface cut by waves (WRS, Swift, 1968; Nummedal and Swift, 1987) or tides (TRS, Allen and Posamentier, 1993). RSs may be overlain by lag deposits (Kidwell, 1989) and are commonly demarcated by substrate-controlled ichnofacies (e.g., MacEachern et al., 1992; Pemberton et al., 1992; MacEachern et al., 2012; Zecchin and Catuneanu, 2013; Zecchin et al., 2019). Most RSs occurring within the Dina-Cummings-Lloydminster interval occur within FAC-F and FAC-G (Fig. 4.5). All of these RSs are interpreted as WRSs. WRS surfaces within this interval are commonly overlain by lag deposits consisting primarily of glauconite, pyrite, organic detritus, and shell debris and commonly display omission suites of the *Glossifungites* ichnofacies. TRSs are interpreted at two stratigraphic intervals, the base of fluvio-tidal or tidal channel deposits in HF Sequence 1, and the base of incised valley fills of the Lloydminster where the TRS has reworked the sequence boundary defining the top of MF Sequence 1 (i.e., TRS/SU)

4.5.1.4 *Maximum Flooding Surface - MFS*

The maximum flooding surface (MFS) corresponds to the seafloor at the peak of shoreline transgression (Posamentier et al., 1988; Van Wagoner et al., 1988) and marks the change from

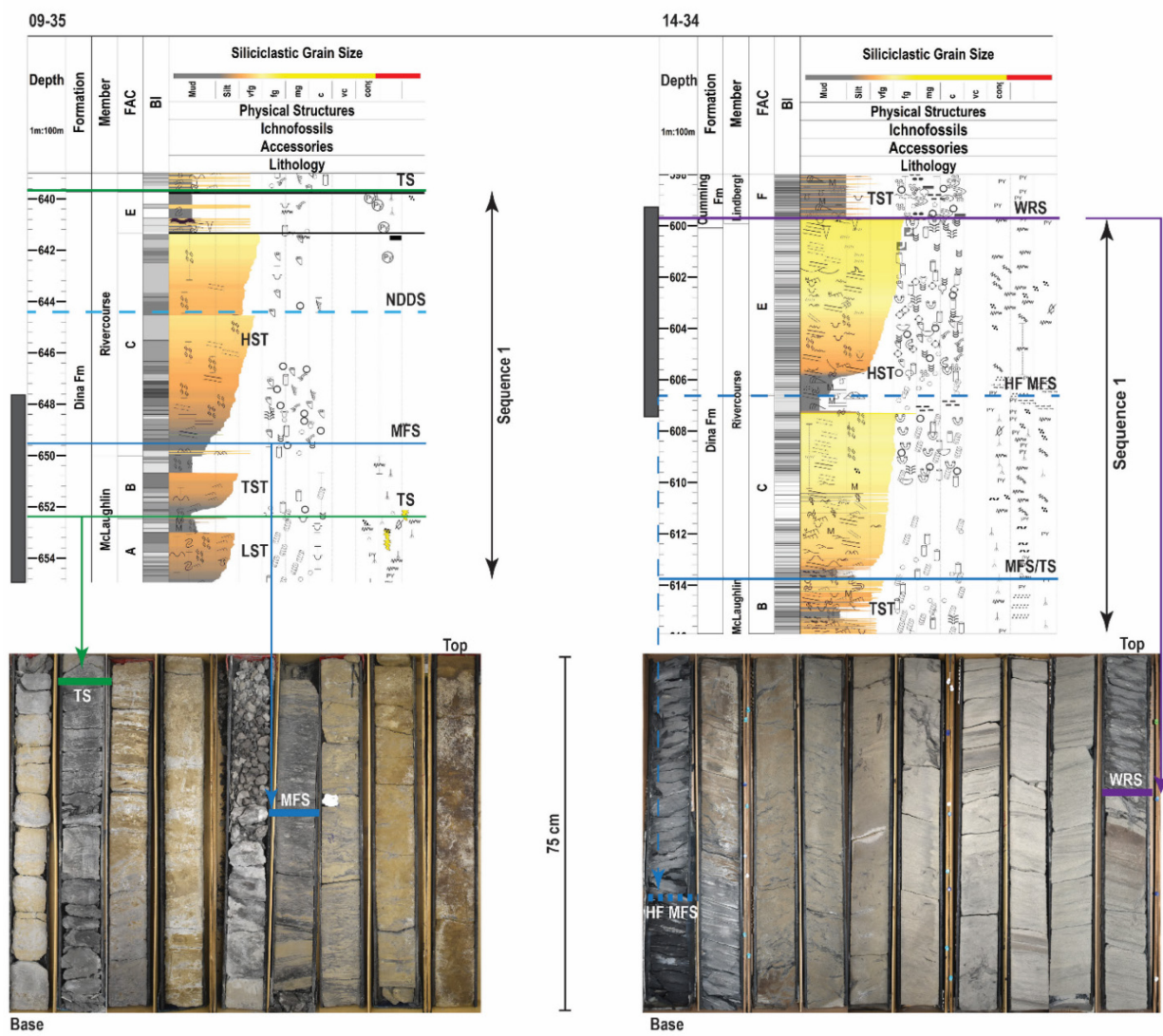
transgressive to normal regressive shoreline trajectories (Helland-Hansen and Martinsen, 1996). MFSs can be recognized at two scales, both of which are of sequence stratigraphic significance. The higher-frequency MFS occurs at or slightly above the base of the open embayment strata of FAC-C (Fig. 4.5, Fig. 4.6). This surface corresponds to the zone of maximum ichnological diversity, bioturbation intensity, and maximum water depth in HF Sequence 1, and marks the change from a retrogradational to a progradational stratal geometry. The MFS of HF Sequence 2 marks the furthest landward extent of sea level and represent the most distal marine facies preserved within LF Sequence 1.

4.5.2 Sedimentological Surfaces

Within HF sequences 1 and 2 are discontinuity surfaces where bounding strata resemble facies juxtapositions of stratigraphic surfaces but do not mark changes in stratal stacking pattern and, therefore, are not regional in nature. Where these surfaces occur, they are given the same terminology as stratigraphic surfaces, with the addition of the abbreviation HF (e.g., HF MFS). One additional term is the use of non-depositional discontinuity surfaces (NDDS) (*sensu* Hampson and Storms, 2003). NDDSs are identified by abrupt decreases in event bed thicknesses, increases in bioturbation intensity, and anomalous interfingering of facies (Hampson and Storms, 2003). NDDSs may form as a result of a decrease in storm frequency, a change from high-energy to lower-energy wave climate, or minor rises in relative sea-level (Hampson and Storms, 2003). These surfaces are most abundant at the contacts between stacked facies associations of FAC-C and within the prograding cycles of the regional Lloydminster Member.

The most readily discernible difference between stratigraphic and sedimentologic contacts in core is the magnitude of apparent environmental juxtaposition, or the emergence or disappearance of particular sedimentological or ichnological attributes. For example, lower delta plain interdistributary bay facies commonly occur as stacked coarsening-upward cycles typically less than 2 metres thick. They are bound by rooted, bioturbated paleosol horizons and within each successive cycles, changes in ichnological and sedimentological characteristics are gradual. In contrast, a distinct or permanent change in facies characteristics occurs across stratigraphic contacts. In the case of the lowest TS in HF Sequence 1, the sedimentological and lithological juxtaposition is minor, but the appearance and permanent presence of brackish-water trace fossils and tidally generated structures suggests the turnaround from regression to transgression. Other examples may be more pronounced. The MFS-TS or MFS at the contact between open embayment strata FAC-C and overlying estuarine facies is lithologically similar to the juxtaposition of lower delta plain over continental facies (paleosol overlain by bioturbated mudstone). However, the difference in ichnological diversity across the sequence stratigraphic MFS is higher (14 ichnogenera versus 10) than that across the sedimentological contact between stacked lower delta plain cycles (essentially equal).

Systems Tracts of High-Frequency Sequence 1



4-6) Core Logs and Photos of HF Sequence 1

Core log and associated core photos showing the facies relationships across the TS, MFS, and WRS of high-frequency sequence 1. The TS marks the transition from the lowstand to transgressive systems tract. The MFS (solid blue line) marks the transition from the transgressive to highstand systems tract. Grey rectangles beside the depth track of each core log represents the core displayed in the photographs below.

4.6 Depositional Sequences

4.6.1 High-Frequency Depositional Sequence 1

4.6.1.1 Lowstand Systems Tract

The lowstand systems tract is defined by normal regression during a period of lowered base level and is bound at the base by the SU/CC, and at the top by the TS/MRS. LST strata of HF Sequence 1 consist of continental facies consisting of fluvial channel, point-bar, and floodplain strata that lack detectable

evidence of brackish-water sedimentation or tidal influence (Fig. 4.6, Fig. 4.7 A-C). This corresponds to A-FA1 and A-FA2 in Table 4.1. The basal sequence boundary is placed at the base of fluvial or estuarine channel strata of A-FA1, -FA3, or B-FA-4 (Fig. 4.2 B). Where the sequence boundary is overlain by tide-influenced channel facies of B-FA4, it is regarded to be a co-planar TRS-SU and the LST is not preserved. The preservation of LST strata is influenced by topographic variability along the sub-Cretaceous unconformity. Within the LST are a number of sedimentological cycles bound by surface corresponding to discontinuity surfaces where pedogenically altered horizons are buried by periodic influxes of sedimentation. The overlying cycle then itself becomes progressively pedogenically altered resulting in stacked paleosol horizons. These internal HF SU surfaces are not regionally mappable and commonly appear to be eroded by fluvial, fluvio-tidal, and estuarine channels.

The contact between LST and TST facies represents a transgressive surface, which is a broadly conformable surface separating regressive deposits below from early transgressive deposits above (Fig. 4.6 well 09-35). This contact is best identified in core, as the sedimentological and ichnological changes across this surface are subtle and not always identifiable on wireline logs. In core, the TS is placed at the base of the first facies association with evidence of brackish-water conditions or of tidal modulation which are inferred to record basal transgressive strata (Gingras et al., 2012b) (Fig. 4.6, well 09-35). Specific ichnogenera associated with brackish-water conditions include *Cylindrichnus*, *Gyrolithes*, and *Teichichnus* (e.g., Pemberton et al., 1982; Beynon et al., 1988, Gingras et al., 2016).

4.6.1.2 Transgressive Systems Tract

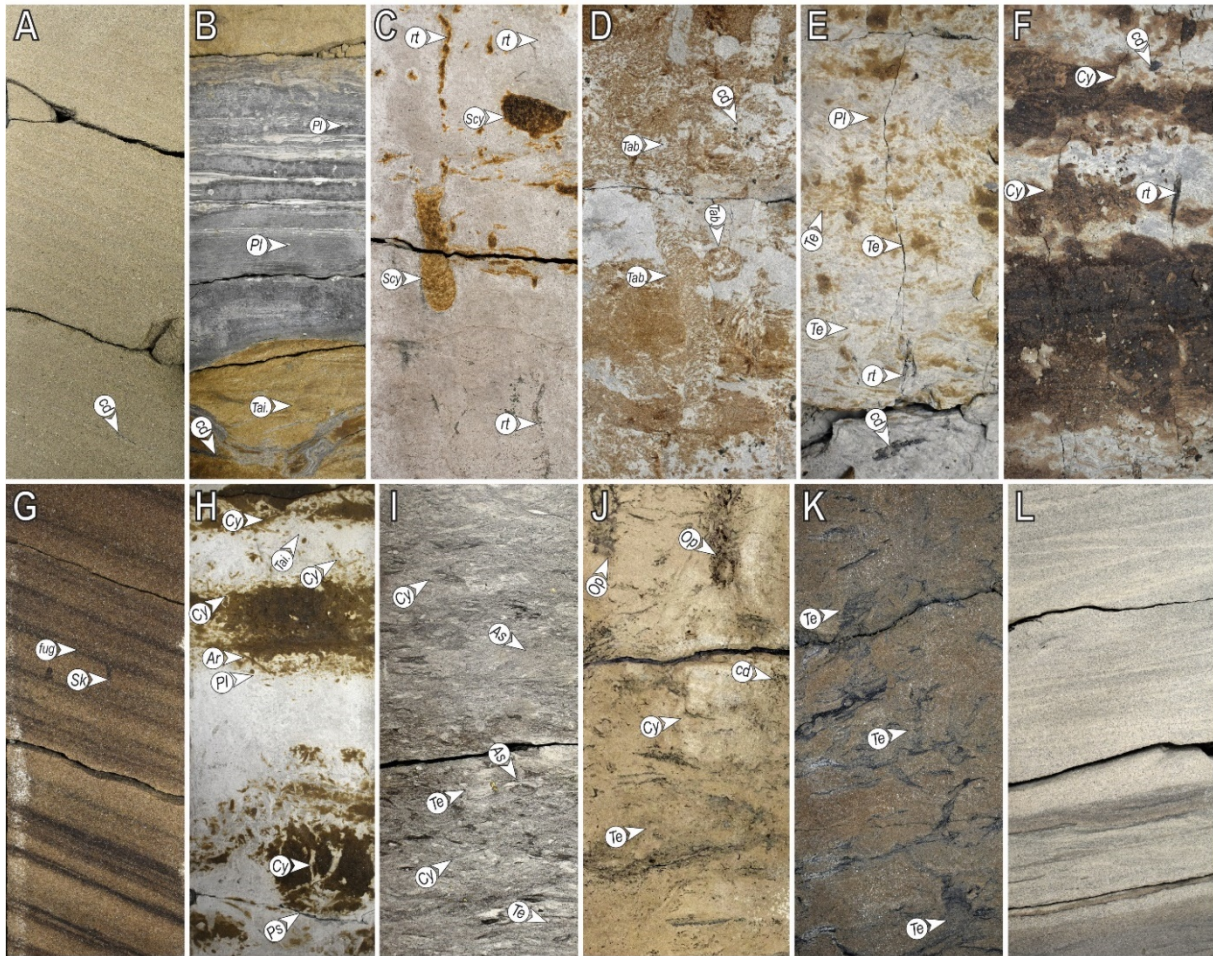
The transgressive systems tract is comprised of retrogradational strata bound at the base by the TS and at the top by the MFS. The TST of HF Sequence 1 is characterized by multiple thin, coarsening- and fining-upward facies associations consisting of lower coastal plain interdistributary bay and channel fills, tide- and wave-influenced bay-margin deltas, tidal channel, tidal bar, and tidal flat facies (Fig. 6, Fig. 7D-H). Lateral facies variability is high, and correlation of distinct internal surfaces is spatially limited. The contacts between individual facies associations are often demarcated by poorly to moderately developed paleosol horizons with variable thicknesses of unmodified sediment between (HF SUs). In the classification of paleosol profiles by Marriott and Wright, (1993) these features correspond to composite and compound profiles which indicate relatively intermittent rapid accumulation of moderate to large amounts of sediment (Marriott and Wright, 1993; Tabor and Myers, 2015). The sedimentological and ichnological differences between TST and LST facies include: 1) the presence of tidal sedimentation in the form of double mudstone drapes and apparent rhythmicity, 2) presence of oscillation ripples and minor hummocky cross-stratification; and 3) the presence of brackish-water ichnogenera (e.g., *Cylindrichnus*,

Gyrolithes, *Teichichnus*). Brackish-water trace fossils are overprinted by continental suites in coastal plain deposits suggesting alternating conditions of brackish-water submergence and sub-aerial exposure. Deposition of tide- and wave-influenced bay, tidal channel, tidal bar, and tidal flat facies appear to be deposited under persistently brackish-water conditions and progressively overly delta plain strata. The TST is thickest in the north-west of the study where overall accommodation is greatest, and onlaps underlying LST, Jurassic, and Paleozoic strata in a south-east and east-ward direction (Fig. 4.8).

The contact between the transgressive and highstand systems tracts represents the maximum flooding surface of HF Sequence 1 wherein pedogenically altered TST facies are sharply overlain by brackish to stressed marine open embayment deposits of the HST (Fig. 4.6). The MFS may occur at the facies contact between paleosol strata of the transgressive and bioturbated mudstone of the highstand systems tract, or slightly above this contact where the bioturbated mudstone transitions from fining-to coarsening-upward (e.g., Fig. 4.6, well 09-35).

4.6.1.3 Highstand Systems Tract

The highstand systems tract is characterized by normal regression and is bounded at the base by the MFS and at the top by the SU, RSME, or BSFR if followed by the falling stage systems tract, or a TS if followed by transgression (Catuneanu, 2019b). Highstand deposits of HF Sequence 1 consist of two to five stacked, progradational wave- and river-dominated deltaic and open embayment cycles (FAC-C and -E) with local tidal channel and mouth-bar facies (FAC-D) (Fig. 4.6, Fig. 4.7 I-L, Fig. 4.8). Progradational facies associations within the highstand systems tract are bound by both HF MFSs, which may be sharp or gradational, and non-depositional discontinuity surfaces (NDDSs) (*sensu* Hampson and Storms, 2003) (Fig. 4.5, Fig. 4.6). The highstand systems tract of HF Sequence 1 is capped by a regional coal seam (the “E” coal, Chapter 2) which is used as the datum for cross-sections in Figure 4.8. The sedimentological and ichnological characteristics of highstand strata are distinct from the thinner, less laterally continuous transgressive systems tract facies associations below. Sedimentologically, facies associations of the HST are characterized by wave-generated (e.g., hummocky cross-stratification, oscillation ripple cross-lamination, planar lamination) and fluvially generated (e.g., normal- and reverse-graded beds, synaeresis cracks, and phytodetriral pulses) structures (Fig. 7I-L). Tidally generated structures such as double mudstone drapes and rhythmites are still present, but significantly less prevalent than in the TST (with the exception of tidal channels of FAC-D). Ichnologically, the trace fossil suites of highstand facies are more diverse (18 (HST) vs. 10 (TST) distinct ichnogenera). Ichnogenera include *Berguaeria*, *Chondrites*, *Cylindrichnus*, *Diplocraterion*, *fugichnia*, *Lockeia*, *Macaronichnus*, *navichnia*, *Ophiomorpha*, *Palaeophycus*, *Phycosiphon*, *Planolites*, *Rhizocorralium*, *Rosselia*, *Skolithos*, *Teichichnus*, and *Thalassinoides*.



4-7) Facies of HF Sequence 1

Facies of High-frequency Sequence 1. A-C) Fluvial channel, point-bar facies, and floodplain facies of A-FA1 strata characterized by a low-diversity continental ichnological assemblage with *Planolites* (*Pl*), *Scoyenia* (*Scy*) and *Taenidium boweni* (*Tab*). Photo A from 15-25-047-01W4, depth 651.7m, photo B from Well 16-03-049-03W4, depth 732.1m, photo C from well 02-30-051-04W4, depth 592.3m. D) Pedogenically altered lower delta plain strata with continental overprinting of brackish-water deposits with a monospecific assemblage of *Taenidium boweni* (*Tab*). Photo from 09-35-047-01W4, depth 653.2m, E-H) Upper to middle estuary strata of the transgressive systems tract including muddy interdistributary bay (E, F), and tidal channel and muddy point-bar (G, H) characterized by a low-diversity brackish-water ichnological assemblage consisting of *Arenicolites* (*Ar*), *Cylindrichnus* (*Cy*), *Planolites* (*Pl*), *Psilonichnus* (*Ps*), *Skolithos* (*Sk*), *Taenidium isp* (*Tai*), *Teichichnus* (*Te*) with rootlets (*rt*), and carbonaceous detritus (*cd*). Photo E and F, well 03-13-055-06W4, depths 611.4 m and 609.7m, photo G, well 16-03-049-03W4, depth 729.8m, photo H, well 09-25-054-01W4, depth 545.6m. I, L) Bioturbated open embayment (I, J) and storm-dominated deltaic (K, L) facies of the highstand systems tract. Trace fossil diversity is elevated in comparison to the TST facies associations, with ichnogenera including *Asterosoma* (*As*), *Cylindrichnus* (*Cy*), and *Teichichnus* (*Te*). Photo I from well 02-32-053-05W4, core depth 601.3m, photo j from well 06-24-048-01W4, core depth 637.6 m, photos K, L from well 14-34-054-06W4, depths 605.1m and 601.8m. All scale bars are 5 cm.

4.6.2 Sequence 1 – 2 Bounding Surface

The surface bounding HF sequences 1 and 2 represents a regional-scale stratigraphic break across which a significant landward shift in depositional environments occurs. This surface is compound in nature and represents a co-planar transgressive surface-maximum flooding surface in wells south-east of approximately Township 53 (Fig. 4.8, Fig. 4.9). North of that township, the TS/MRS is progressively reworked by lower-order ravinement surfaces (RS) that separate facies associations of HF Sequence 2 (Fig. 4.9).

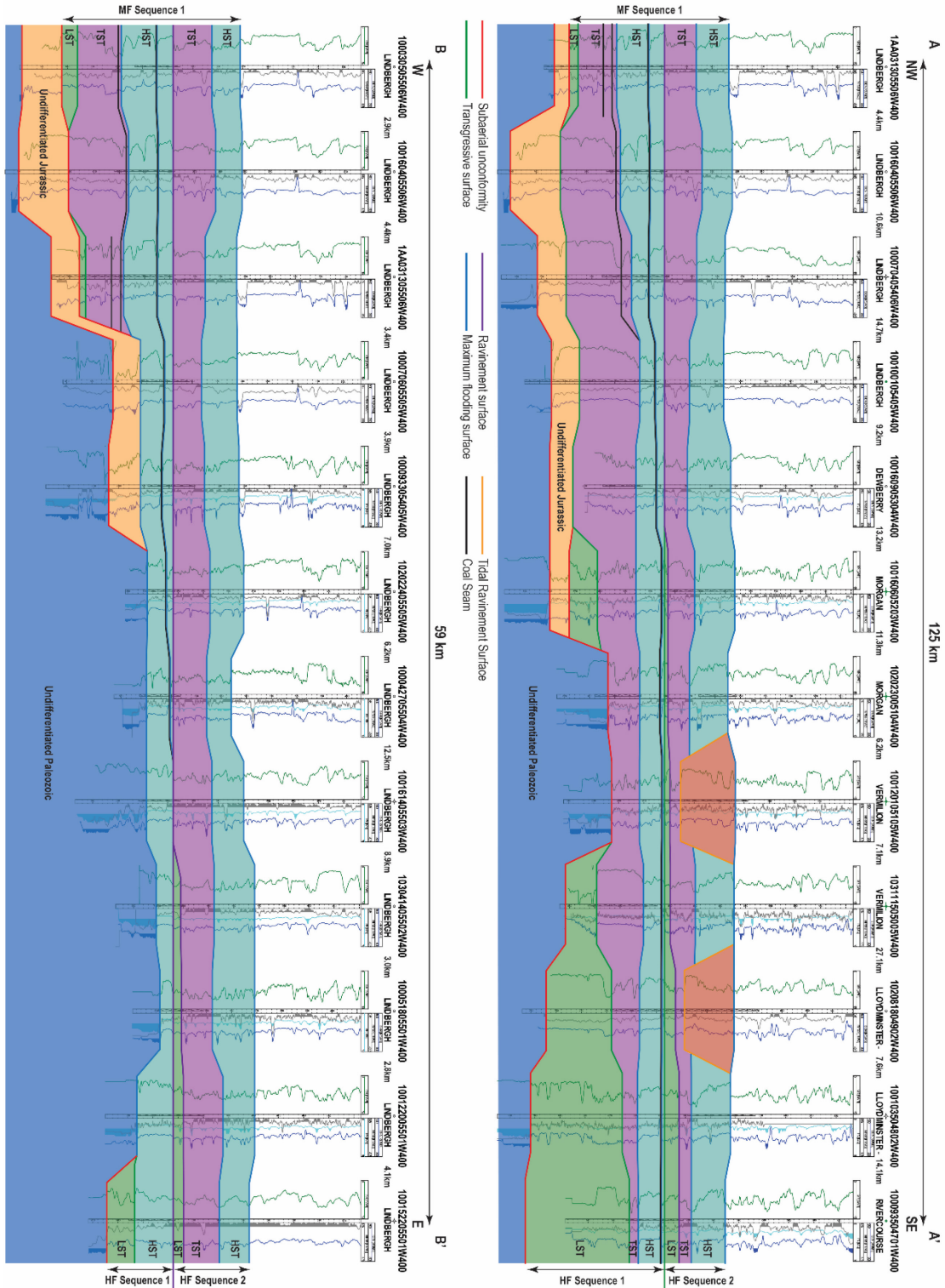
4.6.3 High-Frequency Depositional Sequence 2

4.6.3.1 Lowstand Systems Tract

The lowstand systems tract of HF Sequence 2 consist of thin (2-3 metre), coarsening-upward wave- and river-influenced deltaic cycles of FAC-F bound by HF TS-MFS and WRSs. Near complete coarsening-upward cycles from prodelta to delta front/delta plain are only observed in the south-east of the study (Fig. 8, NW-SE section, wells 10-35 and 09-35, Fig. 4.10, Fig. 4.11A-F). In a basinward direction (moving from SE to NW) these coarsening-upward deltaic facies become progressively truncated by the wave ravinement surface associated with the base of the transgressive systems tract (Fig. 4.8). Deltaic cycles of the LST preserved in the NE corner of the study (Fig. 8, E-W section, wells east of and including 04-14) consist only of prodelta to proximal prodelta/distal delta front. The contact between deltaic deposits of FAC-F and shoreface to shelf strata of FAC-G is demarcated by a ravinement surface characterized by a moderately well-to well-developed *Glossifungites* Ichnofacies-demarcated omission surface that can be traced across the entire study area in a northwest-southeast direction; a distance of greater than 125 km (Fig. 4.8).

4.6.3.2 Transgressive Systems Tract

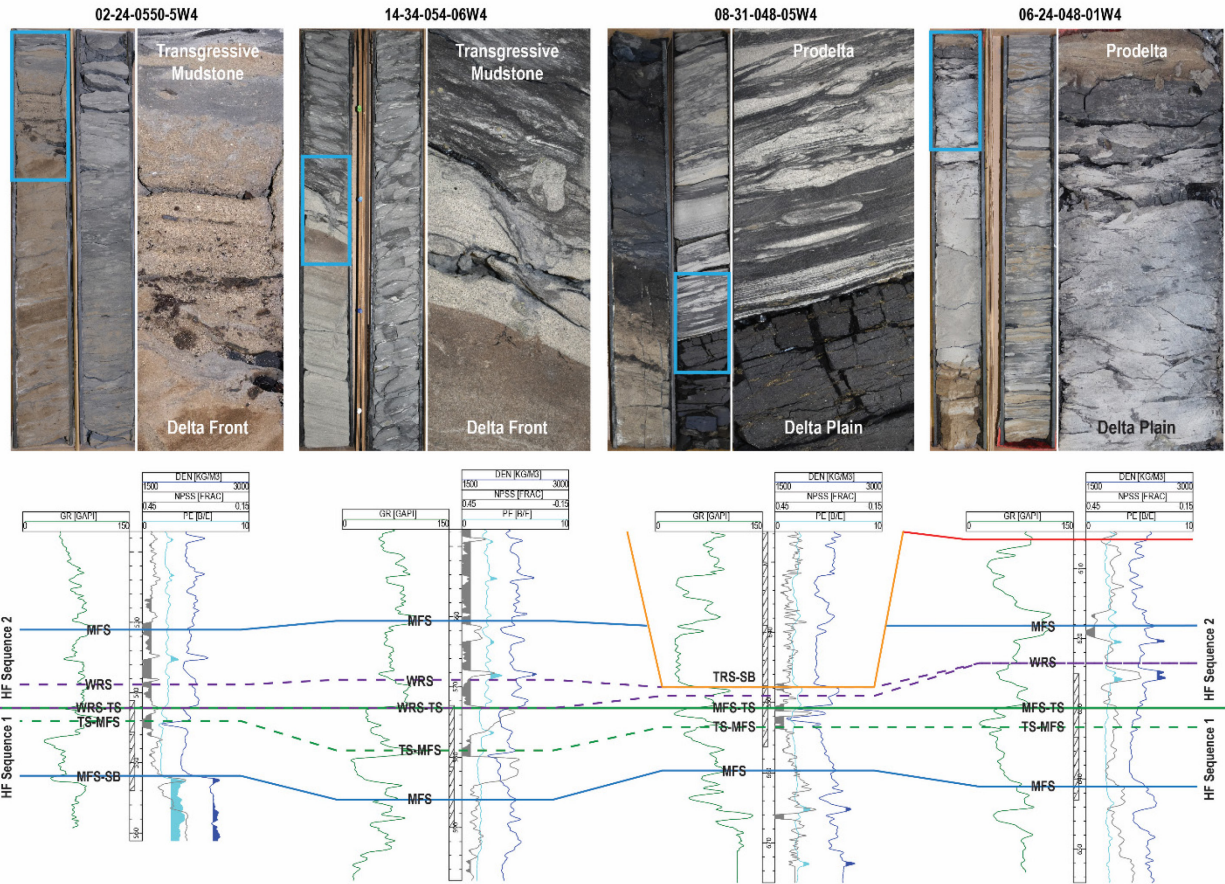
TST strata consist of multiple coarsening-upward to weakly fining-upward cycles of glauconitic marine strata deposited from lower shoreface to upper shelf environments. Cycles are relatively thin (typically < 5 m), with the contacts between cycles demarcated by weakly to moderately developed omission suites of the *Glossifungites* Ichnofacies accompanied by lag deposits consisting primarily of coarse glauconite (Fig. 4.5). While the available core dataset is small, the cycles comprising FAC-G are retrogradationally stacked, with the basal bioturbated mudstone of each successive cycle representing a more distal offshore location.



4-8) NW-SE and W-E Cross-Sections

NW-SE and W-E oriented cross-sections illustrating the interpreted subsurface correlation of sequence stratigraphic surfaces and systems tracts. Note that the cross-sections are not of equal length making the vertical exaggeration in the W-E cross-section larger.

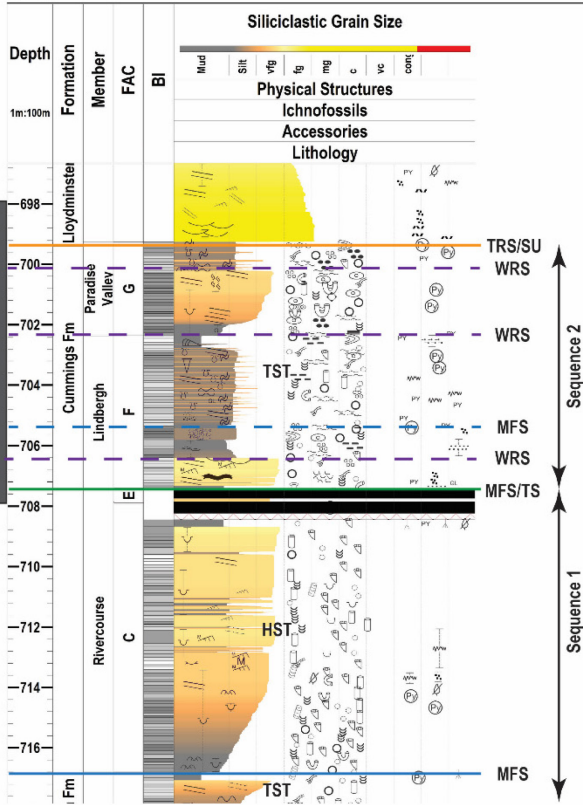
HF Sequence 1 - HF Sequence 2 Stratigraphic Contact



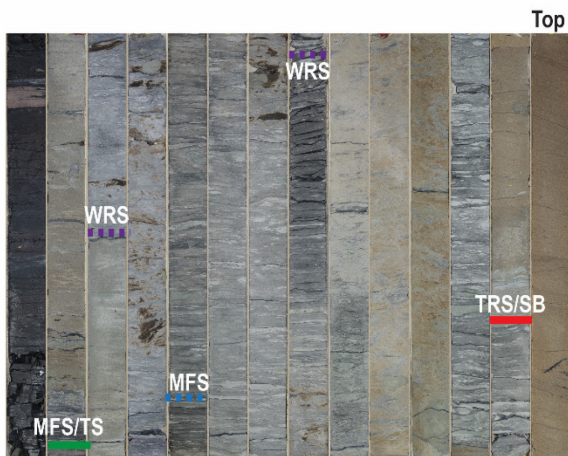
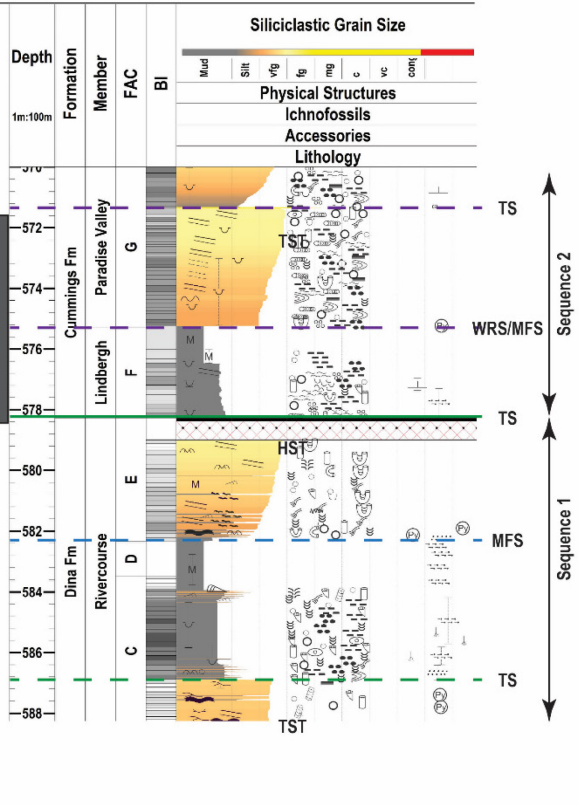
4-9) Core and Petrophysical Characteristics of HF Sequence 1-2 Contact

Proximal (06-25) to distal (02-24) expression of the contact between high-frequency sequences 1 and 2. In proximal locations the contact is sharp, with no appreciable erosion. In distal locations the contact becomes reworked during transgression with the development of a wave-ravinement surface mantled by a coarse-grained lag in the most distal location.

08-18



09-33



4-10) Core Logs and Photos of HF Sequence 2

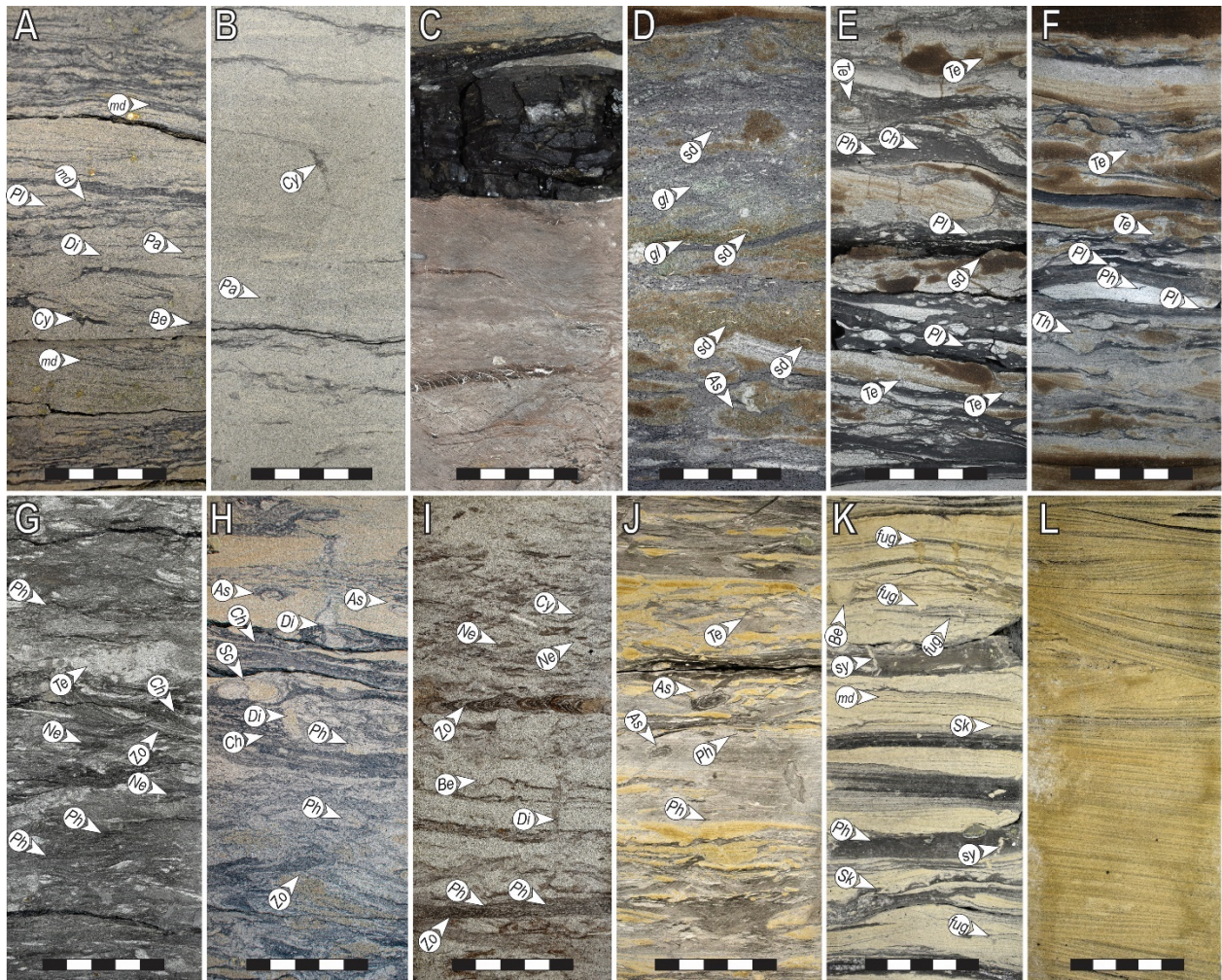
Core log and associated core photos showing the facies relationships across the TS, MFS, WRS, and TRS/SU of high-frequency sequence 2. Grey rectangles beside the depth track of each core log represents the core displayed in the photographs below.

The contact between deltaic and shoreface-shelf strata of HF Sequence 2 can be interpreted in at least 2 ways. Given the moderate to well-developed *Glossifungites* Ichnofacies- demarcated omission surface, this contact could be interpreted as a regressive surface of marine erosion (RSME, Plint, 1988; Plint and Nummedal, 2000), wherein FAC-G would represent shoreface deposits of the falling stage systems tract. This interpretation could apply to core examples where overlying shoreface strata preserve deposition above fair-weather wave base (base of lower shoreface) as the RSME is cut by wave erosion in the lower shoreface during base level fall. Alternatively, this surface could represent a wave-ravinement surface (WRS) cut by waves during transgression resulting in deposition of a transgressively incised shoreface. MacEachern et al. (1999) review and discuss the sedimentological differences in bounding facies between forced and normal regressive incised shorefaces to those of transgressively incised shorefaces in their analysis of the Viking Formation in the Joffre Field of Alberta. One of the critical observations outlined in MacEachern et al. (1999) is the nature of shoreface strata overlying the discontinuity surface. In the case of FSST or LST shoreface deposits, the surface demarcated by the *Glossifungites* Ichnofacies can only extend to the most basinward location of the lower shoreface. This limits the environmental range of facies above the ravinement surface to fair-weather wave-base or shallower. In contrast, the erosional discontinuity at the base of transgressively incised shorefaces is cut prior to shoreface progradation while sea level is lower (MacEachern et al., 1999). In this scenario, facies overlying the erosional surface can consist of sediment that was deposited below fair-weather wave base. Given these criteria, sedimentological observations of facies associations above and below the contact between FAC-F and FAC-G are most consistent with a transgressive surface of erosion associated with transgressively incised shoreface deposits. While often coarser grained, FAC-G facies directly overlying this contact are often thoroughly bioturbated with little or no preservation of oscillatory- or current-generated structures (oscillation ripple cross-lamination) or unburrowed tempestite beds. This suggests that sediment deposited below fair-weather wave base do overlie this well-developed erosional surface.

4.6.3.3 Highstand Systems Tract

Highstand systems tract strata consists of deltaic and shoreface cycles of the regional Lloydminster Member (Table 4.11, Fig. 4.8, Fig. 4.11J-K). The regional Lloydminster Member consists of one or more metre-scale coarsening-upward cycles of lenticular-bedded mudstone, heterolithic sandstone and mudstone, and sandstone. Physical sedimentary features of the Lloydminster Member include common low-angle, planar, hummocky, and trough cross-stratification, oscillation, and combined flow ripple cross-lamination with common graded beds, syneresis cracks, and soft-sediment deformation structures (Fig. 4.11J-K). Trace fossil distribution is sporadic, and diversity is lower than in the underlying transgressive

strata, although marine forms including *Phycosiphon* and *Asterosoma* are still present. The contact between highstand and transgressive systems tract strata of HF Sequence 2 is a MFS, is gradational to sharp, and occurs predominantly within a variably thick mudstone interval (Fig. 4.8). The contact is equivalent to the lithostratigraphic boundary between the Lloydminster Member and Cummings Formation and is also the lower-upper Mannville Group contact (Chapter 3). The upper sequence boundary of HF Sequence 2 occurs at the top of the regional Lloydminster Member and at the base of the younger Lloydminster Member incised valley complexes (Fig. 4.8).



4-11) Facies of HF Sequence 2

A, B) Distal (A) and proximal (B) delta front facies of F-FA2 displaying double mudstone drapes (dmd) and an ichnological assemblage consisting of *Planolites* (*Pl*), *Berguaria* (*Be*), *Lockeia* (*Lo*), and *Chondrites* (*Ch*). Photos from well 09-35-047-01W4, depths 638.5 (A) and 637.6m (B). D, E, F) Prodelta and transgressive facies of F-FA1 with abundant glauconite (*gl*), shell debris (*sd*), dark-grey massive fluid mudstone beds and a low-diversity, sporadically distributed trace fossil assemblage of *Asterosoma* (*As*), *Chondrites* (*Ch*), *Palaeophycus* (*Pa*), *Phycosiphon* (*Ph*), *Planolites* (*Pl*), and *Teichichnus* (*Te*) indicating a stressed environment with

rapid deposition of river-derived sediment. Photo D, E from well 04-14-055-02W4, depths 503.6m, and 501.9m, photo F from well 13-09-054-01W4, depth 515.1m. G-I) Bioturbated glauconitic marine sandy mudstone and muddy sandstone facies of marine shoreface deposits (FAC-G). Bioturbation intensities and ichnological diversity are high and forms are robust. Trace fossils include *Asterosoma* (*As*), *Berguaeria* (*Be*), *Chondrites* (*Ch*), *Diplocraterion* (*Di*), *Nereites* (*Ne*), *Phycosiphon* (*Ph*), *Scolicia* (*Sc*), and *Zoophycos* (*Zo*). Photos from wells 09-33-054-05W4, depths 571.1 m (G), and 572.5 m (I), and well 15-25-047-01W4, depth 625.5 m. J-L) Deltaic facies of the regional Lloydminster Member comprising the highstand systems tract. Facies are characterized by abundant phytodetrital material (K), low- to high-angle and hummocky cross-stratification (L) indicating significant influence of wave- and river-induced reworking and deposition. Marine forms are still present in the form of *Asterosoma* (*As*), *Phycosiphon* (*Ph*), accompanied by *Berguaeria* (*Be*), *Teichichnus* (*Te*), and *Skolithos* (*Sk*) with abundant *fugichnia* (*fug*). Photo J from well 06-09-048-04W4, depth 656.3 m, photos K and L from well 05-25-048-02W4, depths 638.8 m (K), and 638.25 m (L). All scale bars are 5 cm.

4.7 Depositional Evolution

The medium-frequency depositional sequence consisting of high-frequency sequences 1 and 2 records the preserved cycle of sedimentation from landward of the shoreline associated with the Boreal Sea to the point of maximum transgression and onset of regression. The initial influence of this transgression occurs at the base of the transgressive systems tract and is indicated by the first occurrence of tidal sedimentation and brackish-water influence (Fig. 4.12, green star above the first TS). The transgressive systems tract of medium frequency sequence 1 is significantly thicker than that of the LST and overlying HST and consists predominantly of progradational cycles bounded by high-frequency TS-MFS and MFSs. Fining-upward transgressive cycles are preserved in the NW, but are absent in the SE (e.g., Fig. 4.10, well 09-33). The TST transitions upward from thin, discontinuous tide-influenced strata of FAC-B to thicker, laterally continuous wave- and river-dominated deltaic cycles of FAC-C and FAC-E (Fig. 12). This records a progressive change from an embayed coastal morphology protected from high-energy wave processes to more open marine conditions as topographic lows became progressively infilled. The open embayment deltaic facies of FAC-C also mark the first incursion of near marine salinities in the northern part of the study area and is marked by the presence of marine trace fossils including *Cosmorhappe*, *Nereites*, and *Phycosiphon* (Fig. 4.10, well 09-33). The continuation of transgression resulted in deposition of thin, laterally continuous marine deltaic and shoreface to shelf cycles which preserve the first significant fining-upward transgressive deposits of the medium-frequency transgressive systems tract (FAC-F and -G, Figs. 4.8, Fig. 4.9, Fig. 4.12). Deposition of these facies associations also records the onset of fully marine salinities, evidenced by their associated high-diversity, robust to very robust trace fossil assemblages and the presence of numerous marine-indicative ichnogenera (i.e., abundant, robust *Asterosoma*, and *Cosmorhappe*, *Nereites*, *Phycosiphon*, *Scolicia*, and *Zoophycos*) (Fig. 4.12, dark blue stars). Maximum incursion of the Boreal Sea occurs at the maximum flooding surface demarcating the TST-HST contact,

after which sedimentation became progradational. The HST consists of high-energy, coarsening-upward shoreface to deltaic strata that downlap onto the MFS. The incision of thick estuarine channels fills (up to 40 metres) cutting down as far as to the contact between HF sequence 1 and 2 represents a significant fall in base level following normal regressive highstand conditions (Fig. 4.12, well 08-18). The base of these channels represents a co-planar TRS/SU, as the channels observed in core display sedimentological and ichnological evidence of deposition in response to tides and within brackish-water (i.e., display double mudstone drapes, bioturbated inclined heterolithic stratification).

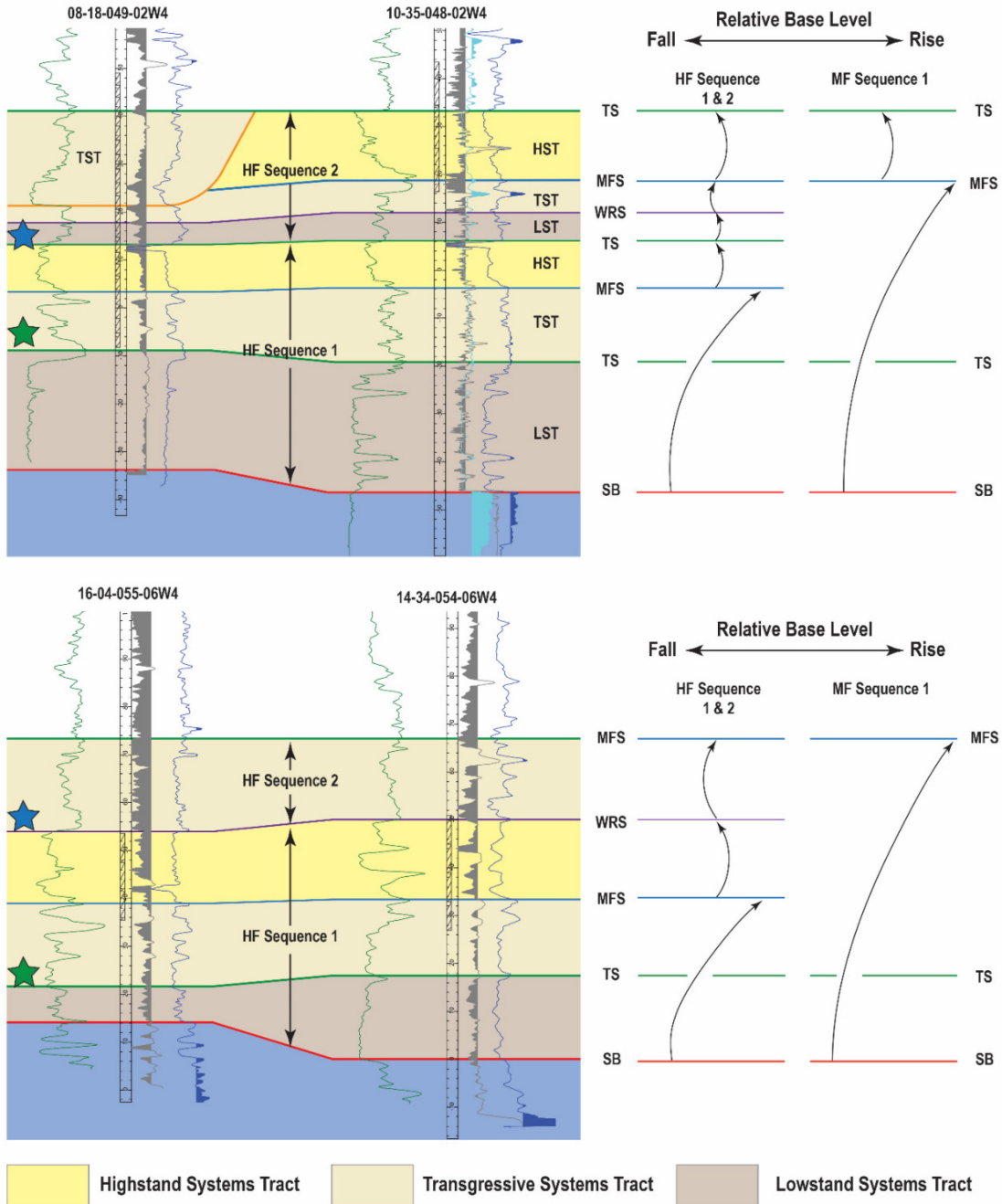
4.8 Conclusions

A high-resolution sequence stratigraphic analysis was conducted on the Lower Cretaceous Dina, Cummings, and Lloydminster lithostratigraphic units leveraging the high-resolution facies analysis of (Chapter 2). The sedimentological and ichnological characteristics of facies associations and facies association complexes documented in that work were used to identify the presence and rank of bounding discontinuities having sequence stratigraphic or sedimentological significance. Sequence stratigraphic surfaces were observed to mark significant facies dislocations in which sedimentological and ichnological criteria changed in a fundamental way. Significant dislocations pertaining to changing base-level include the appearance across stratigraphic surfaces of key ichnological assemblages such as brackish-water or marine-associated suites, changes in the dominant physical processes involved in sediment deposition and distribution (i.e., from tide-dominated to wave-dominated), and the appearance of mineralogical changes including the abrupt occurrence of glauconite across the contact of FAC-E and FAC-F. Sedimentological contacts, while generally having similar lithological juxtaposition commonly display a repetitive stacking of facies, with incremental changes throughout the stacked succession. Sequence stratigraphic surfaces were documented to extend beyond the boundaries of depositional environments, a key characteristic of their identification (MacEachern et al., 2012), whereas sedimentological surfaces were confined to their specific depositional environment.

The surfaces of sequence stratigraphic significance were then used to define systems tracts and establish the presence of depositional sequences. Two hierarchies of sequences were identified, one medium-frequency depositional sequence (MF Sequence 1) and two higher-frequency sequences nested within it (HF sequences 1 and 2). HF Sequence 1 consists of lowstand, transgressive, and highstand systems tracts encompassing of facies association complexes A to E, whereas the systems tracts of HF Sequence 2 consist of facies association complexes F and G, as well as the regional, coarsening-upward strata of the Lloydminster Member. Medium-frequency Sequence 1 preserves the record of deposition from landward

of the shoreline of the Boreal Sea to the point of maximum landward extent marked by the maximum flooding surface separating the lithostratigraphic Cummings Formation and Lloydminster Member.

This study advances the sequence stratigraphic understanding of the Dina, Cummings, and Lloydminster lithostratigraphic units in the east-central plains of Alberta. A study incorporating sedimentary facies and sequence stratigraphic analysis at this resolution for this area has not previously been published. The results presented herein provide a framework within which higher-resolution studies at the scale of hydrocarbon pools can be placed and provides criteria that may aid in identifying the genetic nature of bounding discontinuities. As the production of hydrocarbons from this interval declines, the presence of subsurface pore space that may be useful for disposal of fluids or CO₂ will become of higher importance. It is hoped that this framework can be utilized to inform the presence and connectivity of key disposal intervals, and the presence and extent of confining strata in the development and regulation of any future sub-surface disposal or storage projects.



4.12) Depositional Evolution in Response to Base Level

Illustrative diagram relating the stacking of systems tracts to changes in base level. Green star represents the first occurrence of brackish-water sedimentation, blue star represents the first occurrence of fully marine trace fossil assemblages. LST strata of HF Sequence 2 are present in the landward cross-section (08-18 & 10-35) and absent in the basinward location (16-04 & 14-34) due to erosion. The TST of HF Sequence 2 is also significantly thicker in the basinward location due to higher accommodation.

4.9 References

- Ahmad, W. and Gingras, M.K., 2022, Ichnology and Sedimentology of the Lower Cretaceous Wabiskaw Member (Clearwater Formation) Alberta, Canada: *Marine and Petroleum Geology*, v. 143, Article 105775.
- Allen, G.P., and Posamentier, H.W., 1993, Sequence stratigraphy and facies model of an incised valley fill: the Gironde estuary, France. *Journal of Sedimentary Petrology*, 63, 378-391.
- Banerjee, I., Kalkreuth, W., and Davies, E.H., 1996, Coal seam splits and transgressive-regressive coal couplets: A key to stratigraphy of high-frequency sequences: *Geology*, v. 24, no. 11, p. 1001-1004.
- Bann, K.L., and Fielding, C.R., 2004, An integrated ichnological and sedimentological comparison of non-deltaic shoreface and subaqueous delta deposits in Permian reservoir units of Australia: Geological Society, London, Special Publication v. 228, p. 273-310.
- Bauer, D.B., Hubbard, S.M., Leckie, D.A., and Dolby, G., 2009, Delineation of a sandstone-filled incised valley in the Lower Cretaceous Dina–Cummings interval: implications for development of the Winter Pool, west-central Saskatchewan: *Bulletin of Canadian Petroleum Geology*, v. 57, no. 4, p. 409-429.
- Bayet-Goll., R., Samani, P.N., de Carvalho, C.N., Monaco, P., Khodaie, N., Pour, M.M., Kazemeini, H., and Zareiyan, M.H., 2017, Sequence stratigraphy and ichnology of Early Cretaceous reservoirs, Gadvan Formation in southwestern Iran: *Marine and Petroleum Geology*, v. 81, p. 294-319.
- Beynon, B.M., Pemberton, S.G., Bell, D.F., and Logan, C.A., 1988, Environmental implications of ichnofossil from the Lower Cretaceous Grand Rapids Formation, Cold Lake oil sands deposit, *in*: James, D.P., and Leckie, D.A., editors, *Sequences, Stratigraphy, and Sedimentology: Surface and Subsurface*, Canadian Society of Petroleum Geologists, Memoir 15, p. 275-290.
- Bhattacharya, J.P., and MacEachern, J.A., 2009, Hyperpycnal rivers and prodeltaic shelves in the Cretaceous seaway of North America: *Journal of Sedimentary Research*, v. 79, p. 184–209.
- Bromley, R.G., 1975, Trace fossils at omission surfaces, *in*: Frey, R.W., editor, *The Study of Trace Fossils*, Springer-Verlag, New York, p. 399-428.
- Bromley, R.G., and Ekdale, A.A., 1984, *Chondrites*: a trace fossil indicator of anoxia in sediments: *Science*, v. 224, p. 872-874.
- Buatois, L.A., Mangano, M.G., and Pattison, S.A., 2019, Ichnology of prodeltaic hyperpycnite-turbidite channel complexes and lobes from the upper Cretaceous Prairie Canyon member of the Mancos Shale, Book Cliffs, Utah, USA: *Sedimentology*, v. 66, p. 1825-1860.
- Cant, D.J., 1996, Sedimentological and sequence stratigraphic organization of a foreland clastic wedge, Mannville Group, Western Canada Basin: *Journal of Sedimentary Research*, v. 66, no. 6, p. 1137-1147.

- Cant, D.J., and Abrahamson, B., 1996, Regional distribution and internal stratigraphy of the Lower Mannville: *Bulletin of Canadian Petroleum Geology*, v. 44, no. 3, 508-529.
- Cattaneo, A., and Steel, R.J., 2003, Transgressive deposits: a review of their variability: *Earth Science Reviews*, v. 62, no. 3, p. 187-228.
- Catuneanu, O., 2006, *Principles of Sequence Stratigraphy*: Amsterdam, Elsevier, 375 p.
- Catuneanu, O., 2019a, Scale in sequence stratigraphy: *Marine and Petroleum Geology*, v. 106, p. 128-159.
- Catuneanu, O., 2019b, Model independent sequence stratigraphy: *Earth-Science Reviews*, v. 188, p. 312-388.
- Catuneanu, O., and Zecchin, M., 2013, High-resolution sequence stratigraphy of clastic shelves II: Controls on sequence development: *Marine and Petroleum Geology*, v. 39, p. 26-38.
- Chalmers, R.L., Boyd, R., and Diessel, C.F.K., 2013, Accommodation-based coal cycles and significant surface correlation of low-accommodation Lower Cretaceous coal seams, Lloydminster heavy oil field, Alberta, Canada: Implications for coal quality distribution: *American Association of Petroleum Geologists Bulletin*, v. 97, no. 8, p. 1347-1369.
- Chateau, C.C.F., Dashtgard, S.E., MacEachern, J.A., and Hauck, T.E., 2019, Parasequence architecture in a low-accommodation setting, impact of syndepositional carbonate epikarstification, McMurray Formation, Alberta, Canada: *Marine and Petroleum Geology*, v. 104, p. 168-179.
- Christopher, J., 1997, Evolution of the Lower Cretaceous Mannville Sedimentary Basin in Saskatchewan, *in*: Pemberton, S.G., and James, D.P., editors, *Petroleum Geology of the Cretaceous Mannville Group, Western Canada*: Canadian Society of Petroleum Geologists, Memoir 18, p. 191-210.
- Deschamps, R., Sale, S.O., Chauveau, B., Fierens, R., and Euzen, T., 2017, The coal-bearing strata of the Lower Cretaceous Mannville Group (Western Canadian Sedimentary Basin, South Central Alberta). Part 1: Stratigraphic architecture and coal distribution controlling factors: *International Journal of Coal Geology*, v. 179, 113-129.
- Ekdale, A.A., Bromley, R.G., Pemberton, S.G., 1984. *Ichnology: The Use of Trace Fossils in Sedimentology and Stratigraphy*. Society of Economic Paleontologist and Mineralogists Short Course Notes 15, 1–316.
- Fielding, C.R., Bann, K.L., and Trueman, J.D., 2007, Resolving the Architecture of a Complex, Low-Accommodation Unit Using High-Resolution Sequence Stratigraphy and Ichnology: The Late Permian Freitag Formation in the Denison Trough, Queensland, Australia, *in*: MacEachern, J.A., Bann, K.L., Gingras, M.K., and Pemberton, S.G., editors, *Applied Ichnology*. Society of Economic Paleontologists and Mineralogists, Short Course Notes 52, p. 179-208.

- Fuglem 1970, M.O., 1970, Use of core in evaluation of productive sands, Lloydminster area, *in*: Brindele, J.E., and Holmerg, R.A., editors, Saskatchewan Mesozoic Core Seminar, Saskatchewan Geological Society, 12 p.
- Gingras, M.K., MacEachern, J.A. and Dashtgard, S.E., 2011. Process ichnology and the elucidation of physico-chemical stress. *Sedimentary Geology*, v. 237, no. 3, p.115–134.
- Gingras, M.K., MacEachern, J.A., Dashtgard, S.E., Ranger, M.J., and Pemberton, S.G., 2016, The significance of trace fossils in the McMurray Formation, Alberta, Canada: *Bulletin of Canadian Petroleum Geology*, v. 64, no. 2, p. 233-250.
- Gross, A.A., 1980, Mannville Channels in east-central Alberta: Lloydminster and Beyond: Geology of Mannville Hydrocarbon, *in*: Beck, L.S., Christopher, J.E., and Kent, D.M., editors, Lloydminster and Beyond: Geology of Mannville Hydrocarbon Reservoirs: Saskatchewan Geological Society, Special Publication 5. p. 33–63.
- Hampson, G.J., and Storms, J.E.A., 2003, Geomorphological and sequence stratigraphic variability in wave-dominated, shoreface-shelf parasequences: *Sedimentology*, v. 50, p. 667-701.
- Hayes, B.J.R., Christopher, J.E., Rosenthal, L.L., McKercher, B., Minken, D., Tremblay, Y.M., and Fennel, J., 1994, Cretaceous Mannville Group of the Western Canada Sedimentary Basin, *in*: Mossop, G.D., and Shetson, I., editors, Geological Atlas of the Western Canada Sedimentary Basin, Canadian Society of Petroleum Geologists and Alberta Research Council, Special Report 4.
- Helland-Hansen, W., and Gjelberg, J.G., 1994, Conceptual basis and variability in sequence stratigraphy: a different perspective: *Sedimentary Geology*, v. 92, no. 1-2, p. 31-52.
- Helland-Hansen, W., and Martinsen, O.J., 1996, Shoreline trajectories and sequences: description of variable depositional-dip scenarios: *Journal of Sedimentary Research*, v. 66, no. 4, 670-688.
- Hildred, G.V., Ratcliff, K.T., Wright, A.M., Zaitlin, B.A., and Wray, D.S., 2010, Chemostratigraphic applications to low-accommodation fluvial incised-valley settings: an example from the lower Mannville Formation of Alberta, Canada: *Journal of Sedimentary Research*, v. 80, p. 1032-1045.
- Holz, M., Kalkreuth, W., and Banerjee, I., 2002, Sequence stratigraphy of paralic coal-bearing strata: an overview: *International Journal of Coal Geology*, v. 48, p. 147-179.
- Hunt, D., and Tucker, M.E., 1992, Stranded parasequences and the forced regressive wedge systems tract: deposition during base-level fall: *Sedimentary Geology*, v. 81, no. 1-2, p. 1-9.
- Kent, D.M., 1959, The Lloydminster oil and gas field, Alberta: University of Saskatchewan, M.Sc. thesis, 92 p.

- Kidwell, S.M., 1989, Stratigraphic condensation of marine transgressive records; origin of major shell deposits in the Miocene of Maryland: *Journal of Geology*, v. 97, p. 1-24.
- Leckie, D.A., Vanbeselaere, N.A., and James, D.P., 1997, Regional sedimentology, sequence stratigraphy and petroleum geology of the Mannville Group: southwestern Saskatchewan, *in*: Pemberton, S.G., and James, D.P., editors, *Petroleum Geology of the Cretaceous Mannville Group, Western Canada*, Canadian Society of Petroleum Geologists, Memoir 18, p. 211-262.
- MacEachern, J.A., and Pemberton, S.G., 1994, Ichnological character of incised valley fill systems from the Viking Formation of the Western Canada Sedimentary Basin, Alberta, Canada, *in*: Dalrymple, R., Boyd, R., Zaitlin, B., editors, *Incised-Valley Systems: Origin and Sedimentary Sequences*. Society of Economic Paleontologists and Mineralogists, Special Publication, vol. 51, p. 129–157.
- MacEachern, J.A., Bechtel, D.J., and Pemberton, S.G., Ichnology and sedimentology of transgressive deposits, transgressively related deposits and transgressive systems tracts in the Viking Formation of Alberta, *in*: Pemberton, S.G., editor, *Applications of Ichnology to Petroleum Exploration: A Core Workshop*, Society of Economic Paleontologists and Mineralogists, Core Workshop Notes 17, p. 251-290.
- MacEachern, J.A., Zaitlin, B.A., and Pemberton, S.G., 1999, A sharp-based sandstone of the Viking Formation, Joffre field, Alberta, Canada: criteria for recognition of transgressively incised shoreface complexes: *Journal of Sedimentary Research*, v. 69, no. 4, p. 876-892.
- MacEachern, J.A., Bann, K.L., Bhattacharya, J.P., and Howell, C.D., 2005, Ichnology of deltas: organism responses to the dynamic interplay of rivers, waves, storms and tides, *in*: Bhattacharya, J.P., and Giosan, L., editors, *River Deltas: Concepts, Models and Examples*, Society of Economic Paleontologists and Mineralogists, Special Publication 83, pp. 49–85.
- MacEachern, J.A., Gingras, M.K., Bann, K.L., Pemberton, S.G., and Dafoe, L.T., 2007a, Applications of ichnology to high-resolution genetic stratigraphic paradigms, *in*: MacEachern, J.A., Bann, K.L., Gingras, M.K., and Pemberton, S.G., editors, *Applied Ichnology*. Society of Economic Paleontologists and Mineralogists, Short Course Notes 52, p. 95–129.
- MacEachern, J.A., Pemberton, S.G., Gingras, M.K., Bann, K.L., and Dafoe, L.T., 2007b, Use of trace fossils in genetic stratigraphy, *in*: Miller III, W., editor, *Trace Fossils. Concepts, Problems, and Prospects*. Elsevier, Amsterdam, p. 105-128.
- MacEachern, J.A., Dashtgard, S.E., Knaust, D., Catuneanu, O., Bann, K.L., and Pemberton, S.G., 2012, Sequence Stratigraphy *in*: Knaust, D., and Bromley, R.G., editors, *Trace fossils as indicators of sedimentary environments*. *Developments in Sedimentology*, v. 64, p. 157-194.

- Marriott, S.B., and Wright, V.P., 1993, Paleosols as indicators of geomorphic stability in two Old Red Sandstone alluvial suites, South Wales: *Journal of the Geological Society of London*, v. 150, p. 1109-1120.
- McPhee, D., and Pemberton, S.G., 1997, Sequence stratigraphy of the Lower Cretaceous Mannville Group of east Alberta:
- Morshedian, A., MacEachern, J.A., Dashtgard, S.E., Bann, K.L., and Pemberton, S.G., 2019, Systems tracts and their bounding surfaces in the low- accommodation Upper Mannville group, Saskatchewan, Canada: *Marine and Petroleum Geology*, v. 110, p. 35-54.
- Nauss, A.W., 1945, Cretaceous stratigraphy of Vermillion area, Alberta, Canada: *Bulletin of the American Association of Petroleum Geologists*, v. 29, no. 11, p. 1605-1629.
- Newitt, K.J., and Pederson, P.K., 2022, Observational data-based sequence stratigraphy of a clastic wedge within an active foreland basin, Spirit River Formation, west-central Alberta, Canada: *MPG*, v. 140, 105681.
- Nummedal, D., and Swift, D.J.P., 1987, Transgressive stratigraphy at sequence-bounding unconformities: some principles derived from the Holocene and Cretaceous examples, *in*: Nummedal, D., Pilkey, O.H., and Howard, J.D., editors, *Sea-level Fluctuation and Coastal Evolution*, Society of Economic Paleontologists and Mineralogists, Special Publication, v. 41, p. 241-260.
- Orr, R.D., Johnston, J.R., and Manko, E.M., 1977, Lower Cretaceous geology and heavy-oil potential of the Lloydminster area: *Bulletin of Canadian Petroleum Geology*, v. 25, no. 6, p. 1187-1221.
- Pearson, N.J., Mangano, M.G., Buatois, L.A., Casadio, and Raising, M.R., 2012, Ichnology, sedimentology, and sequence stratigraphy of outer-estuarine and coastal-plain deposits: Implications for the distinction between allogenic and autogenic expressions of the Glossifungites Ichnofacies: *Palaeogeography, Palaeoclimatology, Palaeoecology*, v. 333, 192-217.
- Pemberton, S.G., Flach, P.D., and Mossop, G.D., 1982, Trace fossils from the Athabasca Oil Sands, Alberta, Canada: *Science*, v. 217, p. 825–827.
- Pemberton, S.G., MacEachern, J.A., and Frey, R.W., 1992, Trace fossil facies models: environmental and allostratigraphic significance, *in*: Walker, R.G., and James, N.P., editors, *Facies Models: Response to Sea Level Change*, Geological Association of Canada, Toronto, p. 47-72.
- Pemberton, S.G., and MacEachern, J.A., 1995, The sequence stratigraphic significance of trace fossils: examples from the Cretaceous foreland basin of Alberta, Canada. *in*: Van Wagoner, J.C., and Bertram, G., editors, *Sequence Stratigraphy of Foreland Basin Deposits: Outcrop and Subsurface Examples from*

- the Cretaceous of North America, American Association of Petroleum Geologists, Memoir 64, p. 429–475.
- Pemberton, S.G., MacEachern, J.A., and Gingras, M.K., 2000, Significance of ichnofossil to genetic stratigraphy: Science in China, v. 43, no. 5, p. 541-560.
- Pemberton, S.G., MacEachern, J.A., and Saunders, T.D.A., 2004, Stratigraphic applications of substrate-specific ichnofacies: delineating discontinuities in the rock record. *in*: McIlroy, D., editor, The Application of Ichnology to Palaeoenvironmental and Stratigraphic Analysis. Geological Society of London, Special Publication, vol. 228, p. 29–62.
- Plint, A.G., 1988, Sharp-based shoreface sequences and “offshore bars” in the Cardium Formation of Alberta: their relations to relative changes in sea level, *in*: Wilgus, C.K., Hastings, B.S., Kendall, C.G.St.C., Posamentier, H.W., Ross, C.A., and Van Wagoner, J.C., editors, Sea Level Changes: an Integrated Approach, Society of Economic Paleontologists and Mineralogist, Special Publication, vol. 42, p. 357-370.
- Plint, A.G., and Nummedal, D., 2000, The falling stage systems tract: recognition and importance in sequence stratigraphic analysis, *in*: Hunt, D., and Gawthorpe, R.L., editors, Sedimentary Response to Forced Regression, Geological Society of London Special Publication, v. 172, p. 1-17.
- Posamentier, H.W., and Vail, P.R., 1988, Eustatic controls on clastic deposition, II: sequence and systems tract models, *in*: Wilgus, C.K., Hastings, B.S., Kendall, C.G.St.C., Posamentier, H.W., Ross, C.A., and Van Wagoner, J.C., editors, Sea Level Changes: an Integrated Approach, Society of Economic Paleontologists and Mineralogist, Special Publication, vol. 42, p. 125-154.
- Pouderoux, H., Coderre, A.B., Pedersen, P.K., and Cronkwright, D.J., 2016, Characterization, architecture, and controls of Cold Lake marginal-marine oil sands: the Grand Rapids Formation (Upper Mannville) of east-central Alberta, Canada: Bulletin of Canadian Petroleum Geology, v. 64, no. 2, p. 119-146.
- Ratcliffe, K.T., Wright, A.M., Hallsworth, C., Morton, A., Zaitlin, B.A., Potocki, D., and Wray, D.S., 2004, An example of alternative correlation techniques in a low-accommodation setting, nonmarine hydrocarbon system: The (Lower Cretaceous) Mannville Basal Quartz succession of southern Alberta: American Association of Petroleum Geologists Bulletin, v. 88, no. 10, p. 1419-1432.
- Rodriguez, W., Buatois, L.A., Mangano, M.G., and Solórzano, E., 2018, Sedimentology, ichnology, and sequence stratigraphy of the Miocene Oficina Formation, Junín and Boyacá areas, Orinoco Oil Belt, Eastern Venezuela Basin: Marine and Petroleum Geology, v. 92, p. 213-233.

- Rodriguez-Tovar, F.J., Perez-Valera, F., and Perez-Lopez, A., 2007, Ichnological analysis in high-resolution sequence stratigraphy: The *Glossifungites* ichnofacies in Triassic successions from the Betic Cordillera (southern Spain): *Sedimentary Geology*, v. 198, p. 293-307.
- Sarzalejo, S., and Hart, B.S., 2006, Stratigraphy and lithologic heterogeneity in the Mannville Group (southeast Saskatchewan) defined by integrating 3-D seismic and log data: *Bulletin of Canadian Petroleum Geology*, v. 54. no. 2, p. 138-151.
- Savrda, C.E., and Bottjer, D.J., 1989, Trace-fossil model for reconstructing oxygenation histories of ancient marine bottom waters: application to Upper Cretaceous Niobrara Formation, Colorado: *Palaeogeography, Palaeoclimatology, Palaeoecology*, v. 74, p. 49–74.
- Schultz, S.K., MacEachern, J.A., Catuneanu, O., Dashtgard, S.E., and Diaz, N., 2022, High-resolution sequence stratigraphic framework for the late Albian Viking Formation in central Alberta: *Marine and Petroleum Geology*, v. 139, 105627.
- Sloss, L.L., Krumbein, W.C., and Dapples, E.C., 1949, Integrated facies analysis, *in*: Longwell, C.R., editor, *Sedimentary Facies in Geologic History*, Geological Society of America, Memoir 39, p. 91-124.
- Silva, S.E.S., and Hart, B.S., 2013, Advanced seismic-stratigraphic imaging of depositional elements in a Lower Cretaceous (Mannville) heavy oil reservoir, west-central Saskatchewan, Canada, *in*: Hein, F.J., Leckie, D.A., Larter, S., Suter, J.R., editors, *Heavy-oil and oil-sand petroleum systems in Alberta and beyond: American Association of Petroleum Geologists Studies in Geology* 64, p. 359-371.
- Smaili, M., and Hart, B.S., 2018, Pushing the envelope of seismic stratigraphic interpretation: a case study from the Mannville Group using small 3-D surveys: *Bulletin of Canadian Petroleum Geology*, v. 66, no. 4, 752-772.
- Swift, D.J.P., 1968, Coastal erosion and transgressive stratigraphy: *Journal of Geology*, v. 76, 444-456.
- Tabor, N.J., Myers, T.S., and Michel, L.A., 2017, Sedimentologists guide for recognition, description, and classification of paleosol: *in*: Zeigler, K.E., and Parker, W.G., editors, *Terrestrial Depositional Systems: Deciphering complexities through multiple stratigraphic methods*, Elsevier, p. 165-208.
- Vail, P.R., Audemard, F., Bowman, S.A., Eisner, P.N., and Perez-Cruz, C., 1991, The stratigraphic signatures of tectonics, eustasy, and sedimentology – an overview, *in*: Einsele, G., Ricken, W., and Seilacher, A, editors, *Cycles and Events in Stratigraphy*, Springer-Verlag, p. 617-659.
- Van Wagoner, J.C., Posamentier, H.W., Mitchum, R.M., Vail, P.R., Sarg, J.F., Loutit, T.S., and Hardenbol, J., 1988, An overview of the fundamentals of sequence stratigraphy and key definitions, *in*: Wilgus, C.K., Hastings, B.S., Kendall, C.G.St.C., Posamentier, H.W., Ross, C.A., and Van Wagoner, J.C., editors, *Sea*

Level Changes: an Integrated Approach, Society of Economic Paleontologists and Mineralogist, Special Publication, vol. 42, p. 39-45.

Van Wagoner, J.C., Mitchum, R.M., Campion, K.M., and Rahamanian, V.D., 1990, Siliciclastic sequence stratigraphy in well logs, cores, and outcrops, in: American Association of Petroleum Geologists Methods in Exploration Series, v. 7, 55 p.

Vigrass, L.W., 1977, Trapping of Oil at Intra-Mannville (Lower Cretaceous) Disconformity in Lloydminster Area, Alberta, and Saskatchewan: The American Association of Petroleum Geologists Bulletin, v. 61, no. 7, p. 1010-1028.

Vossler, S.M., and Pemberton, S.G., 1988, Ichnology of the Cardium Formation (Pembina oilfield): implications for depositional and sequence stratigraphic interpretations, *in*: James, D.P., and Leckie, D.A., editors, Sequences, Stratigraphy, Sedimentology: Surface and Subsurface. Canadian Society of Petroleum Geology, Memoir 15, p. 237–253.

Wadsworth, J., Boyd, R., Diessel, C., and Leckie, D., 2002, Stratigraphic style of coal and non-marine strata in a tectonically influenced intermediate accommodation setting: the Mannville Group of the Western Canadian Sedimentary Basin, south-central Alberta: Bulletin of Canadian Petroleum Geology, v. 50, no. 4, p. 507-541.

Wellner, R.W., Varban, B.L., Roca, X., Flaum, J.A., Stewart, E.K., and Blum, M.D., 2018, Simple is better when it comes to sequence stratigraphy: The Clearwater Formation of the Mannville Group reinterpreted using a genetic body approach: American Association of Petroleum Geologists Bulletin, v. 102, no. 3, p. 447-482.

Wickenden, R.T.D., 1948, The Lower Cretaceous of the Lloydminster oil and gas area, Alberta, and Saskatchewan: Geological Survey of Canada, Paper 48-21, 15 p.

Wilson, M., 1984, Depositional environments of the Mannville Group (Lower Cretaceous) in the Tangleflags area, Saskatchewan, *in*: Lorscheider, J.A., and Wilson, M., editors, Oil and Gas in Saskatchewan: Saskatchewan Geological Society, Special Publication Number 7, p. 119-134.

Zaitlin, B.A., and Schultz, B.C., 1984, An estuarine-embayment fill model from the Lower Cretaceous Mannville Group, west-central Saskatchewan, *in*: Stott, D.F., and Glass, D.J., editors, The Mesozoic of Middle North America: Canadian Society of Petroleum Geologists, Memoir 9, p. 455-469.

Zaitlin, B.A., Warren, M.J., Potocki, D., Rosenthal, L., and Boyd, R., 2002, Depositional styles in a low accommodation foreland basin setting: an example from the Basal Quartz (Lower Cretaceous), southern Alberta: Bulletin of Canadian Petroleum Geology, v. 50, no. 1, p. 31-72.

- Zavala, C., Arcuri, M., and Blanco-Valiente, L., 2012, The importance of plant remains as diagnostic criteria for the recognition of ancient hyperpycnites: *Revue De Paleobiologie*, Special Volume 11, p. 457-469
- Zecchin, M., and Catuneanu, O., 2013, High-resolution sequence stratigraphy of clastic shelves I: Units and bounding surfaces: *Marine and Petroleum Geology*, v. 39, p. 1-25.
- Zecchin, M., and Catuneanu, O., 2015, High-resolution sequence stratigraphy of clastic shelves III: Applications to reservoir geology: *Marine and Petroleum Geology*, v. 62, p. 161-175.
- Zecchin, M., Catuneanu, O., and Caffau, M., 2017, High-resolution sequence stratigraphy of clastic shelves V: criteria to discriminate between stratigraphic sequences and sedimentological cycles: *Marine and Petroleum Geology*, v. 85, p. 259-271.
- Zecchin, M., Catuneanu, O., and Caffau, M., 2019, Wave-ravinement surfaces: Classification and key characteristics: *Earth-Science Reviews*, v. 188. p. 210-239.

5 Summary and Conclusions

The chapters of this dissertation provide previously unpublished information on three main geological aspects of the Lower Cretaceous Dina and Cummings lithostratigraphic units in the subsurface of the east-central plains region of Alberta.

5.1 Sedimentary Facies and Depositional Environments

A major focus of this thesis was applying sedimentological and ichnological principles to a core dataset to establish the affinity and range of depositional environments preserved within the Dina and Cummings interval. Through the integration of sedimentological, ichnological, and lithological observations seven facies association complexes (FAC-A to FAC-G) were identified. These seven facies association complexes are comprised of twenty-one facies associations, which are in turn comprised of a diversity of sandstone, heterolithic sandstone and mudstone, mudstone, paleosol, and coal facies. Ichnological analysis played a key role in identifying the geographical location of deposition for each facies association complex and the range of physical and chemical stresses present during sedimentation. Continental deposits were recognized by the presence of low-diversity *Scoyenia* Ichnofacies assemblages (i.e., *Scoyenia*, *Taenidium boweni*) and a lack of trace fossils associated with brackish-water conditions (i.e., *Cylindrichnus*, *Gyrolithes*, *Teichichnus*). The overprinting of brackish-water assemblages by continental ichnogenera (i.e., *Scoyenia*, *Taenidium boweni*) enabled the recognition of strata deposited at the interface between continental and paralic deposition which record alternating sub-aqueous – sub-aerial conditions. Ichnological criteria including diversity, distribution, and relative size, in concert with physical sedimentary structures were vital in identifying spatial and temporal changes in depositional environment including salinity, oxygenation, storm magnitude/frequency, riverine influence, and substrate consistency.

Publications providing detailed facies analysis of the Dina and Cummings lithostratigraphic units within the east-central plains region had not been completed prior to this study. The sedimentological observations of Chapter 2 provide the basis for the stratigraphic analysis of chapters 3 and 4.

5.2 Revised Lithostratigraphic Framework

One of the primary goals of this research was to resolve the lithostratigraphic and nomenclatural issues that have persisted from the initial formal definitions of the Dina and Cummings members in 1945. The major issues stem from 3 factors, 1) stratigraphic top placements were based on lithostratigraphic correlations of horizons unsuitable for regional correlation, 2) the initial geological descriptions did not capture the complexity and range of the depositional environments preserved within these

lithostratigraphic intervals, and 3) the original designation of member status for both the Dina and Cummings was based on a very limited dataset. These issues were addressed in the following ways.

Top placement for the Dina and Cummings were revised to conform to regional discontinuity surfaces marking a dislocation in depositional environment above and below. The stratigraphic top of the Dina is now placed at a regional discontinuity surface marking a distinct geological and petrophysical change. The geological change is characterized by the sharp juxtaposition of glauconitic, fully marine strata of the Cummings overlying paralic to coastal plain facies of the Dina and is marked by a regional coal seam or correlative organic shale. Petrophysical analysis documents a significant change in average photoelectric factor (2.78 above 2.2 B/e), density porosity (0.14 over 0.2 frac.), and gamma ray (74 over 54 API) indicating a mineralogical change across the revised Dina-Cummings boundary. The revised Cummings Formation top was moved significantly downward from the original placement. The Cummings is now more restricted in definition and encompasses the glauconitic, marine strata bound between the Dina below, and the higher-energy, more proximal, non-glauconitic Lloydminster Member above.

Issues 2 and 3 were resolved to the extent of the data available (core and petrophysical logs). The facies analysis completed in Chapter 2 provides for significantly more encompassing definitions of both the Dina and Cummings which will enable more consistent interpretations of these lithostratigraphic units within the subsurface. With the revised top placement and geological definitions in place, subsurface correlations using an extensive wireline dataset (ca. 7800 wells) established the regional extent of both the Dina and Cummings. The regional extent and geologic contrasts of the revised Dina and Cummings meets the criteria for elevation in rank from Member to Formation. The same principles of using unconformity surfaces bounding geologically distinct intervals also resulted in the recognition and formal definition of 4 new members, the McLaughlin and Rivercourse members of the Dina Formation, and the Lindbergh and Paradise Valley Members of the Cummings Formation.

5.3 Sequence Stratigraphic Framework

The sequence stratigraphic framework developed in Chapter 2 fills a gap in the understanding of the Dina and Cummings formations at a scale applicable to evaluating the distribution and connectivity of reservoir intervals and barrier/baffle horizons. As seismic data and associated outcrop were not available, the facies analysis of Chapter 2 was an essential component in the construction of the sequence stratigraphic model. Facies observations and wireline correlations were used to identify the presence and significance of discontinuity surfaces as stratigraphic or sedimentological in nature. Surfaces recognized as having sequence stratigraphic significance were used to identify systems tracts and depositional sequences at two scales, referred to as medium-frequency and high-frequency sequences. The high-

frequency sequences are nested within the medium-frequency sequence, which also includes the overlying regional progradational Lloydminster Member. The resolution of the framework is sufficient to establish the distribution of sedimentological cycles at the scale of <5 metres and to predict the lateral continuity of horizons that may function as barriers or baffles to communication between reservoir intervals. This latter application has importance to both industry and regulatory activities.

References

- Ahmad, W. and Gingras, M.K., 2022, Ichnology and Sedimentology of the Lower Cretaceous Wabiskaw Member (Clearwater Formation) Alberta, Canada: *Marine and Petroleum Geology*, v. 143, Article 105775.
- Ainsworth, R.B., Vakarelov, B.K., and Nanson, R.A., 2011, Dynamic spatial and temporal prediction of changes in depositional processes on clastic shorelines: Toward improved subsurface uncertainty reduction and management: *American Association of Petroleum Geologists*, v. 95, no. 2, p. 267-297.
- Alberta Energy and Utilities Board, 2003, Athabasca Wabiskaw-McMurray regional geological study: Alberta Energy and Utilities Board, Report 2003-A, 195 p.
- Allen, G.P., and Posamentier, H.W., 1993, Sequency stratigraphy and facies model of an incised valley fill: the Gironde estuary, France. *Journal of Sedimentary Petrology*, 63, 378-391.
- Allen, J.R.L., 1964, Studies in fluvial sedimentation: six cyclothems from the Lower Old Red Sandstone, Anglo-Welsh Basin: *Sedimentology*, v. 3, p. 163-198.
- Allen, J.R.L., 1970, Studies in fluvial sedimentation: A comparison of fining-upward cyclothems, with special reference to coarse-member composition and interpretation: *Journal of Sedimentary Petrology*, v. 40, p. 298-323.
- Ambler, J.S., 1951, The stratigraphy and structure of the Lloydminster oil and gas area: University of Saskatchewan, M.Sc. thesis.
- Banerjee, I., Kalkreuth, W., and Davies, E.H., 1996, Coal seam splits and transgressive-regressive coal couplets: A key to stratigraphy of high-frequency sequences: *Geology*, v. 24, no. 11, p. 1001-1004.
- Bann, K.L., and Fielding, C.R., 2004, An integrated ichnological and sedimentological comparison of non-deltaic shoreface and subaqueous delta deposits in Permian reservoir units of Australia: *Geological Society, London, Special Publication* v. 228, p. 273-310.
- Bann, K.L., Fielding, C.R., MacEachern, J.A., and Tye, S.C., 2004, Differentiation of estuarine and offshore marine deposits using integrated ichnology and sedimentology: Permian Pebble Beach Formation, Sydney Basin, Australia, *in*: McIlroy, D., editor, *The Application of Ichnology to Palaeoenvironmental and Stratigraphic Analysis*. Geological Society of London, Special Publication, vol. 228, p. 179–211.
- Barton, M.D., 2016, The architecture and variability of valley-fill deposits within the Cretaceous McMurray Formation, Shell Albian sands lease, northeast Alberta: *Bulletin of Canadian Petroleum Geology*, v. 64, no. 2, p. 166-198.

- Bauer, D.B., Hubbard, S.M., Leckie, D.A., and Dolby, G., 2009, Delineation of a sandstone-filled incised valley in the Lower Cretaceous Dina–Cummings interval: implications for development of the Winter Pool, west-central Saskatchewan: *Bulletin of Canadian Petroleum Geology*, v. 57, no. 4, p. 409-429.
- Bayet-Goll, R., Samani, P.N., de Carvalho, C.N., Monaco, P., Khodaie, N., Pour, M.M., Kazemeini, H., and Zareiyani, M.H., 2017, Sequence stratigraphy and ichnology of Early Cretaceous reservoirs, Gadvan Formation in southwestern Iran: *Marine and Petroleum Geology*, v. 81, p. 294-319.
- Beynon, B.M., Pemberton, S.G., Bell, D.F., and Logan, C.A., 1988, Environmental implications of ichnofossil from the Lower Cretaceous Grand Rapids Formation, Cold Lake oil sands deposit, *in*: James, D.P., and Leckie, D.A., editors, *Sequences, Stratigraphy, and Sedimentology: Surface and Subsurface*, Canadian Society of Petroleum Geologists, Memoir 15, p. 275-290.
- Bhattacharya, J.P., 2010, Deltas. *in*: James, N.P., and Dalrymple, R.W., editors, *Facies Models 4*, Geologic Association of Canada, p. 233-264.
- Bhattacharya, J.P., and MacEachern, J.A., 2009, Hyperpycnal rivers and prodeltaic shelves in the Cretaceous seaway of North America: *Journal of Sedimentary Research*, v. 79, p. 184–209.
- Botterill, S.E., Campbell, S.G., Timmer, E.R., Gingras, M.K., and Pemberton, S.G., 2016, Recognition of wave-influenced deltaic and bay-margin sedimentation, Bluesky Formation, Alberta: *Bulletin of Canadian Petroleum Geology*, v. 64, p. 389–414.
- Bown, T.M. and Kraus, M.J., 1987, Integration of channel and floodplain suites in aggrading fluvial systems I. Developmental sequence and lateral relations of lower Eocene alluvial palaeosols, Willwood Formation, Bighorn Basin, Wyoming: *Journal of Sedimentary Petrology*, v. 57, p. 587-601.
- Bromley, R.G., 1975, Trace fossils at omission surfaces, *in*: Frey, R.W., editor, *The Study of Trace Fossils*, Springer-Verlag, New York, p. 399-428.
- Bromley, R.G., and Ekdale, A.A., 1984, *Chondrites*: a trace fossil indicator of anoxia in sediments: *Science*, v. 224, p. 872-874.
- Buatois, L.A., and Mangano, M.G., 1995, The paleoenvironmental and paleoecological significance of the lacustrine Mermia Ichnofacies: an archetypical subaqueous nonmarine trace fossil assemblage: *Ichnos*, v. 4, no. 2, p. 151–161.
- Buatois, L.A., Mangano, M.G., 2011, *Ichnology: Organism-Substrate Interactions in Space and Time*: Cambridge University Press, Cambridge, 358 pp.
- Buatois, L.A., Santiago, N., Parra, K., and Steel, R., 2008, Animal-Substrate interactions in an early Miocene wave-dominated tropical delta: delineating environmental stresses and depositional dynamics (Tacata Field, eastern Venezuela): *Journal of Sedimentary Research*, v. 86, p. 458-479.

- Buatois, L.A., Mangano, M.G., and Pattison, S.A., 2019, Ichnology of prodeltaic hyperpycnite-turbidite channel complexes and lobes from the upper Cretaceous Prairie Canyon member of the Mancos Shale, Book Cliffs, Utah, USA: *Sedimentology*, v. 66, p. 1825-1860.
- Campbell, S.G., Botterill, S.E., Gingras, M.K., and MacEachern, J.A., 2016, Event sedimentation, deposition rate, and paleoenvironment using crowded *Rosselia* assemblages of the Bluesky Formation: *Journal of Sedimentary Research*, v. 86, p. 380-393.
- Cant, D.J., 1996, Sedimentological and sequence stratigraphic organization of a foreland clastic wedge, Mannville Group, Western Canada Basin: *Journal of Sedimentary Research*, v. 66, no. 6, p. 1137-1147.
- Cant, D.J., and Abrahamson, B., 1996, Regional distribution and internal stratigraphy of the Lower Mannville: *Bulletin of Canadian Petroleum Geology*, v. 44, no. 3, 508-529.
- Carmona, N.B., Buatois, L.A., Ponce, J.J., and Mangano, M.G., 2009, Ichnology and sedimentology of a tide-influenced delta, Lower Miocene Chenque Formation, Patagonia, Argentina: trace-fossil distribution and response to environmental stresses: *Palaeogeography, Palaeoclimatology, Palaeoecology*: v. 273, p. 75–86.
- Cattaneo, A., and Steel, R.J., 2003, Transgressive deposits: a review of their variability: *Earth Science Reviews*, v. 62, no. 3, p. 187-228.
- Catuneanu, O., 2006, *Principles of Sequence Stratigraphy*: Amsterdam, Elsevier, 375 p.
- Catuneanu, O., 2019a, Scale in sequence stratigraphy: *Marine and Petroleum Geology*, v. 106, p. 128-159.
- Catuneanu, O., 2019b, Model independent sequence stratigraphy: *Earth-Science Reviews*, v. 188, p. 312-388.
- Catuneanu, O., and Zecchin, M., 2013, High-resolution sequence stratigraphy of clastic shelves II: Controls on sequence development: *Marine and Petroleum Geology*, v. 39, p. 26-38.
- Chalmers, R.L., Boyd, R., and Diessel, C.F.K., 2013, Accommodation-based coal cycles and significant surface correlation of low-accommodation Lower Cretaceous coal seams, Lloydminster heavy oil field, Alberta, Canada: Implications for coal quality distribution: *American Association of Petroleum Geologists Bulletin*, v. 97, no. 8, p. 1347-1369.
- Chateau, C.C.F., Dashtgard, S.E., MacEachern, J.A., and Hauck, T.E., 2019, Parasequence architecture in a low-accommodation setting, impact of syndepositional carbonate epikarstification, McMurray Formation, Alberta, Canada: *Marine and Petroleum Geology*, v. 104, p. 168-179.

- Christopher, J., 1997, Evolution of the Lower Cretaceous Mannville Sedimentary Basin in Saskatchewan, *in*: Pemberton, S.G., and James, D.P., editors, Petroleum Geology of the Cretaceous Mannville Group, Western Canada: Canadian Society of Petroleum Geologists, Memoir 18, p. 191-210.
- Dalrymple, R.W. 2010, Tidal Depositional Systems. *in*: James, N.P., Dalrymple, R.W. editors, Facies Models 4, Geologic Association of Canada, p. 199-208.
- Dalrymple, R.W., and Choi, K., 2004, Morphological and facies trends through the fluvial-marine transition in tide-dominated depositional systems: a schematic framework for environmental and sequence stratigraphic interpretation, *Earth-Science Reviews*, v. 81, no. 3-4, p. 135-174.
- Demchuk, T. D., Dolby, G., McIntyre, D.J., and Suter, J.R., 2007, The utility of palynofloral assemblages for the interpretation of depositional paleoenvironments and sequence-stratigraphic systems tracts in the McMurray Formation at Surmont, Alberta, *in*: Suter, J.R., Leckie, D.A., and Larter, S., editors, Heavy oil and bitumen in foreland basins: From processes to products, American Association of Petroleum Geologists Hedberg Research Conference, Banff, Alberta, Canada, 5 p.
- Deschamps, R., Sale, S.O., Chauveau, B., Fierens, R., and Euzen, T., 2017, The coal-bearing strata of the Lower Cretaceous Mannville Group (Western Canadian Sedimentary Basin, South Central Alberta). Part 1: Stratigraphic architecture and coal distribution controlling factors: *International Journal of Coal Geology*, v. 179, 113-129.
- Dolby, G., Demchuk, T.D., and Suter, J.R., 2013, The significance of palynofloral assemblages from the Lower Cretaceous McMurray Formation and associated strata, Surmont and surrounding areas in north-central Alberta, *in*: Hein, F.J., Leckie, D.A., Larter, S., and Suter, J.R., editors, Heavy-oil and oil-sand petroleum systems in Alberta and beyond, American Association of Petroleum Geologists Studies in Geology 64, p. 251-272.
- Dott, R.H., Jr and Bourgeois, J., 1982, Hummocky cross-stratification: significance of its variable bedding sequences: *Geological Society of America Bulletin*, v. 93, p. 663-680.
- Duke, W.L., 1985, Hummocky cross-stratification, tropical hurricanes, and intense storms: *Sedimentology*, v. 32, p. 167-194.
- Dumas, S., and Arnott, R.W.C., 2006, Origin of hummocky and swaley cross-stratification – The Controlling influence of unidirectional current strength and aggradation rate: *Geology*, v. 34, p. 1073-1076.
- Dumas, S., Arnott, R.W.C., and Southard, J.B., 2005, Experiments on oscillatory-flow and combined-flow bed forms: implications for interpreting parts of the shallow-marine sedimentary record: *Journal of Sedimentary Research*, v. 75, p. 501-513.

- Ekdale, A.A., Bromley, R.G., Pemberton, S.G., 1984. Ichnology: The Use of Trace Fossils in Sedimentology and Stratigraphy. Society of Economic Paleontologist and Mineralogists Short Course Notes 15, 1–316.
- Fielding, C.R., Bann, K.L., and Trueman, J.D., 2007, Resolving the Architecture of a Complex, Low-Accommodation Unit Using High-Resolution Sequence Stratigraphy and Ichnology: The Late Permian Freitag Formation in the Denison Trough, Queensland, Australia, *in*: MacEachern, J.A., Bann, K.L., Gingras, M.K., and Pemberton, S.G., editors, Applied Ichnology. Society of Economic Paleontologists and Mineralogists, Short Course Notes 52, p. 179-208.
- Frey, R.W., Pemberton, S.G., Fagerstrom, J.A., 1984. Morphological, ethological, and environmental significance of the ichnogenera *Scoyenia* and *Ancorichnus*. *J. Paleontol.* 58, 511–528.
- Frey, R.W., Pemberton, S.G., and Saunders, T.D.A., 1990, Ichnofacies and bathymetry: a passive relationship: *Journal of Paleontology*, v. 64, no. 1, p. 155-158.
- Fuglem 1970, M.O., 1970, Use of core in evaluation of productive sands, Lloydminster area, *in*: Brindele, J.E., and Holmerg, R.A., editors, Saskatchewan Mesozoic Core Seminar, Saskatchewan Geological Society, 12 p.
- Gingras, M.K., MacEachern, J.A., and Pemberton, S.G., 1998, A comparative analysis of the ichnology of wave- and river-dominated allomembers of the Upper Cretaceous Dunvegan Formation; *BGGP*, v. 46, vol. 1, p. 51-73.
- Gingras, M.K., Pemberton, S.G., Saunders, T. and Clifton, H.E. 1999. The ichnology of modern and Pleistocene brackish-water deposits at Willapa Bay, Washington; variability in estuarine settings. *Palaios*, v. 14, no. 4, p. 352–374.
- Gingras, M.K., MacEachern, J.A. and Dashtgard, S.E., 2011. Process ichnology and the elucidation of physico-chemical stress. *Sedimentary Geology*, v. 237, no. 3, p.115–134.
- Gingras, M.K., MacEachern, J.A. and Dashtgard, S.E., 2012. The potential of trace fossils as tidal indicators in bays and estuaries. *Sedimentary Geology*, v. 279, p. 97–106.
- Gingras, M.K., MacEachern, J.A., Dashtgard, S.E., Ranger, M.J., and Pemberton, S.G., 2016, The significance of trace fossils in the McMurray Formation, Alberta, Canada: *Bulletin of Canadian Petroleum Geology*, v. 64, no. 2, p. 233-250.
- Gross, A.A., 1980, Mannville Channels in east-central Alberta: Lloydminster and Beyond: *Geology of Mannville Hydrocarbon*, *in*: Beck, L.S., Christopher, J.E., and Kent, D.M., editors, *Lloydminster and Beyond: Geology of Mannville Hydrocarbon Reservoirs*: Saskatchewan Geological Society, Special Publication 5. p. 33–63.

- Hampson, G.J., and Storms, J.E.A., 2003, Geomorphological and sequence stratigraphic variability in wave-dominated, shoreface-shelf parasequences: *Sedimentology*, v. 50, p. 667-701.
- Harms, J.C., Southard, J.B., Spearing, D.R., and Walker, R.G., 1975, Depositional environments as interpreted from primary sedimentary structures and stratification sequences: *Society of Economic Paleontologists and Mineralogists Short Course 2*, 161 p.
- Hasiotis, S.T. 2002, Continental Trace Fossils: *Society of Economic Mineralogist and Palaeontologists. Short Course No. 51*, 132 p.
- Hasiotis, S.T., 2007, Continental ichnology: fundamental processes and controls on trace fossil distribution, *in: Miller, W., Trace Fossil Concepts, Problems, and Prospects*, Elsevier, Amsterdam, p. 268-284.
- Hauck, T.E., Dashtgard, S.E., and Gingras, M.K., 2009, Brackish-water ichnological trends in a microtidal barrier island/embayment system, Kouchibouguac National Park, New Brunswick, Canada: *Palaios*, v. 24, p. 478–496.
- Hayes, B.J.R., Christopher, J.E., Rosenthal, L.L., McKercher, B., Minken, D., Tremblay, Y.M., and Fennel, J., 1994, Cretaceous Mannville Group of the Western Canada Sedimentary Basin, *in: Mossop, G.D., and Shetson, I., editors, Geological Atlas of the Western Canada Sedimentary Basin*, Canadian Society of Petroleum Geologists and Alberta Research Council, Special Report 4.
- Helland-Hansen, W., and Martinsen, O.J., 1994, Shoreline trajectories and sequences: description of variable depositional-dip scenarios: *Journal of Sedimentary Research*, v. 66, no. 4, 670-688.
- Helland-Hansen, W., and Gjelberg, J.G., 1994, Conceptual basis and variability in sequence stratigraphy: a different perspective: *Sedimentary Geology*, v. 92, no. 1-2, p. 31-52.
- Hembree, D., 2018, The role of continental trace fossils in Cenozoic paleoenvironmental and paleoecological reconstructions, *in: Croft, D.A., Su, D.F., and Simpson, S.W., editors, Methods in Paleoecology: Reconstructing Cenozoic Terrestrial Environments and Ecological Communities, Vertebrate Paleobiology and Paleoanthropology Series*, p. 185-214.
- Hildred, G.V., Ratcliff, K.T., Wright, A.M., Zaitlin, B.A., and Wray, D.S., 2010, Chemostratigraphic applications to low-accommodation fluvial incised-valley settings: an example from the lower Mannville Formation of Alberta, Canada: *Journal of Sedimentary Research*, v. 80, p. 1032-1045.
- Holz, M., Kalkreuth, W., and Banerjee, I., 2002, Sequence stratigraphy of paralic coal-bearing strata: an overview: *International Journal of Coal Geology*, v. 48, p. 147-179.
- Howard, J.D., Elders, C.A., and Heinbokel, J.F., 1975, Animal-sediment relationships in estuarine point bar deposits, Ogeechee River-Ossabaw Sound: *Estuaries of the Georgia Coast, U.S.A.: Sedimentology and Biology V, Senckenbergiana Maritima*, v. 7, p. 181-203.

- Hubbard, S.M., Pemberton, S.G. and Howard, E.A. 1999, Regional geology and sedimentology of the basal Cretaceous Peace River Oil Sands deposit, north-central Alberta: *Bulletin of Canadian Petroleum Geology*, v. 47, p. 270–297.
- Hubbard, S.M, Gingras, M.K., and Pemberton, S.G., 2004, Paleoenvironmental implications of trace fossils in estuary deposits of the Cretaceous Bluesky Formation, Cadotte region, Alberta, Canada: *Fossils and Strata*, v. 51, p. 68–87.
- Hunt, D., and Tucker, M.E., 1992, Stranded parasequences and the forced regressive wedge systems tract: deposition during base-level fall: *Sedimentary Geology*, v. 81, no. 1-2, p. 1-9.
- Ichaso, A.A., and Dalrymple, R.W., 2009, Tide- and wave-generated fluid mud deposits in the Tilje Formation (Jurassic), offshore Norway, *Geology*, v. 37, p. 539-542.
- Kent, D.M., 1959, The Lloydminster oil and gas field, Alberta: University of Saskatchewan, M.Sc. thesis, 92 p.
- Kidwell, S.M., 1989, Stratigraphic condensation of marine transgressive records; origin of major shell deposits in the Miocene of Maryland: *Journal of Geology*, v. 97, p. 1-24.
- Kohlruss, D. J., 2012, Stratigraphic architecture and facies analysis of the Lower Cretaceous Dina Member of the Mannville Group in northwest Saskatchewan: University of Regina, M.Sc. thesis, 200 p.
- Kraus, M.J., 1999, Paleosols in clastic sedimentary rocks: their geologic applications: *Earth-Science Reviews*, v. 47, p. 41-70.
- Kvale, E.P. 2012. Tidal constituents of modern and ancient tidal rhythmites: criteria for recognition and analyses, *in*: Davis, R.A., Davis Jr, R.A., and Dalrymple, R.W., editors, *Principles of Tidal Sedimentology*, Springer Netherlands, p. 1–17.
- Kvale, E.P., Johnson, H.W., Sonett, C.P., Archer, A.W. and Zawistoski, A. 1999. Calculating lunar retreat rates using tidal rhythmites. *Journal of Sedimentary Research*, v. 69, no. 6. 1154-1168.
- Leckie, D.A., Vanbeselaere, N.A., and James, D.P., 1997, Regional sedimentology, sequence stratigraphy and petroleum geology of the Mannville Group: southwestern Saskatchewan, *in*: Pemberton, S.G., and James, D.P., editors, *Petroleum Geology of the Cretaceous Mannville Group, Western Canada*, Canadian Society of Petroleum Geologists, Memoir 18, p. 211-262.
- Longhitano, S.G., Mellere, D., Steel, R.J., and Ainsworth, R.B., 2012, Tidal depositional systems in the rock record: A review and new insights: *Sedimentary Geology*, v. 279, p. 2-22.
- MacEachern, J.A., and Pemberton, S.G., 1992, Ichnological aspects of Cretaceous shoreface successions and shoreface variability in the Western Interior Seaway of North America, *in*: Pemberton, S.G., editor, *Applications of Ichnology to Petroleum Exploration, A Core Workshop*, Core Workshop 17,

Society of Economic Paleontologist and Mineralogists Society for Sedimentary Geology, Tulsa, OK. p. 57–84.

MacEachern, J.A., and Pemberton, S.G., 1994, Ichnological character of incised valley fill systems from the Viking Formation of the Western Canada Sedimentary Basin, Alberta, Canada, *in*: Dalrymple, R., Boyd, R., Zaitlin, B., editors, *Incised-Valley Systems: Origin and Sedimentary Sequences*. Society of Economic Paleontologists and Mineralogists, Special Publication, vol. 51, p. 129–157.

MacEachern, J.A., Zaitlin, B.A., and Pemberton, S.G., 1999, A sharp-based sandstone of the Viking Formation, Joffre field, Alberta, Canada: criteria for recognition of transgressively incised shoreface complexes: *Journal of Sedimentary Research*, v. 69, no. 4, p. 876-892.

MacEachern, J.A., and Gingras, M.K., 2007, Recognition of brackish-water trace fossil suites in the Cretaceous Western Interior Seaway of Alberta, Canada, *in*: Bromley, R.G., Buatois, L.A., Mangano, G., Genise, J.F., and Melchor, R.N., editors, *Sediment-Organism Interactions: A Multifaceted Ichnology*, Society of Economic Paleontologists and Mineralogists Special Publication, v. 88, p. 50–59.

MacEachern, J.A., Pemberton, S.G., Gingras, M.K., Bann, K.L., and Dafoe, L.T., 2007b, Use of trace fossils in genetic stratigraphy, *in*: Miller III, W., editor, *Trace Fossils. Concepts, Problems, and Prospects*. Elsevier, Amsterdam, p. 105-128.

MacEachern, J.A., and Bann, K.L., 2008, The role of ichnology in refining shallow marine facies models, *in*: Hampson, G., Steel, R., Burgess, P., and Dalrymple, R.W., editors, *Recent Advances in Models of Siliciclastic Shallow-Marine Stratigraphy*. Society of Economic Paleontologist and Mineralogists Special Publication, v. 90, p. 73-116.

MacEachern, J.A., Gingras, M.K., Bann, K.L., Pemberton, S.G., and Dafoe, L.T., 2007, Applications of ichnology to high-resolution genetic stratigraphic paradigms, *in*: MacEachern, J.A., Bann, K.L., Gingras, M.K., and Pemberton, S.G., editors, *Applied Ichnology*. Society of Economic Paleontologists and Mineralogists, Short Course Notes 52, p. 95–129.

MacEachern, J.A., and Bann, K.L., 2020, The Phycosiphon ichnofacies and Rosselia ichnofacies: two new ichnofacies for marine deltaic environments: *Journal of Sedimentary Research*, v. 90, p. 855-886.

MacEachern, J.A., Bann, K.L., Bhattacharya, J.P., and Howell, C.D., 2005, Ichnology of deltas: organism responses to the dynamic interplay of rivers, waves, storms and tides, *in*: Bhattacharya, J.P., and Giosan, L., editors, *River Deltas: Concepts, Models and Examples*, Society of Economic Paleontologists and Mineralogists, Special Publication 83, pp. 49–85.

- MacEachern, J.A., Pemberton, S.G., Gingras, M.K., and Bann, K.L., 2010, Ichnology and facies models. *in*: James, N.P., and Dalrymple, R.W. editors, *Facies Models*, edition 4: Geological Association of Canada, St. Johns, Newfoundland, p. 19–58.
- MacEachern, J.A., Dashtgard, S.E., Knaust, D., Catuneanu, O., Bann, K.L., and Pemberton, S.G., 2012, Sequence Stratigraphy *in*: Knaust, D., and Bromley, R.G., editors, *Trace fossils as indicators of sedimentary environments*. *Developments in Sedimentology*, v. 64, p. 157-194.
- Mack, G.H., James, W.C., and Monger, H.C., 1993, Classification of paleosols: *Geological Society of America Bulletin*, v. 105, p. 129-136.
- MacKay, D.A. and Dalrymple, R.W., 2011, Dynamic mud deposition in a tidal environment: the record of fluid-mud deposition in the Cretaceous Bluesky Formation, Alberta Canada: *Journal of Sedimentary Research*, v. 81, p. 901-920.
- Martin, K.D., 2004. A re-evaluation of the relationship between trace fossils and dysoxia, *in*: McIlroy, D. editor, *The Application of Ichnology to Paleoenvironmental and Stratigraphic Analysis*: Geological Society of London, Special Publication, v. 228, p. 141–156.
- Marriott, S.B., and Wright, V.P., 1993, Paleosols as indicators of geomorphic stability in two Old Red Sandstone alluvial suites, South Wales: *Journal of the Geological Society of London*, v. 150, p. 1109-1120.
- McIlroy, D., 2004, Some Ichnological Concepts, Methodologies, Applications, and Frontiers: Geological Society of London, Special Publication, v. 288, p. 3-27.
- McPhee, D., and Pemberton, S.G., 1997, Sequence stratigraphy of the Lower Cretaceous Mannville Group of east Alberta:
- Melchor, R.N., Genise, J.F., Buatois, L.A., and Umazano, A.M., 2012, Fluvial environments, *in*: Knaust, D., Bromley, R.G. editors, *Trace fossils as indicators of sedimentary environments*. *Developments in Sedimentology*, v. 64, p. 329-378.
- Melnyk, S., and Gingras, M.K., 2020, Using ichnological relationships to interpret heterolithic fabrics in fluvio-tidal settings: *Sedimentology*, v. 67, p. 1069-1083.
- Metz, R., 2020, Trace fossils in fluvial deposits of the uppermost Stockton Formation (Late Triassic), Newark Basin, New Jersey: *Ichnos*, v. 27, no. 2, p. 142-151.
- Miall, A.D. 2006. *The geology of fluvial deposits: Sedimentary facies, basin analysis, and petroleum geology*. Springer-Verlag, Berlin.

- Morshedjian, A., MacEachern, J.A., Dashtgard, S.E., Bann, K.L., and Pemberton, S.G., 2019, Systems tracts and their bounding surfaces in the low- accommodation Upper Mannville group, Saskatchewan, Canada: *Marine and Petroleum Geology*, v. 110, p. 35-54.
- Moslow, T.F., and Pemberton, S.G., 1988, An integrated approach to the sedimentological analysis of some Lower Cretaceous shoreface and delta front sandstone sequences, *in*: James, D.P., and Leckie, D.A., editors, *Sequences, Stratigraphy, and Sedimentology: Surface and Subsurface*, Canadian Society of Petroleum Geologists, *Memoir 15*, p. 373-386.
- Mulder, T., and Alexander, J., 2001, The physical character of subaqueous sedimentary density currents and their deposits: *Sedimentology*, v. 48, p. 269-299.
- Mulder, T., Syvitski, J.P.M., Migeon, S., Faugères, J.C., and Savoye, B., 2003, Marine hyperpycnal flows: initiation, behaviour, and related deposits. A review: *Marine and Petroleum Geology*, v. 20p. 861-882.
- North American Commission on Stratigraphic Nomenclature, 2005, North American Stratigraphic Code: *American Association of Petroleum Geologists Bulletin*, v. 89, no. 11, p. 1547-1491.
- Nauss, A.W., 1945, Cretaceous stratigraphy of Vermillion area, Alberta, Canada: *Bulletin of the American Association of Petroleum Geologists*, v. 29, no. 11, p. 1605-1629.
- Newitt, K.J., and Pederson, P.K., 2022, Observational data-based sequence stratigraphy of a clastic wedge within an active foreland basin, Spirit River Formation, west-central Alberta, Canada: *MPG*, v. 140, 105681.
- Nio, S.D., and Yang, C.S., 1991, Diagnostic attributes of clastic tidal deposits: a review, *in*: Smith, D.G., Reinson, C.G., Zaitlin, B.A., and Rahmani, R.A., editors, *Clastic Tidal Sedimentology*, Canadian Society of Petroleum Geology, *Memoir 16*, p. 3-28.
- Nummedal, D., and Swift, D.J.P., 1987, Transgressive stratigraphy at sequence-bounding unconformities: some principles derived from the Holocene and Cretaceous examples, *in*: Nummedal, D., Pilkey, O.H., and Howard, J.D., editors, *Sea-level Fluctuation and Coastal Evolution*, Society of Economic Paleontologists and Mineralogists, *Special Publication*, v. 41, p. 241-260.
- Orr, R.D., Johnston, J.R., and Manko, E.M., 1977, Lower Cretaceous geology and heavy-oil potential of the Lloydminster area: *Bulletin of Canadian Petroleum Geology*, v. 25, no. 6, p. 1187-1221.
- Pearson, N.J., Mangano, M.G., Buatois, L.A., Casadio, and Raising, M.R., 2012, Ichnology, sedimentology, and sequence stratigraphy of outer-estuarine and coastal-plain deposits: Implications for the distinction between allogenic and autogenic expressions of the Glossifungites Ichnofacies: *Palaeogeography, Palaeoclimatology, Palaeoecology*, v. 333, 192-217.

- Pemberton, S.G., Flach, P.D., and Mossop, G.D., 1982, Trace fossils from the Athabasca Oil Sands, Alberta, Canada: *Science*, v. 217, p. 825–827.
- Pemberton, S.G., MacEachern, J.A., and Frey, R.W., 1992, Trace fossil facies models: environmental and allostratigraphic significance, *in*: Walker, R.G., and James, N.P., editors, *Facies Models: Response to Sea Level Change*, Geological Association of Canada, Toronto, p. 47-72.
- Pemberton, S.G., and MacEachern, J.A., 1995, The sequence stratigraphic significance of trace fossils: examples from the Cretaceous foreland basin of Alberta, Canada. *in*: Van Wagoner, J.C., and Bertram, G., editors, *Sequence Stratigraphy of Foreland Basin Deposits: Outcrop and Subsurface Examples from the Cretaceous of North America*, American Association of Petroleum Geologists, Memoir 64, p. 429–475.
- Pemberton, S.G., and MacEachern, J.A., 1997, The ichnological signature of storm deposits: the use of trace fossils in event stratigraphy, *in*: Brett, C.E. editor, *Paleontological Event Horizons: Ecological and Evolutionary Implications*, Columbia University Press, p. 73-109.
- Pemberton, S.G., MacEachern, J.A., and Gingras, M.K., 2000, Significance of ichnofossil to genetic stratigraphy: *Science in China*, v. 43, no. 5, p. 541-560.
- Pemberton, S.G., MacEachern, J.A., and Saunders, T.D.A., 2004, Stratigraphic applications of substrate-specific ichnofacies: delineating discontinuities in the rock record. *in*: McIlroy, D., editor, *The Application of Ichnology to Palaeoenvironmental and Stratigraphic Analysis*. Geological Society of London, Special Publication, vol. 228, p. 29–62.
- Pemberton, S.G., MacEachern, J.A., Dashtgard, S.E., Bann, K.L., Gingras, M.K., and Zonneveld, J.P., 2012, Shorefaces. *in*: Knaust, D., and Bromley, R.G., editors, *Trace fossils as indicators of sedimentary environments*. *Developments in Sedimentology*, v. 64, p. 563-603.
- Plint, A.G., 1988, Sharp-based shoreface sequences and “offshore bars” in the Cardium Formation of Alberta: their relations to relative changes in sea level, *in*: Wilgus, C.K., Hastings, B.S., Kendall, C.G.St.C., Posamentier, H.W., Ross, C.A., and Van Wagoner, J.C., editors, *Sea Level Changes: an Integrated Approach*, Society of Economic Paleontologists and Mineralogist, Special Publication, vol. 42, p. 357-370.
- Plint, A.G., and Nummedal, D., 2000, The falling stage systems tract: recognition and importance in sequence stratigraphic analysis, *in*: Hunt, D., and Gawthorpe, R.L., editors, *Sedimentary Response to Forced Regression*, Geological Society of London Special Publication, v. 172, p. 1-17.
- Plummer, P.S., and Gostin, V.A., 1981, Shrinkage cracks: desiccation or syneresis? *Journal of Sedimentary Petrology*, v. 51, no. 4, p. 1147-1156.

- Posamentier, H.W., and Vail, P.R., 1988, Eustatic controls on clastic deposition, II: sequence and systems tract models, *in*: Wilgus, C.K., Hastings, B.S., Kendall, C.G.St.C., Posamentier, H.W., Ross, C.A., and Van Wagoner, J.C., editors, *Sea Level Changes: an Integrated Approach*, Society of Economic Paleontologists and Mineralogist, Special Publication, vol. 42, p. 125-154.
- Pouderoux, H., Coderre, A.B., Pedersen, P.K., and Cronkwright, D.J., 2016, Characterization, architecture, and controls of Cold Lake marginal-marine oil sands: the Grand Rapids Formation (Upper Mannville) of east-central Alberta, Canada: *Bulletin of Canadian Petroleum Geology*, v. 64, no. 2, p. 119-146.
- Ratcliffe, K.T., Wright, A.M., Hallsworth, C., Morton, A., Zaitlin, B.A., Potocki, D., and Wray, D.S., 2004, An example of alternative correlation techniques in a low-accommodation setting, nonmarine hydrocarbon system: The (Lower Cretaceous) Mannville Basal Quartz succession of southern Alberta: *American Association of Petroleum Geologists Bulletin*, v. 88, no. 10, p. 1419-1432.
- Reading, H.G., and Collinson, J.D., 1996, *Clastic Coasts*, *in*: Reading, H.G., editor, *Sedimentary Environments: Processes, Facies and Stratigraphy*, Third Addition, Blackwell, p. 154-231.
- Reineck, H.E., 1967. Parameter von Schichtung und bioturbation. *Geologische Rundschau*, v. 56, p. 420–438.
- Reineck, H.E., 1975, German North Sea tidal flats: *in*: Ginsburg, R.N., editor, *Tidal Deposits: A casebook of recent examples and fossil counterparts*, Springer-Verlag, New York.
- Retallack, G.J., 1984, Field recognition of paleosols: *in*: Reinhardt, J., and Sigleo, W.R., editors, *Paleosols and weathering through geologic time*, Geological Society of America Special Paper, v. 2016, p. 1-20
- Rinke-Hardekopf, L., Dashtgard, S.E., MacEachern, J.A., and Gingras, M.K., 2022, Resolving stratigraphic architecture and constraining ages of paralic strata in a low-accommodation setting, Firebag Tributary, McMurray Formation, Canada, *Depositional Record*, v. 8, p. 754-785.
- Rodriguez, W., Buatois, L.A., Mangano, M.G., and Solórzano, E., 2018, Sedimentology, ichnology, and sequence stratigraphy of the Miocene Oficina Formation, Junín and Boyacá areas, Orinoco Oil Belt, Eastern Venezuela Basin: *Marine and Petroleum Geology*, v. 92, p. 213-233.
- Rodriguez-Tovar, F.J., Perez-Valera, F., and Perez-Lopez, A., 2007, Ichnological analysis in high-resolution sequence stratigraphy: The *Glossifungites* ichnofacies in Triassic successions from the Betic Cordillera (southern Spain): *Sedimentary Geology*, v. 198, p. 293-307.
- Sarzalejo, S., and Hart, B.S., 2006, Stratigraphy and lithologic heterogeneity in the Mannville Group (southeast Saskatchewan) defined by integrating 3-D seismic and log data: *Bulletin of Canadian Petroleum Geology*, v. 54. no. 2, p. 138-151.

- Savrda, C.E., and Bottjer, D.J., 1989, Trace-fossil model for reconstructing oxygenation histories of ancient marine bottom waters: application to Upper Cretaceous Niobrara Formation, Colorado: *Palaeogeography, Palaeoclimatology, Palaeoecology*, v. 74, p. 49–74.
- Shchepetkina, A., Ponce, J.J., Carmona, N.B., Mangano, M.G., Buatois, L.A., Ribas, S., and Benvenuto, M.C.V., 2020, Sedimentological and ichnological analyses of the continental to marginal-marine Centenario formation (Cretaceous), Neuquén basin, Argentina: reservoir implications: *Marine and Petroleum Geology*, v. 119, 104471.
- Schultz, S.K., MacEachern, J.A., Catuneanu, O., Dashtgard, S.E., and Diaz, N., 2022, High-resolution sequence stratigraphic framework for the late Albian Viking Formation in central Alberta: *Marine and Petroleum Geology*, v. 139, 105627.
- Seilacher, A., 1978, Use of trace fossil assemblages for recognizing depositional environments: *Trace Fossil Concepts*, Society of Economic Paleontologists and Mineralogists, Special Publication 5, p. 185-201.
- Silva, S.E.S, and Hart, B.S., 2013, Advanced seismic-stratigraphic imaging of depositional elements in a Lower Cretaceous (Mannville) heavy oil reservoir, west-central Saskatchewan, Canada, *in*: Hein, F.J., Leckie, D.A., Larter, S., Suter, J.R., editors, *Heavy-oil and oil-sand petroleum systems in Alberta and beyond: American Association of Petroleum Geologists Studies in Geology* 64, p. 359-371.
- Sloss, L.L., Krumbein, W.C., and Dapples, E.C., 1949, Integrated facies analysis, *in*: Longwell, C.R., editor, *Sedimentary Facies in Geologic History*, Geological Society of America, Memoir 39, p. 91-124.
- Smali, M., and Hart, B.S., 2018, Pushing the envelope of seismic stratigraphic interpretation: a case study from the Mannville Group using small 3-D surveys: *Bulletin of Canadian Petroleum Geology*, v. 66, no. 4, 752-772.
- Solórzano, E.J., Buatois, L.A., Rodriguez, W.J., and Mangano, M.G., 2017, From freshwater to fully marine: exploring animal-substrate interactions along a salinity gradient (Miocene Oficina Formation of Venezuela): *Palaeogeography, Palaeoclimatology, Palaeoecology*, v. 482, p. 30-47.
- Swift, D.J.P., 1968, Coastal erosion and transgressive stratigraphy: *Journal of Geology*, v. 76, 444-456.
- Tabor, N.J., Myers, T.S., and Michel, L.A., 2017, Sedimentologists guide for recognition, description, and classification of paleosol: *in*: Zeigler, K.E., and Parker, W.G., editors, *Terrestrial Depositional Systems: Deciphering complexities through multiple stratigraphic methods*, Elsevier, p. 165-208.
- Taylor, A.M. and Goldring, R. 1993. Description and analysis of bioturbation and ichnofabric; Organisms and sediments; relationships and applications. *Journal of the Geological Society of London*, v. 150, p. 141–148. Thomas et al., 1987

- Thomas, R.G., Smith, D.G., Wood, J.M., Visser, J., Calverley-Range, E.A. and Koster, E.H. 1987. Inclined heterolithic stratification—terminology, description, interpretation, and significance. *Sedimentary Geology*, v. 53, no. 1, p. 123–179.
- Timmer, E.R., Gingras, M.K., Morin, M.L., Ranger, M.J., and Zonneveld, J.P., 2016, Laminae-scale rhythmicity of inclined heterolithic stratification, Lower Cretaceous McMurray Formation, NE Alberta, Canada: *Canadian Society of Petroleum Geology*, v. 64, no. 2, 199-217.
- Seilacher, A., 1978, Use of trace fossil assemblages for recognizing depositional environments, *in*: Basan, B., editor, *Trace Fossil Concepts: Society of Economic Paleontologists and Mineralogists: Short Course*, 5, p. 167–181.
- Vail, P.R., Audemard, F., Bowman, S.A., Eisner, P.N., and Perez-Cruz, C., 1991, The stratigraphic signatures of tectonics, eustasy, and sedimentology – an overview, *in*: Einsele, G., Ricken, W., and Seilacher, A, editors, *Cycles and Events in Stratigraphy*, Springer-Verlag, p. 617-659.
- Van Wagoner, J.C., Posamentier, H.W., Mitchum, R.M., Vail, P.R., Sarg, J.F., Loutit, T.S., and Hardenbol, J., 1988, An overview of the fundamentals of sequence stratigraphy and key definitions, *in*: Wilgus, C.K., Hastings, B.S., Kendall, C.G.St.C., Posamentier, H.W., Ross, C.A., and Van Wagoner, J.C., editors, *Sea Level Changes: an Integrated Approach*, Society of Economic Paleontologists and Mineralogist, Special Publication, vol. 42, p. 39-45.
- Van Wagoner, J.C., Mitchum, R.M., Campion, K.M., and Rahamanian, V.D., 1990, Siliciclastic sequence stratigraphy in well logs, cores, and outcrops, *in*: American Association of Petroleum Geologists Methods in Exploration Series, v. 7, 55 p.
- Velde, B., 2014, Green Clay Minerals: *in*: Mackenzie, F.T., editor, *Sediments, Diagenesis, and Sedimentary Rocks*, *in*: Holland, H.D., and Turekian, K.K., editors, *Treatise on Geochemistry*, v. 7, Elsevier-Pergamon, Oxford
- Vigrass, L.W., 1977, Trapping of Oil at Intra-Mannville (Lower Cretaceous) Disconformity in Lloydminster Area, Alberta, and Saskatchewan: *The American Association of Petroleum Geologists Bulletin*, v. 61, no. 7, p. 1010-1028.
- Vossler, S.M., and Pemberton, S.G., 1988, Ichnology of the Cardium Formation (Pembina oilfield): implications for depositional and sequence stratigraphic interpretations, *in*: James, D.P., and Leckie, D.A., editors, *Sequences, Stratigraphy, Sedimentology: Surface and Subsurface*. Canadian Society of Petroleum Geology, Memoir 15, p. 237–253.
- Wadsworth, J., Boyd, R., Diessel, C., and Leckie, D., 2002, Stratigraphic style of coal and non-marine strata in a tectonically influenced intermediate accommodation setting: the Mannville Group of the

- Western Canadian Sedimentary Basin, south-central Alberta: *Bulletin of Canadian Petroleum Geology*, v. 50, no. 4, p. 507-541.
- Walker, R.G., and Cant, D.J. 1984, Sandy fluvial systems. *in*: Walker, R.G., editor, *Facies models*, Second Edition: Geological Association of Canada, 1984.
- Weleschuk, Z.P., and Dashtgard, S.E., 2019, Evolution of an ancient (Lower Cretaceous) marginal-marine system from a tide-dominated to wave-dominated deposition, McMurray Formation: *Sedimentology*, v. 66, p. 2354-2391.
- Wellner, R.W., Varban, B.L., Roca, X, Flaum, J.A., Stewart, E.K., and Blum, M.D., 2018, Simple is better when it comes to sequence stratigraphy: The Clearwater Formation of the Mannville Group reinterpreted using a genetic body approach: *American Association of Petroleum Geologists Bulletin*, v. 102, no. 3, p. 447-482.
- Wickenden, R.T.D., 1948, The Lower Cretaceous of the Lloydminster oil and gas area, Alberta, and Saskatchewan: Geological Survey of Canada, Paper 48-21, 15 p.
- Wilson, M., 1984, Depositional environments of the Mannville Group (Lower Cretaceous) in the Tangleflags area, Saskatchewan, *in*: Lorscheider, J.A., and Wilson, M., editors, *Oil and Gas in Saskatchewan: Saskatchewan Geological Society, Special Publication Number 7*, p. 119-134.
- Zaitlin, B.A., and Schultz, B.C., 1984, An estuarine-embayment fill model from the Lower Cretaceous Mannville Group, west-central Saskatchewan, *in*: Stott, D.F., and Glass, D.J., editors, *The Mesozoic of Middle North America: Canadian Society of Petroleum Geologists, Memoir 9*, p. 455-469.
- Zaitlin, B.A., Warren, M.J., Potocki, D., Rosenthal, L., and Boyd, R., 2002, Depositional styles in a low accommodation foreland basin setting: an example from the Basal Quartz (Lower Cretaceous), southern Alberta: *Bulletin of Canadian Petroleum Geology*, v. 50, no. 1, p. 31-72.
- Zavala, C., Arcuri, M., and Blanco-Valiente, L., 2012, The importance of plant remains as diagnostic criteria for the recognition of ancient hyperpycnites: *Revue De Paleobiologie, Special Volume 11*, p. 457-469,
- Zecchin, M., and Catuneanu, O., 2013, High-resolution sequence stratigraphy of clastic shelves I: Units and bounding surfaces: *Marine and Petroleum Geology*, v. 39, p. 1-25.
- Zecchin, M., and Catuneanu, O., 2015, High-resolution sequence stratigraphy of clastic shelves III: Applications to reservoir geology: *Marine and Petroleum Geology*, v. 62, p. 161-175.
- Zecchin, M., Catuneanu, O., and Caffau, M., 2017, High-resolution sequence stratigraphy of clastic shelves V: criteria to discriminate between stratigraphic sequences and sedimentological cycles: *Marine and Petroleum Geology*, v. 85, p. 259-271.

Zecchin, M., Catuneanu, O., and Caffau, M., 2019, Wave-ravinement surfaces: Classification and key characteristics: *Earth-Science Reviews*, v. 188. p. 210-239.

Appendix

Core Logs

Legend

Core Logs

Sedimentary Structures

| | | | |
|---|-------------------------------------|--|---------------------------|
| M | Massive | | Sedimentary scour |
| | Low-angle cross-lamination | | Convolute bedding |
| | High-angle cross-lamination | | Dish structures |
| | Hummocky cross-lamination | | Synsedimentary fault |
| | Herringbone cross-lamination | | Mottled |
| | Planar cross-stratification | | Flame structure |
| | Trough cross-stratification | | Injection feature |
| | Bioturbated | | Gutter cast |
| | Crypto-bioturbation | | Fracture |
| | Vague low-angle cross-lamination | | Soft sediment deformation |
| | Oscillation ripple cross-lamination | | Slickensides |
| | Isolated wave ripples | | Loaded ripples |
| | Combined flow ripple cross-lam | | Undiff cross-bedding |
| | Current ripple cross-lamination | | Lenticular bedding |
| | Climbing ripple cross-lamination | | Flaser bedding |
| | Starved wave ripples | | Dewatering structure |
| | Wavy bedded | | Lenses |
| | Normally graded beds | | Contorted |
| | Reverse graded beds | | Boudinage |
| | Load structures | | Bioturbated mud laminae |
| | Synaeresis cracks | | Bioturbated mud beds |
| | Double mud drape | | Wavy mud beds |
| | Mud crack | | Pinstrip bedding |
| | Reactivation surface | | |

Accessories

| | | | |
|------|---------------------|---|-------------------|
| | Coal laminae | | Granule/pebble |
| | Coal fragment | | Siderite layer |
| | Mudstone interclast | | Shale laminae |
| PY | Pyrite | | Sand laminae |
| GL | Glauconite | | Silt laminae |
| | Wood fragments | | Plant debris |
| | Carbonaceous debris | K | Kaolinite |
| | Carbonaceous drapes | | Mud-filled crack |
| (SI) | Siderite nodules | | Sand-filled crack |
| | Rootlets | | |

Ichnofossils

| | | | |
|--|---------------------|--|----------------|
| | Skolithos | | Cylindrichnus |
| | Diplocraterion | | Bergaueria |
| | Asterosoma | | Rhizocorallium |
| | Chondrites | | Arenicolites |
| | Zoophycos | | Gyrolithes |
| | Palaeophycus | | Taenidium isp. |
| | fugichnia | | Scolicia |
| | Thalassinoides | | Macaronichnus |
| | Planolites | | Nereites |
| | Ophiomorpha | | Cosmoraphe |
| | Rosselia | | Conichnus |
| | Schaubcylindrichnus | | Navichnia |
| | Helminthopsis | | Undiff Burrow |
| | Phycosiphon | | Lockeia |
| | Teichichnus | | Shell Debris |

Surfaces

| | |
|--|----------------------------|
| | Formation Contact |
| | Member Unit Contact |
| | Depositional Unit Contact |
| | Facies Association Contact |
| | Unconformity |

Bioturbation Index



Lithology

| | |
|--|--------------|
| | Missing core |
| | Coal |

Facies Abbreviation Codes

Lithology

| | |
|---|----------------|
| G | = Gravel |
| S | = Sand |
| H | = Heterolithic |
| F | = Fines |
| P | = Paleosol |
| C | = Coal |

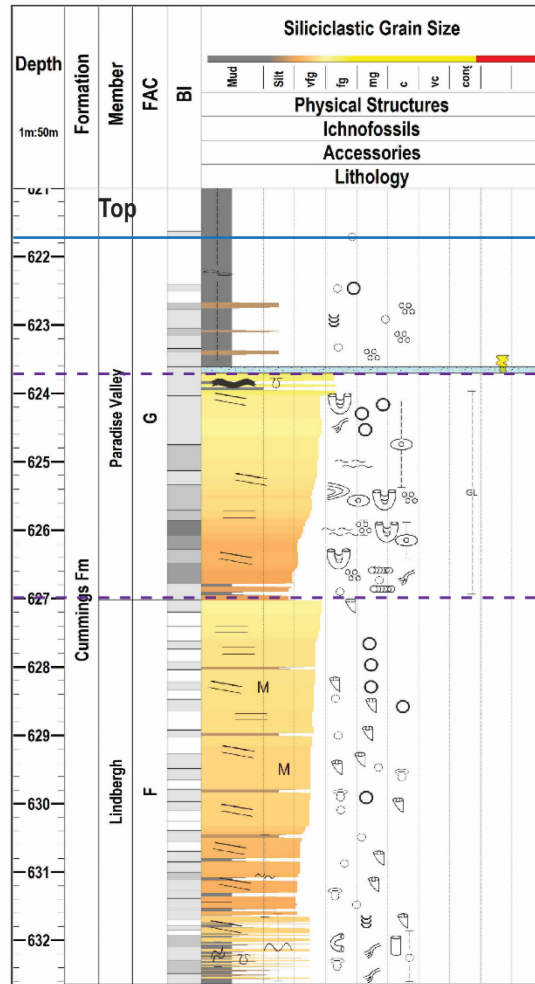
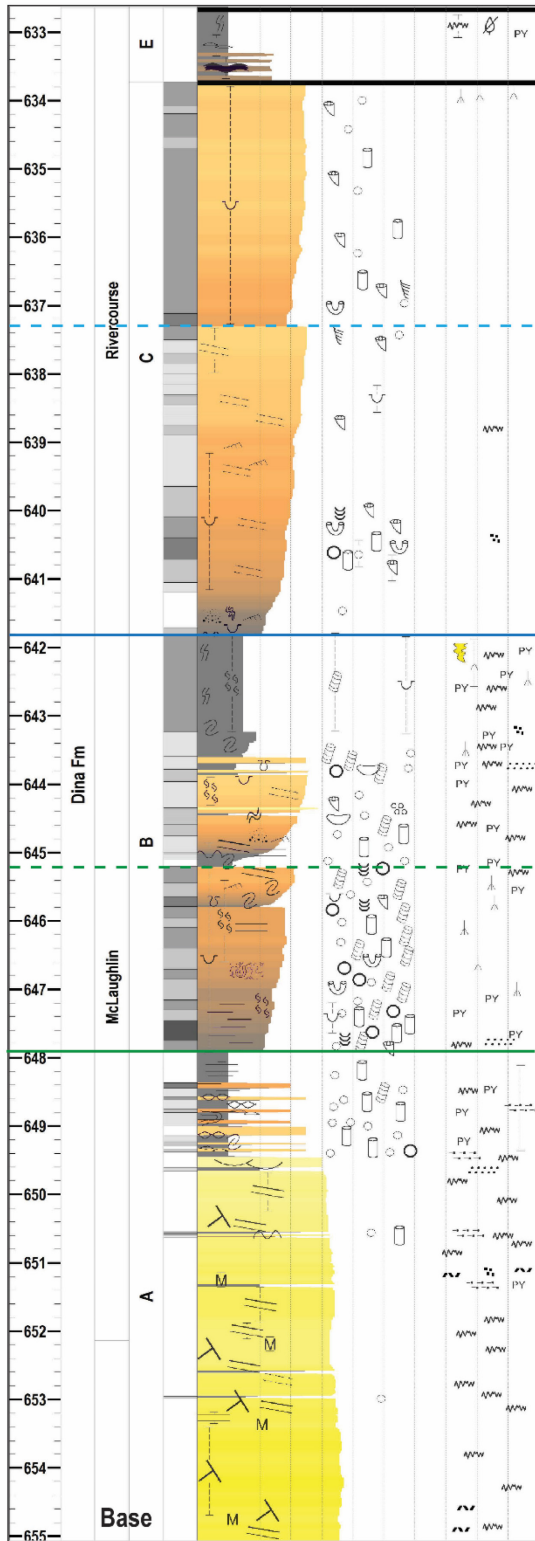
Lithology Modifiers

| | |
|-----|---|
| t | = trough cross-bedding |
| l | = low-angle cross-lamination |
| h | = horizontal bedding |
| c | = curvilinear cross-lamination |
| p | = planar cross-beds |
| or | = oscillation ripple cross-lamination |
| cr | = current ripple cross-lamination |
| cfr | = combined flow ripple cross-lamination |
| m | = massive |
| s | = scours |
| mb | = mud clast breccia |
| f | = flaser bedding |
| ln | = lenticular bedding |
| sm | = sand - silt/mud |
| ms | = silt/mud - sand |
| r | = massive, roots, biot. |
| mm | = matrix supported, weak grading |
| mg | = matrix supported, graded |
| ci | = clast supported, inverse grading |
| cm | = clast supported, massive |

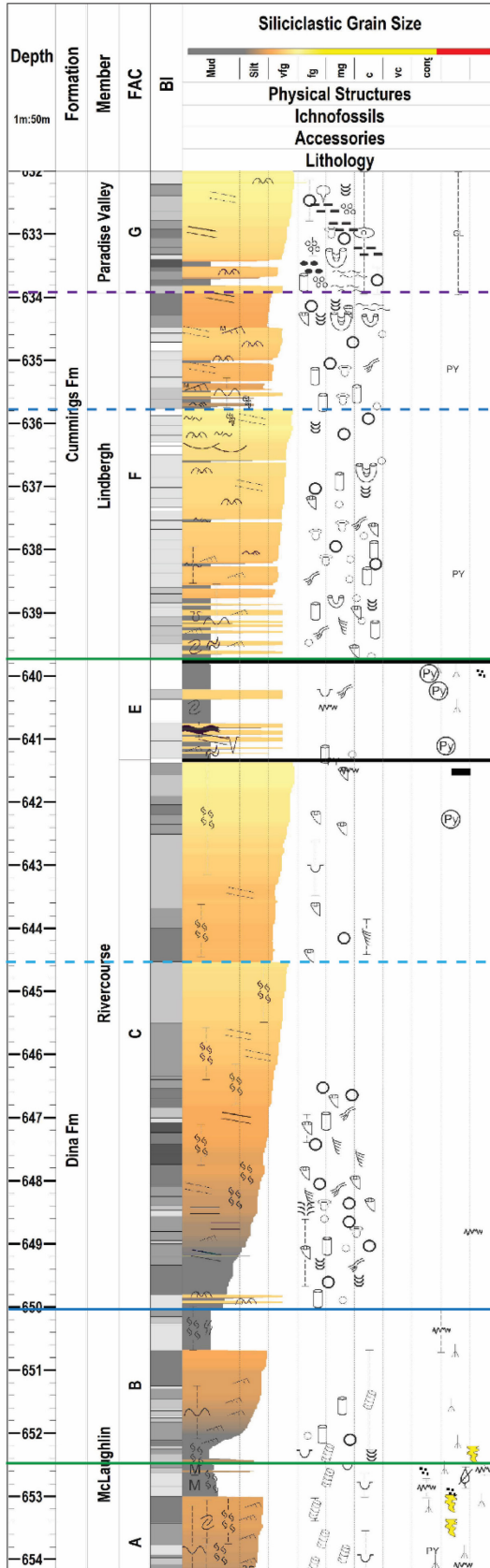
Paleosol Modifiers

| | |
|---|--------------|
| h | = Histosol |
| p | = Protosol |
| v | = Vertisol |
| g | = Gleysol |
| c | = Calcisol |
| g | = Gypsisol |
| a | = Argillisol |
| s | = Spodosol |
| o | = Oxisol |

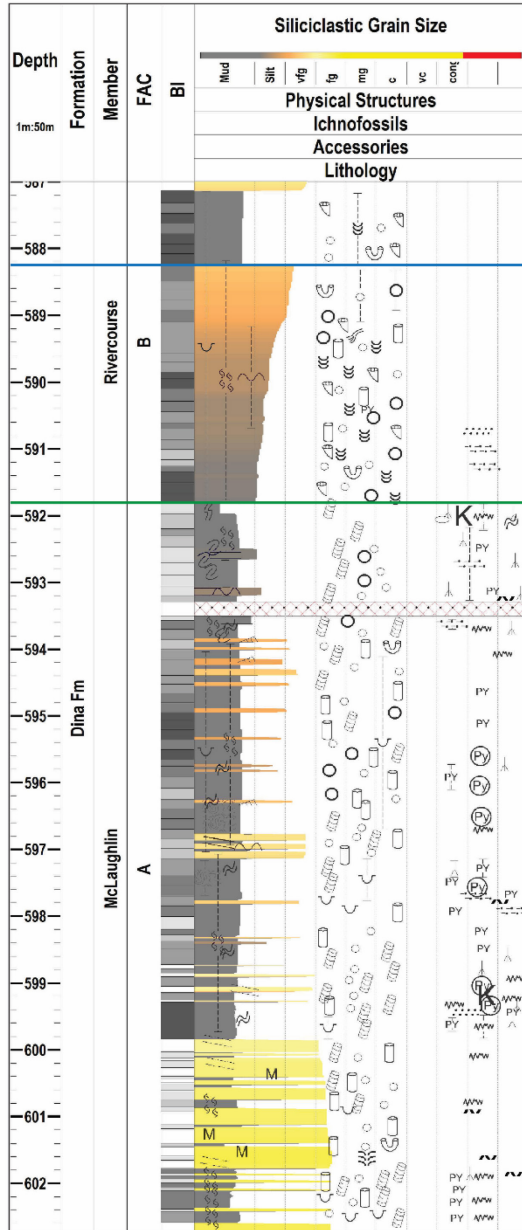
15-25-047-01W4



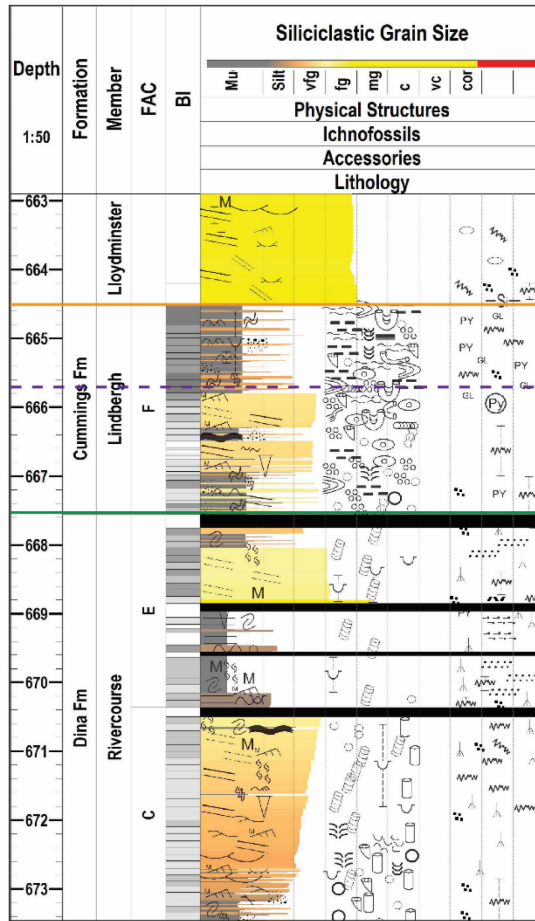
09-35-047-01W4



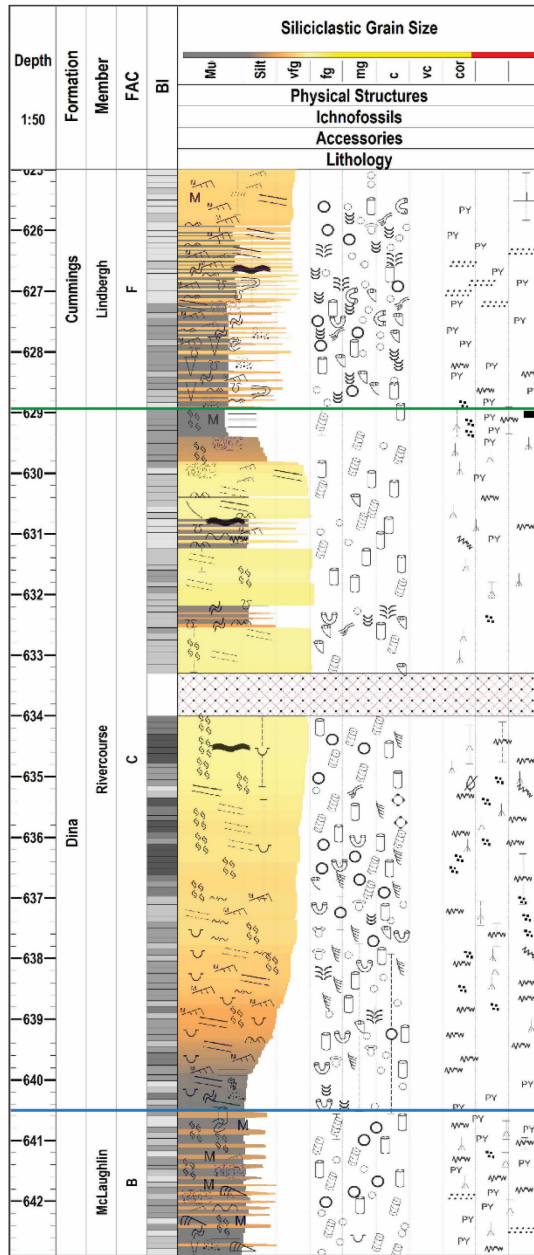
16-09-053-04W4

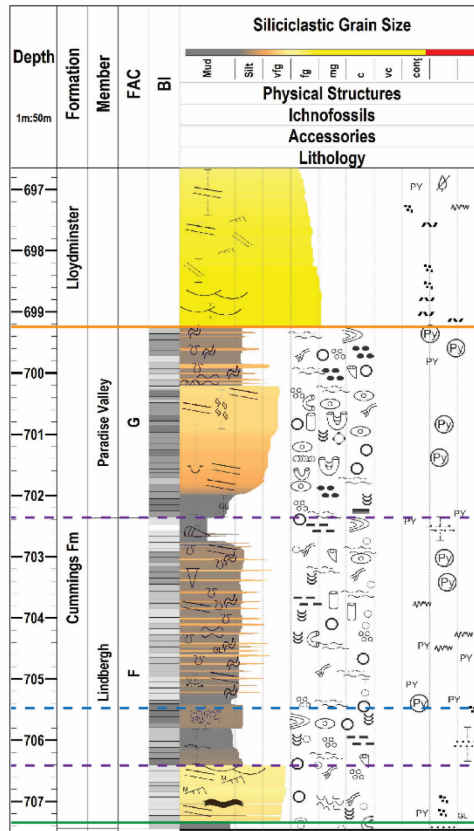
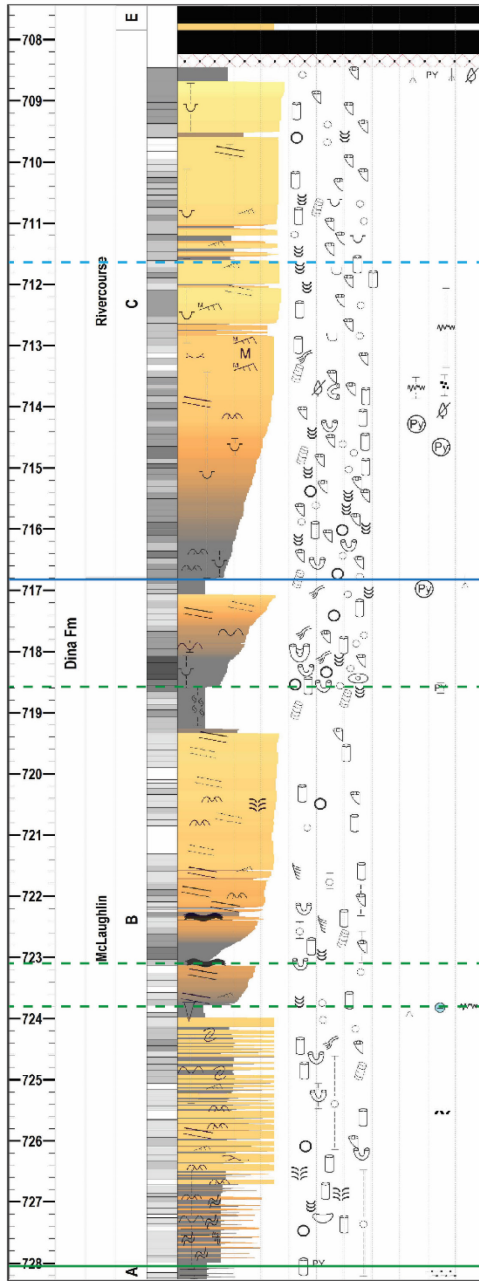


08-31-048-05W4

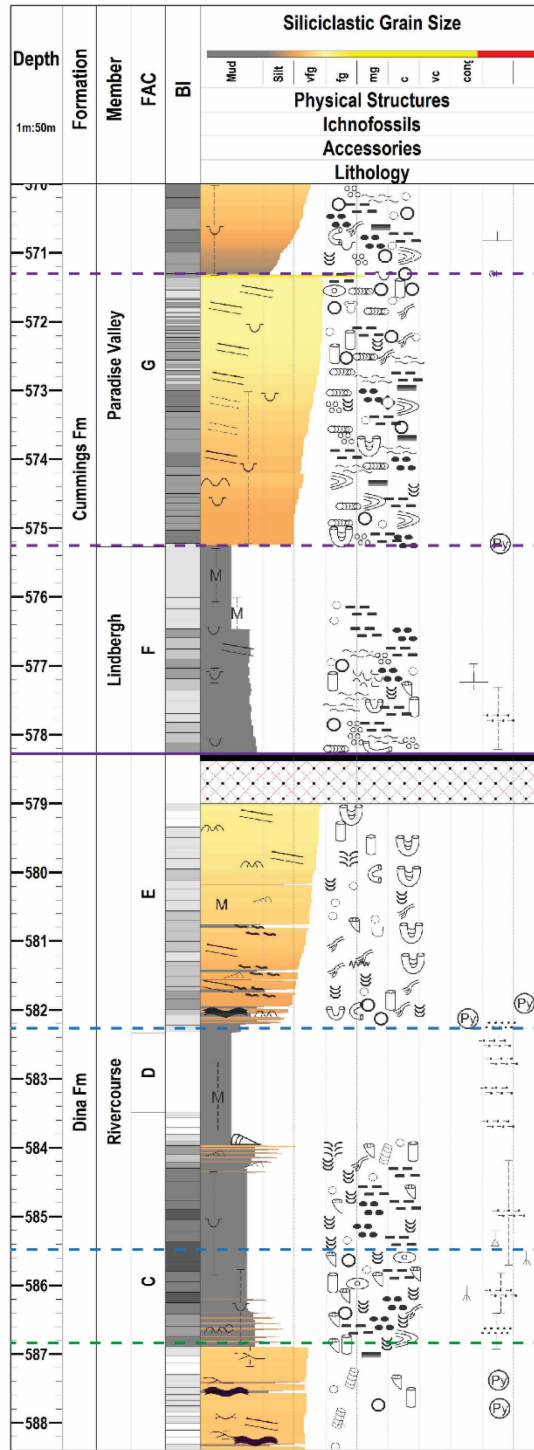


06-24-048-01W4

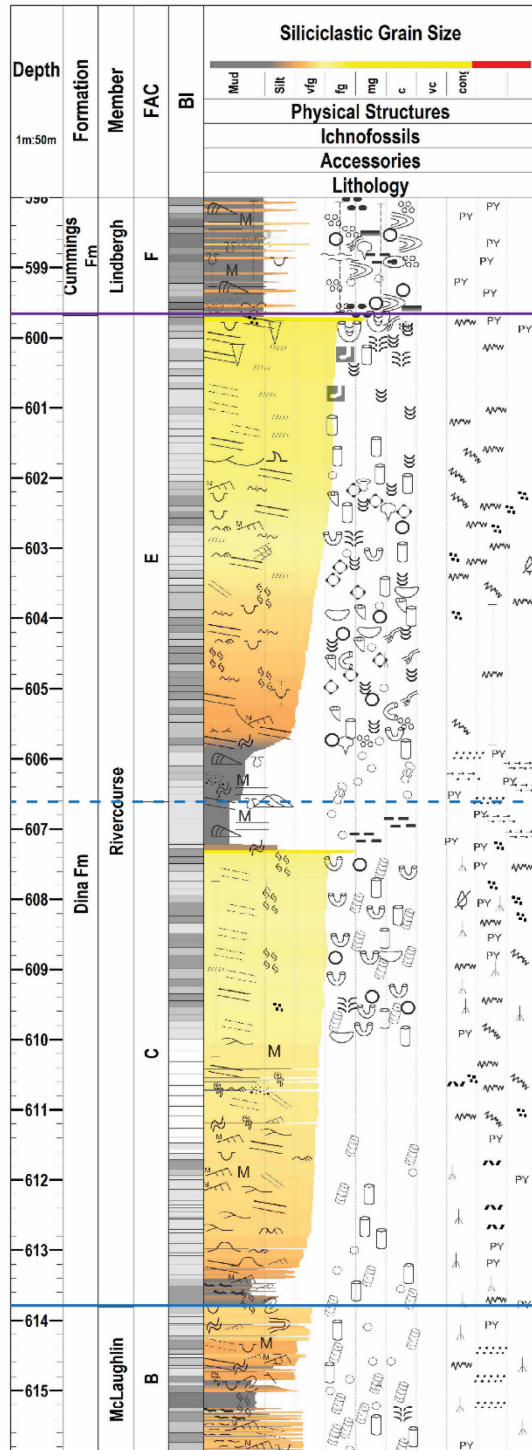




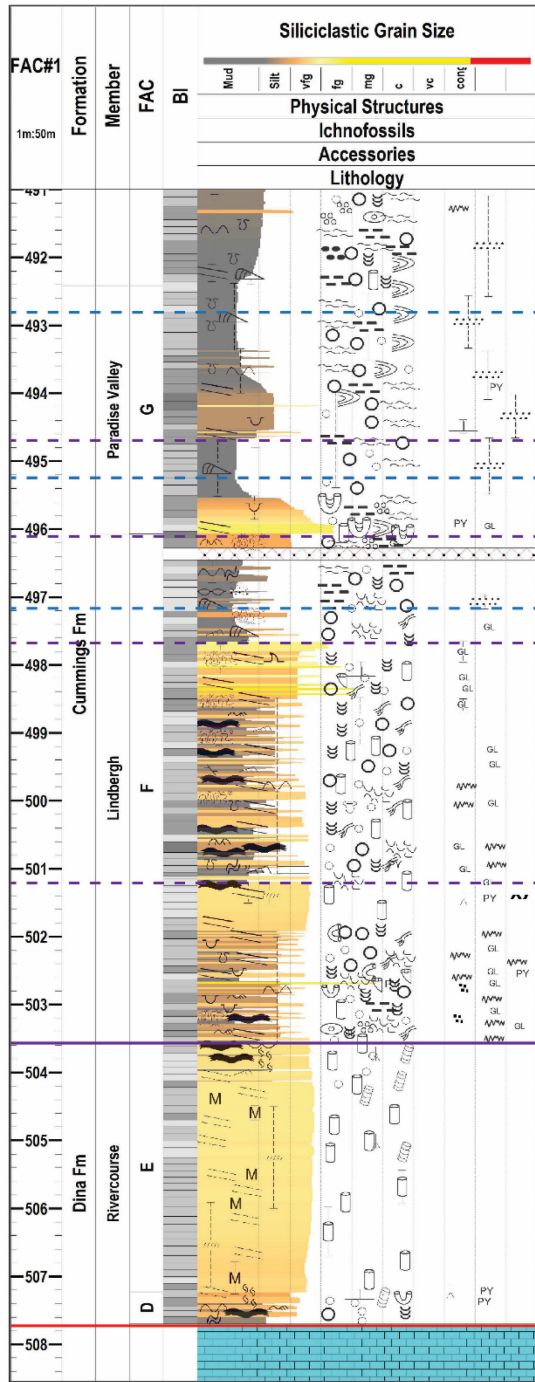
09-33-054-05W4



14-34-054-06W4



05-18-055-01W4



15-22-055-01W4

